ADAPTATION AND PHENOTYPIC PLASTICITY TO CLIMATE CHANGE

EDITED BY: Timothy Ravasi, Jennifer Marie Donelson, Jose M. Eirin-Lopez and Lisa N. S. Shama

PUBLISHED IN: Frontiers in Marine Science

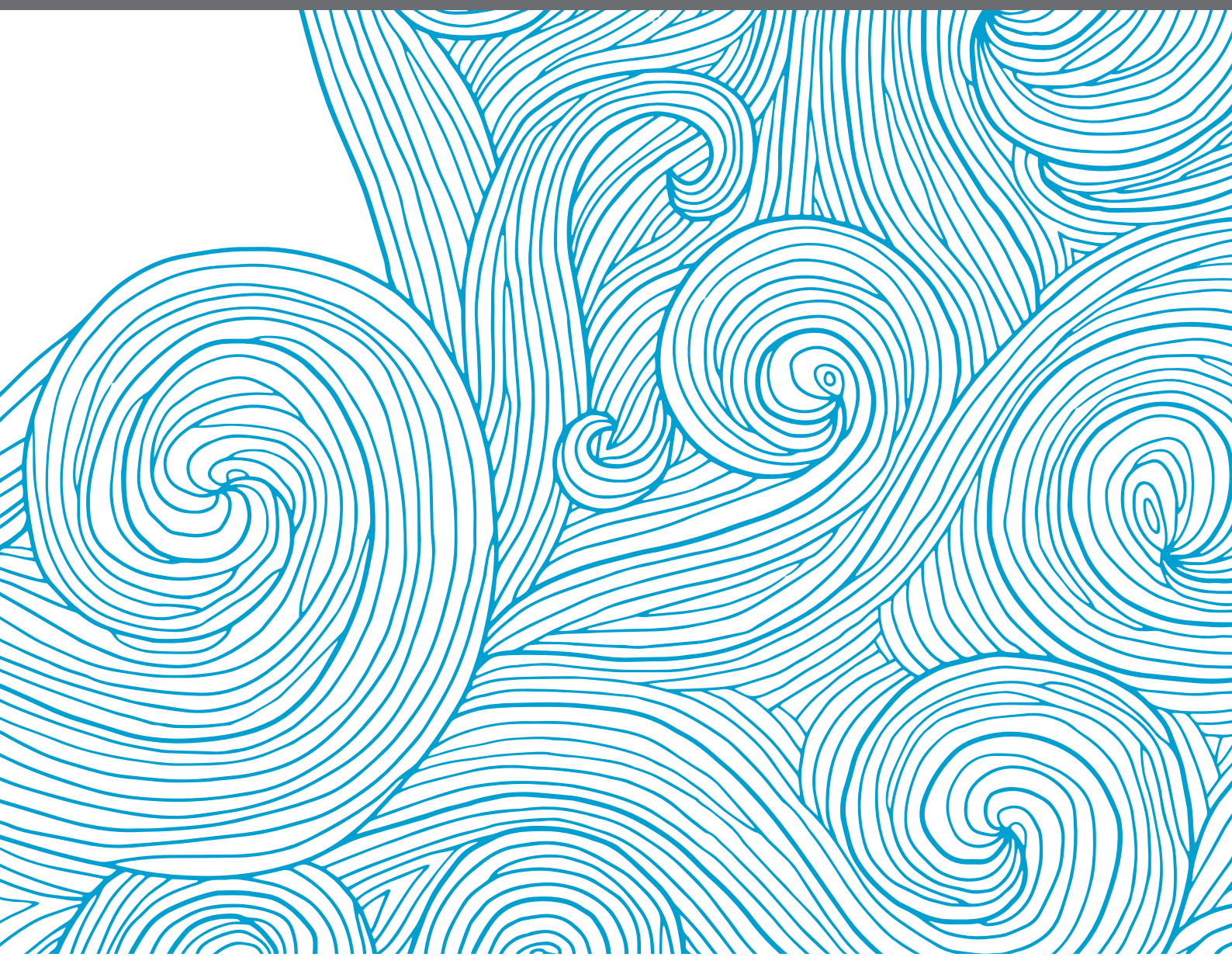

frontiers Research Topics

ISSN 1664-8714
ISBN 978-2-88976-131-9
DOI 10.3389/978-2-88976-131-9

About Frontiers

Frontiers is more than just an open-access publisher of scholarly articles: it is a pioneering approach to the world of academia, radically improving the way scholarly research is managed. The grand vision of Frontiers is a world where all people have an equal opportunity to seek, share and generate knowledge. Frontiers provides immediate and permanent online open access to all its publications, but this alone is not enough to realize our grand goals.

Frontiers Journal Series

The Frontiers Journal Series is a multi-tier and interdisciplinary set of open-access, online journals, promising a paradigm shift from the current review, selection and dissemination processes in academic publishing. All Frontiers journals are driven by researchers for researchers; therefore, they constitute a service to the scholarly community. At the same time, the Frontiers Journal Series operates on a revolutionary invention, the tiered publishing system, initially addressing specific communities of scholars, and gradually climbing up to broader public understanding, thus serving the interests of the lay society, too.

Dedication to Quality

Each Frontiers article is a landmark of the highest quality, thanks to genuinely collaborative interactions between authors and review editors, who include some of the world's best academicians. Research must be certified by peers before entering a stream of knowledge that may eventually reach the public - and shape society; therefore, Frontiers only applies the most rigorous and unbiased reviews.
Frontiers revolutionizes research publishing by freely delivering the most outstanding research, evaluated with no bias from both the academic and social point of view. By applying the most advanced information technologies, Frontiers is catapulting scholarly publishing into a new generation.

What are Frontiers Research Topics?

Frontiers Research Topics are very popular trademarks of the Frontiers Journals Series: they are collections of at least ten articles, all centered on a particular subject. With their unique mix of varied contributions from Original Research to Review Articles, Frontiers Research Topics unify the most influential researchers, the latest key findings and historical advances in a hot research area! Find out more on how to host your own Frontiers Research Topic or contribute to one as an author by contacting the Frontiers Editorial Office: frontiersin.org/about/contact

ADAPTATION AND PHENOTYPIC PLASTICITY TO CLIMATE CHANGE

Topic Editors:
Timothy Ravasi, Okinawa Institute of Science and Technology Graduate University, Japan
Jennifer Marie Donelson, James Cook University, Australia
Jose M. Eirin-Lopez, Florida International University, United States
Lisa N. S. Shama, Wadden Sea Station Sylt, Alfred Wegener Institute Helmholtz Centre for Polar and Marine Research (AWI), Germany

Citation: Ravasi, T., Donelson, J. M., Eirin-Lopez, J. M., Shama, L. N. S., eds. (2022). Adaptation and Phenotypic Plasticity to Climate Change.
Lausanne: Frontiers Media SA. doi: 10.3389/978-2-88976-131-9

Table of Contents

frontiers | Frontiers in Marine Science

EDITORIAL
published: 20 April 2022
doi: 10.3389/fmars.2022.893117

Editorial: Adaptation and Phenotypic Plasticity to Climate Change

Lisa N. S. Shama[1*], *Jennifer M. Donelson*[2*], *Jose M. Eirin-Lopez*[3*] *and Timothy Ravasi*[1,4*]

[1] Coastal Ecology Section, Alfred Wegener Institute Helmholtz Centre for Polar and Marine Research, Wadden Sea Station Sylt, List, Germany, [2] Australian Research Council (ARC) Centre of Excellence for Coral Reef Studies, James Cook University, Townsville, QLD, Australia, [3] Environmental Epigenetics Lab, Florida International University, Miami, FL, United States, [4] Marine Climate Change Unit, Okinawa Institute of Science and Technology (OIST), Okinawa, Japan

Keywords: climate change, adaptation, plasticity, epigenetics, marine, aquatic ectotherm

OPEN ACCESS

Edited and reviewed by:
Carlos M. Duarte,
King Abdullah University of Science and Technology, Saudi Arabia

***Correspondence:**
Lisa N. S. Shama
lisa.shama@awi.de
Jennifer M. Donelson
jennifer.donelson@my.jcu.edu.au
Jose M. Eirin-Lopez
jeirinlo@fiu.edu
Timothy Ravasi
timothy.ravasi@oist.jp

Specialty section:
This article was submitted to Global Change and the Future Ocean, a section of the journal Frontiers in Marine Science

Received: *10 March 2022*
Accepted: *21 March 2022*
Published: *20 April 2022*

Citation:
Shama LNS, Donelson JM, Eirin-Lopez JM and Ravasi T (2022) Editorial: Adaptation and Phenotypic Plasticity to Climate Change. Front. Mar. Sci. 9:893117. doi: 10.3389/fmars.2022.893117

Editorial on the Research Topic

Adaptation and Phenotypic Plasticity to Climate Change

Anthropogenic activities are driving rapid changes in aquatic environments. Numerous studies suggest that climatic shifts and anomalies will convey severe consequences for ecosystems worldwide, leading to disruptions in key processes within populations including larval development, individual growth, and reproductive success. This is further exacerbated by the negative impacts on between-species interactions, and changes to biodiversity and ecosystem services (Munday et al., 2013). Understanding the responses of organisms to environmental shifts is imperative to help predict their fate on a changing planet. Particularly, the capacity of individuals and populations to cope through phenotypic plasticity and adaptation is of critical interest, with advances in genomics and epigenomics techniques helping to unveil the underlying molecular mechanisms (Eirin-Lopez and Putnam, 2019). However, major knowledge gaps remain about the adaptive potential of marine organisms to respond to future ocean conditions. The aim of this Research Topic was to bring together novel research approaches that examine acclimation and adaptation processes in marine organisms, their role in population resilience, and implications for geographical distributions and range shifts under rapid climate change. Contributions to the topic span a broad range of taxa, and investigate a diverse array of response mechanisms such as thermal safety margins (Bennett et al.), thermotolerance *via* endosymbionts and gene expression (Naugle et al.), tolerance *via* changes in allele frequencies (Knöbel et al.), local adaptation and maternal effects (Richards et al.), transgenerational plasticity (TGP; Chang et al.), environment-dependent reproductive success (Wanzenböck et al.), and phenological shifts to long-term seasonal changes (Xia et al.). Furthermore, the importance of environmental variability (not only mean changes) at different time scales, the role of developmental or life history stage in phenotypic responses, as well as future challenges for plasticity research (both within and across generations) are outlined in Bautista and Crespel.

THERMAL TOLERANCE

Organisms can cope with fast changing environments either by staying in place and tolerating local conditions, adjusting *via* plasticity or genetic change, or shifting their distribution to more favourable environments (Gienapp et al., 2007). As discussed in Bennett et al., species distribution models often assume that thermal sensitivity is the same along the species´ geographic distribution, and do not account for local adaptation or thermal plasticity. Bennett et al. conducted a comparative study using populations of four foundation species (two seagrass and two seaweed) that occur across a west-east temperature gradient in the Mediterranean. They found the greatest variability in thermal performance between species, but also site-specific differences in thermal safety margins within species (e.g., *Posidonia oceanica*), and that species retain deep "pre-Mediterranean" evolutionary legacies (genetic differences) for thermal sensitivity. Their study demonstrates differing thermal sensitivities of species despite similarities in realised thermal distributions. Around the island of Tutuila in American Samoa, Naugle et al. investigated thermal tolerance of coral colonies (*Acropora hyacinthus*) from sites with baseline differences in nutrient pollution. This multi-stressor experiment showed that in 2014, polluted sites had more thermotolerant corals due to higher proportions of heat-tolerant endosymbionts, whereas by 2019, there were small difference among sites because most colonies had undergone "symbiont shuffling" towards the heat-tolerant forms. These two studies demonstrate population-specific thermal tolerance, which has important implications for species conservation and management strategies.

GENETIC CHANGE AND NON-GENETIC INHERITANCE

Although it is often assumed that genetic adaptation may be too slow to keep pace with climate change, major shifts in allele frequencies can occur in one generation. Plasticity and non-genetic inheritance are faster and have multiple pathways from which to act. However, how plasticity shapes selection strengths is debated (Merilä and Hendry, 2013). To examine local adaptation to salinity in blue mussels (*Mytilus* spp.), Knöbel et al. conducted a common garden experiment using high salinity "western" and low salinity "eastern" mussels from the Baltic sea and found that laboratory-bred larvae showed local adaptation for several traits. Testing larvae derived from a F1 west-east hybrid population to predicted future desalinisation and warming, they found that when larval populations were exposed to lower salinity, there was a shift toward the "eastern" alleles, indicating that salinity acts as a selection force during the pre-settlement phase driving local adaptation to low salinity, ultimately shaping the genetic composition of populations along the salinity gradient.

Both within- and across-generation plasticity have been shown to contribute to the adaptive potential of populations (Donelson et al., 2018). Exposing six populations of the foundation species, red mangrove (*Rhizophora mangle*), to both increased salinity and nitrogen in a common garden setting, Richards et al. found plasticity in response to salinity for some traits, but that other trait responses co-varied with both stressors. Significant population effects in the common garden suggest local adaptation and/or heritable plasticity, but the strongest predictor for nearly all traits was maternal family, indicating non-genetic inheritance mechanisms. Maternal effects are known to play a large role in offspring phenotypic variation, however, paternal effects are starting to gain attention (Crean and Bonduriansky, 2014). Using laboratory-bred F3 generation sheepshead minnows (*Cypriniodont variegatus*) as parental fish, Chang et al. exposed both parents and offspring to two temperatures in a split-cross TGP experiment. They found that offspring growth was lowest when there was no thermal history match among parents and offspring, but highest when all three matched. That is, TGP effects were additive across the sire-offspring and dam-offspring interactions. Strong paternal effects suggest an epigenetic basis underlying TGP.

REPRODUCTIVE BEHAVIOUR

In addition to shaping key fitness-related traits such as growth, changing environmental conditions can also influence reproductive behaviours like mate choice and the onset of breeding (Fox et al., 2019). Using a mesocosm experiment, Wanzenböck et al. tested for differential reproductive success among stickleback (*Gasterosteus aculeatus*) plate morph phenotypes by genotyping egg clutches laid in either ambient or +4°C conditions. They found that low-plated males sired more eggs at +4°C, likely due to their smaller size (relative to other morphs), and hence, lower metabolic demands at higher temperature. However, more low-plated fish under ocean warming may have implications for range shifts, since their migration distance is limited due to missing keel plates. In silver carp (*Hypophthalmichthys molitrix*), spawning periods are influenced by both temperature and river discharge (which can affect oviposition habitat). By correlating time-series data of temperature and hydrological regimes with larval fish abundance, Xia et al. found that spawning times of populations showed local adaptation, and that the spawning period has shortened over the last decade, with clear implications for reproductive output of this commercially important species.

FUTURE CHALLENGES

The diverse array of mechanisms to cope with rapid climate change compiled in this Research Topic are reviewed in Bautista and Crespel. They highlight that within-generation responses such as thermal tolerance, plasticity and/or relocation are a first line of defence. If organisms manage to reproduce, then climate change effects can be transferred across generations *via* genetic change (adaptation) and/or non-genetic inheritance *via* parental effects, TGP and/or heritable epigenetic modifications. Importantly, they advocate for the inclusion of more environmental variability in future experiments to provide ecologically relevant predictions, and to investigate consequences of early exposure on later stages (carryover effects) and fitness traits. Key research areas for the

future include the role of non-genetic inheritance in evolution, neutral and quantitative genetic adaptive potential, interactions between within- and transgenerational plasticity, and coupling genetic sequence data with epigenetic patterns to assess the heritability of epigenetic marks. The collection of papers in this Research Topic demonstrate empirically how adaptation and phenotypic plasticity contribute to population resilience, and propose new research directions to further understanding of their importance under future climate change.

AUTHOR CONTRIBUTIONS

LS, JD, JE-L and TR together wrote this editorial. All authors contributed to the article and approved the submitted version.

FUNDING

JD was supported by and ARC Future Fellowship (FT190100015).

REFERENCES

Crean, A. J., and Bonduriansky, R. (2014). What Is a Paternal Effect? *Trends. Ecol. Evol.* 29, 554–559. doi: 10.1016/j.tree.2014.07.009

Donelson, J. M., Salinas, S., Munday, P. L., and Shama, L. N. S. (2018). Transgenerational Plasticity and Climate Change Experiments: Where Do We Go From Here? *Global Change Biol.* 24, 13–34. doi: 10.1111/gcb.13903

Eirin-Lopez, J. M., and Putnam, H. M. (2019). Marine Environmental Epigenetics. *Ann. Rev. Mar. Sci.* 11, 335–368. doi: 10.1146/annurev-marine-010318-095114

Fox, R. J., Fromhage, L., and Jennions, M. D. (2019). Sexual Selection, Phenotypic Plasticity and Female Reproductive Output. *Phil. Trans. R. Soc.* 374, 20180184. doi: 10.1098/rstb.2018.0184

Gienapp, P., Teplisky, C., Alho, J. S., Mills, J. A., and Merilä, J. (2007). Climate Change and Evolution: Disentangling Environmental and Genetic Responses. *Mol. Ecol.* 17, 1–12. doi: 10.1111/j.1365-294X.2007.03413.x

Merilä, J., and Hendry, A. P. (2013). Climate Change, Adaptation, and Phenotypic Plasticity: The Problem and the Evidence. *Evol. Appl.* 7, 1–14. doi: 10.1111/eva.12137

Munday, P. L., Warner, R. R., Monro, K., Pandolfi, J. M., and Marshall, D. J. (2013). Predicting Evolutionary Responses to Climate Change in the Sea. *Ecol. Lett.* 16, 1488–1500. doi: 10.1111/ele.12185

Conflict of Interest: The authors declare that the research was conducted in the absence of any commercial or financial relationships that could be construed as a potential conflict of interest.

frontiers in Marine Science

ORIGINAL RESEARCH
published: 13 August 2021
doi: 10.3389/fmars.2021.692078

OPEN ACCESS

Edited by:
Lisa N. S. Shama, Wadden Sea Station Sylt, Alfred Wegener Institute Helmholtz Centre for Polar and Marine Research (AWI), Germany

Reviewed by:
Marta Paterno, University of Salerno, Italy
Roman Wenne, Institute of Oceanology, Polish Academy of Sciences, Poland
Ronghua Li, Ningbo University, China

***Correspondence:**
Heiko Stuckas
heiko.stuckas@senckenberg.de
Frank Melzner
fmelzner@geomar.de

† These authors have contributed equally to this work and share first authorship

‡Present address:
Jennifer C. Nascimento-Schulze College of Life and Environmental Sciences, University of Exeter, Exeter, United Kingdom
Trystan Sanders, School of Ocean and Earth Science, National Oceanography Centre Southampton, University of Southampton, Southampton, United Kingdom
Francisco R. Barboza, Estonian Marine Institute, University of Tartu, Tallinn, Estonia

§ These authors have contributed equally to this work and share senior authorship

Specialty section:
This article was submitted to Global Change and the Future Ocean, a section of the journal Frontiers in Marine Science

Received: *07 April 2021*
Accepted: *05 July 2021*
Published: *13 August 2021*

Citation:
Knöbel L, Nascimento-Schulze JC, Sanders T, Zeus D, Hiebenthal C, Barboza FR, Stuckas H and Melzner F (2021) Salinity Driven Selection and Local Adaptation in Baltic Sea Mytilid Mussels. Front. Mar. Sci. 8:692078. doi: 10.3389/fmars.2021.692078

Salinity Driven Selection and Local Adaptation in Baltic Sea Mytilid Mussels

Loreen Knöbel[1†], Jennifer C. Nascimento-Schulze[2†‡], Trystan Sanders[2†‡], Dominique Zeus[1], Claas Hiebenthal[2], Francisco R. Barboza[2‡], Heiko Stuckas[1§] and Frank Melzner[2*§]*

[1] Senckenberg Natural History Collections Dresden, Senckenberg Leibniz Institution for Biodiversity and Earth System Research, Dresden, Germany, [2] Marine Ecology, GEOMAR Helmholtz Centre for Ocean Research Kiel, Kiel, Germany

Baltic blue mussels can colonise and dominate habitats with far lower salinity (<10 psu) than other *Mytilus* congeners. Pervasive gene flow was observed between Western Baltic *Mytilus edulis* living at high salinity conditions and Eastern Baltic *M. trossulus* living at lower salinites, with highest admixture proportions within a genetic transition zone located at intermediate salinities (Darss Sill area). Yet, we do not understand the impacts of low salinity on larval performance, and how salinity may act as an early selective pressure during passive larval drift across salinity gradients. This study tested whether larvae originating from two different populations along the natural salinity cline in the Baltic Sea have highest fitness at their native salinities. Our results suggest that Eastern Baltic *M. trossulus* (Usedom, 7 psu) and Western Baltic *M. edulis* (Kiel, 16 psu) larvae display better performance (fitness components: growth, mortality, settlement success) when reared at their respective native salinities. This suggests that these populations are adapted to their local environment. Additionally, species diagnostic markers were used for genetic analyses of transition zone (Ahrenshoop, 11 psu) mussel larvae exposed to low salinity. This revealed that low salinity selection resulted in a shift towards allele frequencies more typical for Eastern Baltic *M. trossulus*. Thus, salinity acts as a selective pressure during the pre-settlement phase and can shape the genetic composition of Baltic mussel populations driving local adaptation to low salinity. Future climate change driven desalination, therefore, has the potential to shift the Baltic Sea hybrid gradient westward with consequences for benthic ecosystem structure.

Keywords: hybrid swarm, *Mytilus edulis*, *Mytilus trossulus*, laboratory experiments, mussel larvae

INTRODUCTION

The pronounced natural salinity gradient in the Baltic Sea, ranging from 30 psu at the transition to the North Sea to less than 4 psu in the innermost sub-basins (Bothnian Bay and inner Gulf of Finland) offers a natural context in which to explore evolutionary mechanisms underlying the colonisation of extreme environmental conditions (Johannesson et al., 2011; Wennerström et al., 2013). Apart from evolutionary questions, understanding how Baltic organisms cope with extreme environmental conditions holds the key to predicting and mitigating consequences of global change on marine biodiversity (Reusch et al., 2018). In this marginal sea, climate models predict a decrease

of sea surface salinities by ca. 2 psu and a westward shift of the salinity gradient by the end of the century (Gräwe et al., 2013). Additionally, the Baltic Sea has been identified as one of the fastest warming marine basins on the planet (Belkin, 2009).

Mytilid mussels have successfully colonised the Baltic Sea presumably 9000-8000 years ago after the last freshwater stage (Berglund et al., 2005; Witkowski et al., 2005; Behre, 2007; Kostecki and Janczak-Kostecka, 2011). Today, the two species *Mytilus edulis* and *M. trossulus* occur in the Baltic Sea (e.g., Koehn, 1991). Both are important foundation species which contribute significantly to benthic ecosystem function and nutrient turnover (Norling and Kautsky, 2008; Heckwolf et al., 2021). *Mytilus edulis* colonizes the Western Baltic (e.g., Kattegat, Belt Sea) at salinities between 12 and 25 psu and *M. trossulus* is found in the Eastern Baltic (e.g., Baltic Proper) at salinities between 4.5 and 8 psu (e.g., Stuckas et al., 2009, 2017; Kijewski et al., 2019). Whilst gene flow between these species is restricted on the Atlantic coastline of Northern America, a hybrid swarm is found in the Baltic (e.g., Riginos and Cunningham, 2005; Wenne et al., 2020). However, pervasive interspecific gene flow does not lead to an amalgamation of the gene pools. Instead, a pronounced genetic structure is found where Western Baltic *M. edulis* and Eastern Baltic *M. trossulus* are dominated by their species-specific alleles (e.g., Stuckas et al., 2009, 2017; Fraïsse et al., 2016; Kijewski et al., 2019; Simon et al., 2019). Species-specific allele frequencies change gradually resulting in allele frequency clines and a transition zone that is situated along longitude 12–13°E (a virtual line between Öresund and Darss Sill). This is an area of maximum genetic admixture where repeated backcrossing results in the coexistence of individuals with highly different proportions of alleles specific to *M. edulis* (ME-alleles) and *M. trossulus* (MT-alleles). Consequently, the species identity of transition zone mussels is best described by a hybrid index, e.g., continuously ranging from 0 (100% ME-alleles) via 0.5 (F1-like hybrid) to 1 (100% MT-alleles) (Stuckas et al., 2017). Despite of pervasive interspecific gene flow between Baltic mussels, substantial dissimilarities in shell morphology and physiology between Western Baltic *M edulis* and Eastern Baltic *M. trossulus* still exist (Kautsky et al., 1990; Tedengren et al., 1990; Telesca et al., 2018).

Adaptation to local salinity conditions is presumed to be one mechanism underlying the maintenance of distinct phenotypic differences in Baltic Sea *Mytilus*. This hypothesis was tested in field transplantation experiments of adult mussels. These analyses documented negative impacts of low salinities (<10 psu) particularly on Western Baltic *M. edulis,* with reduced filtration and growth rates as well as extremely high mortalities (Kautsky et al., 1990; Kossak, 2006; Riisgård et al., 2012, 2013, 2014). However, growth, survival, and feeding rates of Baltic *M. trossulus* individuals were comparable to those of Baltic *M. edulis* populations at high salinities (25–30 psu) (Kautsky et al., 1990; Tedengren et al., 1990; Riisgård et al., 2014). These specific responses of Baltic *Mytilus* species to salinity do not only hint toward the existence of local adaptation to salinity but also suggests that Baltic *M. trossulus* adults have a broader salinity tolerance window.

However, the implications of salinity changes on pre-settlement stages of Baltic mussel populations are yet to be understood. This is an important research topic, as larvae can drift for long distances during their several-week long pelagic life phase, thereby being exposed to fluctuating salinities (Larsson et al., 2016; Stuckas et al., 2017). In addition, mussel early life stages have been shown to be much more susceptible to abiotic stressors than adults, with a particularly high sensitivity to low calcium concentrations in low saline basins such as the Baltic (Thorson, 1950; Thomsen et al., 2015, 2017; Ramesh et al., 2017).

Here we explored how salinity impacts pelagic larvae during the pre-settlement life stage addressing two main questions: (i) whether larvae of both Baltic *Mytilus* species as well as transition zone mussels show differential salinity dependent performance (mortality, growth, settlement success) and (ii) whether salinity stress acts as a selective pressure in these early life stages, possibly shaping the genetic composition of mussel populations along the salinity gradient.

We first conducted a population comparison experiment using a common garden design with larvae originating from Western Baltic *M. edulis* (Kiel – KIE -, genotypes dominated by ME alleles, **Figure 1**) and Eastern Baltic *M. trossulus* (Usedom – USE -, genotypes dominated by MT alleles, **Figure 1**). Larval performance was quantified at both native and reciprocal salinities. A second experiment utilised larvae raised from transition zone mussel parents (Ahrenshoop, - AHP -, genotypes with intermediate frequencies of both ME- and MT-alleles, **Figure 1**). Although methodologically challenging, we used laboratory larval rearing trials for the first time at salinities <10 psu. These larvae were reared at low salinities analogous to what they could be exposed to during eastward drift trajectories along the southern Baltic coast. Performance of larvae was monitored in response to lowered salinity and at two temperatures prior to genotyping with species diagnostic markers upon settlement. Under the assumption of local adaptation to distinctly different habitat salinity regimes, both experiments were expected to show better performance of larvae under native compared to altered salinity. In addition, we hypothesised that low salinity treatment under laboratory conditions causes selection on transition zone mussels and predicted a significant enrichment of hybrid genotypes dominated by *M. trossulus* specific alleles.

MATERIALS AND METHODS

Broodstock Sampling and Maintenance

Adult Baltic *Mytilus* individuals were collected from three populations along the Baltic Sea coastline at the localities (KIE, average salinity 16 psu), Ahrenshoop (AHP, average salinity 11 psu), and (USE, average salinity 7 psu) (**Figure 1** and **Table 1**) in spring 2016. Average salinities at each locality were analysed over a 2 to 3-year period and this information was used to calculate average salinity conditions for experimental procedures described below (Sanders et al., 2021). Considering the high levels of interspecific gene flow (see introduction), we will refer to Baltic mussels as "Western Baltic *M. edulis*" (KIE), "transition zone mussels" (AHP), and "Eastern Baltic *M. trossulus*" (USE)

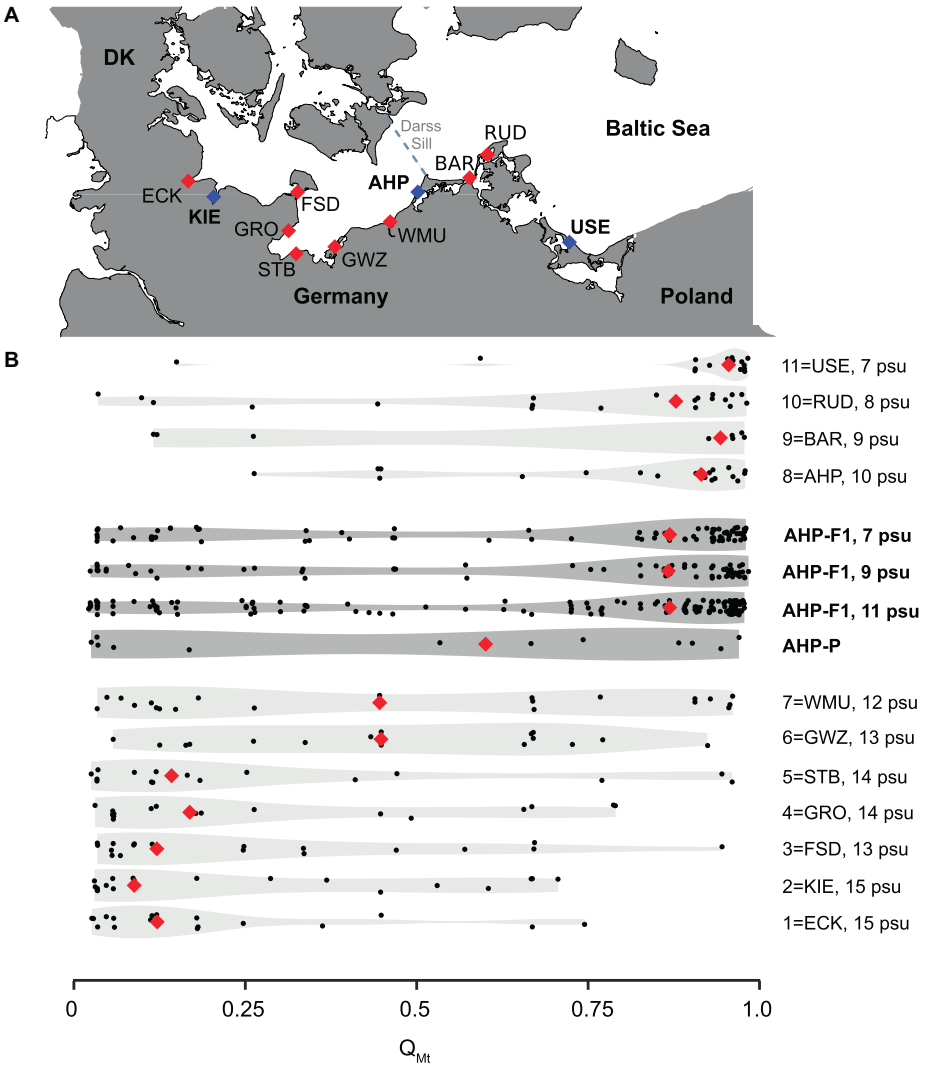

FIGURE 1 | Distribution of Baltic *Mytilus* species and sampling localities. **(A)** Sampling locations for the population comparison (Kiel, KIE; Usedom, USE) and the desalination (Ahrenshoop, AHP) experiments. Further references locations for genetic analyses are shown ECK, Eckernförde; FSD, Fehmarnsund; GRO, Grömitz; STB, Steinbeck; GWZ, Gollwitz; WMU, Warnemünde; BAR, Barhöft; RUD, Rügen Island (Dranske); USE, Usedom (see further information in **Supplementary Figure 5**). **(B)** Distribution of hybrid classes expressed as Q_{MT}-values (0 = genotypes dominated by *M. edulis* alleles, 1 = genotypes dominated by *M. trossulus* alleles). Experimental data (dark grey, animals sampled in 2016 in AHP, parental animals: AHP-P, larval offspring populations: AHP-F1 and reference data from Stuckas et al. (2017) (light grey, animals sampled in 2013, including average salinity values) are given as violin plots. Median Q_{MT} values are indicated by red diamonds. Compare to **Supplementary Figure 3** for full dataset and STRUCTURE bar plots. Salinity is given for each locality based on hydrodynamic model data obtained from Stuckas et al. (2017).

throughout the manuscript. Mussels (15–50 mm shell length) were collected and transported to GEOMAR in continuously aerated, cooling boxes and kept at 10°C in 10 L plastic aquaria (N = 20 mussels per aquarium) with 20 μm – filtered sea water (FSW) at their native salinities (**Table 1**). Water (ca. 50% of tank volume) was changed daily.

Population Comparison Experiment (Kiel vs. Usedom)

The experiment aimed at testing whether larval stages originating from Western Baltic *M. edulis* collected in KIE and Eastern Baltic *M. trossulus* collected in USE are adapted to local salinity regimes and whether they can rapidly acclimate to salinity changes. The experimental design is depicted in **Supplementary Figures 1, 2**. Two separate larval pools originating from parental mussels from each of the two populations were compared under high and low experimental salinity conditions. Larvae used in the experiment were generated using a group spawning approach, followed by pooling gametes within each population to obtain offspring representing all possible parental combinations. Although this method may potentially mask the intra-population variability compared to analyses of individual families, it guaranties absolute synchronous spawning of mussels

TABLE 1 | Parental mussel sampling sites and abiotic conditions.

Sampling location	Coordinates	Collection date	Field conditions				Spawning date	Lab conditions			
			S	T	pH	A_T		S	T	pH	A_T
Kiel (KIE)	54°19′45.7″, 10°8′55.5″	20/04/2016	15.5	10.2	7.82	2071	16/05/2016	16	10	8.04	1973
Ahrenshoop (AHP)	54°23′07.3″, 12°25′24.1″	03/05/2016	12.4	11.3	8.18	1859	12/05/2016	11	10	7.98	1812
Usedom (USE)	54°3′17.8″, 14°0′43.8″	14/04/2016	7.1	11.9	8.12	1857	16/05/2016	7	10	7.93	1790

Western Baltic M. edulis were taken from Kiel (KIE), Eastern Baltic M. trossulus were taken from Usedom (USE), and specimens from the transition zone were taken from Ahrenshoop (AHP). Given are the field conditions at their native sites at the collection date and conditions in the laboratory to maintain mussels until spawning to rear larvae for the population comparison experiment (KIE, USE) and the desalination experiment (AHP). Detailed field monitoring data can be found in Sanders et al. (2021). Lab conditions were chosen to represent annual means, except for temperature which was kept at 10°C to prevent spawning before the experiments started. S, salinity; T, temperature in °C; A_T, total alkalinity in μmol·kg^{-1} seawater, pH (NBS scale).

and imitates the natural diversity of family representation in the larval pool.

All spawning and fertilisations were conducted within each population (KIE, USE) separately at their native salinity. Spawning was induced by increasing water temperature (10 to 18°C within 30 min) and individuals were immediately isolated in 1 L beakers containing filtered seawater (FSW). Once spawning started, water was gently, periodically stirred and gamete quality was checked (active sperm, circular eggs). After 30 min, gametes were counted under the microscope for each individual and pooled at equal ratios separately for males and females to ensure equal representation from each parent. Pooled gametes of 4 females and 6 males were mixed at a 1:100 egg to sperm ratio. Fertilisation success was determined by monitoring the presence of a polar body and/or cell cleavage within 30 min of gamete mixing. Embryo pools from each population were split into two salinity treatments (16 and 7 psu, 4 treatments in total; with 6 technical replicates). The adjustment to reciprocal salinities (Baltic *M. edulis*: from 16 to 7 psu; Baltic *M. trossulus*: from 7 to 16 psu) was performed at a rate of 3 psu per day conducting 50% water changes daily for the first three days (see further details of water changes below). Larvae were cultured in 10 L glass Duran bottles (Schott, Germany) at a density of 15 larvae·mL^{-1} at 17°C for the first 36 h until shell formation. Afterwards shelled D-veliger larvae were transferred to custom made 14 L plastic (PVC) conical culturing vessels at a density of 10 larvae·mL^{-1} (**Supplementary Figure 2**). Mild aeration (ca. 50 mL air min^{-1}) from below prevented sedimentation and mechanical damage to larvae.

From 3 days post fertilisation (dpf) onward, larval density and growth measurements were performed every third day on larvae contained in triplicate 5 mL water samples which were taken with a Pasteur pipette. Water changes were performed every third day, by gently draining experimental water through cylindrical 65 μm mesh filters keeping larvae submerged at all times. Subsequently, filters containing larvae were inverted and gently rinsed back into experimental vessels with freshly prepared FSW. Pilot experiments revealed that this method did not alter larval densities. Larvae were fed daily (from 3 to 16 dpf) with live cultures of *Isochrysis galbana* (Prymnesiophyceae) at a final concentration of 15000 cells·mL^{-1} with a cell diameter of ca. 4 μm, which is optimal for early-stage mussel larvae. After 16 dpf, larvae were fed larger *Rhodomonas* sp. (Cryptophyceae; cell diameter of ca. 7 μm) for the remainder of the experiment at a final concentration of 3000 cells·mL^{-1}. Larvae were fixed in Para-formaldehyde (4% PFA, pH = 8, corresponding salinity) for quantitative analyses using a stereo microscope and camera at 100x magnification (Leica Microsystems GmbH, Wetzlar, Germany). Larval size was determined for ca. 15 larvae per replicate culture vessel by measuring shell length using ImageJ 1.x (Schneider et al., 2012) at multiple time points up until 23 dpf, despite this experiment running for 33 days in total. This was due to the loss of larger individuals from the water column due to settlement after 23 dpf. Larval mortality was expressed as the decrease in larval density (percentage of the initial number of larvae·mL^{-1}) over time and monitored until the termination of the experiment at 33 dpf. At this point of time, settlement success was quantified after removing settled larvae from culture tanks with a 5 cm × 5 cm × 5 cm synthetic sponge and rinsing onto a 65 μm mesh. Collected juvenile mussels were counted using a stereo microscope and settlement success was expressed as the ratio of settled individuals to initial absolute number of larvae.

Desalination Experiment (Ahrenshoop)

This experiment exposed larvae from transition zone parents collected in AHP to native habitat salinity (11 psu) and two lower salinities (9, 7 psu). These reduced salinities reflect the range that is expected during eastward passive drift and approximates the range of predicted desalination of their native habitat over the next century (see introduction). By using a parental population with intermediate frequencies of both ME- and MT-alleles, we tested for significant enrichment of species-specific alleles in the group of surviving F1 offspring reared at lower salinities.

The experimental design is depicted in **Supplementary Figures 3, 4**. Larval rearing, maintenance, feeding and measurements of fitness proxies were conducted as described in the population comparison experiment with the following modifications: mussels were placed individually in 100 mL plastic beakers containing 50 mL of 11 psu FSW in a 10°C water bath. Spawning was induced by increasing the water temperature to 18°C over 30 min. Gametes of 6 females (F1–F6) and 6 males (M1–M6) were mixed in a pairwise fashion in equal numbers to generate six families. After successful fertilisation, 40,000 embryos from each of the six families were pooled in 3 separate new vessels (1 L) in equal ratios (240,000 embryos per vessel). The volume of each of the 3 vessels was then divided equally

into 10 × 2 L glass Duran bottles (a total of 30 experimental vessels). Each bottle contained an equal ratio of the 6 families (24,000 embryos in total; 4,000 from each family with a larval density of 12 larvae mL^{-1}). Salinity in 10 experimental bottles was kept at 11 psu. In the remaining 20 bottles, salinity was reduced to 9 psu (10 bottles) and 7 psu (10 bottles), each at a rate of 1 psu every 12 h. Within each salinity treatment, half of the bottles (5) were maintained at 12 ± 0.01°C while the other half (5) were maintained at 15 ± 0.04°C, following a two-day temperature adjustment period (1.5°C day^{-1}). In summary, the experiment consisted of 6 salinity-temperature treatment combinations with 5 technical replicates containing 12 embryos mL^{-1} (**Supplementary Figure 3**). Tanks were aerated via 20 mL plastic Pasteur pipettes at a rate of ca. 50 mL air min^{-1} to provide fully air saturated conditions without causing mechanical damage to larvae. Shell growth (relative increase in shell length over time) and mortality (relative decrease in larval density over time) were recorded until 45 dpf despite the experimental period lasting for 67–69 days. This was because of the onset of settlement. Finally, settlement success (relative number of larvae settled) was estimated at the end of the experiment at 67–69 dpf and settled juvenile mussels were collected for genotyping at this time point.

Statistics

Statistical analyses were performed with Rstudio v0.1.0.44 (RStudio Team, 2015) using R v0.3.3.2 (R Core Team, 2014). Growth rates (increases in shell length at widest point over time) were described using the von Bertalanffy growth model (VBGM) modified by Beverton and Holt (1957). In this model, growth proceeds toward a maximum asymptotic size limit, decreasing as the size approaches the maximum limit (L_∞). This was done using the equation $\cdot L(t) = L_\infty(1 - e^{-k(t-t0)})$, where L(t) is the expected or average length at time (age) t, L_∞ is the asymptotic average length, K is the body growth rate coefficient, and t0 is a modelling artefact to represent time/age when average length was zero. For both experiments, parameters for the general VBGM model (L_∞ and K and t0) were estimated using the FSA R package. For comparison between treatments, subset models were created using a common t0 value (one for each experiment) and L_∞ and K separately estimated for each the treatment level of both the simulated desalination (factors: salinity and temperature) and population comparison (factors: salinity, population) experiments. Designating a common t0 is justified, as larvae used in different treatments originated from the same cohort. For each individual experiment, the Akaike Information Criterion (AIC) was used to define the most parsimonious model representing the shell length data. Mortality rates (changes in larval densities over time) were analysed using two-way ANCOVA (covariable: time (dpf), fixed factors: population and salinity or, salinity and temperature), and pairwise comparison among means of the different groups were tested with the Tukey's HSD *post hoc* test. Mortality/density data related to the population comparison experiment were visually inspected for homogeneity of variances (data distribution in the residual vs. fitted plot) and deviations from normality (density plot and QQ plot). Data obtained from the desalination experiment were checked for homogeneity of variances using a Fligner-Killeen test and checks for normality were performed using a Shapiro-Wilk test. Larval settlement was analysed by comparing the settlement probability between treatment using a Generalised Linear Model (GLM) with binomial distribution and logit link function for both the simulated desalination (factors: temperature, salinity) and population comparison (factors: salinity, population) experiments.

Genetic Analyses Associated to the Desalination Experiment

Genotyping

Genetic analyses of specimens aimed to identify ME- and MT-alleles. Genotyping included parental mussels sampled at AHP in spring 2016 (AHP-P, six females and six males, **Table 1** and **Figure 1**) and successfully settled individuals (juvenile mussels) sampled at the end of the desalination experiment from different treatments (AHP-F1, experimental populations). DNA extraction from AHP-P mussels was performed as described in Stuckas et al. (2017). Juvenile mussels from each replicate were rinsed with PBS and stored at −20°C until DNA extraction in 20 µL LoTEPA buffer according to Zhan et al. (2008). Genotyping of AHP-P and AHP-F1 was performed at four species diagnostic single copy nuclear markers that targeted non-coding (Glu5′, EFbis, mac-1) and coding (M7 lysin) genomic loci. These markers were intensively used for *Mytilus* genotyping, species identification and hybrid zone analyses and, therefore, used to characterize the distribution of Western Baltic *M. edulis*, transition zone mussels, and Eastern Baltic *M. trossulus* (e.g., Riginos and Cunningham, 2005; Stuckas et al., 2009, 2017). Protocols were adapted to juvenile mussel genotyping (**Supplementary Tables 1, 2**).

Simulated Reference Populations

The analyses of whether salinity change has an effect on the genetic composition of experimental larval populations would ideally be based on genetic profiling before and after laboratory treatments. However, sampling of individuals shortly after fertilisation (before treatment) was not feasible. This problem was circumvented by predicting the before treatment genetic profile of larval populations using simulations (simulated reference populations). This was done using the genetic data from AHP-P and mimicking the breeding scheme used for the desalination experiment (see above, **Supplementary Figure 3**). In a first step, 4,000 offspring genotypes of each of six parent couples were simulated using Hybrid Lab v0.1.0 (Nielsen et al., 2006) and assuming random association of parental gametes and alleles. Second, simulated offspring genotypes of these six couples were pooled (24,000 simulated genotypes in total), randomly mixed, and split into 10 virtual populations (2,400 simulated individuals each). Finally, random mortality was simulated by randomly drawing 20 virtual individuals ("survivors") from each simulated population. This procedure was repeated three times (accounting for the three salinity treatments, **Supplementary Figure 3**) resulting in three sets of simulated reference populations (AHP-F1, simulation 1–3). They reflect the genetic composition of larval cohorts before salinity selection under genetic drift expectations.

Hybrid Indices Using Bayesian Inference

Bayesian inference (STRUCTURE v0.2.3.3; Falush et al., 2003) was used to estimate the proportion of ME-alleles and MT-alleles in each individual. This method used genetic data from the genotyping step (see above) and assigns individuals to genetic clusters fulfilling Hardy-Weinberg and linkage equilibrium expectations. Assignment probabilities to a given genetic cluster is expressed as *Q*-value ranging from 0 (no assignment) to 1 (full assignment) while values between 0 and 1 indicate admixture between clusters. Thus, *Q*-values can be interpreted as hybrid indices expressing to what proportion the genome of each individual is composed of alleles from one or the other genetic cluster. Bayesian inference was performed for individuals of (i) AHP-P, (ii) AHP-F1 (experimental populations), and (iii) AHP-F1 (simulations 1–3). This was done with reference to genetically pure populations of *M. edulis* (Helgoland, North Sea, coordinates: 54.18, 07.89), *M. trossulus* (Penn Cove, North America, coordinates: 48.21, −122.70), and 19 populations of Baltic mussels analysed in a previous investigation (Stuckas et al., 2017). This included previously analysed samples from KIE, AHP, and USE that were collected in 2013. A complete list of samples included in Bayesian inference is shown in **Supplementary Table 3**.

Analyses were performed using the admixture model under the assumption of correlated allele frequencies (Falush et al., 2003). All other parameters were set to default. The possibility for K 1–10 genetic clusters was tested performing 20 independent runs for each K and a Markov Chain length of 10^6 including a 25% burn-in period. The best K was chosen following Evanno et al. (2005). Further analyses of STRUCTURE *Q*-value distribution were performed with Rstudio v0.1.0.44 (RStudio Team, 2015) using R v0.3.3.2 (R Core Team, 2014). As settled larvae could only be recovered from 9 out of 15 replicate units at 12°C and from 14 out of 15 replicates at 15°C, we decided to pool temperature replicates for the analysis of the influence of salinity treatment on *Q*-value distributions. This was done as a Welch *t*-test suggested that temperature (across salinity treatments) did not significantly impact *Q*-value distribution. The effect of salinity treatment on *Q*-value distribution of the three F1 animal groups at salinities of 7, 9, and 11 psu in comparison to the three simulated F1 populations was then analysed using one-way ANOVA followed by Tukey's HSD tests after visually verifying normal distribution and homoscedasticity (see above). Data were displayed as violin plots (using geom_violin in ggplot2).

Ethical Approval

All applicable international, national and/or institutional guidelines for the care and use of animals were followed.

RESULTS

Population Comparison Experiment

With our improved larval culturing system, we successfully reared Baltic Sea mussel larvae at low salinities (<10 psu) to settlement for the first time in Western Baltic *M. edulis* originated from KIE (16 psu) and Eastern Baltic *M. trossulus* from USE (7 psu). Low salinity had an effect on fitness-related parameters in both Baltic *M. trossulus* and Baltic *M. edulis* larvae. Developmental delay was observed in both populations at 7 psu compared to 16 psu with a ca. 12 h delay in formation of the complete D-veliger shell, accompanied by significantly slower growth rates at 7 psu in both populations (**Figures 2A,C** and **Supplementary Tables 4, 5**). Final shell lengths were approximately 17% lower at 7 psu than at 16 psu at 23 dpf, i.e., the end of the period analysed for shell growth (**Figure 2**). Larval mortality estimated from larval density changes was significantly higher at 7 psu than at 16 psu (ANCOVA, $F_{(1,259)} = 6.6$, $p < 0.001$; **Supplementary Table 6** and **Figure 3A**) only in Baltic *M. edulis* (ANCOVA, Tukey HSD *post hoc* test, $p < 0.001$; **Supplementary Tables 6, 7** and **Figure 3A**). Mortality rates of Baltic *M. trossulus* did not differ significantly between both salinities (ANCOVA $p = 0.41$; **Supplementary Table 7**), indicating that Baltic *M. trossulus* larvae exhibit better performance at low salinity than Baltic *M. edulis* larvae. Settlement began in all treatments at ca. 25 dpf and the experiment was terminated at 33 dpf when no larvae remained in the water column. Low salinity decreased settlement success in both populations (GLM, $p < 0.001$; **Supplementary Table 8** and **Figure 3B**), with settlement probability of Baltic *M. edulis* at 7 psu being particularly poor (0.3% compared with 1.89% at 16 psu). Yet, Baltic *M. edulis* larvae had a higher settlement success at 16 psu compared to Baltic *M. trossulus* (Tukey HSD, $p < 0.001$; **Supplementary Table 9** and **Figure 3B**), and Baltic *M. trossulus* exhibited higher settlement success than Baltic *M. edulis* at 7 psu (Tukey HSD, $p < 0.001$; **Supplementary Table 9** and **Figure 3B**).

Desalination Experiment: Larval Performance

Exposing larvae from transition zone mussels (AHP, 11 psu) to desalination and warming revealed strong impacts on larval fitness components. Exposure to desalination reduced shell length growth rates of transition zone larvae (**Figures 2B,D** and **Supplementary Tables 4, 5**) with slower rates of growth at both 9 and 7 psu. Mortality rate expressed as larval density change was also higher at low salinities (ANCOVA, $F_{(2,558)} = 8.9$, $p < 0.001$; **Supplementary Table 6** and **Figure 3C**) with mortality being highest in the 7 psu treatment (ANCOVA *post hoc* test, $p < 0.001$; **Supplementary Table 7**) and not significantly different between 9 and 11 psu (ANCOVA *post hoc* test, $p = 1.0$, **Supplementary Table 7**). Settlement probability was negatively impacted by both desalination and temperature (GLM, $p < 0.001$; **Supplementary Tables 8, 9** and **Figure 3D**) with larval settlement being significantly different between all three salinities only at 15°C (Tukey HSD, $p < 0.001$; **Supplementary Table 9**). At 12°C, settlement success was significantly higher only at 11 psu compared to both 9 and 7 psu treatments (Tukey HSD, $p < 0.001$; **Supplementary Table 9**). At all salinities, settlement success was higher at the higher temperature (15°C) (**Figure 3D**). A significant interaction between salinity and temperature was also observed for mortality and shell length growth, i.e., shell growth and mortality were more strongly reduced by low salinity at 12°C, compared to 15°C (Tukey HSD, **Supplementary Table 7**

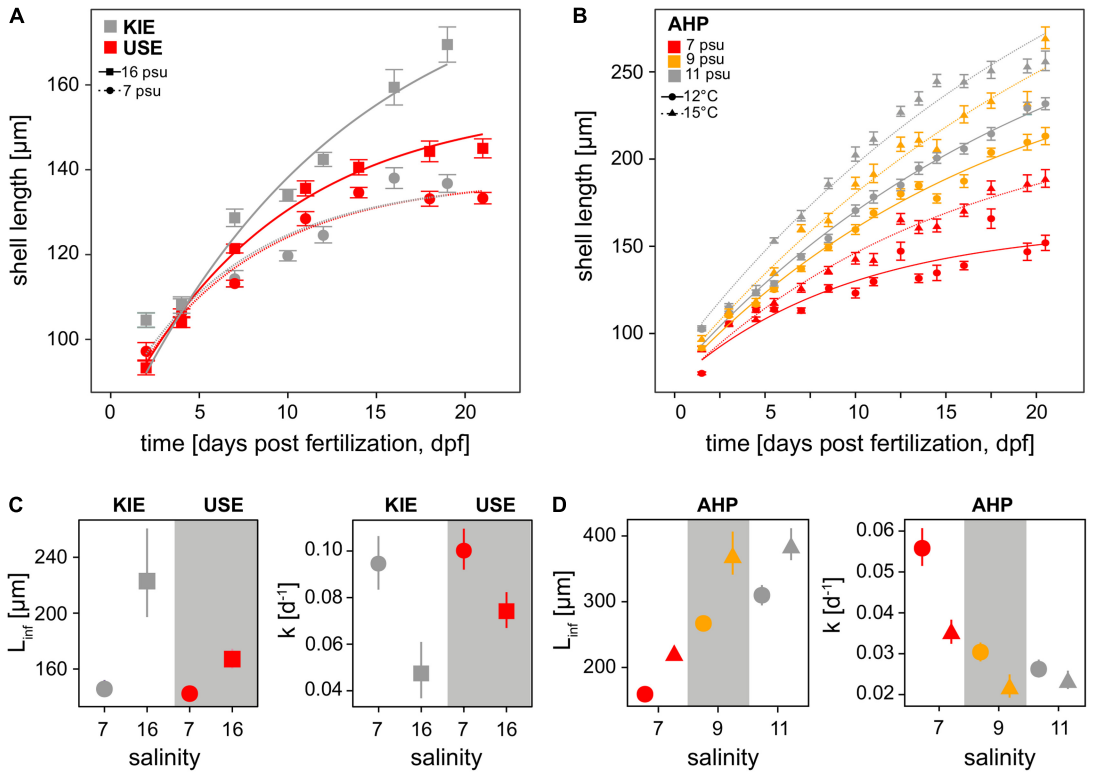

FIGURE 2 | Growth rates. Shell length (µm) increase over time of all treatments throughout the course of populations comparison **(A)** and desalination experiments **(B)** fitted to von Bertalanffy growth models (VBGM). Mean asymptotic average length (L_∞) and mean Brody growth coefficient (K) estimated using the VBGM for the different treatments of the population comparison and simulated desalination experiments are represented in panels **(C,D)**, respectively. Symbols represent means and 95% confidence interval.

and **Figures 2B,D,3C**). This demonstrates the interactive role of both temperature and salinity in influencing fitness related parameters in Baltic *Mytilus* larvae.

Desalination Experiment: Genetic Analyses

A total of 296 settled juveniles (<1 mm shell length; AHP-F1, experimental populations) from the six treatments of the desalination experiment were genotyped along with parental animals (AHP-P, 6 males, 6 females). Subsequently, genotypes of parental animals were used to predict the genetic profile of their offspring (simulated reference populations; AHP-F1, simulation 1–3) reflecting genetic drift expectations. These genetic data were used for Bayesian inference along with reference animals from the North Sea (genetically pure *M. edulis*), and the western Pacific Ocean (genetically pure *M. trossulus*), and additional Baltic reference populations from a previous survey in 2013 (**Figure 1A**, **Supplementary Figure 5** and **Supplementary Table 3**; Stuckas et al., 2017). These individuals were assigned with different probabilities to two genetic clusters, an *M. edulis*-cluster (expressed by the Q_{ME}-value) and an *M. trossulus*-cluster (expressed by an Q_{MT}-value). As both Q-values add to 1, we only use the Q_{MT}-values to describe assignment results and to express the hybrid index, i.e., the relative proportion of MT-alleles. An excerpt of the complete results (**Supplementary Figure 4A**; STRUCTURE bar plots) is presented **Figures 1B**, **4**. In **Figure 1B**, we show the distribution of Q_{MT}-values of AHP-P and experimental AHP-F1, with all animals pooled for each salinity group. Animals were pooled for this visualisation, as we observed no significant differences in Q_{MT}-values between temperatures (Welch's *t*-test, $t = -0.76$, df = 20.9, $p > 0.45$). We also added Q_{MT}-distributions for animals collected in 2013 for our previous study (Stuckas et al., 2017). From this depiction it becomes apparent, that AHP-P includes roughly equal proportions of animals with very low (*M. edulis* – dominated genotypes) and high (*M. trossulus* – dominated genotypes) Q_{MT}-values, resulting in a median Q_{MT} - value around 0.6. Interestingly, this median value and distribution is more similar to that of populations further west of AHP sampled in 2013 (e.g., Warnemünde – WMU -, Gollwitz - GWZ -, **Figure 1**). However, experimental offspring (AHP-F1) from all three salinity treatments closely resemble Q_{MT} distribution of the 2013 AHP animals and populations further east (e.g., Barhöft – BAR -, Dranske at Rügen Isand - RUD -, USE), with a Q_{MT}-median in all three salinity groups >0.75, indicating a shift to more *M. trossulus* - dominated genotypes. This is also illustrated by the shift in violin shape in **Figure 1B**. Simulated offspring populations (AHP-F1, simulation 1–3) are characterised by a similar distribution of Q_{MT}-values as their parents (AHP-P) with a low median

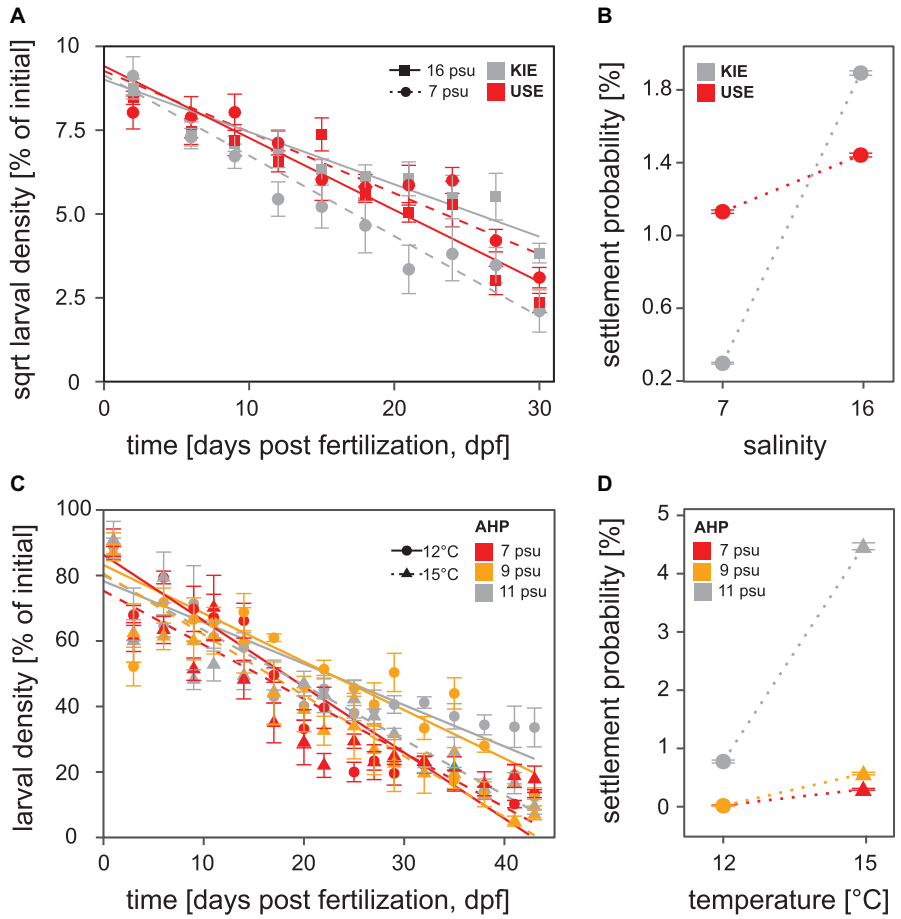

FIGURE 3 | Larval density in cultures and probability of settlement success for all treatments throughout the course of the population comparison **(A,B)** and simulated desalination experiments **(C,D)**. Plots **(A)** and **(C)** represent changes in larval density over time which indicates mortality and **(B)** and **(D)** the probability of settlement success. Symbols represent means and SE.

Q_{MT}-value of <0.25 (**Figure 4A**). Experimental AHP-F1 larvae raised to settlement at all three salinities were characterised by significantly higher Q_{MT}-values than the AHP-F1-simulation groups, with substantial enrichment of animals with Q_{MT}-values > 0.75 (ANOVA; $F_{(5,47)} = 12.44$, $p < 0.0001$, Tukey HSD $p < 0.01$; **Supplementary Tables 10, 11**, **Figure 4B**). There were no significant differences in Q_{MT} - values between the different F1 salinity groups (Tukey HSD $p > 0.05$).

DISCUSSION

Salinity Dependent Local Adaptation and Differential Survival in Baltic *Mytilus* Larvae

To our best knowledge, this is the first study in which Baltic *Mytilus* larvae were spawned and reared at extremely low salinities (<10 psu) under laboratory conditions. We explored whether larvae of Baltic *Mytilus* species from three Baltic model populations are adapted to local salinity regimes, and to test whether individuals with a high proportion of *M. trossulus* alleles have a higher tolerance of low salinity.

Our findings on pre-settlement stages of mussels representing different Baltic *Mytilus* species point towards local adaptation to comparatively high (>10 psu; Baltic *M. edulis,* KIE) and low salinities (<10 psu; Baltic *M. trossulus,* USE). This is primarily shown in the population comparison experiment where larvae originating from both localities show a better performance (mortality, growth, settlement success) under ambient compared to non-ambient conditions. Additional support comes from the desalination experiment, where transition zone mussels from AHP generally perform better at their ambient salinity (11 psu) compared to lowered salinities (9, 7 psu). Transition zone mussels show differential performance under low salinity conditions (7–11 psu) associated with a generally higher settlement success of larvae with a high proportion of *M. trossulus* specific alleles, as indicated by high Q_{MT}-values. In other words, hybrids with *M. trossulus* – dominated genotypes perform better under experimental low salinities. Our findings are in line with the existing knowledge on adult stages which suggests that salinity driven selection during the entire mussel life cycle can maintain

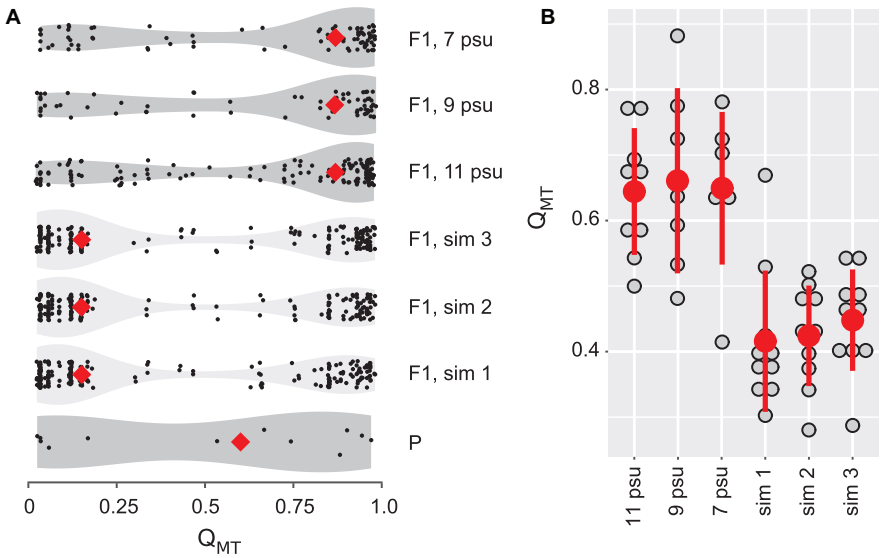

FIGURE 4 | Distribution of hybrid classes expressed as Q_{MT}-values among parental animals (AHP-P), pooled simulated reference populations (AHP-F1 sim 1–3), and pooled treatment data at different salinities (AHP-F1_7psu, AHP-F1_9psu, AHP-F1_11psu). **(A)** Violin plots represent the distribution of individual Q_{MT}-values and medians (red diamonds). **(B)** Comparison between experimental (AHP-F1) and simulated offspring (AHP-F1-sim) populations depicting culture (replicate) bottle mean Q_{MT}-values (grey dots), with temperatures pooled for each salinity step, overall treatment mean values (red dot) and SD.

genotypic and phenotypic differences between Baltic *M. edulis* and Baltic *M. trossulus,* despite of pervasive gene flow.

In a strict sense, the local adaptation observed in our experiments must be interpreted as a combination of genetically fixed phenotypic differences and acclimation and (transgenerational) epigenetic mechanisms (Palumbi et al., 2014; Donelson et al., 2018). Accordingly, future experimental approaches following multigenerational laboratory breeding of populations under common garden conditions (e.g., Sanford and Kelly, 2011) are required to help quantify the contribution of these factors to the observed performance trends, and to investigate the underlying mechanisms (e.g., Dupont et al., 2013; Shama et al., 2016).

Salinity driven selection in the laboratory shifted the genetic composition of experimental AHP-F1 animals toward the median hybrid index observed at low salinity (<11 psu) in eastern Baltic habitats, i.e., from median Q_{MT} – values of approx. 0.6 in AHP-P to values > 0.75 for experimental AHP-F1 resembling distributions observed for AHP, BAR, RUD, and USE (**Figure 1B**). The Q_{MT} – distribution of parental animals (AHP-P) sampled for our experiment in 2016 did not resemble that of the AHP reference population sampled in 2013 (**Figure 1B**; Stuckas et al., 2017). In fact, if we had started our experiment with a similar Q_{MT} distribution as in the reference sample from 2013, we most likely would not have detected a selection signal toward *M. trossulus* - dominated genotypes. The sampling bias in the AHP-P population toward a high number of *M. edulis* - dominated genotypes could be either due to random effects associated with the low sample size (12 parental animals) (**Figure 1B**). On the other hand, a shift in the position of the hybrid zone further eastward between 2013 and 2016 seems equally likely: the winter of 2014 experienced the third strongest wind-driven influx event of high saline North Sea water into the Baltic Sea in the last century, elevating salinity in the Darss Sill area (Mohrholz et al., 2015). This could have led to an increase in the fraction of *M. edulis* – dominated genotypes in the transition zone near AHP. AHP salinity monitoring data records indicate that salinity fluctuates strongly at this site and that salinity was relatively high in 2016 (Sanders et al., 2021).

Despite of the genetic shift toward high Q_{MT} - values observed in our experiment, differences between experimental AHP-F1 and naturally occurring populations still exist (**Figure 1B**), with a substantial number of *M. edulis*-like genotypes still present. This was observed in all experimental cohorts and the outcome was similar irrespective of the different salinity and temperature conditions. These observations allow forwarding two testable hypotheses: We suggests that below a salinity threshold of ca. 11 psu *M. trossulus*-like hybrids have a generally better performance than other hybrid classes. Presuming a threshold salinity as a trigger for differential performances explains why different experimental salinities basically resulted in similar genetic composition of settled larval cohorts. This explanation also fits to previous observations on naturally occurring populations east of Darss Sill (**Figure 1B**). Furthermore, given the effect of salinity driven selection on the pre-settlement phase, genetic differences between experimental AHP-F1 and natural occurring populations are best explained by the action of additional, post-settlement selection, as observed in a US East coast *Mytilus* population (Koehn et al., 1980).

Positive effects of increased temperature on growth and settlement success were observed in the simulated warming and desalination experiment - but also negative effects such

as increased mortality. This may suggest that higher metabolic rates induced by increased temperatures may not fully buffer the negative effects of low salinity (Sprung, 1984; Sanders et al., 2018). Previous studies support the positive effect of higher temperatures on larval growth and developmental pace in *Mytilus* (Sprung, 1984; Beaumont et al., 2004; Sánchez-Lazo and Martínez-Pita, 2012). The warming treatment used in this experiment was within the lower part of the range of current interannual temperature variability in the natural habitat during the reproductive season (Pansch et al., 2018). Whether future warming will influence larval mussel survival and developmental energetics largely depends on whether spawning windows will shift toward earlier time points in the year. It is not unlikely that such phenological shifts will enable mussels to reproduce in thermal environments that are comparable to the ones they experience now. Strong phenological shifts with warming have been observed for Baltic plankton communities (Sommer and Lewandowska, 2011). More research on potential phenological shifts of mussel spawning windows under simulated warming is necessary to understand the combined impacts of desalination and warming on future larval mussel ecology in the Baltic Sea.

Overall, in combination with previous knowledge from post-settlement stages, this study has significance for predicting consequences for Baltic *Mytilus* abundance and distribution in the context of climate change. Given our experiments, predicted desalination and a westward shift in low salinities across the Baltic Sea have the potential to shift the *M. edulis*-*M. trossulus* distribution range and genetic transition zone westward (Meier et al., 2006; Gräwe et al., 2013). Even though elevated temperatures may benefit larval development by increasing developmental pace and reducing the length of the planktonic larvae phase, negative synergistic effects of high temperatures and extremely low salinities may be observed when temperatures exceed the species' tolerance threshold.

What Mechanisms Underlie Salinity Driven Selection in Baltic *Mytilus* Species?

Our results suggest that *M. trossulus* – dominated hybrids are the outperforming genotypes under predicted future salinity conditions in the Baltic Sea. However, the putative mechanisms underlying these physiological differences between genotypes in the Baltic Sea remains elusive. Marine euryhaline molluscs are osmoconformers, meaning their extra- and intracellular environments remain iso-osmotic with surrounding seawater. Intracellular osmolarity is maintained primarily through adjustments in intracellular concentrations of compatible organic osmolytes (amino acids and amino acid derivatives), but also changes in inorganic ion concentrations (Berger and Kharazova, 1997; Yancey, 2005).

Under low salinity conditions, the depletion of intracellular ions, organic osmolytes, or both, to critical concentrations may impede cellular function (Podbielski et al., 2016). Thus, genotypic differences in salinity tolerance may depend on species-specific abilities to maintain physiological function at low intracellular osmotic pressures. Physiological costs associated with overcoming extremely low intracellular osmotic pressures such as increased active transport of inorganic ions (Maar et al., 2015) or reduced energetic efficiency of protein turnover (Tedengren and Kautsky, 1986) may underly the poorer performance of Baltic *M. edulis* genotypes at salinities <11 compared to Baltic *M. trossulus*. Biomineralisation processes may also play a key role in low salinity adaptation. In fact, reciprocal transplantation experiments demonstrated the reduced ability of adult Baltic *M. edulis* to calcify under low salinity conditions (Riisgård et al., 2014). Accordingly, salinities below 11 psu were shown to invoke higher costs of calcification in juvenile Baltic *Mytilus* with these costs potentially being related to limited availability of $[Ca^{2+}]$ (<4 mmol·kg^{-1}) below 11 psu (Sanders et al., 2018; Thomsen et al., 2018; 2021). Furthermore, a higher tolerance to lowered calcium concentrations has been observed in Baltic *M. trossulus* larvae when compared with Baltic *M. edulis* (Thomsen et al., 2018). This supports our observations of local adaptation to low salinity/$[Ca^{2+}]$ in this study and suggests that calcification substrate transport pathways may be under selection during adaptation to low salinity habitats. Interestingly, high genetic divergence in genomic regions associated with ion and osmoregulation have been identified in Baltic cod (6 psu) compared to North Sea cod (35 psu) suggesting these processes are targets of selection in low salinity environments, at least in vertebrates (Berg et al., 2015). Overall, it is likely that alleles at genetic loci associated with key physiological processes (e.g., osmoregulation, or biomineralisation) are targets of salinity driven selection and cause an indirect genome wide allele shift of species diagnostic markers. In fact, adaptive phenotypes related to physiological processes such as biomineralisation are polygenic traits (Hüning et al., 2016; Arivalagan et al., 2017) and complex selection regimes are expected to affect the entire genome.

In summary, the above cited example studies list putative mechanisms underlying salinity driven selection and show that there already is some evidence for species-specific responses to Baltic Sea salinity variation. Identifying genomic loci that are associated with salinity adaptation will enable us to better characterize the mechanistic basis for salinity adaptation in Baltic *Mytilus* species.

CONCLUSION AND FUTURE PERSPECTIVES

This study provides the first experimental evidence suggesting that (i) pre-settlement stages of Baltic *Mytilus* populations exhibit local adaptation to their native salinities (Baltic *M. edulis*, KIE; Baltic *M. trossulus*, USE) and that (ii) larvae with a high proportion of *M. trossulus* alleles (transition zone mussels, AHP) show a higher tolerance to low salinity conditions (11 psu and lower). Future work utilising complementary approaches and (multi-generational) laboratory experiments are key to elucidate ongoing selection and adaptation in this system. One task is to unravel the physiological mechanisms which modulate mussel performance under different environmental conditions. This is important to further test our prediction of a westward shift of the *M. edulis* - *M. trossulus* distribution range. Given the morphological and physiological differences between both species, these range shifts may have impacts on

ecosystem functioning (nutrient and organic matter turnover) and biodiversity. A further task is to identify genomic loci causing salinity adaptation. In fact, while our genetic assay had a taxonomic focus (i.e., distinguishing between Baltic *M. edulis*, Baltic *M. trossulus*, and their hybrids), the molecular targets of salinity driven selection (genomic loci and their alleles) have not yet been identified. Overall, this study highlights the value of using the Baltic Sea environmental gradient as a model system to investigate the role of environmental factors in shaping physiological and genetic differences between populations and species (Berg et al., 2015; Guo et al., 2015; Reusch et al., 2018).

DATA AVAILABILITY STATEMENT

The datasets presented in this study can be found in online repositories. The names of the repository/repositories and accession number(s) can be found below as: https://doi.org/10.1594/PANGAEA.892875.

AUTHOR CONTRIBUTIONS

HS and FM conceived and designed the study. LK, JN-S, TS, DZ, and CH performed laboratory and field work. LK, JN-S, TS, DZ, FB, HS, and FM analyzed the data. HS and FM wrote the manuscript with support by LK, JN-S, and TS. All authors contributed to revisions.

FUNDING

Funding was provided by the Marie Curie ITN network "CACHE" (EU 7'th Framework Programme grant 605051) and the Paul Ungerer Stiftung. Technical funding and support was provided by the Kiel Marine Organism Culture Centre (KIMOCC) of the Kiel Cluster of Excellence "Future Ocean." FB received financial support from the German Academic Exchange Service (DAAD) through the Doctoral Programmes 2015/16 (57129429).

ACKNOWLEDGMENTS

The authors thank Ulrike Panknin, Julia Haegyeong Lee, Jörn Thomsen, and Anja Rauh for technical support. Earlier versions of this manuscript are part of two Ph.D. theses by TS (Sanders, 2018) and LK (Knöbel, 2019). The authors also thank three reviewers for valuable suggestions to improve the manuscript.

SUPPLEMENTARY MATERIAL

The Supplementary Material for this article can be found online at: https://www.frontiersin.org/articles/10.3389/fmars.2021.692078/full#supplementary-material

REFERENCES

Arivalagan, J., Yarra, T., Marie, B., Sleight, V. A., Duvernois-Berthet, E., Clark, M. S., et al. (2017). Insights from the shell proteome: biomineralization to adaptation. *Mol. Biol. Evol.* 34, 66–77. doi: 10.1093/molbev/msw219

Beaumont, A. R., Turner, G., Wood, A. R., and Skibinski, D. O. F. (2004). Hybridisations between *Mytilus edulis* and *Mytilus galloprovincialis* and performance of pure species and hybrid veliger larvae at different temperatures. *J. Exp. Mar. Biol. Ecol.* 302, 177–188. doi: 10.1016/j.jembe.2003.10.009

Behre, K.-E. (2007). A new Holocene sea-level curve for the southern North Sea. *Boreas* 36, 82–102. doi: 10.1111/j.1502-3885.2007.tb01183.x

Belkin, I. M. (2009). Rapid warming of large marine ecosystems. *Prog. in Oceanogr.* 81, 207–213. doi: 10.1016/j.pocean.2009.04.011

Berg, P. R., Jentoft, S., Star, B., Ring, K. H., Knutsen, H., Lien, S., et al. (2015). Adaptation to low salinity promotes genomic divergence in Atlantic cod (*Gadus morhua* L.). *Genome Biol. Evol.* 7, 1644–1663. doi: 10.1093/gbe/evv093

Berger, V. J., and Kharazova, A. (1997). "Mechanisms of salinity adaptations in marine molluscs," in *Developments in Hydrobiology: Interactions and Adaptation Strategies of Marine Organisms*, eds A. D. Naumov, H. Hummel, A. A. Sukhotin, and J. S. Ryland (Dordrecht: Springer), 115–126. doi: 10.1007/978-94-017-1907-0_12

Berglund, B. E., Sandgren, P., Barnekow, L., Hannon, G., Jiang, H., Skog, G., et al. (2005). Early Holocene history of the Baltic Sea, as reflected in coastal sediments in Blekinge, southeastern Sweden. *Q. Int.* 130, 111–139. doi: 10.1016/j.quaint.2004.04.036

Beverton, R. J. H., and Holt, S. J. (1957). *On the Dynamics of Exploited Fish Populations. Fisheries Investigations (Series 2)*. London: United Kingdom Ministry of Agriculture and Fisheries, 19.

Donelson, J. M., Salinas, S., Minday, P., and Shama, L. N. (2018). Transgenerational plasticity and climate change experiments: where do we go from here. *Glob. Change Biol.* 24, 13–34. doi: 10.1111/gcb.13903

Dupont, S., Dorey, N., Stumpp, M., Melzner, F., and Thorndyke, M. (2013). Long-term and trans-life-cycle effects of exposure to ocean acidification in the green sea urchin *Strongylocentrotus droebachiensis*. *Mar. Biol.* 160, 1835–1843. doi: 10.1007/s00227-012-1921-x

Evanno, G., Regnaut, S., and Goudet, J. (2005). Detecting the number of clusters of individuals using the software STRUCTURE: a simulation study. *Mol. Ecol.* 14, 2611–2620. doi: 10.1111/j.1365-294X.2005.02553.x

Falush, D., Stephens, M., and Pritchard, J. K. (2003). Inference of population structure using multilocus genotype data: linked loci and correlated allele frequencies. *Genetics* 164, 1567–1587. doi: 10.1093/genetics/164.4.1567

Fraïsse, C., Belkhir, K., Welch, J. J., and Bierne, N. (2016). Local interspecies introgression is the main cause of extreme levels of intraspecific differentiation in mussels. *Mol. Ecol.* 25, 269–286. doi: 10.1111/mec.13299

Gräwe, U., Friedland, R., and Burchard, H. (2013). The future of the western Baltic Sea: two possible scenarios. *Ocean Dyn.* 63, 901–921. doi: 10.1007/s10236-013-0634-0

Guo, B., DeFaveri, J., Sotelo, G., Nair, A., and Merilä, J. (2015). Population genomic evidence for adaptive differentiation in Baltic Sea three-spined sticklebacks. *BMC Biol.* 13:19. doi: 10.1186/s12915-015-0130-8

Heckwolf, M. J., Peterson, A., Jänes, H., Horne, P., Künne, J., Liversage, K., et al. (2021). From ecosystems to socio-economic benefits: a systematic review of coastal ecosystem services in the Baltic Sea. *Sci. Total Environ.* 755:142565. doi: 10.1016/j.scitotenv.2020.142565

Hüning, A. K., Lange, S. M., Ramesh, K., Jacob, D. E., Jackson, D. J., Panknin, U., et al. (2016). A shell regeneration assay to identify biomineralization candidate genes in mytilid mussels. *Mar. Genomics* 27, 57–67. doi: 10.1016/j.margen.2016.03.011

Johannesson, K., Smolarz, K., Grahn, M., and André, C. (2011). The future of Baltic Sea populations: local extinction or evolutionary rescue? *AMBIO* 40, 179–190. doi: 10.1007/s13280-010-0129-X

Kautsky, N., Johannesson, K., and Tedengren, M. (1990). Genotypic and phenotypic differences between Baltic and North Sea populations of *Mytilus edulis* evaluated through reciprocal transplantations. *I. Growth and morphology. Mar. Ecol. Prog. Ser.* 59, 203–210. doi: 10.3354/meps059203

Kijewski, T., Zbawicka, M., Strand, J., Kautsky, H., Kotta, J., Ratsep, M., et al. (2019). Random forest assessment of correlation between environmental factors and genetic differentiation of populations: case of marine mussels Mytilus. *Oceanologia* 61, 131–142. doi: 10.1016/j.oceano.2018.08.002

Knöbel, L. (2019). *Analyses of the Baltic Mytilus Hybrid Zone: Implications for Exploring Evolutionary Processes and Global Change Effects*. Dissertation. Dresden: University of Technology Dresden.

Koehn, K. R. (1991). The genetics and taxonomy of species in the genus *Mytilus*. *Aquaculture* 94, 125–145. doi: 10.1016/0044-8486(91)90114-m

Koehn, R. K., Newell, R. I. E., and Immermann, F. (1980). Maintenance of an aminopeptidase allele frequency cline by natural selection. *Proc. Natl. Acad. Sci. U.S.A.* 77, 5385–5389. doi: 10.1073/pnas.77.9.5385

Kossak, U. (2006). *How Climate Change Translates into Ecological Change: Impacts of Warming and Desalination on Prey Properties and Predator-Prey Interactions in the Baltic Sea*. Dissertation, Kiel: Christian-Albrechts-University Kiel.

Kostecki, R., and Janczak-Kostecka, B. (2011). Holocene evolution of the Pomeranian Bay environment, southern Baltic Sea. *Oceanologia* 53, 471–487. doi: 10.5697/oc.53-1-ti.471

Larsson, J., Lind, E. E., Corell, H., Grahn, M., Smolarz, K., and Lönn, M. (2016). Regional genetic differentiation in the blue mussel from the Baltic Sea area. *Estuar. Coast. Shelf. Sci* 195, 98–109. doi: 10.1016/j.ecss.2016.06.016

Maar, M., Saurel, C., Landes, A., Dolmer, P., and Petersen, J. K. (2015). Growth potential of blue mussels (*M. edulis*) exposed to different salinities evaluated by a dynamic energy budget model. *Mar. Syst.* 148, 48–55. doi: 10.1016/j.jmarsys.2015.02.003

Meier, H., Kjellström, E., and Graham, L. (2006). Estimating uncertainties of projected Baltic Sea salinity in the late 21st century. *Geophys. Res. Lett.* 33:L15705. doi: 10.1029/2006GL026488

Mohrholz, V., Naumann, M., Nausch, G., Krüger, S., and Gräwe, U. (2015). Fsh oxygen for the Baltic Sea-an exceptional saline inflow after a decade of stagnation. *J. Mar. Syst.* 148, 152–166. doi: 10.1016/j.jmarsys.2015.03.005

Nielsen, E. E., Bach, L. A., and Kotlicki, P. (2006). HYBRIDLAB (version 1.0): a program for generating simulated hybrids from population samples. *Mol. Ecol. Resour.* 6, 971–973. doi: 10.1111/j.1471-8286.2006.01433.x

Norling, P., and Kautsky, N. (2008). Patches of the mussel *Mytilus* sp. are islands of high biodiversity in subtidal sediment habitats in the Baltic Sea. *Aquat. Biol.* 4, 75–87. doi: 10.3354/ab00096

Palumbi, S. R., Barshis, D. J., Traylor-Knowles, N., and Bay, R. A. (2014). Mechanisms of reef coral resistance to future climate change. *Science* 344, 895–898. doi: 10.1126/science.1251336

Pansch, C., Scotti, M., Barboza, F. R., Al-Janabi, B., Brakel, J., Briski, E., et al. (2018). Heat waves and their significance for a temperate benthic community: a near-natural experimental approach. *Glob. Change Biol.* 24, 4357–4367. doi: 10.1111/gcb.14282

Podbielski, I., Bock, C., Lenz, M., and Melzner, F. (2016). Using the critical salinity (S_{crit}) concept to predict invasion potential of the anemone *Diadumene lineata* in the Baltic Sea. *Mar. Biol.* 163:227. doi: 10.1007/s00227-016-2989-5

R Core Team (2014). *R: A Language and Environment for Statistical Computing*. Vienna: R Foundation for Statistical Computing.

Ramesh, K., Hu, M. Y., Thomsen, J., Bleich, M., and Melzner, F. (2017). Mussel larvae modify calcifying fluid carbonate chemistry to promote calcification. *Nat. Commun.* 8:1709. doi: 10.1038/s41467-017-01806-8

Reusch, T. B. H., Dierking, J., Andersson, H. C., Bonsdorff, E., Carstensen, J., Casini, M., et al. (2018). The Baltic Sea as a time machine for the future coastal ocean. *Sci. Adv.* 4:eaar8195.

Riginos, C., and Cunningham, C. W. (2005). Invited review: local adaptation and species segregation in two mussel (*Mytilus edulis* × *Mytilus trossulus*) hybrid zones. *Mol. Ecol.* 14, 381–400. doi: 10.1111/j.1365-294X.2004.02379.x

Riisgård, H. U., Bøttiger, L., and Pleissner, D. (2012). Effect of salinity on growth of mussels, *Mytilus edulis*, with special reference to Great Belt (Denmark). *OJMS* 2, 167–176. doi: 10.4236/ojms.2012.24020

Riisgård, H. U., Larsen, P. S., Turja, R., and Lundgreen, K. (2014). Dwarfism of blue mussels in the low saline Baltic Sea - growth to the lower salinity limit. *Mar. Ecol. Prog. Ser.* 517, 181–192. doi: 10.3354/meps11011

Riisgård, H. U., Lüskow, F., Pleissner, D., Lundgreen, K., and López, M. ÁP. (2013). Effect of salinity on filtration rates of mussels *Mytilus edulis* with special emphasis on dwarfed mussels from the low-saline Central Baltic Sea. *Helgol. Mar. Res.* 67, 591–598. doi: 10.1007/s10152-013-0347-2

RStudio Team (2015). *RStudio: Integrated Development for R*. Avaliable online at: http://www.rstudio.com/ (accessed July 1, 2018).

Sánchez-Lazo, C., and Martínez-Pita, I. (2012). Induction of settlement in larvae of the mussel *Mytilus galloprovincialis* using neuroactive compounds. *Aquaculture* 344, 210–215. doi: 10.1016/j.aquaculture.2012.03.021

Sanders, T. (2018). *Bioenergetics of Calcification in Mytilid Bivalves Along the Baltic Sea Salinity Gradient*. Dissertation, Kiel: Christian-Alberts-University of Kiel.

Sanders, T., Schmittmann, L., Nascimento-Schulze, J. C., and Melzner, F. (2018). High calcification costs limit mussel growth at low salinity. *Front. Mar. Sci.* 5:352. doi: 10.3389/fmars.2018.00352

Sanders, T., Thomsen, J., Müller, J. D., Rehder, G., and Melzner, F. (2021). Decoupling salinity and carbonate chemistry: low calcium ion concentration rather than salinity limits calcification in Baltic Sea mussels. *Biogeosciences* 18, 2573–2590. doi: 10.5194/bg-18-2573-2021

Sanford, E., and Kelly, M. W. (2011). Local adaptation in marine invertebrates. *Annu. Rev. Mar. Sci.* 3, 509–539. doi: 10.1146/annurev-marine-120709-142756

Schneider, C. A., Rasband, W. S., and Eliceiri, K. W. (2012). NIH Image to ImageJ: 25 years of image analysis. *Nat. Methods* 9, 671–675. doi: 10.1038/nmeth.2089

Shama, L. N. S., Mark, F. C., Strobel, A., Lokmer, A., John, U., and Wegner, K. M. (2016). Transgenerational effects persist down the maternal line in marine sticklebacks: gene expression matches physiology in warming ocean. *Evol. Appl.* 9, 1096–1111. doi: 10.1111/eva.12370

Simon, A., Fraïsse, C., El Ayari, T., Liautard-Haag, C., Strelkov, P., Welch, J. J., et al. (2019). How do speies barriers decay? Concordance and local introgression in mosaic hybrid zones of mussels. *J. Evol. Biol.* 34, 208–223. doi: 10.1111/jeb.13709

Sommer, U., and Lewandowska, A. (2011). Climate change and the phytoplankton spring bloom: warming and overwintering zooplankton have similar effects on phytoplankton. *Glob. Change Biol.* 17, 154–162. doi: 10.1111/j.1365-2486.2010.02182.x

Sprung, M. (1984). Physiological energetics of mussel larvae (*Mytilus edulis*). I. Shell growth and biomass. *Mar. Ecol. Prog. Ser.* 18, 283–293. doi: 10.3354/meps017283

Stuckas, H., Knöbel, L., Schade, H., Breusing, C., Hinrichsen, H. H., Bartel, M., et al. (2017). Combining hydrodynamic modelling with genetics: can passive larval drift shape the genetic structure of Baltic *Mytilus* populations? *Mol. Ecol.* 26, 2765–2782. doi: 10.1111/mec.14075

Stuckas, H., Stoof, K., Quesada, H., and Tiedemann, R. (2009). Evolutionary implications of discordant clines across the Baltic *Mytilus* hybrid zone (*Mytilus edulis* and *Mytilus trossulus*). *Heredity* 103, 146–156. doi: 10.1038/hdy.2009.37

Tedengren, M., André, C., Johannesson, K., and Kautsky, N. (1990). Genotypic and phenotypic differences between Baltic and North Sea populations of *Mytilus edulis* evaluated through reciprocal transplantations. III. *Physiol. Mar. Ecol. Prog. Ser.* 59, 221–227. doi: 10.3354/meps059221

Tedengren, M., and Kautsky, N. (1986). Comparative study of the physiology and its probable effect on size in blue mussels (*Mytilus edulis* L.) from the North Sea and the northern Baltic proper. *Ophelia* 25, 147–155. doi: 10.1080/00785326.1986.10429746

Telesca, L., Michalek, K., Sanders, T., Peck, L. S., Thyrring, J., and Harper, E. M. (2018). Blue mussel shell shape plasticity and natural environments: a quantitative approach. *Sci. Rep.* 8:2865. doi: 10.1038/s41598-018-20122-9

Thomsen, J., Haynert, K., Wegner, K. M., and Melzner, F. (2015). Impact of seawater carbonate chemistry on the calcification of marine bivalves. *Biogeosciences* 12, 1543–1571. doi: 10.5194/bgd-12-1543-2015

Thomsen, J., Ramesh, K., Sanders, T., Bleich, M., and Melzner, F. (2018). Calcification in a marginal sea–influence of seawater [Ca 2+] and carbonate chemistry on bivalve shell formation. *Biogeosciences* 15, 1469–1482. doi: 10.5194/bg-15-1469-2018

Thomsen, J., Stapp, L. S., Haynert, K., Schade, H., Danelli, M., Lannig, G., et al. (2017). Naturally acidified habitat selects for ocean acidification-tolerant mussels. *Sci. Adv.* 3:e1602411. doi: 10.1126/sciadv.1602411

Thorson, G. (1950). Reproductive and larval ecology of marine bottom invertebrates. *Biol. Rev.* 25, 1–45. doi: 10.1111/j.1469-185X.1950.tb00585.x

Wenne, R., Zbawicka, M., Bach, L., Strelkov, P., Gantsevich, M., Kukliński, P., et al. (2020). Trans-atlantic distribution and introgression as inferred from single

nucleotide polymorphism: mussels *Mytilus* and environmental factors. *Genes* 11:530. doi: 10.3390/genes11050530

Wennerström, L., Laikre, L., Ryman, N., Utter, F. M., Ghani, N. I. A., Andre, C., et al. (2013). Genetic biodiversity in the Baltic Sea: species-specific patterns challenge management. *Biodivers. Conserv.* 22, 3045–3065. doi: 10.1007/s10531-013-0570-9

Witkowski, A., Broszinski, A., Bennike, O., Janczak-Kostecka, B., Bo Jensen, J., Lemke, W., et al. (2005). Darss Sill as a biological border in the fossil record of the Baltic Sea: evidence from diatoms. *Q. Int.* 130, 97–109. doi: 10.1016/j.quaint.2004.04.035

Yancey, P. H. (2005). Organic osmolytes as compatible, metabolic and counteracting cytoprotectants in high osmolarity and other stresses. *J. Exp. Biol.* 208, 2819–2830. doi: 10.1242/jeb.01730

Zhan, A., Bao, Z., Hu, X., Lu, W., Wang, S., Peng, W., et al. (2008). Accurate methods of DNA extraction and PCR-based genotyping for single scallop embryos/larvae long preserved in ethanol. *Mol. Ecol. Resour.* 8, 790–795. doi: 10.1111/j.1755-0998.2007.02066.x

Conflict of Interest: The authors declare that the research was conducted in the absence of any commercial or financial relationships that could be construed as a potential conflict of interest.

Publisher's Note: All claims expressed in this article are solely those of the authors and do not necessarily represent those of their affiliated organizations, or those of the publisher, the editors and the reviewers. Any product that may be evaluated in this article, or claim that may be made by its manufacturer, is not guaranteed or endorsed by the publisher.

frontiers in Marine Science

ORIGINAL RESEARCH
published: 16 September 2021
doi: 10.3389/fmars.2021.708109

Elevated Temperatures Shorten the Spawning Period of Silver Carp (*Hypophthalmichthys molitrix*) in a Large Subtropical River in China

*Yuguo Xia[1,2], Xinhui Li[1,2], Jiping Yang[1,2], Shuli Zhu[1,2], Zhi Wu[1,2], Jie Li[1,3,4] and Yuefei Li[1,2]**

[1] Pearl River Fisheries Research Institute, Chinese Academy of Fishery Sciences, Guangzhou, China, [2] Experimental Station for Scientific Observation on Fishery Resources and Environment in the Middle and Lower Reaches of Pearl River, Ministry of Agriculture and Rural Affairs of the People's Republic of China, Zhaoqing, China, [3] Guangzhou Scientific Observing and Experimental Station of National Fisheries Resources and Environment, Guangzhou, China, [4] Key Laboratory of Aquatic Animal Immune Technology of Guangdong Province, Guangzhou, China

Global warming is influencing the life history traits of fishes globally. However, the impacts of elevated temperature on fish reproduction are diverse in different regions. Previous studies have revealed that the spawning timing of silver carp (*Hypophthalmichthys molitrix*) in the Pearl River, in China, has changed over the past decade. However, few studies have explored the potential reasons, which are critical for determining fishing-moratorium periods and developing sustainable fisheries. The current study used discharge suitability index (DSI), temperature suitability index (TSI), correlation and time-series analyses to determine (i) the optimal discharge and temperature for silver carp spawning; (ii) relationships among the thermal regime, hydrological parameters, and spawning timing based on an 11-year time-series dataset. Our results indicated that the most suitable discharge and temperature for silver carp spawning were 13,000–15,000 m^3/s and 25–26°C, respectively. The start date of spawning fluctuated with a slight tendency to delay, while the spawning peak and end date obviously occurred earlier during the study period. Correlation analyses suggested that the increasing average temperature between January and March likely caused the initial spawning delay. Moreover, elevated temperatures in August and September probably promoted the anticipated end of silver carp spawning. However, increases in discharge did not significantly correlate with the start of spawning but were significantly and positively correlated with the spawning peak. These results indicated that elevated temperatures shorten the spawning period of silver carp in the Pearl River. Moreover, the initial spawning of silver carp seems to be triggered by temperature rather than changes in discharge; flow pulses can probably create more suitable spawning niches for *H. molitrix*. This study enhances our understanding of the effect of warming on fish reproduction in subtropical regions.

Keywords: fish reproduction, thermal regime, fish larvae, Pearl River (China), hydrological regime

OPEN ACCESS

Edited by:
Jennifer Marie Donelson, James Cook University, Australia

Reviewed by:
Heather Diana Veilleux, University of Alberta, Canada
Vânia Baptista, University of Algarve, Portugal

***Correspondence:**
Yuefei Li
liyuefei815@163.com

Specialty section:
This article was submitted to Global Change and the Future Ocean, a section of the journal Frontiers in Marine Science

Received: *11 May 2021*
Accepted: *27 August 2021*
Published: *16 September 2021*

Citation:
Xia Y, Li X, Yang J, Zhu S, Wu Z, Li J and Li Y (2021) Elevated Temperatures Shorten the Spawning Period of Silver Carp (Hypophthalmichthys molitrix) in a Large Subtropical River in China. Front. Mar. Sci. 8:708109. doi: 10.3389/fmars.2021.708109

INTRODUCTION

Global warming is a critical concern in spawning ecology of fishes, especially in freshwater (Alix et al., 2020; Zhang et al., 2021). By 2017, the Earth's surface temperature had increased by approximately 1.0°C relative to pre-industrial (1850–1900) levels, with average temperatures rising by 0.2°C per decade over the past three decades (IPBES, 2019). It is predicted that temperatures will rise even faster over the next 25 years than it did over the previous two decades (Smith et al., 2018). The impact of warming is likely to be stronger in freshwater than in terrestrial and marine systems, because discrete ecosystem boundaries in rivers limit fish migrations to follow optimal temperature conditions (Perry et al., 2005; Chen et al., 2011). More specifically, fish reproduction, controlled by the brain-pituitary-gonadal axis, may be more sensitive to warming than fish biodiversity, species interactions, and distributions (Walther et al., 2002; Miranda et al., 2013).

Determining the impact of global warming on fish spawning (e.g., spawning time) is challenging, since spawning characteristics are also regulated by other factors such as hydrographic parameters, spawning population stocks (Gillet and Dubois, 2007; Paumier et al., 2020). Generally, warm temperature and increases in river discharge can trigger spawning initiation (Yu et al., 2018), while spawning stock abundance mainly determines the interannual variability in larvae production (Glover et al., 2020). However, in some cases (e.g., a cold winter), temperature and river discharge affect larval abundance of some species (e.g., *Clupea harengus membras*) more significantly than spawning stock size (Ojaveer et al., 2011). Temperature and natural river floods can also affect oviposition amount and hatchability (O'Brien et al., 2012; Garcia et al., 2013; Wakefield et al., 2015). Therefore, understanding the influences of changes in temperature and hydrological conditions on fish reproduction is essential to preserving fish resources and developing sustainable fisheries practices.

For freshwater fish species that form spawning aggregations, understanding how global warming and other factors influence their spawning time is of great interest, since such information can be vital for determining management policies such as closed fishing seasons (Tuz-Sulub and Brulé, 2015; van Overzee and Rijnsdorp, 2015). Mature fishes that form transient aggregates to spawn at specific times and places are productivity hubs and vulnerable to overfishing (Erisman et al., 2017). Generally, the timing of spawning is influenced by the age of the spawning fish, water temperature, and hydrological conditions (Wang et al., 2014; Li et al., 2020). The age of mature fish slightly influences the spawning time, in that large individuals tend to produce eggs later than small ones (Gillet and Dubois, 2007; Gordoa and Carreras, 2014). Low-temperature can delay fish spawning by inhibiting vitellogenesis or reducing the mature fish size (Kjesbu, 1994; Carscadden et al., 1997; Wang et al., 2014), although low temperature may contribute to earlier spawning migration in temperate fish species (Sims et al., 2004). Extreme high temperatures seem to be more readily impair or even quit some fish (e.g., *Odontesthes bonariensis*) spawning by inhibiting gene expression throughout the brain-pituitary-gonad axis (Miranda et al., 2013). Hydrological conditions such as flood peaks during spawning seasons can promote fish spawning by favoring gonad development (Bailly et al., 2008), stimulating spawning migration (Thorstad et al., 2008), generating eddies that promote fertilization (Yi et al., 1988), and assisting the eggs and larvae in drifting downstream (Zhang et al., 2018).

Silver carp (*Hypophthalmichthys molitrix*) is a common freshwater fish that forms large spawning aggregations and is widely distributed in Asia, especially in China's rivers. As one of the four major Chinese carp, it is a commercially important fish species in the Pearl River in southern China, accounting for about 13.6% of the total weight of the catches (Zhang et al., 2020). Mature silver carp form transient aggregations in spawning grounds in flood seasons and produce semi-buoyant eggs that drift with the flow for hundreds of kilometers in Asia (Yi and Liang, 1964; Zhang et al., 2000). Spawning characteristics of silver carp populations around the world demonstrated high local adaptation. Their spawning timings vary slightly in different regions: mid-May to the beginning of July in the Caspian Basin (Abdusamadov, 1987); from mid-May to mid-June in Arkansas (Freeze and Crawford, 1983); from June to early August in the Amur River (Gorbach and Krykhtin, 1989); from May to August in the Yangtze River (Zhang et al., 2000); and early April to early October in the Pearl River in China (Shuai et al., 2018). In China, some researchers consider the occurrences of silver carp eggs and larvae to be stimulated by high water discharge (Shuai et al., 2018; Yu et al., 2018). However, this fish can reproduce in the Wabash River without changes in discharges (Coulter et al., 2016). Notably, the spawning of silver carp in China is impacted by changes in thermal and hydrological regimes caused by the construction of dams (Wang et al., 2014; Li et al., 2016). In general, thermally stratified reservoirs releasing hypolimnetic water could reduce the temperature below large dams (Preece and Jones, 2002; Wang et al., 2014), while small surface-release dams could increase downstream temperatures by releasing warm epilimnetic water (Lessard and Hayes, 2003).

Currently, we lack a clear understanding of the impacts of global warming and other factors upon the spawning characteristics of silver carp in one of its largest habitats, the Pearl River in China (Shuai et al., 2018). First, there is a debate on the change of spawning timing of silver carp (delayed vs. advanced) in the Pearl River. Based on fish larvae data from 2006 to 2008, Tan et al. (2010) reported silver carp spawning delays in the Pearl River. In contrast, Shuai et al. (2018) reported that the spawning peak of this fish occurred at an earlier date from 2006 to 2013 in the same region. The spawning processes of fish have natural fluctuations, and long-term data are required to reveal the dynamics. Second, few studies have examined the possible reasons that drive the changes in spawning characteristics of silver carp in this river (Shuai et al., 2016).

The present study uses a long time-series dataset (2006–2013 and 2017–2019) to reveal the changing spawning characteristics of silver carp in the Pear River and the underlying drivers. We focus on answering the following three questions: (1) what are the temperature and hydrological requirements for spawning of silver carp in the river; (2) how has their spawning timing varied (delayed or advanced) over the past decade; (3) which factors

(e.g., global warming, river discharge) were mainly correlated with such variation?

MATERIALS AND METHODS

Study Area

The Pearl River is the largest river in southern China, with a total length of 2,214 km and a mean annual discharge of 3.3×10^{11} m^3. The sampling location, i.e., Zhaoqing section, is in the lower reach of the Pearl River, about 180 km upstream from the estuary (**Figure 1**). The annual average air temperature, annual rainfall, and annual discharge of this section are about 22.0°C, 1,644.5 mm, and 6,810 m^3/s, respectively (Lu, 1990). There are 76 fish species recorded in the lower reach of the Pearl River, excluding the estuary area (Zhang et al., 2020). Over the past century, 18 spawning grounds of silver carp have been reported in the middle and upper reaches of the Pearl River (Committee of Pearl River Fishery Resources Investigation, 1985), and approximately 26 dams had been built near the spawning grounds by 2007. Our long-term monitoring results (unpublished data), along with a recent study (Gao et al., 2020), indicate that only the spawning grounds in the lower reaches of the tributary Liujiang River and the Laibin–Pingnan section of the mainstream still exist after 2007.

For our samples, the spawning grounds are located in the Guiping–Pingnan section, estimated by the development periods of captured larvae and water velocity (Pearl River Water Resources Commission, unpublished data). Eleven dams have been constructed in the mainstream of the Pearl River. All these dams were completed before 2005 and are located at the upper reaches, except for two downstream dams: Changzhou Dam and Datengxia Dam (Chen et al., 2018). The Changzhou Dam is a low head dam (height < 30 m, highest water level = 16 m) built in 2007 with only a daily discharge regulation. The Datengxia Dam began to impound in 2020, with a maximum water level of 61 m expected in 2023. Taken together, all large dams were located in the headwater and upper reaches of the Pearl River before 2019, far away from the current silver carp spawning grounds. Therefore, the impoundment would not influence the water temperature in the current spawning grounds during the study period (2006–2019).

Data Collection

We sampled three times a day (06:00–08:00, 13:00–15:00, and 19:00–21:00) every other day throughout the year. Larval fish were collected using a pyramid trap net (mesh size = 0.5 mm, length = 6 m). The net had a rectangular mouth (width × height: 1.5 m × 1.0 m), and the end opened to a larval collection cage (0.8 m × 0.4 m × 0.4 m) (Shuai et al., 2018). A cup-type flowmeter (LS45-2) was fixed at the net mouth center to measure the water volume flowing through the net. The net was submerged in the water with mouth open and facing the river flow. The net position would change slightly with the rise and fall of the water level, but it was kept 10–15 m away from the bank, where the flow velocity was approximately 0.3 m/s. Sampling was initially conducted at S1 (23°2′40″ N, 112°27′5″ E) from 2006 to 2013. But the location was changed to S2 (23°9′54″ N, 112°16′58″ E, about 28 km upstream of S1) from 2017 to 2019, because cargo ships anchored near S1 (**Figure 1**). No samples were collected from 2014 to 2016.

Larvae samples were kept in a 5% formalin solution immediately after collection. The larvae of silver carp were identified (based on morphological characteristics) and counted by an experienced researcher in the laboratory (Yi et al., 1988). The abundance of larvae was calculated as the number of larvae per 24 h. The collected silver carp larvae were mainly at two developmental stages: the emergence of air bladder and one-chamber air bladder. Spawning dates of larvae were estimated using back-calculation methods from the captured dates (Yi et al., 1988). The spawning date of larvae was defined as the day of spawning occurrence.

We collected daily water temperatures and discharges at the Dahuangjiangkou (DHJK) gauge station to represent the environmental conditions of the spawning ground from 2006 to 2019 (**Figure 1**). Daily water temperature was collected by an automatic water temperature monitor, which recorded the temperature at least four times a day. Daily river discharge (Dis) was obtained from the Pearl River Water Resources Commission.

Data Analysis

We back-calculated the earliest birth date of the captured larvae, date of the spawning peak, and the end date of spawning by subtracting their development periods from the capturing dates of the larvae. These variables were used to describe the spawning period across our study. A previous study reported that the minimum discharge required to observe the occurrence of silver carp larvae was 10,000 m^3/s in the Pearl River (Shuai et al., 2018). Thus, we used the first date of the discharge increased to 10,000 and 13,000 m^3/s to index the possible flow-related reasons for changes in spawning timing. The minimum water temperature for silver carp spawning was 18°C (Yi et al., 1988). We counted the number of days with a temperature not lower than 18°C (hereafter, N_18) prior to the spawning season (from January to March). The threshold temperature for initial gonad development of adult silver carp was 15°C. We thus regarded the date when the water temperature reached 15°C during spring as the start date of stage IV (Wang et al., 2014). The end date of stage V denoted the date when larval abundance reached 5% of the total observed annual abundance. The cumulative temperature from stages IV to V was calculated by the sum of daily water temperature from stages IV to V in the year. The above variables and the mean monthly water temperature of the spawning ground were used to describe the changes in water temperature of spawning and cumulative temperature. Using the day of year calendar, the date is a sequential day number starting with day 1 on January 1.

The discharge suitability index (DSI) and the temperature suitability index (TSI) were applied to define the discharge and temperature suitability for silver carp' spawning (Yu et al., 2018). The DSI was calculated as $DSI_i = \frac{D_i}{D_{max}}$, where DSI_i is the discharge suitability index of the discharge bin i, D_i is the value of larvae abundance weighted by the number of spawning

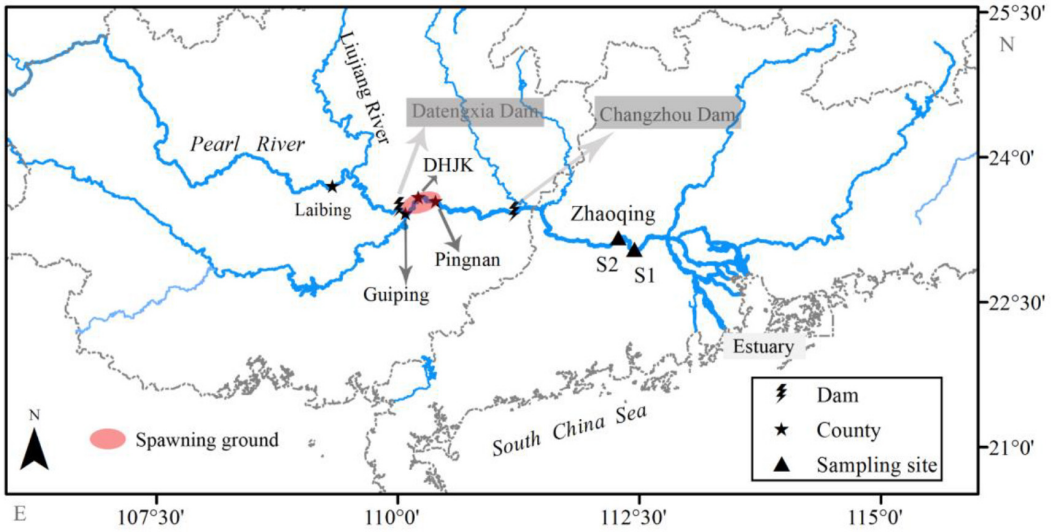

FIGURE 1 | Locations of dams near the spawning ground, sampling sites, and spawning ground of the collected larvae in the Pearl River (China). Sampling of larvae was conducted during 2006–2013 and 2017–2019. The daily temperatures and discharges of the spawning ground were collected from the DHJK gauge station from 2006 to 2019.

occurrences of the discharge bin i, D_{max} is the maximum value of larvae abundance weighted by the number of spawning occurrences across all discharge bins. The TSI was calculated as $TSI_j = \frac{T_j}{T_{max}}$, where TSI_j is the temperature suitability index of the temperature bin j, T_j is the value of larvae abundance weighted by the number of spawning occurrences of the temperature bin j, T_{max} is the maximum value of larvae abundance weighted by the number of spawning occurrences across all temperature bins.

All datasets of discharge, temperature, and abundance of larvae have normal distributions. The analysis were performed using Shapiro–Wilk tests in the "stats" package in R 3.6.1 (R Core Team, 2019). Pearson correlation analysis was used to determine the statistical significance of correlations between the spawning timing, discharge increase, and monthly temperature variables. The correlation analysis was performed using SPSS 13.0. Data for daily temperature (from January to March, August to September) was converted to weekly time-series for trend analysis using the "stats" package in R. The structural change in a time-series was detected by the chow test/F statistic using the "strucchange" package in R to plot the corresponding p-values (Zeileis et al., 2002). Differences were considered statistically significant at $p < 0.05$.

RESULTS

Discharge and Temperature Suitability for Silver Carp Spawning

The silver carp started to spawn when the river discharge reached 2,310 m^3/s (**Figure 2A**). The occurrence of spawning gradually increased with increased discharge before 7,000–9,000 m^3/s, and then decreased (**Figure 2A**). However, the highest discharge suitability index (DSI) was observed at a discharge of 13,000–15,000 m^3/s (**Figure 2A**). Moreover, there was a relatively lower peak of DSI at a discharge of 19,000–21,000 m^3/s (**Figure 2A**).

The lowest temperature observed for the occurrence of silver carp spawning was 20.7°C (**Figure 2B**). The occurrence of spawning gradually increased with increasing temperature before 27–28°C, slowly declined after that, and then plummeted (**Figure 2B**). The temperature suitability index (TSI) stayed at a low level when the temperature was lower than 22°C, then sharply increased to the peak at 25–26°C. Then TSI rapidly declined and remained at a relatively stable level at temperatures of 26–28°C after that; finally, it sharply decreased at temperatures above 28°C (**Figure 2B**).

Increased Temperature Shortening Spawning Period of Silver Carp

Variation of Spawning Timing and Temperature Variables

Silver carp' spawning began with the onset of floods at the end of April, peaking by June/July (**Figure 3**). The onset of spawning (spawning start; **Figure 3**) fluctuated from 2006 to 2017, with a delay of 55 days in 2017 relative to 2009 (the trough). By 2019, the onset of spawning was 47 days earlier than in 2017. In contrast, there were relatively stronger temporal trends in peak and end of spawning dates in that they were both earlier (**Figure 3**). For instance, peak spawning occurred earlier stepwise from 2006 to 2012, with the earliest peak occurring in 2012. Specifically, peak spawning was 80-days earlier in 2012 than 2006; in 2019, peak spawning was delayed by 18 compared to 2012. A similar temporal trend was also observed for the end of the spawning season, which tended to occur earlier stepwise from 2006 to 2011, with the earliest end date in 2011. This 2011 end date was 61-days earlier than 2006 and

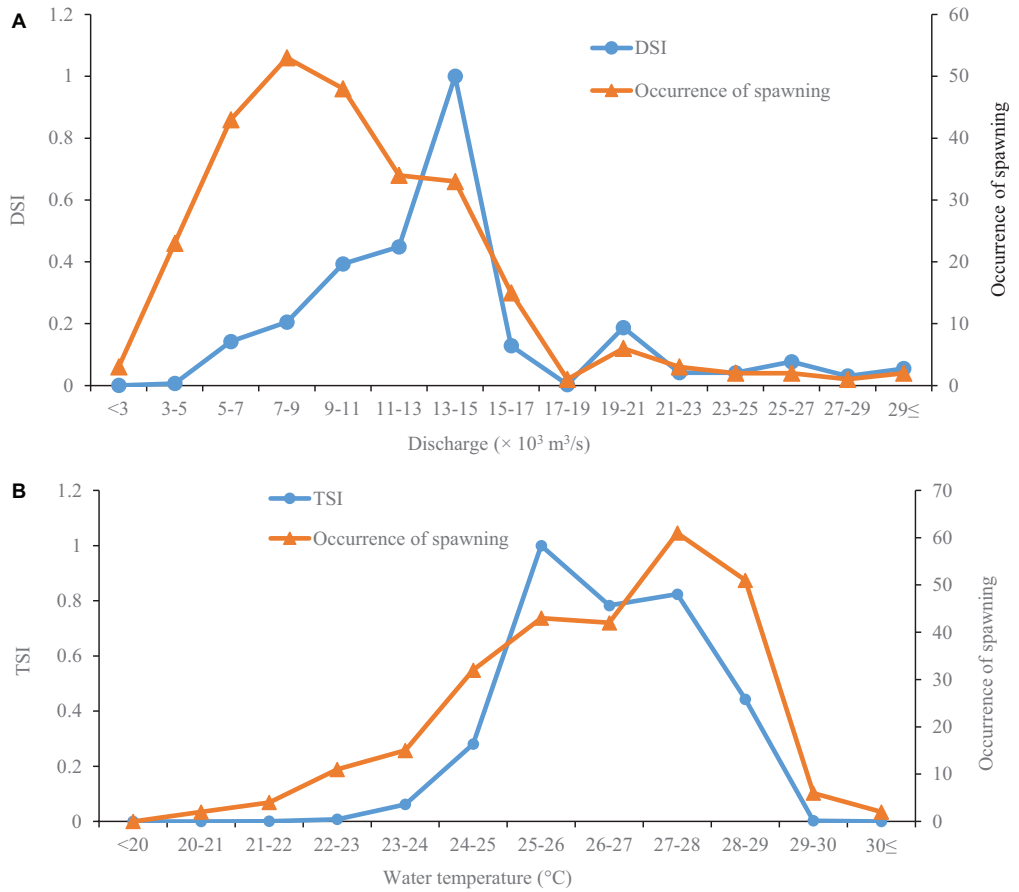

FIGURE 2 | Discharge **(A)** and temperature **(B)** suitability curves for the spawning of silver carps. The data are collected in the Pearl River (China) during 2006–2013 and 2017–2019. The occurrence of spawning represents the number of spawning days at a given discharge or temperature. The discharge suitability index (DSI) and temperature suitability index (TSI) range from 0–1.

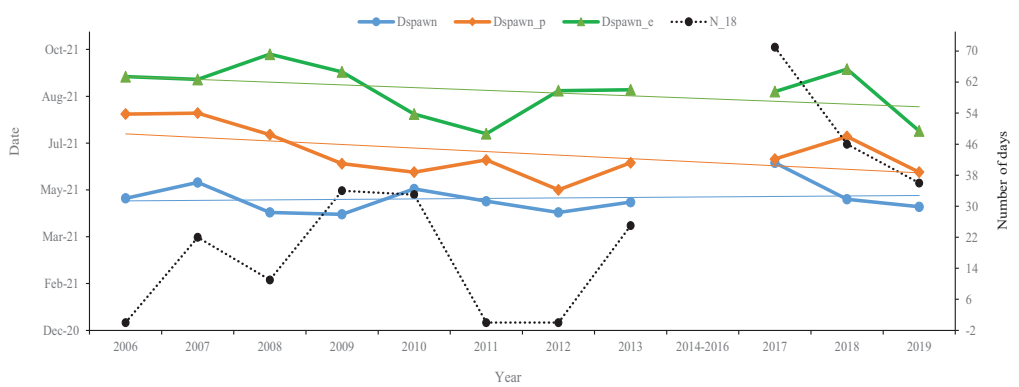

FIGURE 3 | Variations in the timing of silver carps' spawning characteristics and the number of days with a temperature greater than or equal to 18°C from January to March (N_18). The data are collected in the Pearl River (China) during 2006–2013 and 2017–2019. The earliest date of spawning (blue; Dspawn), the peak spawning date (orange; Dspawn_p), the end of spawning (green; Dspawn_e). Faint lines of similar colors denote the trend lines.

only 3 days earlier than in 2019. Consequentially, the interval between the onset and the end of spawning decreased from 130 days in 2006 to 81 days in 2019. In contrast, the number of days temperatures were greater than or equal to 18°C from January to March (N_18) generally increased. The N_18 first gradually increased from 0 in 2006 to 71 in 2017 (the peak), although there were two zeros in 2011 and 2012 and the peak value halved by 2019.

Correlation Between Flow and Temperature Variables and Spawning Timing

Pearson correlation coefficients between timings of silver carp spawning, thermal regime, and discharge variables are shown in **Table 1**. The number of days with a temperature greater than or equal to 18°C from January to March (N_18) and the mean temperature in January (T1) were significantly and positively correlated with the initial spawning date (Dspawn) ($p < 0.05$), but significantly and negatively correlated with the days of spawning occurrence (Occu) ($p < 0.05$). Spawning peak (Dspawn_p) was significantly and positively correlated with (i) the end of spawning (Dspawn_e), (ii) the onset of the discharge increased to 10,000 m^3/s (Ddis_1), and (iii) the cumulative temperature from stages IV to V (DdegdayIV-V) ($p < 0.05$). The Dspawn_e was positively correlated with the mean temperature in April (T4, $p < 0.05$), but negatively correlated with mean temperatures in August (T8) and September (T9) (both $p < 0.05$). The onset of the discharge increased to 13,000 m^3/s (Ddis_13) was positively correlated with Ddis_1, DdegdayIV-V, and mean temperatures in January (T1), April (T4), May (T5), and December (T12) (all $p < 0.05$). The Ddis_1 was positively correlated with Dspawn_p, Ddis_13, DdegdayIV-V, and mean temperature in May (T5) (all $p < 0.05$). The Occu was negatively correlated with Dspawn, N_18, and mean temperatures in January (T1) and February (T2) (all $p < 0.05$).

Interannual Fluctuations of Temperature

The temperature before the spawning season (from January to March) fluctuated and can be generally viewed from two periods: before and after 2012 (**Figure 4**). Prior to 2012, the temperature fluctuated without significant trends. After 2012, there was a warming trend by 2019 (all p values < 0.05, except those in 2019). During 2006–2019, the average minimum and maximum temperatures from January to March increased by approximately 0.95 and 1.76°C, respectively.

The temperature from August to September (during the late period of the spawning season) can be viewed from three periods: 2006–2011, 2011–2015, and 2015–2019 (**Figure 5**). The temperature during the late period of the spawning season showed a generally significant increase trend between 2006 and 2011, when the minimum and maximum temperatures increased by approximately 1.61 and 2.39°C, respectively (**Figure 5**). In contrast, the temperature fluctuated without a significant trend from 2011 to 2015, when the minimum and maximum temperatures decreased by approximately 1.91 and 2.44°C, respectively. From 2015 to 2019, however, there existed another warming trend, and the minimum and maximum temperatures increased by approximately 1.73 and 2.49°C, respectively.

DISCUSSION

Discharge and Temperature Suitability for Silver Carp Spawning

Spawning environment suitability of fish in rivers is determined by hydrodynamic, geomorphological, and biological interactions that generate complex and localized linkages (Alvarez-Mieles et al., 2019). The same species distributed over a variety of environmental conditions could probably demonstrate different ecological and hydrological requirements for spawning. The silver carp is distributed all over the world and has high local adaptation in reproduction characteristics. The initiation of silver carp spawning without changes in discharge was noted in the Wabash River, but the occurrences of eggs and larvae of this fish seemed to be triggered by flood pulses in the Yangtze River and Pearl River (Coulter et al., 2016; Shuai et al., 2018; Yu et al., 2018). The most suitable discharge and temperature of silver carp' spawning habitats in the middle and lower reaches of the Yangtze River were 15,000–21,300 m^3/s and 21–24°C, respectively (Yi et al., 1988; Yu et al., 2018). In contrast, the current study demonstrated that spawning in the Pearl River was initiated when discharge was much lower, approximately 2,310 m^3/s, indicating that the fish can start to spawn without significant increases in discharge. The most suitable discharge for silver carp' spawning in this study (13,000–15,000 m^3/s) was also lower than that in the Yangtze River. The distance between the middle and lower reaches of the Yangtze River and those of the Pearl River is approximately 800 km, and there is a relatively high genetic distance between these two silver carp populations (Ji et al., 2009). Therefore, different hydrological requirements for silver carp spawning in those two large rivers in China could probably attribute to local adaptation.

Our study provides some new insights about the mechanisms of how river discharge affects the spawning characteristics of silver carp. First, our findings suggest that the spawning peak of silver carp, rather than the initial spawning, is probably triggered by flow increase in the Pearl River. This was evidenced by the fact that the start date of spawning was not significantly correlated with high discharge (Ddis_1 and Ddis_13), while the spawning peak was significantly and positively correlated with high discharge (Ddis_1). Second, we showed that spawning occurrence of silver carp occurred at a relatively low discharge level, but with relatively lower daily larvae abundance. This finding is likely because only part of the mainstream is suitable for fish spawning when the discharge is at a low level. Then as the discharge gradually increases, some hydro-fluctuation zones become suitable for spawning, which explains why the highest average daily larvae appeared at high discharge. Flow pulses can probably create more suitable spawning niches for fish.

We indicate that the minimum and most suitable temperatures for silver carp' spawning in the Pearl River were higher than those in the Yangtze River (Yi et al., 1988). Temperature can both affect the development of gonad and trigger spawning of fish (Morgan et al., 2013). In the present study, silver carp spawned at 20.7–30.1°C in the Pearl River, while they spawned at 18–28°C in the Yangtze River (Chen et al., 2009). Fish are very capable of finding habitat patches with suitable spawning temperature (Górski et al., 2010), which might explain why silver carp can spawn at a wide range of temperatures. The lowest temperature for silver carp spawning is 18°C indicating that water temperature is not a limiting factor in the Pearl River where average annual water temperature in spawning grounds is approximately 23°C (Yi et al., 1988). Although there is a wide range of temperatures for silver carp

TABLE 1 | Pearson correlation coefficients among thermal, discharge, and spawning timing variables in the Pearl River (China) during 2006–2013 and 2017–2019.

	Dspawn	Dspawn_p	Dspawn_e	Ddis_13	Ddis_1	N_18	DdegdaylV-V	Occu	T1	T2	T3	T4	T5	T6	T7	T8	T9	T10	T11	T12
Dspawn	1																			
Dspawn_p	0.22	1																		
Dspawn_e	−0.11	**0.53***	1																	
Ddis_13	0.46	0.37	0.23	1																
Ddis_1	0.07	**0.60***	0.34	**0.75****	1															
N_18	**0.59***	−0.13	0.02	0.52	0.12	1														
DdegdaylV-V	0.38	**0.79****	0.45	**0.75****	**0.75****	0.26	1													
Occu	−**0.56***	−0.09	0.40	−0.49	−0.21	−**0.56***	−0.41	1												
T1	**0.61***	0.24	0.25	**0.76****	0.34	**0.85****	**0.62***	−**0.54***	1											
T2	0.50	−0.03	−0.21	0.31	0.06	**0.77****	0.19	−**0.61***	**0.55***	1										
T3	0.33	0.16	0.22	0.25	0.32	**0.72****	0.29	−0.26	0.50	**0.65***	1									
T4	0.02	0.27	**0.55***	**0.56***	0.44	0.46	0.50	−0.16	**0.59***	0.30	0.49	1								
T5	0.20	0.28	0.35	**0.70***	**0.57***	0.26	0.44	−0.26	0.40	0.10	0.21	**0.76****	1							
T6	0.17	0.26	0.09	0.31	0.27	0.38	0.17	−0.48	0.33	0.40	0.42	**0.57***	**0.65***	1						
T7	−0.06	0.19	−0.13	−0.29	0.11	−0.23	−0.14	−0.10	−0.44	0.02	0.27	−0.02	0.23	**0.54***	1					
T8	−0.17	−0.26	−**0.65***	−0.42	−0.29	−0.09	−0.47	−0.34	−0.32	0.07	−0.10	−0.47	−0.36	0.31	0.42	1				
T9	−0.34	−0.54	−**0.63***	−0.31	−0.32	0.07	−0.44	−0.20	−0.15	0.25	−0.13	−0.41	−**0.60***	−0.17	−0.22	**0.67***	1.			
T10	0.01	0.20	0.18	0.32	0.06	0.16	0.34	−0.13	0.34	0.45	−0.04	0.50	0.23	0.11	−0.38	−0.40	0.00	1		
T11	−0.06	0.26	−0.37	0.19	0.14	−0.20	0.20	−0.52	0.00	0.09	−0.44	−0.10	0.07	0.32	0.04	0.50	0.37	0.34	1	
T12	0.29	0.12	−0.32	**0.58***	0.45	0.33	0.22	−0.37	0.40	0.32	0.04	−0.08	0.10	0.18	−0.25	0.23	0.33	0.08	0.46	1

Dspawn, Dspawn_p, and Dspawn_e denote the earliest date of spawning, date of the spawning peak, and the end date of the spawning, respectively; Ddis_1 and Ddis_13 denote the first date of the discharge increased to 10,000 m^3/s and 13,000 m^3/s, respectively; N_18 denotes the number of days with a temperature greater than or equal to 18°C from January to March; DdegdaylV-V denotes the cumulative temperature from stages IV to V; Occu denotes the days of spawning occurrence in a whole year; T1–T12 denote the mean monthly water temperature of spawning ground across the year.

Significant results using a one-tailed test of significance are shown in bold.

***Significant at the 0.01 level.*

**Significant at the 0.05 level.*

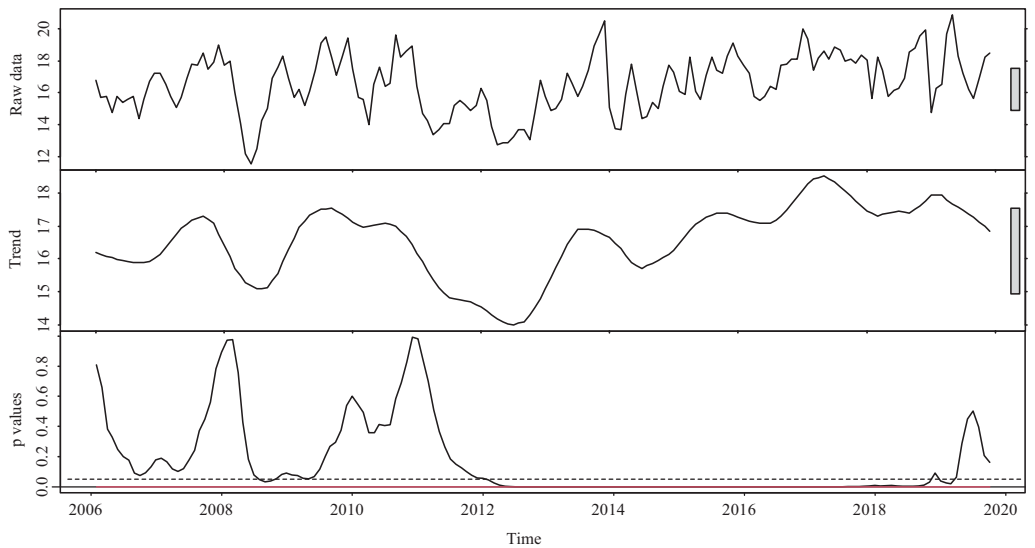

FIGURE 4 | The temperature (two components: raw data and trend) and corresponding *p*-value before the spawning season (from January to March) during 2006–2019 in the Pearl River (China). The gray boxes represent the relative magnitude of variation in each component. The trend component is derived by locally weighted scatterplot smoothing. The red line represents the corresponding *p*-value of the boundary of the F statistics at the confidence level of 99%. The dotted line shows where the *p*-value equals 0.05.

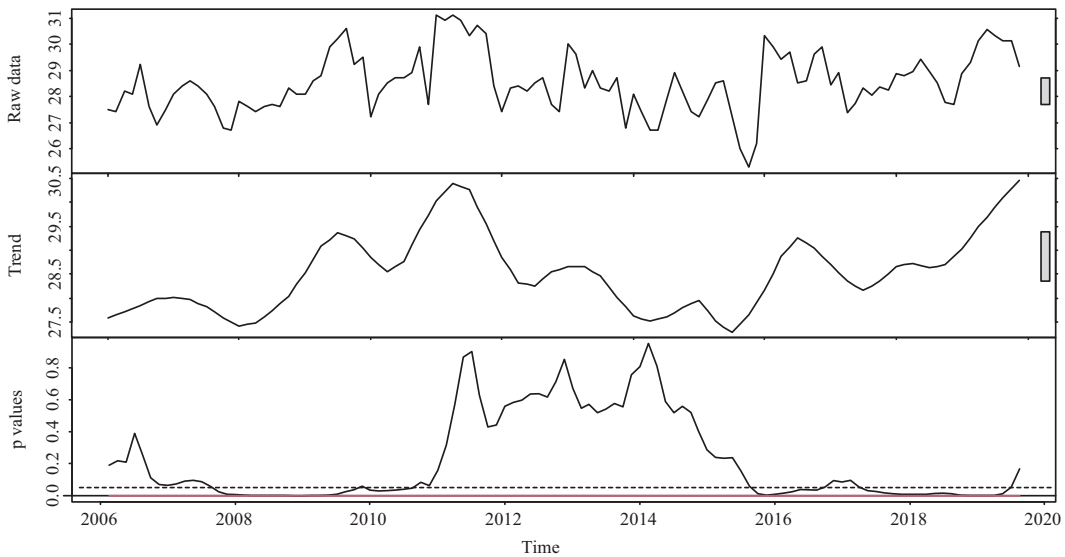

FIGURE 5 | The temperature (two components: raw data and trend) and corresponding *p*-value from August to September during 2006–2019 in the Pearl River (China). The gray boxes represent the relative magnitude of variation in each component. The trend component is derived by locally weighted scatterplot smoothing. The red line represents the corresponding *p*-value of the boundary of the F statistics at the confidence level of 99%. The dotted line shows where the *p*-value equals 0.05.

spawning in the present study, the most suitable temperature was closely related to the flood season.

Increased Temperature Shortening Spawning Period of Silver Carp

We showed that the spawning period of silver carp has been gradually shortened, given the start date of spawning fluctuated with a slight tendency to delay, while the spawning peak and end date obviously occurred earlier over the years. The start date of spawning of silver carp in the Pear River was largely regulated by water temperature, and warmer temperature prior to the spawning season can delay the spawning (Warren et al., 2012). The temperature-related changes in spawning timing are evident in a large number of freshwater fish species. For example, elevated water temperatures caused earlier spawning of rainbow

smelt (*Osmerus mordax*) in the Great Lakes (O'Brien et al., 2012). Warmer temperatures prompted earlier phenology that led to 17 species of larval fishes occurring earlier in the year in southern California (Asch, 2015). In the Yangtze River, a water temperature decline of 2–4°C between March and May resulting from the Three Gorges Dam impoundment led to a delay in silver carp spawning (Wang et al., 2014). However, the rising temperature can also delay fish spawning. It has been reported that the elevated summer temperature caused delayed spawning of brook trout (*Salvelinus fontinalis*) and reduce spawning activities in Rock Lake (Warren et al., 2012). Likewise, in our study, the results suggest that rising temperature from January to March (prior to the spawning season) may delay the spawning start date and decreases the occurrence of spawning. Given the uncertainty between 2014 and 2016 and the limited time-series points, our analyses and conclusions on the trend of Dspawn should be viewed with caution.

We indicated that water temperature increases before the spawning season may be the principal reason for the initial spawning delay in the present study. However, an observed delay in silver carp spawning in the Yangtze River was caused by water temperature declines before spawning (Wang et al., 2014). This could attribute to the reasons that when the mean temperature before the spawning season is lower than 15°C (threshold temperature for gonad development of silver carp), the increase of temperature may favor body growth and promoted gonad development (Yi et al., 1988). However, when the mean temperature substantially exceeds 18°C (threshold temperature for silver carp spawning), we speculated that the elevated temperature would increase metabolism, diverting energy from the fat accumulation, which is needed to complete gonad development, ultimately causing spawning delay (Luksiene and Svedang, 1997; Pankhurst and Munday, 2011). The mean water temperature before and during the spawning season in the spawning ground (DHJK) in the Pearl River were approximately 18 and 26°C, respectively. However, in the spawning grounds of silver carp in the Yangtze River, the mean water temperatures before and during the spawning period were approximately 13 and 21°C, respectively (Wang, 2016). These differences in ambient temperatures might be the principal reason for the divergence in warming effects on the onset of spawning. Although temperature-dependent adaptation allows parents to adjust the spawning time so that the larvae match the timing of the food source (Neuheimer et al., 2018), most studies consider that temperature-related spawning time variations can be attributed to changes in effective accumulated temperature (Robinson et al., 2010; Chezik et al., 2014; Hansen et al., 2017). The initiation of spawning in the present study did not significantly correlate with cumulative temperature. Although cumulative degree-day is an important factor affecting spawning initiation, it is not the main limiting factor in a subtropical river with high temperatures (Wang et al., 2014; Hansen et al., 2017).

The average temperature in August and September was significantly and negatively correlated with the end of spawning, indicating that high temperature in August and September promotes the earlier termination of silver carp spawning. The mean water temperature in the Pearl River between August and September is approximately 28.6°C, which is higher than mean temperatures in other months. The optimum temperature for embryo development of silver carp is 22–28°C (Chen et al., 2009). Therefore, it is likely that silver carp in the Pearl River complete spawning early to avoid the adverse effects of rising temperature on embryo development in a freshwater system with limited thermal refugia (McCullough et al., 2009; Warren et al., 2012).

We revealed that the temperature before the spawning period (from January to March) and near the end of spawning (August and September) were increased during the study period. According to the relationships between the timing of spawning and thermal regime, this warming trend was likely the principal reason for the decreasing trend of the spawning time of silver carp in the present study. Given there was no large dam near the spawning ground during the sampling period, the temperature variation could not be attributed to dam impoundment. It has been reported that the Pearl River basin has been undergoing air temperature increases since the 1950s caused by climate change (Zhang et al., 2012; Tian and Yang, 2017). Therefore, the upward trend in the water temperature in the present study is most likely due to global warming.

CONCLUSION

The discharge suitability index for spawning of silver carp in the Pearl River showed a peak at the discharge of 13,000–15,000 m^3/s. While the temperature suitability index peak was observed at temperatures of 25–26°C, the most suitable temperature for spawning was between 25 and 28°C. In general, the start date of spawning fluctuated with a slight tendency to delay, while the spawning peak and end date obviously occurred earlier during the study period. The initial spawning delay mainly attributed to the increasing temperatures between January and March. In addition, the end date of the spawning became earlier, likely due to elevated temperatures in August and September. Increases in discharge did not significantly correlate with the start of spawning but significantly positively correlated with the spawning peak. These results indicated that (i) the initial spawning of silver carp seems to be triggered by temperature rather than changes in discharge; (ii) flow pulses can probably create more suitable spawning niches for fish; and (iii) elevated temperature has shortened the spawning period of silver carp in the Pearl River.

DATA AVAILABILITY STATEMENT

The raw data supporting the conclusions of this article will be made available by the authors, without undue reservation.

ETHICS STATEMENT

All experiments were performed under the approval of the Ethics Committee of Pearl River Fisheries Research Institute, Chinese Academy of Fishery Sciences. These policies align

with the Chinese Association for the Laboratory Animal Sciences and the Institutional Animal Care and Use Committee (IACUC) protocols.

AUTHOR CONTRIBUTIONS

YX: data analysis, writing—original draft, writing—review and editing, and visualization. XL: conceptualization, methodology, and funding acquisition. JY, SZ, ZW, and JL: sampling collection and data curation. YL: conceptualization, methodology, investigation, and supervision. All authors contributed to the article and approved the submitted version.

FUNDING

This work was supported by the National Key R&D Program of China (2018YFD0900903), the Guangzhou Science Technology Project (202102020270), and the Pearl River Fishery Resources Survey and Evaluation Innovation Team Project (2020TD10, 2020ZJTD-04).

ACKNOWLEDGMENTS

The authors are grateful to technicians Shaofang Su and Zhirong Zhi for their assistance with fieldwork and larvae collection.

REFERENCES

Abdusamadov, A. S. (1987). Biology of white Amur (*Ctenopharyngodon idella*), silver carp (*Hypophthalmichthys molitrix*), and bighead (*Aristichthys nobilis*), acclimatized in the Terek Region of the Caspian Basin. *J. Ichthyol.* 26, 41–49.

Alix, M., Kjesbu, O. S., and Anderson, K. C. (2020). From gametogenesis to spawning: how climate-driven warming affects teleost reproductive biology. *J. Fish Biol.* 97, 607–632. doi: 10.1111/jfb.14439

Alvarez-Mieles, G., Corzo, G., and Mynett, A. E. (2019). "Spatial and temporal variations' of habitat suitability for fish: a case study in Abras de Mantequilla Wetland, Ecuador," in *Spatiotemporal Analysis of Extreme Hydrological Events*, eds G. Corzo and E. A. Varouchakis (Amsterdam: Elsevier), 113–141.

Asch, R. G. (2015). Climate change and decadal shifts in the phenology of larval fishes in the California Current ecosystem. *Proc. Natl. Acad. Sci. U.S.A.* 112, E4065–E4074. doi: 10.1073/pnas.1421946112

Bailly, D., Agostinho, A. A., and Suzuki, H. I. (2008). Influence of the flood regime on the reproduction of fish species with different reproductive strategies in the Cuiaba River, upper Pantanal, Brazil. *River Res. Appl.* 24, 1218–1229. doi: 10.1002/rra.1147

Carscadden, J., Nakashima, B. S., and Frank, K. T. (1997). Effects of fish length and temperature on the timing of peak spawning in capelin (*Mallotus villosus*). *Can. J. Fish. Aquat. Sci.* 54, 781–787. doi: 10.1139/f96-331

Chen, F., Lei, H., Zheng, H., Wang, W., Fang, Y., Yang, Z., et al. (2018). Impacts of cascade reservoirs on fishes in the mainstream of Pearl River and mitigation measures. *J. Lake Sci.* 30, 1097–1108. doi: 10.18307/2018.0422

Chen, I. C., Hill, J. K., Ohlemüller, R., Roy, D. B., and Thomas, C. D. (2011). Rapid range shifts of species associated with high levels of climate warming. *Science* 333, 1024–1026. doi: 10.1126/science.1206432

Chen, Y. B., Liao, W. G., Peng, Q. D., Chen, D. Q., and Gao, Y. (2009). A summary of hydrology and hydrodynamics conditions of Four Chinese Carps' spawning. *J. Hydroecol.* 2, 130–133. doi: 10.15928/j.1674-3075.2009.02.023

Chezik, K. A., Lester, N. P., Venturelli, P. A., and Tierney, K. (2014). Fish growth and degree-days I: selecting a base temperature for a within-population study. *Can. J. Fish. Aquat. Sci.* 71, 47–55. doi: 10.1139/cjfas-2013-0295

Committee of Pearl River Fishery Resources Investigation (1985). *Investigation Report on Fishery Resources in the Pearl River*, Vol. 6. 33–54. (Guangzhou: Unpublished report).

Coulter, A. A., Bailey, E. J., Keller, D., and Goforth, R. R. (2016). Invasive Silver Carp movement patterns in the predominantly free-flowing Wabash River (Indiana, USA). *Biol. Invasions* 18, 471–485. doi: 10.1007/s10530-015-1020-2

Erisman, B., Heyman, W., Kobara, S., Ezer, T., Pittman, S., Aburto-Oropeza, O., et al. (2017). Fish spawning aggregations: where well-placed management actions can yield big benefits for fisheries and conservation. *Fish Fish.* 18, 128–144. doi: 10.1111/faf.12132

Freeze, M., and Crawford, T. (1983). Fall spawning of silver carp. *Prog. Fish Cult.* 45:133.

Gao, M., Wu, Z., Tan, X., Huang, L., Huang, H., and Liu, H. (2020). Composition and abundance of drifting fish eggs on the upper reaches of Xijiang River, China, after the formation of the cascade reservoirs. *BioRxiv* [preprint] doi: 10.1101/2020.01.13.904110

Garcia, T., Jackson, P. R., Murphy, E. A., Valocchi, A. J., and Garcia, M. H. (2013). Development of a fluvial egg drift simulator to evaluate the transport and dispersion of Asian carp eggs in rivers. *Ecol. Modell.* 263, 211–222. doi: 10.1016/j.ecolmodel.2013.05.005

Gillet, C., and Dubois, J. P. (2007). Effect of water temperature and size of females on the timing of spawning of perch Perca fluviatilis L. in Lake Geneva from 1984 to 2003. *J. Fish Biol.* 70, 1001–1014. doi: 10.1111/j.1095-8649.2007.01359.x

Glover, R. S., Soulsby, C., Fryer, R. J., Birkel, C., and Malcolm, I. A. (2020). Quantifying the relative importance of stock level, river temperature and discharge on the abundance of juvenile Atlantic salmon (*Salmo salar*). *Ecohydrology* 13:e2231. doi: 10.1002/eco.2231

Gorbach, E. I., and Krykhtin, M. L. (1989). Migration of the white Amur, *Ctenopharyngodon idella*, and silver carp, *Hypophthalmichthys molitrix*, in the Amur River Basin. *J. Ichthyol.* 28, 47–53.

Gordoa, A., and Carreras, G. (2014). Determination of temporal spawning patterns and hatching time in response to temperature of Atlantic bluefin tuna (*Thunnus thynnus*) in the western Mediterranean. *PLoS One* 9:e90691. doi: 10.1371/journal.pone.0090691

Górski, K., Winter, H. V., De Leeuw, J. J., Minin, A. E., and Nagelkerke, L. A. J. (2010). Fish spawning in a large temperate floodplain: the role of flooding and temperature. *Freshw. Biol.* 55, 1509–1519. doi: 10.1111/j.1365-2427.2009.02362.x

Hansen, G. J., Read, J. S., Hansen, J. F., and Winslow, L. A. (2017). Projected shifts in fish species dominance in Wisconsin lakes under climate change. *Glob. Change Biol.* 23, 1463–1476. doi: 10.1111/gcb.13462

IPBES. (2019). "Summary for policymakers of the global assessment report on biodiversity and ecosystem services of the Intergovernmental Science-Policy Platform on Biodiversity and Ecosystem Services," in *IPBES Secretariat*, eds S. Díaz, J. Settele, E. S. Brondizio, H. T. Ngo, M. Guèze, J. Agard, et al. (Bonn: IPBES), 13.

Ji, C., Gu, J., Mao, R., Zhu, X., and Sun, X. (2009). Analysis of genetic diversity among wild silver carp (*Hypophthalmichthys molitrix*) populations in the Yangtze River, Helongjiang and Pearl River using microsatellite markers. *J. Fish. China* 33, 364–371. doi: 10.3321/j.issn:1000-0615.2009.03.002

Kjesbu, O. S. (1994). Time of start of spawning in Atlantic cod (*Gadus morhua*) females in relation to vitellogenic oocyte diameter, temperature, fish length and condition. *J. Fish Biol.* 45, 719–735. doi: 10.1111/j.1095-8649.1994.tb00939.x

Lessard, J. A. L., and Hayes, D. B. (2003). Effects of elevated water temperature on fish and macroinvertebrate communities below small dams. *River Res. Appl.* 19, 721–732. doi: 10.1002/rra.713

Li, F., Wei, J., Qiu, J., and Jiang, H. (2020). Determining the most effective flow rising process to stimulate fish spawning via reservoir operation. *J. Hydrol.* 582:124490. doi: 10.1016/j.jhydrol.2019.124490

Li, M., Duan, Z., Gao, X., Cao, W., and Liu, H. (2016). Impact of the three Gorges Dam on reproduction of four major Chinese carps species in the middle reaches of the Changjiang River. *Chin. J. Oceanol. Limn.* 34, 885–893. doi: 10.1007/s00343-016-4303-2

Lu, K. (1990). *Fisheries Resources in Pearl River*. Guangzhou: Guangdong science and Technology Press, 1–5.

Luksiene, D., and Svedang, H. (1997). *A Review on Fish Reproduction With Special Reference to Temperature Anomalies*. Öregrund: Fiskeriverket, Kustlaboratoriet, 35.

McCullough, D. A., Bartholow, J. M., Jager, H. I., Beschta, R. L., Cheslak, E. F., Deas, M. L., et al. (2009). Research in thermal biology: burning questions for coldwater stream fishes. *Rev. Fish. Sci.* 17, 90–115. doi: 10.1080/10641260802590152

Miranda, L. A., Chalde, T., Elisio, M., and Strüssmann, C. A. (2013). Effects of global warming on fish reproductive endocrine axis, with special emphasis in pejerrey *Odontesthes bonariensis*. *Gen. Comp. Endocr.* 192, 45–54. doi: 10.1016/j.ygcen.2013.02.034

Morgan, M. J., Wright, P. J., and Rideout, R. M. (2013). Effect of age and temperature on spawning time in two gadoid species. *Fish. Res.* 138, 42–51. doi: 10.1016/j.fishres.2012.02.019

Neuheimer, A. B., MacKenzie, B. R., and Payne, M. R. (2018). Temperature-dependent adaptation allows fish to meet their food across their species' range. *Sci. Adv.* 4:eaar4349. doi: 10.1126/sciadv.aar4349

O'Brien, T. P., Taylor, W. W., Briggs, A. S., and Roseman, E. F. (2012). Influence of water temperature on rainbow smelt spawning and early life history dynamics in St. Martin Bay, Lake Huron. *J. Great Lakes Res.* 38, 776–785. doi: 10.1016/j.jglr.2012.09.017

Ojaveer, E., Arula, T., Lankov, A., and Shpilev, H. (2011). Impact of environmental deviations on the larval and year-class abundances in the spring spawning herring (*Clupea harengus* membras L.) of the Gulf of Riga (Baltic Sea) in 1947–2004. *Fish. Res.* 107, 159–168. doi: 10.1016/j.fishres.2010.11.001

Pankhurst, N. W., and Munday, P. L. (2011). Effects of climate change on fish reproduction and early life history stages. *Mar. Freshw. Res.* 62, 1015–1026. doi: 10.1071/MF10269

Paumier, A., Drouineau, H., Boutry, S., Sillero, N., and Lambert, P. (2020). Assessing the relative importance of temperature, discharge, and day length on the reproduction of an anadromous fish (*Alosa alosa*). *Freshw. Biol.* 65, 253–263. doi: 10.1111/fwb.13418

Perry, A. L., Low, P. J., Ellis, J. R., and Reynolds, J. D. (2005). Climate change and distribution shifts in marine fishes. *Science* 308, 1912–1915. doi: 10.1126/science.1111322

Preece, R. M., and Jones, H. A. (2002). The effect of Keepit Dam on the temperature regime of the Namoi River, Australia. *River Res. Appl.* 18, 397–414. doi: 10.1002/rra.686

R Core Team (2019). *R: A Language and Environment for Statistical Computing*. Vienna: R Foundation for Statistical Computing.

Robinson, J. M., Josephson, D. C., Weidel, B. C., and Kraft, C. E. (2010). Influence of variable interannual summer water temperatures on brook trout growth, consumption, reproduction, and mortality in an unstratified Adirondack Lake. *Trans. Am. Fish. Soc.* 139, 685–699. doi: 10.1577/T08-185.1

Shuai, F., Lek, S., Baehr, C., Park, Y. S., Li, Y., and Li, X. (2018). Silver carp larva abundance in response to river flow rate revealed by cross-wavelet modelling. *Ecol. Modell.* 383, 98–105. doi: 10.1016/j.ecolmodel.2018.05.020

Shuai, F., Li, X., Li, Y., Li, J., Yang, J., and Lek, S. (2016). Temporal patterns of larval fish occurrence in a large subtropical river. *PLoS One* 11:e0146441. doi: 10.1371/journal.pone.0146441

Sims, D. W., Wearmouth, V. J., Genner, M. J., Southward, A. J., and Hawkins, S. J. (2004). Low-temperature-driven early spawning migration of a temperate marine fish. *J. Anim. Ecol.* 73, 333–341. doi: 10.1111/j.0021-8790.2004.00810.x

Smith, D. M., Scaife, A. A., Hawkins, E., Bilbao, R., Boer, G. J., Caian, M., et al. (2018). Predicted chance that global warming will temporarily exceed 1.5 °C. *Geophys. Res. Lett.* 45, 895–811,903. doi: 10.1029/2018GL079362

Tan, X., Li, X., Lek, S., Li, Y., Wang, C., Li, J., et al. (2010). Annual dynamics of the abundance of fish larvae and its relationship with hydrological variation in the Pearl River. *Environ. Biol. Fish.* 88, 217–225. doi: 10.1007/s10641-010-9632-y

Thorstad, E. B., Økland, F., Aarestrup, K., and Heggberget, T. G. (2008). Factors affecting the within-river spawning migration of Atlantic salmon, with emphasis on human impacts. *Rev. Fish Biol. Fish.* 18, 345–371. doi: 10.1007/s11160-007-9076-4

Tian, Q., and Yang, S. (2017). Regional climatic response to global warming: trends in temperature and precipitation in the Yellow, Yangtze and Pearl River basins since the 1950s. *Quatern. Int.* 440, 1–11. doi: 10.1016/j.quaint.2016.02.066

Tuz-Sulub, A., and Brulé, T. (2015). Spawning aggregations of three protogynous groupers in the southern Gulf of Mexico. *J. Fish Biol.* 86, 162–185. doi: 10.1111/jfb.12555

van Overzee, H. M. J., and Rijnsdorp, A. D. (2015). Effects of fishing during the spawning period: implications for sustainable management. *Rev. Fish Biol. Fisher.* 25, 65–83. doi: 10.1007/s11160-014-9370-x

Wakefield, C. B., Potter, I. C., Hall, N. G., Lenanton, R. C. J., and Hesp, S. A. (2015). Marked variations in reproductive characteristics of snapper (*Chrysophrys auratus*, Sparidae) and their relationship with temperature over a wide latitudinal range. *ICES J. Mar. Sci.* 72, 2341–2349. doi: 10.1093/icesjms/fsv108

Walther, G. R., Post, E., Convey, P., Menzel, A., Parmesan, C., Beebee, T. J. C., et al. (2002). Ecological responses to recent climate change. *Nature* 416, 389–395.

Wang, J. N., Li, C., Duan, X. B., Luo, H. H., Feng, S. X., Peng, Q. D., et al. (2014). The relationship between thermal regime alteration and spawning delay of the four major Chinese carps in the Yangtze River below the three Gorges Dam. *River Res. Appl.* 30, 987–1001. doi: 10.1002/rra.2691

Wang, Y. F. (2016). *The Three Gorges Project on Downstream River Eco-Hydrological Impact Assessment Study*. Master Dissertation. Zhengzhou: North China University of Water Resources and Electric Power.

Warren, D. R., Robinson, J. M., Josephson, D. C., Sheldon, D. R., and Kraft, C. E. (2012). Elevated summer temperatures delay spawning and reduce redd construction for resident brook trout (*Salvelinus fontinalis*). *Glob. Change Biol.* 18, 1804–1811. doi: 10.1111/j.1365-2486.2012.02670.x

Yi, B. L., and Liang, Z. S. (1964). Natural conditions of the spawning grounds of the "domestic fishes" in Yangtze River and essential external factor for spawning. *Acta Hydrobiol. Sin.* 5, 1–15.

Yi, B. L., Liang, Z. S., Yu, Z. T., Lin, R. D., and He, M. J. (1988). "A comparative study on the early development of grass carp, black carp, silver carp and big head of the Yangtze River," in *Gezhouba Water Control Project and Four Famous Fishes in Yangtze River*, eds B. L. Yi, Z. T. Yu, and Z. S. Liang (Wuhan: Hubei Science and Technology Press), 69–116.

Yu, L., Lin, J., Chen, D., Duan, X., Peng, Q., and Liu, S. (2018). Ecological flow assessment to improve the spawning habitat for the four major species of carp of the Yangtze River: a study on habitat suitability based on ultrasonic telemetry. *Water* 10:600. doi: 10.3390/w10050600

Zeileis, A., Leisch, F., Hornik, K., and Kleiber, C. (2002). Strucchange: an R package for testing for structural change in linear regression models. *J. Stat. Softw.* 7, 1–38.

Zhang, F., Lei, X., Jiang, Y., and Bai, J. (2012). Analysis on character of temperature variation in upstream of Pearl River basin during 55 years. *J. Water Res. Water Eng.* 23, 20–25.

Zhang, G. H., Chang, J. B., and Shu, G. F. (2000). Applications of factor-criteria system reconstruction analysis in the reproduction research on grass carp, black carp, silver carp and bighead in the Yangtze River. *Int. J. Gen. Syst.* 29, 419–428.

Zhang, P., Li, K., Wu, Y., Liu, Q., Zhao, P., and Li, Y. (2018). Analysis and restoration of an ecological flow regime during the *Coreius guichenoti* spawning period. *Ecol. Eng.* 123, 74–85. doi: 10.1016/j.ecoleng.2018.08.009

Zhang, P., Qiao, Y., Grenouillet, G., Lek, S., Cai, L., and Chang, J. (2021). Responses of spawning thermal suitability to climate change and hydropower operation for typical fishes below the Three Gorges Dam. *Ecol. Indic.* 121:107186. doi: 10.1016/j.ecolind.2020.107186

Zhang, Y., Huang, D., Li, X., Liu, Q., Li, J., Li, Y., et al. (2020). Fish community structure and environmental effects of West River. *S. China Fish. Sci.* 16, 42–52. doi: 10.12131/20190142

Conflict of Interest: The authors declare that the research was conducted in the absence of any commercial or financial relationships that could be construed as a potential conflict of interest.

frontiers in Marine Science

PERSPECTIVE
published: 22 September 2021
doi: 10.3389/fmars.2021.729194

Within- and Trans-Generational Environmental Adaptation to Climate Change: Perspectives and New Challenges

Naim M. Bautista[1,2]* *and Amélie Crespel*[3]*

[1] Department of Biology, Aarhus University, Aarhus, Denmark, [2] School of Biological Sciences, University of Nebraska-Lincoln, Lincoln, NE, United States, [3] Department of Biology, University of Turku, Turku, Finland

The current and projected impacts of climate change are shaped by unprecedented rates of change in environmental conditions. These changes likely mismatch the existing coping capacities of organisms within-generations and impose challenges for population resilience across generations. To better understand the impacts of projected scenarios of climate change on organismal fitness and population maintenance, it is crucial to consider and integrate the proximate sources of variability of plastic and adaptive responses to environmental change in future empirical approaches. Here we explore the implications of considering: (a) the variability in different time-scale events of climate change; (b) the variability in plastic responses from embryonic to adult developmental stages; (c) the importance of considering the species life-history traits; and (d) the influence of trans-generational effects for individual survival and population maintenance. Finally, we posit a list of future challenges with questions and approaches that will help to elucidate knowledge gaps, to better inform conservation and management actions in preserving ecosystems and biodiversity.

Keywords: climate fluctuation, evolution, developmental plasticity, trans-generational effects, adaptation, life-history trait

OPEN ACCESS

Edited by:
Timothy Ravasi, Okinawa Institute of Science and Technology Graduate University, Japan

Reviewed by:
Heather Diana Veilleux, University of Alberta, Canada
Yuan-Ye Zhang, Xiamen University, China

***Correspondence:**
Amélie Crespel
amelie.crespel@gmail.com
orcid.org/0000-0002-6351-9008
Naim M. Bautista
naimbautista05@gmail.com
orcid.org/0000-0003-0634-0842

Specialty section:
This article was submitted to Global Change and the Future Ocean, a section of the journal Frontiers in Marine Science

Received: *22 June 2021*
Accepted: *26 August 2021*
Published: *22 September 2021*

Citation:
Bautista NM and Crespel A (2021) Within- and Trans-Generational Environmental Adaptation to Climate Change: Perspectives and New Challenges. Front. Mar. Sci. 8:729194. doi: 10.3389/fmars.2021.729194

INTRODUCTION

Global climate change is projected to continue modifying environmental conditions at unprecedented rates (Lüthi et al., 2008; IPCC, 2014). These changes have dramatic consequences for ecosystems and communities by reducing species abundance and in extreme cases causing species extinction (Thomas et al., 2004; Willis et al., 2008; Hoffmann and Sgrò, 2011), leading to decreased biodiversity (Parmesan and Yohe, 2003; Landman et al., 2005; Burlakova et al., 2014; Zhang et al., 2018). In aquatic systems, the effects of climate change include, among others, fluctuations in oxygen availability, increased acidification, and extreme stochastic temperature events (Caldeira and Wickett, 2005; IPCC, 2014; Jenny et al., 2016; Dahlke et al., 2020). The magnitude, duration, and periodicity of these changes likely mismatch the existing evolved coping capacities of species, compromising population maintenance and resilience (Johansen et al., 2021). Mitigation of the effects of climate change can take place within and across generations. Within-generational mitigation can occur through relocation to more favorable environments (Pinsky et al., 2013). However, when relocation is not feasible, within-generational mitigation can then

occur through individual acclimatization by phenotypic plasticity (Crozier and Hutchings, 2014). If individuals of a population survive and are able to reproduce, the effects of climate change can then be attenuated across generations via non-genetic inheritance or genetic adaptation (Gienapp et al., 2008; Andrewartha and Burggren, 2012; Ryu et al., 2020).

To better understand the impacts of projected scenarios of climate change on individual fitness, population maintenance, and species resilience, it is thus crucial to frame future experimental studies under an integrative approach that considers how the proximate environmental causes of individual variability that affect plastic responses can influence the ultimate functional and potential adaptive responses to environmental change. As the number of studies on climate change increases, the complexity of its effects becomes more evident. In fact, these advances bring along new challenges for the scientific community, such as providing more ecologically relevant predictions that integrate natural-field conditions in experimental designs while overcoming technological and logistic constraints.

In this perspective we focus on aquatic systems to first highlight the importance of considering different time scales of fluctuations in environmental conditions, for example, comparing the effects of short-term variations (i.e., daily fluctuations) to long-term projected scenarios (i.e., average changes of climate change). Second, depending on the environmental condition, the organismal physiological capacities to cope with disturbances partially depend on the "maturity" of its organs and systems. Therefore, variability in plastic responses to environmental challenges within a population will likely arise based on the organism's developmental stage. Third, species' life history traits (e.g., life span, generational time, and reproductive strategy) rely on the availability of resources through time and location. However, variability within and across habitats imposes challenges on fitness. Thus, it becomes important to determine how climatic variability will impact life history traits, as well as to determine if the response to these challenges will be similar across species with different life histories. Fourth, we discuss how within-generational responses to fluctuations in environmental conditions can affect the phenotype of subsequent offspring generations, and potentially induce genetic adaptation. Finally, we list potential directions for future experimental studies that will provide more realistic predictions of the consequences of climate change on populations.

TIME-SCALE EVENTS: WEATHER, CLIMATE, AND CLIMATE CHANGE

Climate change refers to significant long-term changes in average environmental conditions. These changes include, among others, modifications of temperature cycles, carbon dioxide and oxygen levels, pH of water, precipitation, and wind patterns (Burroughs, 2007; Bopp et al., 2013). Although these variables fluctuate naturally and impose constant challenging conditions for individuals and populations, their occurrence, variability, amplitude, and unpredictability have been exacerbated since the industrial revolution (Jenny et al., 2016; Johansen et al., 2021; **Figure 1A**). Strikingly, most of the studies aimed at understanding the effects of climate change consider discrete stepwise changes of a selected "stressor" that reflect the mean values of long-term predicted scenarios. Commonly, after exposing the study species to the new steady level, a description of the organismal (or population) responses and speculations about their adaptive capacity are provided (e.g., Rosa et al., 2014; Rummer et al., 2014; Dixson et al., 2015; Faria et al., 2018; Johansen et al., 2021). For example, studies investigating the effects of global warming and ocean acidification generally expose the individuals to a constant + 3°C or – 0.3 pH units, respectively, before assessing individual fitness related traits, such as growth and survival (Sheppard-Brennand et al., 2010; McLeod et al., 2013; Rasconi et al., 2015; Crespel et al., 2017; Qui-Minet et al., 2019). However, in nature, ambient conditions rarely, if ever, change in a stepwise fashion, and organisms face fluctuations in environmental conditions at time scales of hours, days, months, and years (Burggren, 2018). Recent studies have highlighted that the responses of individuals within a population will vary when exposed to a constant or fluctuating conditions (Drake et al., 2017; Hannan et al., 2020). Therefore, to better understand the impacts of climate change on organisms and populations, it is necessary to integrate more naturally relevant variability of environmental conditions in experimental designs and to differentiate the effects of stochastic *weather* events –short-term every day and weekly changes in ambient conditions– from those of *climate* –seasonal and yearly changes in ambient conditions– and *climate change* –predicted changes in mean values of environmental parameters across decades and centuries- (Burroughs, 2007; **Figure 1A**).

Habitats vary in their capacities for buffering changes in environmental conditions (Malhi et al., 2020), and their resident species reflect this variation. Nonetheless, even if organisms are physiologically able to cope with the environmental stress imposed by a single extreme event (e.g., heat waves), it is possible that repeated and long-term exposure to unpredictable conditions will likely outweigh their existing evolved coping capacities (Le Nohaïc et al., 2017; Johansen et al., 2021)– compromising survival and contribution to future generations. For example, thermally resistant corals from Northwestern Australia that have been able to thrive in daily temperatures up to 37°C, experienced severe mass bleaching (<80.6%) in 2016 due to extreme heatwaves of 4.5–9.3° heating weeks for about 5 months (Le Nohaïc et al., 2017). This study highlights the importance of considering both, stochastic extreme weather events as well as medium- and long-term natural climatic variability in experimental designs.

Noteworthy is the fact that the combination of environmental stressors –which is the norm more than the exception in nature- can have antagonistic, additive or synergetic effects on organisms and populations (Darling and Côté, 2008; Lefevre, 2016; Montgomery et al., 2019). For example, oxygen consumption of marine ectotherms is more commonly affected by additive or antagonistic interactions between ocean warming and acidification than by a synergistic effect (see Lefevre, 2016; Pistevos et al., 2016; Leo et al., 2017). Consequently, the empirical

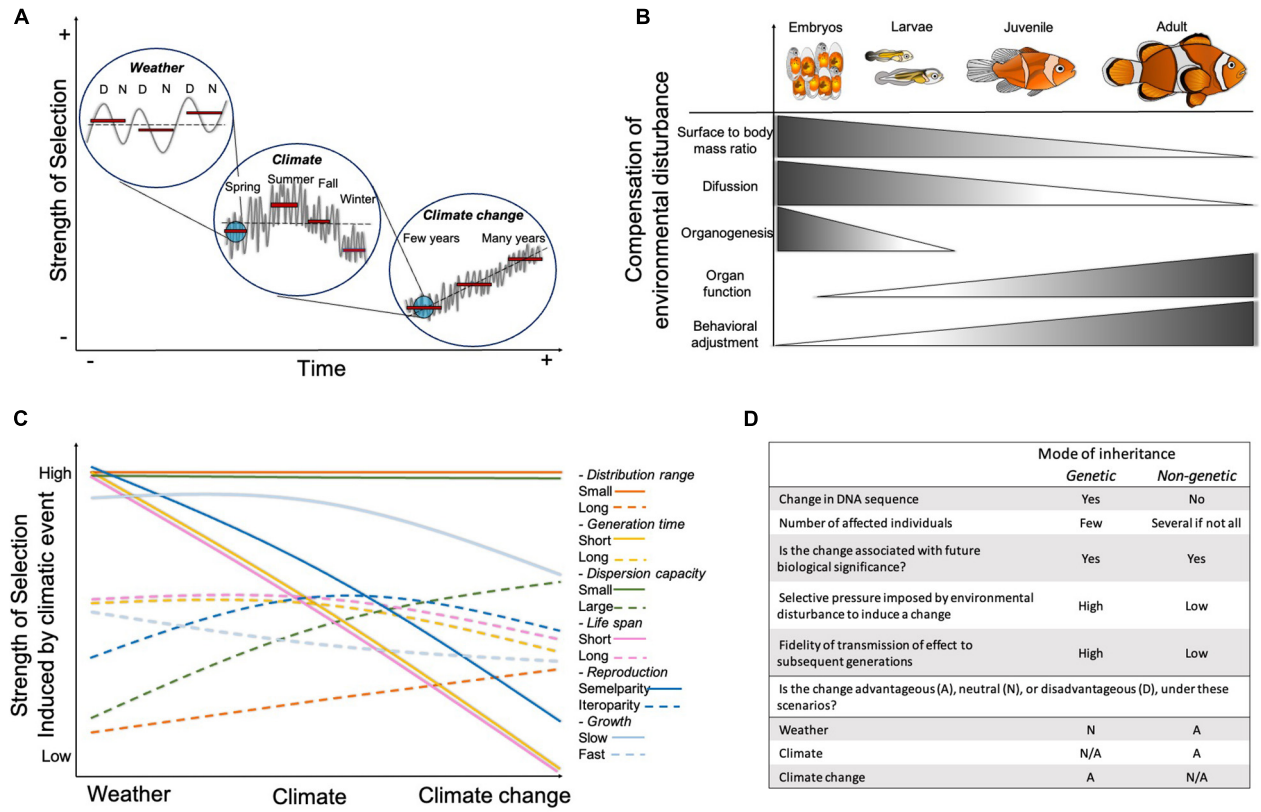

D

	Mode of inheritance	
	Genetic	*Non-genetic*
Change in DNA sequence	Yes	No
Number of affected individuals	Few	Several if not all
Is the change associated with future biological significance?	Yes	Yes
Selective pressure imposed by environmental disturbance to induce a change	High	Low
Fidelity of transmission of effect to subsequent generations	High	Low
Is the change advantageous (A), neutral (N), or disadvantageous (D), under these scenarios?		
Weather	N	A
Climate	N/A	A
Climate change	A	N/A

FIGURE 1 | Factors affecting the variability of plastic and adaptive responses to environmental change. **(A)** Strength of selection induced by different time-scale events of climate change. The gray line depicts variation in a measured variable (e.g., temperature) in a "real world scenario" highlighting the mismatch with the classic experimental approach of choosing stepwise/discrete mean values (red bars) at different time scales. D, day and N, night; **(B)** Factors affecting the variability in plastic responses from embryonic to adult developmental stages. Triangles represent the absence (white) and the emergence/presence (dark) of these factors across development; **(C)** Strength of selection on life-history traits at the species level. Colored lines represent two extremes (slow/small/short = solid lines vs. fast/large/long = dotted lines) for each trait, each line should be interpreted under independent *y* axis; and **(D)** Comparison of the influence of the mode of inheritance (genetic vs. non-genetic) for trans-generational effects affecting individual survival and population maintenance under climatic change events.

consideration of multi-stressor interactions will render a better understanding of the effects of climate change.

VARIABILITY IN PLASTIC RESPONSES WITHIN A GENERATION

Developmental Stage

Individual plastic responses to weather and climate events are expected to vary across developmental stages. Embryonic and larval stages are considered to be more sensitive to variable environmental conditions in comparison to adult stages, because of reduced plastic capacity (Burggren and Bautista, 2019; Dahlke et al., 2020). Inherent to early development is the progressive maturing of rudimentary morphological structures and physiological functions that allow organisms to regulate homeostatic disturbances (**Figure 1B**). In fish for example, as development progresses and the surface to body mass ratio decreases, homeostatic regulation by diffusion through skin is gradually replaced by the interrelated functions of the forming organ systems (Rombough, 1998, 2002; Burggren et al., 2017). During organogenesis, disturbances induced by challenging environmental conditions can compromise the survival of early life stages (Réalis-Doyelle et al., 2016). However, if they survive, the effects can remain present later in life potentially compromising metabolic rates, reproduction, and population replenishment (Jonsson and Jonsson, 2014; Durtsche et al., 2021). In contrast, the experience of environmental challenges early in life can also have positive phenotypic effects. For example, improvement of skeletal development (faster mineralization) was reported in larvae of the seabass exposed to hypercapnic conditions (Crespel et al., 2017). Worth mentioning is the fact that early exposures in life can also lead to positive effects in later developmental stages and not only at the exposed stage (Gobler and Talmage, 2013; Vanderplancke et al., 2015; Spinks et al., 2019). For instance, zebrafish embryos incubated up to hatching in colder or warmer temperatures, exhibited improved swimming performance as adults when exposed to temperatures resembling their temperature of incubation (Scott and Johnston, 2012). However, to date we still have poor understanding of the plastic capacities at the whole organismal level in developing organisms (e.g., thermal limits and tolerance

ranges), as well as of the actual partitioning of their regulatory mechanisms in organ and systems (e.g., acid-base regulation), and the potential trade-offs with other traits, when facing environmental disturbances (West-Eberhard, 2003; Burggren and Bautista, 2019). This lack of knowledge mainly arises from the intrinsic complexity of studying the effects of climate change in tiny sized organisms, and the inherent technological challenge of developing and implementing reproducible techniques for such specialized measurements.

Although adult life stages exhibit well established physiological acid-base and thermoregulatory capacities, as well as the capacity for adjusting their behavior in response to their surrounding environment, their plasticity and susceptibility to environmental disturbances can vary depending on their reproductive status. Indeed, scenario-based projections of climate change suggest that spawning adults have significantly narrower thermal tolerances (Dahlke et al., 2020). In addition, environmental variation can induce alteration in neuroendocrine pathways, modifying metabolism, disrupting homeostasis and exacerbating production of reactive oxygen species, leading to acceleration of development and aging (Burraco et al., 2020). Therefore, different developmental stages are likely to respond to stressors through distinct mechanisms and with different sensitivity and plasticity. Because populations are composed of individuals of different developmental stages, a particular sensitivity or lack of plasticity in one of the stages may lead to the collapse of the entire population. Therefore, investigating the effects of weather and climate events in all developmental life stages is crucial to provide more reliable information on how populations could be affected by future conditions (**Figure 1B**).

Life History Traits

Availability of resources varies with seasonality and across habitats with different environmental conditions. Furthermore, organisms' life history traits represent how variable the environmental changes are in their habitat (Hovel et al., 2017; Chaparro-Pedraza and de Roos, 2019). Consequently, changes in the species geographic distribution and its realized niche induced by climate variability can impact these traits (de Roos and Persson, 2013; Wang et al., 2020; Chaudhary et al., 2021). For example, the reproductive strategies of the majority of species depend on environmental conditions (e.g., temperature, salinity, light:dark cycles, and food availability). Therefore, a delay or acceleration in the timing for reproduction in semelparous species -characterized by death after first reproduction- can lead to a phenological mismatch between larval exogenous feeding and food availability (Durant et al., 2007; Renner and Zohner, 2018), increasing mortality and compromising effective population size (**Figure 1C**). In comparison, iteroparous species – with multiple reproduction events in their lifetime- may be more capable of buffering the effects of climate variability by regulating parental investment across their clutches (Parker, 2002; Cayuela et al., 2014), although long-term and recurrent scenarios may still threaten population recruitment. Therefore, as different species perceive the changes in environmental conditions depending on the granularity of the habitat that they inhabit (Levins, 1968; van Tienderen, 1991, 1997), it becomes necessary to consider the species' dispersal needs and capacities as well as their migration patterns -if present- when interpreting results from experimental studies (**Figure 1C**).

The effects of climate change can also affect species differentially based on their lifespan and generation time. For example, in comparison to taxa with short-generation times (benthopelagic and reef fishes; up to 5 years), accelerated development and life histories due to global warming can lead to lower mortality and higher fecundity earlier in life in taxa with long-generation times (elasmobranch, bathydemersal, demersal; over 10 years) (Wang et al., 2020). In addition, simulation models suggest that species that possess long lifespans, relative to the change in environmental conditions, may be more plastic in comparison to species with short lifespan (Ratikainien and Kokkoo, 2020). Overall, the differential responses related to life-span and generational time of a particular species will induce inter- and trans-generational effects that will affect the number of generations experiencing climate variability as well as the species potential for evolutionary adaptation (**Figure 1C**).

BEYOND A SINGLE GENERATION: TRANS-GENERATIONAL ACCLIMATION AND ADAPTATION

Evolutionary Adaptation

Within-generational phenotypic plasticity allows organisms to face the challenges directly imposed by variable environmental conditions. However, to persist in the long-term, populations must cope with the continuous environmental challenges through adaptation across generations. Adaptation occurs through genetic inheritance, i.e., evolution (McGuigan et al., 2021; **Figure 1D**). For evolution (genetic adaptation) to occur, empirical evidence must demonstrate that the environmental fluctuations due to climate change can lead to modifications in genetic sequences, and that these changes are the result of natural selection (Merilä and Hendry, 2014; Ehrenreich and Pfennig, 2016). The new environmental pressures are likely to induce selection on specific fitness-related traits, resulting in the shift of the allele frequencies of these traits across generations (Bernatchez, 2016; Manhard et al., 2017). Micro evolutionary changes can occur across a small number of generations and at ecological relevant timescales (Hairston et al., 2005; Carroll et al., 2007; Bell and Aguirre, 2013; Hendry et al., 2018; Reznick et al., 2019). However, the species' evolutionary potential may still be low when the rate of change in the environmental conditions outpaces the rate of the species adaptation. For example, a recent study on thermal tolerance in zebrafish artificially selected over six generations to increase or decrease their upper thermal tolerance, reported that these fish exhibited a slow rate of adaptation compared to the rate of global warming, suggesting that such tropical species may meet adaptive constraints when facing global warming (Morgan et al., 2020).

Taken together these studies highlight the need for determining whether adaptation from existing genetic variation

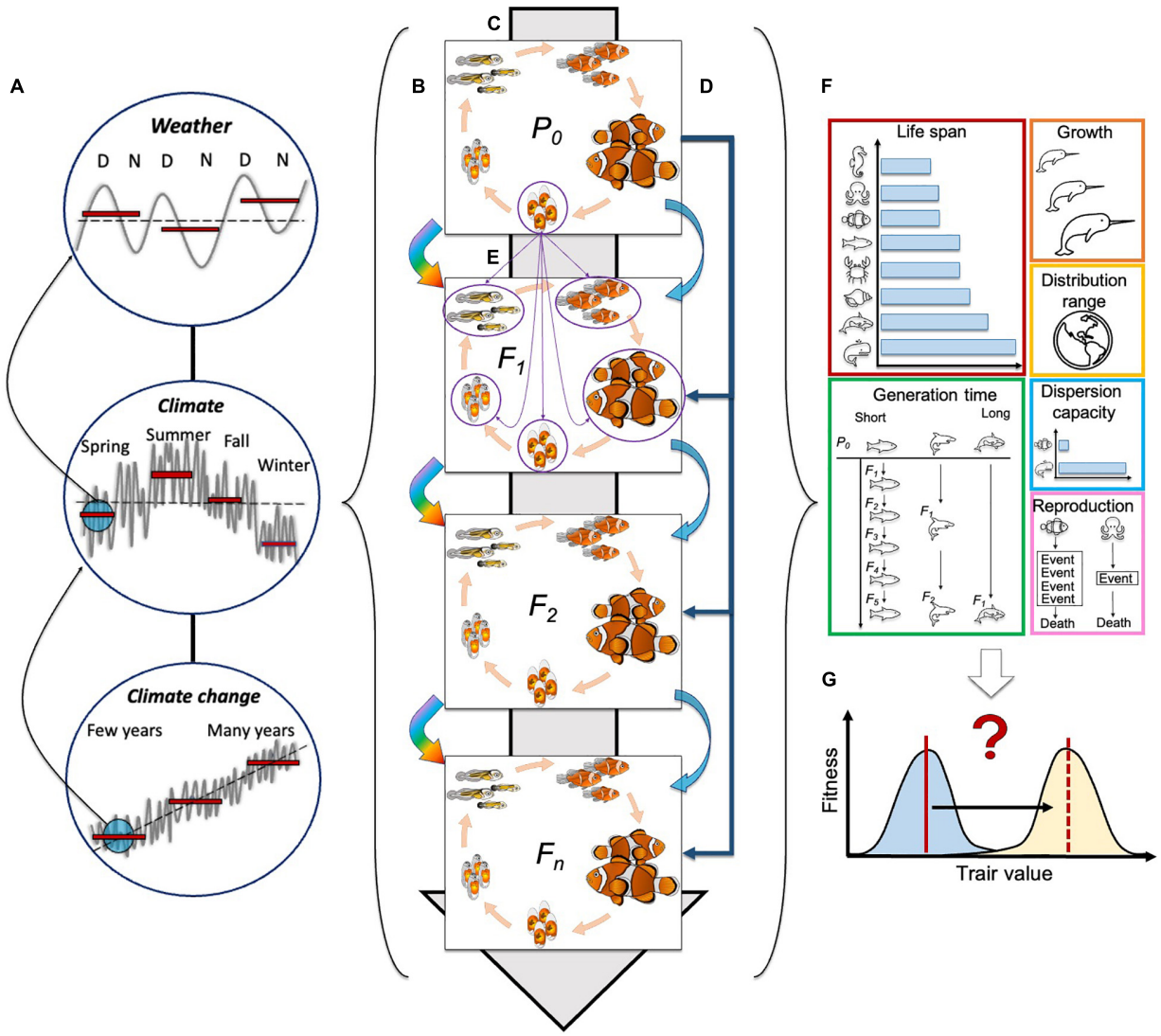

FIGURE 2 | Challenges of within- and trans-generational effects of climatic events on life history traits of species. **(A)** The different scales in the continuum between weather and climate change impose varied selection pressures (e.g., stochastic, cyclic, and unpredictable) on individuals and populations within- and across generations. D, day and N, night; **(B)** Climatic events will impose *within*-generational effects to each generation *per se* (depicted by surrounding squares for each generation); **(C)** *Trans-generational* effects could occur through *genetic* inheritance (gray background arrow) with transmission of DNA sequences under selection by the environmental conditions across generations; **(D)** The experience of climatic events on a parental generation alone can also lead to *non-genetic* trans-generational effects on its subsequent generations (dark blue arrows). Moreover, the experience of climatic events on the F_1, F_2 and, F_n, generation *per se* can also affect their subsequent generation (light blue arrows). **(E)** A question to be answered yet embraces the trans-generational implications of how the experience of climatic events at specific life stages will affect the different life stages. For example: how experience of climatic events at the egg stage will affect phenotypic traits of eggs, embryos, larvae, juveniles and adults, of the following generation? (purple arrows). **(F)** The effects of climatic events will vary among species according to their life history traits. Here we illustrate how the variation in life span, generation time, growth, distribution range, dispersion capacity and reproductive events in different species could be differentially affected by changes in environmental conditions. The impact of life history traits across generations is represented with rainbow arrows. **(G)** Still yet to be answered (?) is if the effects of climatic events (white arrow) will induce a shift (black solid line) of the existing optimum of a trait (blue shaded curve – red solid line) toward a new optimum of the trait (yellow shaded curve – red dotted line) and if this change/adaptation will happen to a rate fast enough to allow species to cope with the effects of climate change.

within populations would be sufficient to cope with the rate of change of climatic variables.

Non-genetic Inheritance

The adaptability of future generations to fluctuating environments can also be influenced by non-genetic inheritance and can happen from one generation to the next (Ezard et al., 2014; Ryu et al., 2018; Bautista and Burggren, 2019; Cavieres et al., 2020). Although not completely understood, the mechanisms responsible for this type of trans-generational acclimation include, maternal provisioning, microbiome transfer, inheritance of epigenetic markers (e.g., DNA methylation,

small RNAs, and histone modifications), and behavioral and cultural processes (Bonduriansky et al., 2012; Burggren, 2016, 2018; Bonduriansky and Day, 2018; Ryu et al., 2018; Bautista et al., 2020; Jablonka and Lamb, 2020; Crespel et al., 2021). Although the role of non-genetic inheritance on adaptation and evolution is still under debate (Laland et al., 2014; Charlesworth et al., 2017), trans-generational effects can be stable and can substantially impact organisms' responses to environmental change over several generations (Ryu et al., 2018; Yin et al., 2019; Jablonka and Lamb, 2020). However, their advantages and disadvantages under the different scenarios of climate change are yet to be determined (Munday, 2014; Morgan et al., 2020; **Figure 1D**). For instance, trans-generational acclimation is particularly advantageous when the change in environmental conditions is slow, and the environmental correlation between parents and offspring is high (Munday, 2014; Uller et al., 2015; Bernal et al., 2018). However, if trans-generational acclimation moves the mean of the phenotype of interest closer to the fitness optima imposed by the environmental change, the strength of selection may be weakened because individuals with different genotypes but with similar phenotypes -induced by non-genetic mechanisms- may exhibit similar fitness (Falconer and Mackay, 1981; Price et al., 2003; Ghalambor et al., 2007; Wild and Traulsen, 2007). Consequently, the rate of genetic adaptation will likely be slowed down (Huey et al., 2009; Donelson et al., 2019), or it can be eliminated in extreme cases (Price et al., 2003). Therefore, more research is still needed to understand this phenomenon and to determine if its buffering capacity would last long enough across generations to lead to genomic fixation (e.g., genetic assimilation). Nonetheless, modeling suggests that when selection acts on genetic and non-genetic mechanisms in the same systems, adaptation takes place at a faster rate than in systems where selection acts just on one mechanism (Klironomos et al., 2013).

FUTURE CHALLENGES AND APPROACHES

Finally, we propose a list of future challenges that can help to elucidate knowledge gaps and better predict, validate, and inform conservation and management actions to preserve ecosystems and biodiversity. Therefore, with this perspective we advocate for future studies to focus on describing the evolutionary implications of the interaction between within- and trans-generational responses to climatic events. The inherent complexity of understanding the effects of climate change -at any of its scales- also highlights the need for interdisciplinary efforts among the scientific community (see **Figure 2**).

Challenge 1: To integrate more realistic and naturally relevant variability of environmental conditions in experimental designs (e.g., stochasticity, daily, or seasonal cycles).

- Include more variability, unpredictable frequency, magnitude, and amplitude of fluctuations in environmental conditions.
- Differentiate the specific effects of weather, climate and climate change events on individual fitness-related traits.
- Consider the interaction between multiple stressors in experimental designs at all scales.

Recommendation: By positioning data loggers in the field, researchers can find information about the magnitude and frequency of natural environmental fluctuations. This information may be also found in public data bases. Microcontrollers (e.g., Arduino, see Drake et al., 2017) or timers can be used on temperature or gas control devices to recreate the fluctuations in experiments. Exposing the studied organisms for different length of time to these conditions will then help to distinguish the impacts of the different climatic events. Furthermore, the recreation of environmental conditions reflecting the interactions between at least two relevant environmental stressors for the organisms (for example among temperature, hypercapnia, hypoxia, pH, and salinity) can be used to provide even more accurate predictions.

Challenge 2: To characterize the effects of climatic events on plastic responses from the cellular to the whole individual level at different developmental stages (embryos, larvae, juveniles, adults, and reproductive adults).

- Document the range of plastic response at the different developmental stages within a population.
- Determine what is the actual partitioning of the roles of specific organs and systems for coping with climatic events as the organism develop.
- Determine the consequences of exposure to climatic events during early life stages for overall species fitness.

Recommendation: For experiments on early development, studies must be guided by specific developmental processes and not by "chronological development." Some things to consider are, for example, when organogenesis or metamorphosis occurs. The use of model species to produce specific knock-out organisms would help to determine the role of specific organs and systems. Experiments on adults could compare the plastic response before, during or after the breeding period in iteroparous species, or at least mention the reproductive status of the individuals under study. Although we acknowledge that there might be technological constraints, we advocate for applying the August Krogh's principle for choosing the right species model to answer the question of interest. Furthermore, analyzing the response of juveniles or adults after an early life stage exposure would provide useful information on the carry-over effects of environmental stress on the species fitness.

Challenge 3: To determine the influence of climatic events (weather, climate, and climate change) on both: individual and combined life-history traits to elucidate its consequences for species resilience.

- Implement more studies considering life history traits to improve experimental designs and interpretation of results.
- Determine the effects of climatic events on the phenology of life history traits.

Recommendation: Studies could include several species representative of different levels across two opposite extremes of any life-history trait of choice in their design or could design and interpret an experiment based on the life history of the species under study. For example, studies will benefit from using more evolutionary approaches for short generation species while focusing on plastic responses for long generations species. In addition, studies could implement re-location of individuals in field studies (under controlled designs) using translocation approaches to see how life-history traits could be modified by the environment. Because of the inherent complexity of integrating a large number of species in these studies, these challenges may be aided by particularly in mathematical modeling.

Challenge 4: To evaluate the limits – if any – of evolutionary adaptation in response to climate change.

- Document if the genetic heterogeneity of populations will be enough to allow for adaptation and relate it with the biology of the species.
- Determine if microevolution can happen in response to climate change and if the rate would be fast enough to overcome its effects.

Recommendation: Studies could determine if future environmental conditions would be able to induce a shift of the optimum values of fitness traits and life-history traits, as well as to determine if species would be able to gradually improve these changes across generations at a rate faster than climate change. Studies could also compare the evolutionary potential of different populations depending on the level of their genetic background or previous experience to new fluctuating environments (e.g., because of geothermal activity). The difference in the genetic basis of the populations either exposed or not could also be evaluated for each generation. This approach will render more precise documentation of the potential and rate of microevolutionary changes. In addition, these experiments would provide even more accurate predictions by including populations composed of individuals at different developmental stages.

Challenge 5: To estimate the limitations and scope (buffering capacities) that trans-generational effects have for species resilience under climatic scenarios.

- Determine the importance of non-genetic inheritance for overcoming environmental challenges, across several generations, by investigating the interaction between within- and trans-generational responses and the specific mechanisms of inheritance.
- Determine how the within generational response of a population can improve or limit the response of future generations.
- Unravel the interplay between genetic and non-genetic molecular basis of physiological, and behavioral responses that help organisms to cope with climatic events, and if these mechanisms can lead to genetic assimilation.

Recommendation: Studies could determine if populations exposed to new environmental challenges are able to adjust their phenotype, transfer it and improve, or limit the response of their offspring over several generations by using common garden experiments. The studies could at the same time document a variety of the different non-genetic mechanisms (for example maternal provisioning, microbiome transfer, or epigenetic markers) to relate to the phenotypic adjustments. Genetic sequencing can also be used in parallel of epigenetic sequencing, to determine if the sequences under epigenetic regulation in one generation match the sequences under genetic evolution in later generations and how those sequences are involved in further non-genetic mechanisms.

DATA AVAILABILITY STATEMENT

The original contributions presented in the study are included in the article/supplementary material, further inquiries can be directed to the corresponding author/s.

AUTHOR CONTRIBUTIONS

NB and AC contributed for conceptualization, manuscript drafting, figure preparation, editing, and revision. Both authors approved the manuscript for submission.

FUNDING

This research was supported by a fellowship from the Kone Foundation (201907804) to AC.

ACKNOWLEDGMENTS

We thank all the many colleagues who through constructive discussions inspired the thoughts covered in this perspective. We also thank the reviewers for their thoughtful comments that helped to improve the manuscript.

REFERENCES

Andrewartha, S. J., and Burggren, W. W. (2012). Transgenerational variation in metabolism and life-history traits induced by maternal hypoxia in *Daphnia magna*. *Physiol. Biochem. Zool.* 85, 625–634. doi: 10.1086/666657

Bautista, N. M., and Burggren, W. W. (2019). Parental stressor exposure simultaneously conveys both adaptive and maladaptive larval phenotypes through epigenetic inheritance in the zebrafish (*Danio rerio*). *J. Exp. Biol.* 222(Pt 17):jeb.208918.

Bautista, N. M., Crespel, A., Crossley, J., Padilla, P., and Burggren, W. (2020). Parental transgenerational epigenetic inheritance related to dietary crude oil exposure in *Danio rerio*. *J. Exp. Biol.* 223(Pt 16):jeb.222224.

Bell, M. A., and Aguirre, W. (2013). Contemporary evolution, allelic recycling, and adaptive radiation of the three- spine stickleback. *Evol. Ecol. Res.* 15, 377–411.

Bernal, M. A., Donelson, J. M., Veilleux, H. D., Ryu, T., Munday, P. L., and Ravasi, T. (2018). Phenotypic and molecular consequences of stepwise temperature increase across generations in a coral reef fish. *Mol. Ecol.* 27, 4516–4528. doi: 10.1111/mec.14884

Bernatchez, L. (2016). On the maintenance of genetic variation and adaptation to environmental change: considerations from population genomics in fishes. *J. Fish Biol.* 89, 2519–2556. doi: 10.1111/jfb.13145

Bonduriansky, R., Crean, A. J., and Day, T. (2012). The implications of nongenetic inheritance for evolution in changing environments. *Evol. Appl.* 5, 192–201. doi: 10.1111/j.1752-4571.2011.00213.x

Bonduriansky, R., and Day, T. (2018). *Extended Heredity: A New Understanding of Inheritance and Evolution*, Vol. 281. Princeton, NJ: Princeton University Press.

Bopp, L., Resplandy, L., Orr, J. C., Doney, S. C., Dunne, J. P., Gehlen, M., et al. (2013). Multiple stressors of ocean ecosystems in the 21st century: projections with CMIP5 models. *Biogeosciences* 10, 6225–6245. doi: 10.5194/bg-10-6225-2013

Burggren, W. (2016). Epigenetic inheritance and its role in evolutionary biology: re-evaluation and new perspectives. *Biology* 5, 1–22. doi: 10.1016/b978-0-12-800049-6.00050-0

Burggren, W. (2018). Developmental phenotypic plasticity helps bridge stochastic weather events associated with climate change. *J. Exp. Biol.* 221:jeb161984.

Burggren, W., and Bautista, N. (2019). Invited review: development of acid-base regulation in vertebrates. *Comp. Biochem. Physiol. A Mol. Integr. Physiol.* 236, 1–14. doi: 10.5005/jp/books/10618_1

Burggren, W. W., Dubansky, B., and Bautista, N. M. (2017). "Cardiovascular development in embryonic and larval fishes," in *Fish Physiology*, eds A. K. Gamperl, T. E. Gillis, A. P. Farrell, and C. J. Brauner (Cambridge, MA: Academic Press), 107–184. doi: 10.1016/bs.fp.2017.09.002

Burlakova, L. E., Karatayev, A. Y., Pennuto, C., and Mayer, C. (2014). Changes in Lake Erie benthos over the last 50years: historical perspectives, current status, and main drivers. *J. Great Lakes Res.* 40, 560–573. doi: 10.1016/j.jglr.2014.02.008

Burraco, P., Orizaola, G., Monaghan, P., and Metcalfe, N. B. (2020). Climate change and ageing in ectotherms. *Glob. Change Biol.* 26, 5371–5381. doi: 10.1111/gcb.15305

Burroughs, W. J. (2007). *Climate Change: A Multidisciplinary Approach*. Cambridge: Cambridge University Press.

Caldeira, K., and Wickett, E. M. (2005). Ocean model predictions of chemistry changes from carbon dioxide emissions to the atmosphere and ocean. *J. Geophys. Res.* 110, 1–12.

Carroll, S. P., Hendry, A. P., Reznick, D. N., and Fox, C. W. (2007). Evolution on ecological time-scales. *Funct. Ecol.* 21, 387–393.

Cavieres, G., Rezende, E. L., Clavijo-Baquet, S., Alruiz, J. M., Rivera-Rebella, C., Boher, F., et al. (2020). Rapid within- and transgenerational changes in thermal tolerance and fitness in variable thermal landscapes. *Ecol. Evol.* 10, 8105–8113. doi: 10.1002/ece3.6496

Cayuela, H., Besnard, A., Bonnaire, E., Perret, H., Rivoalen, J., Miaud, C., et al. (2014). To breed or not to breed: past reproductive status and environmental cues drive current breeding decisions in a long-lived amphibian. *Oecologia* 176, 107–116. doi: 10.1007/s00442-014-3003-x

Chaparro-Pedraza, P. C., and de Roos, A. M. (2019). Environmental change effects on life-history traits and population dynamics of anadromous fishes. *J. Anim. Ecol.* 88, 1178–1190. doi: 10.1111/1365-2656.13010

Charlesworth, D., Barton, N. H., and Charlesworth, B. (2017). The sources of adaptive variation. *Proc. R. Soc. B Biol. Sci.* 284:20162864.

Chaudhary, C., Richardson, A. J., Schoeman, D. S., and Costello, M. J. (2021). Global warming is causing a more pronounced dip in marine species richness around the equator. *Proc. Natl. Acad. Sci.* 11:e2015094118. doi: 10.1073/pnas.2015094118

Crespel, A., Miller, T., Rácz, A., Parsons, K., Lindström, J., and Killen, S. (2021). Density influences the heritability and genetic correlations of fish behaviour under trawling-associated selection. *Evol. Appl.* 00, 1–14.

Crespel, A., Zambonino-Infante, J.-L., Mazurais, D., Koumoundouros, G., Fragkoulis, S., Quazuguel, P., et al. (2017). The development of contemporary European sea bass larvae (*Dicentrarchus labrax*) is not affected by projected ocean acidification scenarios. *Mar. Biol.* 164:155.

Crozier, L. G., and Hutchings, J. A. (2014). Plastic and evolutionary responses to climate change in fish. *Evol. Appl.* 7, 68–87.

Dahlke, F. T., Wohlrab, S., Butzin, M., and Pörtner, H.-O. (2020). Thermal bottlenecks in the life cycle define climate vulnerability of fish. *Science* 369, 65–70.

Darling, E. S., and Côté, I. M. (2008). Quantifying the evidence for ecological synergies. *Ecol. Lett.* 11, 1278–1286.

de Roos, A. M., and Persson, L. (2013). *Population and Community Ecology of Ontogenetic Development*. Princeton, NJ: Princeton University Press.

Dixson, D. L., Jennings, A. R., Atema, J., and Munday, P. L. (2015). Odor tracking in sharks is reduced under future ocean acidification conditions. *Glob. Change Biol.* 21, 1454–1462.

Donelson, J. M., Sunday, J. M., Figueira, W. F., Gaitán-Espitia, J. D., Hobday, A. J., Johnson, C. R., et al. (2019). Understanding interactions between plasticity, adaptation and range shifts in response to marine environmental change. *Philos. Trans. R. Soc. B Biol. Sci.* 374, 1–14.

Drake, M. J., Miller, N. A., and Todgham, A. E. (2017). The role of stochastic thermal environments in modulating the thermal physiology of an intertidal limpet, *Lottia digitalis*. *J. Exp. Biol.* 220, 3072–3083.

Durant, J., Hjermann, D., Ottersen, G., and Stenseth, N. (2007). Climate and the match or mismatch between predator requirements and resource availability. *Clim. Res.* 33, 271–283.

Durtsche, R. D., Jonsson, B., and Greenberg, L. A. (2021). Thermal conditions during embryogenesis influence metabolic rates of juvenile brown trout *Salmo trutta*. *Ecosphere* 12, 1–14.

Ehrenreich, I. M., and Pfennig, D. W. (2016). Genetic assimilation: a review of its potential proximate causes and evolutionary consequences. *Ann. Bot.* 117, 769–779.

Ezard, T. H. G., Prizak, R., and Hoyle, R. B. (2014). The fitness costs of adaptation via phenotypic plasticity and maternal effects. *Funct. Ecol.* 28, 693–701.

Falconer, D. S., and Mackay, T. F. C. (1981). *Introduction to Quantitative Genetics*, 2nd Edn. New York, NY: Longman Group.

Faria, A. M., Lopes, A. F., Silva, C. S. E., Novais, S. C., Lemos, M. F. L., and Gonçalves, E. J. (2018). Reproductive trade-offs in a temperate reef fish under high pCO2 levels. *Mar. Environ. Res.* 137, 8–15.

Ghalambor, C. K., McKay, J. K., Carroll, S. P., and Reznick, D. N. (2007). Adaptive versus non-adaptive phenotypic plasticity and the potential for contemporary adaptation in new environments. *Funct. Ecol.* 21, 394–407.

Gienapp, P., Teplitsky, C., Alho, J. S., Mills, J. A., and Merilä, J. (2008). Climate change and evolution: disentangling environmental and genetic responses. *Mol. Ecol.* 17, 167–178.

Gobler, C. J., and Talmage, S. C. (2013). Short- and long-term consequences of larval stage exposure to constantly and ephemerally elevated carbon dioxide for marine bivalve populations. *Biogeosciences* 10, 2241–2253.

Hairston, N. G., Ellner, S. P., Geber, M. A., Yoshida, T., and Fox, J. A. (2005). Rapid evolution and the convergence of ecological and evolutionary time. *Ecol. Lett.* 8, 1114–1127. doi: 10.1111/j.1461-0248.2005.00812.x

Hannan, K. D., Munday, P. L., and Rummer, J. L. (2020). The effects of constant and fluctuating elevated pCO2 levels on oxygen uptake rates of coral reef fishes. *Sci. Total Environ.* 741:140334. doi: 10.1016/j.scitotenv.2020.140334

Hendry, A. P., Schoen, D. J., Wolak, M. E., and Reid, J. M. (2018). The contemporary evolution of fitness. *Ann. Rev. Ecol. Evol. Syst.* 49, 457–476. doi: 10.1146/annurev-ecolsys-110617-062358

Hoffmann, A. A., and Sgrò, C. M. (2011). Climate change and evolutionary adaptation. *Nature* 470, 479–485. doi: 10.1038/nature09670

Hovel, R. A., Carlson, S. M., and Quinn, T. P. (2017). Climate change alters the reproductive phenology and investment of a lacustrine fish, the three-spine stickleback. *Glob. Change Biol.* 23, 2308–2320. doi: 10.1111/gcb.13531

Huey, R. B., Deutsch, C. A., Tewksbury, J. J., Vitt, L. J., Hertz, P. E., Álvarez Pérez, H. J., et al. (2009). Why tropical forest lizards are vulnerable to climate warming. *Proc. R. Soc. B: Biol. Sci.* 276, 1939–1948. doi: 10.1098/rspb.2008.1957

IPCC (2014). "Climate change 2014: synthesis report," in *Core Writing Team. Contribution of Working Groups I, II and III to the Fifth Assessment Report of the Intergovernmental Panel on Climate Change*, eds R. K. Pachauri and L. A. Meyer (Geneva: IPCC), 151.

Jablonka, E., and Lamb, M. J. (2020). *Inheritance Systems and the Extended Synthesis*. Cambridge: Cambridge University Press. doi: 10.1017/9781108685412

Jenny, J.-P., Francus, P., Normandeau, A., Lapointe, F., Perga, M.-E., Ojala, A., et al. (2016). Global spread of hypoxia in freshwater ecosystems during the last three centuries is caused by rising local human pressure. *Glob. Change Biol.* 22, 1481–1489. doi: 10.1111/gcb.13193

Johansen, J. L., Nadler, L. E., Habary, A., Bowden, A. J., and Rummer, J. (2021). Thermal acclimation of tropical coral reef fishes to global heat waves. *Elife* 10, 1–30. doi: 10.7554/eLife.59162

Jonsson, B., and Jonsson, N. (2014). Early environment influences later performance in fishes. *J. Fish Biol.* 85, 151–188. doi: 10.1111/jfb.12432

Klironomos, F. D., Berg, J., and Collins, S. (2013). How epigenetic mutations can affect genetic evolution: model and mechanism. *Bioessays* 35, 571–578. doi: 10.1002/bies.201200169

Laland, K., Uller, T., Feldman, M., Sterelny, K., Müller, G. B., Moczek, A., et al. (2014). Does evolutionary theory need a rethink? *Nature* 514, 161–164. doi: 10.1038/514161a

Landman, M. J., Van Den Heuvel, M. R., and Ling, N. (2005). Relative sensitivities of common freshwater fish and invertebrates to acute hypoxia. *N. Z. J. Mar. Freshw. Res.* 39, 1061–1067. doi: 10.1080/00288330.2005.9517375

Le Nohaïc, M., Ross, C. L., Cornwall, C. E., Comeau, S., Lowe, R., McCulloch, M. T., et al. (2017). Marine heatwave causes unprecedented regional mass bleaching of thermally resistant corals in northwestern Australia. *Sci. Rep.* 7, 1–11. doi: 10.1038/s41598-017-14794-y

Lefevre, S. (2016). Are global warming and ocean acidification conspiring against marine ectotherms? A meta-analysis of the respiratory effects of elevated temperature, high CO2 and their interaction. *Conserv. Physiol.* 4, 1–31. doi: 10.1093/conphys/cow009

Leo, E., Kunz, K. L., Schmidt, M., Storch, D., Pörtner, H.-O., and Mark, F. C. (2017). Mitochondrial acclimation potential to ocean acidification and warming of Polar cod (*Boreogadus saida*) and Atlantic cod (*Gadus morhua*). *Front. Zool.* 14:21. doi: 10.1186/s12983-017-0205-1

Levins, R. (1968). *Evolution in Changing Environments Some Theoretical Explorations. (MPB-2)*. Princeton, NJ: Princeton University Press. doi: 10.1515/9780691209418

Lüthi, D., Le Floch, M., Bereiter, B., Blunier, T., Barnola, J.-M., Siegenthaler, U., et al. (2008). High-resolution carbon dioxide concentration record 650,000–800,000 years before present. *Nature* 453, 379–382. doi: 10.1038/nature06949

Malhi, Y., Franklin, J., Seddon, N., Solan, M., Turner, M. G., Field, C. B., et al. (2020). Climate change and ecosystems: threats, opportunities and solutions. *Philos. Trans. R. Soc. B Biol. Sci.* 375, 1–8. doi: 10.1098/rstb.2019.0104

Manhard, C. V., Joyce, J. E., and Gharrett, A. J. (2017). Evolution of phenology in a salmonid population: a potential adaptive response to climate change. *Can. J. Fish. Aquat. Sci.* 74, 1519–1527. doi: 10.1139/cjfas-2017-0028

McGuigan, K., Hoffmann, A. A., and Sgrò, C. M. (2021). How is epigenetics predicted to contribute to climate change adaptation? What evidence do we need? *Philos. Trans. R. Soc. B Biol. Sci.* 376, 1–10. doi: 10.1098/rstb.2020.0119

McLeod, I. M., Rummer, J. L., Clark, T. D., Jones, G. P., McCormick, M. I., Wenger, A. S., et al. (2013). Climate change and the performance of larval coral reef fishes: the interaction between temperature and food availability. *Conserv. Physiol.* 1, 1–12. doi: 10.1093/conphys/cot024

Merilä, J., and Hendry, A. P. (2014). Climate change, adaptation, and phenotypic plasticity: the problem and the evidence. *Evol. Appl.* 7, 1–14. doi: 10.1111/eva.12137

Montgomery, D. W., Simpson, S. D., Engelhard, G. H., Birchenough, S. N. R., and Wilson, R. W. (2019). Rising CO2 enhances hypoxia tolerance in a marine fish. *Sci. Rep.* 9:15152. doi: 10.1038/s41598-019-51572-4

Morgan, R., Finnøen, M. H., Jensen, H., Pélabon, C., and Jutfelt, F. (2020). Low potential for evolutionary rescue from climate change in a tropical fish. *Proc. Natl. Acad. Sci.* 117, 33365–33372. doi: 10.1073/pnas.2011419117

Munday, P. L. (2014). Transgenerational acclimation of fishes to climate change and ocean acidification. *F1000prime Rep.* 6, 1–7. doi: 10.12703/P6-99

Parker, T. H. (2002). Maternal condition, reproductive investment, and offspring sex ratio in captive red Junglefowl (*Gallus gallus*). *Auk* 119, 840–845. doi: 10.1642/0004-8038(2002)119[0840:MCRIAO]2.0.CO;2

Parmesan, C., and Yohe, G. (2003). A globally coherent fingerprint of climate change impacts across natural systems. *Nature* 421, 37–42. doi: 10.1038/nature01286

Pinsky, M. L., Worm, B., Fogarty, M. J., Sarmiento, J. L., and Levin, S. A. (2013). Marine taxa track local climate velocities. *Science* 341, 1239–1242. doi: 10.1126/science.1239352

Pistevos, J. C. A., Nagelkerken, I., Rossi, T., and Connell, S. D. (2016). Antagonistic effects of ocean acidification and warming on hunting sharks. *Oikos* 126, 1–21. doi: 10.1111/oik.03182

Price, T. D., Qvarnström, A., and Irwin, D. E. (2003). The role of phenotypic plasticity in driving genetic evolution. *Proc. R. Soc. Lond. Ser. B Biol. Sci.* 270, 1433–1440. doi: 10.1098/rspb.2003.2372

Qui-Minet, Z. N., Coudret, J., Davoult, D., Grall, J., Mendez-Sandin, M., Cariou, T., et al. (2019). Combined effects of global climate change and nutrient enrichment on the physiology of three temperate maerl species. *Ecol. Evol.* 9, 13787–13807. doi: 10.1002/ece3.5802

Rasconi, S., Gall, A., Winter, K., and Kainz, M. J. (2015). Increasing water temperature triggers dominance of small freshwater plankton. *PLoS One* 10:e0140449. doi: 10.1371/journal.pone.0140449

Ratikainen, I. I. and Kokko, H. (2019). The coevolution of lifespan and reversible plasticity. *Nature Commun.* 10, 1–7. doi: 10.1038/s41467-019-08502-9

Réalis-Doyelle, E., Pasquet, A., De Charleroy, D., Fontaine, P., and Teletchea, F. (2016). Strong effects of temperature on the early life stages of a cold stenothermal fish species, Brown Trout (*Salmo trutta* L.). *PLoS One* 11:e0155487. doi: 10.1371/journal.pone.0155487

Renner, S. S., and Zohner, C. M. (2018). Climate change and phenological mismatch in trophic interactions among plants, insects, and vertebrates. *Ann. Rev. Ecol. Evol. Syst.* 49, 165–182. doi: 10.1146/annurev-ecolsys-110617-062535

Reznick, D. N., Losos, J., and Travis, J. (2019). From low to high gear: there has been a paradigm shift in our understanding of evolution. *Ecol. Lett.* 22, 233–244. doi: 10.1111/ele.13189

Rombough, P. (2002). Gills are needed for ionoregulation before they are needed for O2 uptake in developing zebrafish, *Danio rerio*. *J. Exp. Biol.* 205, 1787–1794. doi: 10.1242/jeb.205.12.1787

Rombough, P. J. (1998). Partitioning of oxygen uptake between the gills and skin in fish larvae: a novel method for estimating cutaneous oxygen uptake. *J. Exp. Biol.* 201, 1763–1769. doi: 10.1242/jeb.201.11.1763

Rosa, R., Baptista, M., Lopes, V. M., Pegado, M. R., Ricardo Paula, J., Trübenbach, K., et al. (2014). Early-life exposure to climate change impairs tropical shark survival. *Proc. R. Soc. B Biol. Sci.* 281:20141738. doi: 10.1098/rspb.2014.1738

Rummer, J. L., Couturier, C. S., Stecyk, J. A. W., Gardiner, N. M., Kinch, J. P., Nilsson, G. E., et al. (2014). Life on the edge: thermal optima for aerobic scope of equatorial reef fishes are close to current day temperatures. *Glob. Change Biol.* 20, 1055–1066. doi: 10.1111/gcb.12455

Ryu, T., Veilleux, H. D., Donelson, J. M., Munday, P. L., and Ravasi, T. (2018). The epigenetic landscape of transgenerational acclimation to ocean warming. *Nat. Clim. Change* 8, 504–509. doi: 10.1038/s41558-018-0159-0

Ryu, T., Veilleux, H. D., Munday, P. L., Jung, I., Donelson, J. M., and Ravasi, T. (2020). An epigenetic signature for within-generational plasticity of a reef fish to ocean warming. *Front. Mar. Sci.* 7:284. doi: 10.3389/fmars.2020.00284

Scott, G. R., and Johnston, I. A. (2012). Temperature during embryonic development has persistent effects on thermal acclimation capacity in zebrafish. *Proc. Natl. Acad. Sci.* 109, 14247–14252. doi: 10.1073/pnas.1205012109

Sheppard-Brennand, H., Soars, N., Dworjanyn, S. A., Davis, A. R., and Byrne, M. (2010). Impact of ocean warming and ocean acidification on larval development and calcification in the sea urchin *Tripneustes gratilla*. *PLoS One* 5:e11372. doi: 10.1371/journal.pone.0011372

Spinks, R. K., Munday, P. L., and Donelson, J. M. (2019). Developmental effects of heatwave conditions on the early life stages of a coral reef fish. *J. Exp. Biol.* 222, 1–16. doi: 10.1242/jeb.202713

Thomas, C. D., Cameron, A., Green, R. E., Bakkenes, M., Beaumont, L. J., Collingham, Y. C., et al. (2004). Extinction risk from climate change. *Nature* 427, 145–148. doi: 10.1038/nature02121

Uller, T., English, S., and Pen, I. (2015). When is incomplete epigenetic resetting in germ cells favoured by natural selection? *Proc. R. Soc. B Biol. Sci.* 282, 1–8. doi: 10.1098/rspb.2015.0682

van Tienderen, P. H. (1991). Evolution of generalists and specialists in spatially heterogeneous environments. *Evolution* 45, 1317–1331. doi: 10.1111/j.1558-5646.1991.tb02638.x

van Tienderen, P. H. (1997). Generalists, specialists, and the evolution of phenotypic plasticity in sympatric populations of distinct species. *Evolution* 51, 1372–1380. doi: 10.1111/j.1558-5646.1997.tb01460.x

Vanderplancke, G., Claireaux, G., Quazuguel, P., Madec, L., Ferraresso, S., Sévère, A., et al. (2015). Hypoxic episode during the larval period has long-term effects on European sea bass juveniles (*Dicentrarchus labrax*). *Mar. Biol.* 162, 367–376. doi: 10.1007/s00227-014-2601-9

Wang, H.-Y., Shen, S.-F., Chen, Y.-S., Kiang, Y.-K., and Heino, M. (2020). Life histories determine divergent population trends for fishes under climate warming. *Nat. Commun.* 11, 1–9. doi: 10.1038/s41467-020-17937-4

West-Eberhard, M. J. (2003). *Developmental Plasticity and Evolution*. New York, NY: Oxford University Press. doi: 10.1093/oso/9780195122343.001.0001

Wild, G., and Traulsen, A. (2007). The different limits of weak selection and the evolutionary dynamics of finite populations. *J. Theor. Biol.* 247, 382–390. doi: 10.1016/j.jtbi.2007.03.015

Willis, C. G., Ruhfel, B., Primack, R. B., Miller-Rushing, A. J., and Davis, C. C. (2008). Phylogenetic patterns of species loss in Thoreau's woods are driven by climate change. *Proc. Natl. Acad. Sci.* 105, 17029–17033. doi: 10.1073/pnas.0806446105

Yin, J., Zhou, M., Lin, Z., Li, Q. Q., and Zhang, Y. Y. (2019). Transgenerational effects benefit offspring across diverse environments: a meta-analysis in plants and animals. *Ecol. Lett.* 22, 1976–1986. doi: 10.1111/ele.13373

Zhang, Y., Loreau, M., He, N., Wang, J., Pan, Q., Bai, Y., et al. (2018). Climate variability decreases species richness and community stability in a temperate grassland. *Oecologia* 188, 183–192. doi: 10.1007/s00442-018-4208-1

Conflict of Interest: The authors declare that the research was conducted in the absence of any commercial or financial relationships that could be construed as a potential conflict of interest.

Publisher's Note: All claims expressed in this article are solely those of the authors and do not necessarily represent those of their affiliated organizations, or those of the publisher, the editors and the reviewers. Any product that may be evaluated in this article, or claim that may be made by its manufacturer, is not guaranteed or endorsed by the publisher.

frontiers in Marine Science

ORIGINAL RESEARCH
published: 12 October 2021
doi: 10.3389/fmars.2021.734318

Separating Paternal and Maternal Contributions to Thermal Transgenerational Plasticity

Sarah L. Chang[1], Who-Seung Lee[1,2] and Stephan B. Munch[1]*

[1] Ecology, Evolution, and Behavior, University of California, Santa Cruz, Santa Cruz, CA, United States, [2] Environmental Assessment Group, Korea Environment Institute, Sejong, South Korea

Climate change is rapidly altering the thermal environment in terrestrial and aquatic systems. Transgenerational thermal plasticity (TGP) – which occurs when the temperatures experienced by the parental generation prior to the fertilization of gametes results in a change in offspring reaction norms – may mitigate the effects of climate change. Although "maternal effects" have been widely studied, relatively little is known about TGP effects in vertebrates, particularly paternal contributions. We used artificial fertilization to cross sheepshead minnow (*Cyprinodon variegatus*) parents exposed to either low (26°C) or high (32°C) temperatures and measured growth rates of the offspring over the first 8 weeks of life at both low and high temperatures. A linear mixed effects model was employed to quantify the effects of maternal, paternal, and offspring temperatures on offspring growth and fecundity. We found that the offspring growth rate up to 63 days post-hatch was affected by both the temperature they experienced directly and parental temperatures prior to fertilization. Growth was lowest when neither parents' temperature matched the offspring temperature, indicating a strong transgenerational effect. Notably, offspring growth was highest when all three (offspring, sire, and dam) temperatures matched [although the three-way interaction was found to be marginally non-significant ($P = 0.155$)], suggesting that TGP effects were additive across significant sire-offspring ($P < 0.001$) and dam-offspring interactions ($P < 0.001$). Transgenerational effects on fecundity (GSI) were suggestive for both maternal and paternal effects, but not significant. The finding that thermal TGP is contributed by both parents strongly suggests that it has an epigenetic basis.

Keywords: transgenerational plasticity, paternal effects, maternal effects, *Cyprinodon variegatus*, temperature, growth rate, fecundity

OPEN ACCESS

Edited by:
Lisa N. S. Shama, Wadden Sea Station Sylt, Alfred Wegener Institute Helmholtz Centre for Polar and Marine Research (AWI), Germany

Reviewed by:
Anne Beemelmanns, Memorial University of Newfoundland, Canada
Heather Diana Veilleux, University of Alberta, Canada

****Correspondence:***
Sarah L. Chang
chang.sarahl@gmail.com

Specialty section:
This article was submitted to Global Change and the Future Ocean, a section of the journal Frontiers in Marine Science

Received: *30 June 2021*
Accepted: *22 September 2021*
Published: *12 October 2021*

Citation:
Chang SL, Lee W-S and Munch SB (2021) Separating Paternal and Maternal Contributions to Thermal Transgenerational Plasticity. Front. Mar. Sci. 8:734318. doi: 10.3389/fmars.2021.734318

INTRODUCTION

Global temperatures are predicted to rise by at least 2°C by 2050–2100, a rapid shift that is significantly more than that of the past 420,000 years (Hoegh-Guldberg et al., 2007). Increased ocean temperatures can negatively affect marine organisms, e.g., shifts in metabolic rate (Gillooly et al., 2001), decreased body size at each key developmental stages (Atkinson, 1995), and declines in fish population size (Clark et al., 2003). With accelerating change, potential mismatches between the expected and realized thermal environment are more likely to occur and can substantially

affect key physiological traits across life stages such as reduced growth, maturation, fecundity, and ultimately survival (Kingsolver and Huey, 1998; Pörtner et al., 2001; Hani et al., 2019). However, the ramifications of rapid climate change can be buffered by transgenerational plasticity (TGP), a carryover effect that is characterized by changes in the reaction norms of offspring that are closely correlated to the environment experienced by the parents (Mousseau and Fox, 1998; Donelson et al., 2018). Parental contributions to offspring can therefore alter the strength of selection on organisms during early life stages in response to climate change, allowing for population persistence and adaptation in populations with high genetic diversity (Heckwolf et al., 2018).

Transgenerational plasticity is often described as a generalization of well-studied maternal effects in which the current state of the mother modifies the offspring phenotype. Maternal effects are found in a wide range of both invertebrate and vertebrate taxa (Mousseau and Dingle, 1991; Mousseau and Fox, 1998; Galloway and Etterson, 2007; Shama, 2015; Ruebel and Latham, 2020; McGhee et al., 2021) and arise through a variety of mechanisms, e.g., provisioning of energy or nutrients (Berkeley et al., 2004), hormones (Groothuis and Schwabl, 2008), and antibodies (Grindstaff et al., 2003), or epigenetic mechanisms such as DNA methylation (Cooney et al., 2002) and histone modification (Upadhyaya et al., 2017).

In contrast, paternal effects were initially thought to be minimal or non-existent (Roach and Wulff, 1987). However, increased interest on paternal effects in recent years (Rutkowska et al., 2020) has revealed evidence that non-genetic paternal effects can arise in both mammals and fish through changes in the sperm epigenome and transmission of the paternal DNA methylome that directly affect resulting offspring through DNA methylation (Jiang et al., 2013; Baxter and Drake, 2019; Skvortsova et al., 2019). Effects of epigenetic transfer can be wide ranging, for example, male rats conditioned to fear the smell of acetophenone paired with naive females had produced offspring that also showed an aversion to the same odor (Dias and Ressler, 2014). Offspring sired by male tunicates from low density populations developed faster, a higher hatching success rate, and were more likely to survive when the environment of the offspring matched the environment of the sire (Crean et al., 2013).

With parental effects found to be stronger early in life (Wilson and Reale, 2006), non-genetic paternal effects can play a role in offspring survival across a myriad of taxa that can have long-lasting consequences (Uller, 2008). Importantly, because the mechanisms for non-genetic paternal effects are limited, evidence for paternal effects in TGP provides strong, albeit indirect, evidence that TGP is epigenetic (Curley et al., 2011). Despite growing literature, relatively little is known about non-genetic paternal contributions to thermal performance, particularly in ectothermic vertebrates (but see Shama and Wegner, 2014). Several studies have found that performance is best when the parent and offspring environments match (Shama and Wegner, 2014; Donelson et al., 2018). But when both parents contribute to TGP, which parents' environment is most relevant? Given the more numerous pathways for maternal effects to manifest, we might hypothesize that the maternal environment will have the greatest impact on TGP. Alternatively, since TGP has ostensibly evolved to increase offspring fitness, perhaps TGP is driven by the environment that matches best (or worst). Or more simply, perhaps the contributions of sire and dam are additive, such that TGP is driven by the average parental environment. Distinguishing between these hypotheses would be most relevant for species that have sex-specific aggregations and hence parents with distinct thermal histories, or otherwise display sex differences in life history and behavior before breeding (Tarka et al., 2018). In this situation, to effectively predict transgenerational effects on key offspring fitness traits such as growth rate or reproductive allocation and their implications for population responses to climate change, we would need to determine the interplay between non-genetic maternal and paternal effects. In addition, although the age-specificity of maternal effects is fairly well-studied (e.g., Monteleone and Houde, 1990; Marteinsdottir and Steinarsson, 1998; Gao and Munch, 2013), very little is known about how paternal contributions change over the ontogeny of their offspring.

To fill these gaps, we evaluated the effect of parental temperature on offspring thermal performance, explicitly partitioning sire and dam contributions to growth rate and reproductive allocation using sheepshead minnows (*Cyprinodon variegatus*) as our model organism. Sheepshead minnows are ectothermic fish found on the US East Coast from Massachusetts to Florida and into the Caribbean across a wide range of thermal regimes. They tolerate temperatures between −1.5 and 41.6°C (Bennett and Beitinger, 1997), grow rapidly and mature in under a year (Lee et al., 2017). Moreover, they grow well in individual housings making it possible to eliminate competition for food and social stress as factors influencing growth. Critically, previous studies have found that sheepshead minnows exhibit thermal TGP across multiple generations (Salinas and Munch, 2012; Lee et al., 2020). After 30 days of parental exposure to different temperatures, the fastest growing offspring tend to be individuals whose parents were at the same temperature (Salinas and Munch, 2012; Munch et al., 2021). To control for the possibility of selection on larval survival at different temperatures, the experiment was repeated using the same rearing protocols, but reducing the parental temperature treatment to 7 days. With this brief parental temperature treatment, no effect of the parent temperature was observed. As the only difference between these experiments was the duration of the parent temperature exposure, Salinas and Munch (2012) attributed differences in offspring growth to TGP. However, they used mass-spawning to produce large numbers of fertilized eggs and were thus unable to rigorously control for the possibility of fecundity selection and unable to distinguish between paternal and maternal contributions to phenotype. To resolve these issues, we used artificial fertilization to test for distinct maternal and paternal contributions to offspring growth rate and gonadosomatic index (GSI), key indicators for survival and fecundity that could also be subject to growth-fecundity tradeoffs. Although all husbandry was kept identical to Salinas and Munch (2012), we narrowed the range of acclimation and test temperatures from 21–34°C

down to 24–32°C to reduce concerns about temperature stress and subsequently exposed offspring to parental reproductive temperatures.

MATERIALS AND METHODS

In August 2014, wild juvenile sheepshead minnows (*C. variegatus)* were collected from tidal ponds in South Carolina, United States (32°45′2″ N, 79°53′50″ W) where they typically experienced daily average temperatures between 2.5 and 32.5°C (median temperature = 21.5°C). The fish were acclimated in aquaria held at 24°C at the Southwest Fisheries Science Center, Santa Cruz, California. As sheepshead minnows exhibit grandparental effects (Lee et al., 2020) we maintained breeding populations in the lab under constant temperature (24°C) for three generations, to reduce uncontrolled environmental effects and used F_3 fish as the parents in this experiment.

Fish Crosses

In 2016, we separated F_3 females (n = 40) and males (n = 40) into individual nets for 30 days before the collection of gametes to ensure that eggs were not fertilized before collection. We randomly subdivided these into two groups and acclimated them to experimental temperatures of 26 and 32°C for 30 days which is sufficient to elicit a transgenerational response (Salinas and Munch, 2012). No parents died over this interval.

To examine the degree to which maternal and paternal temperatures affect TGP in F_4 offspring, we artificially crossed males and females from each temperature group in a full factorial design. We anesthetized female fish with MS-222 to reduce handling stress, and conducted strip spawning to collect unfertilized eggs. To obtain sperm, we dissected testes from males euthanized with concentrated MS-222 solution, pulverized the testes in a petri dish and diluted with seawater. Eggs from each female were divided into two petri dishes, with half artificially fertilized with sperm/seawater solution from a randomly selected 26°C male, and the other half by a 32°C male. To ensure fertilization success, the egg-sperm mixture was allowed to sit for ∼30 min. We then subdivided the fertilized eggs from each into separate mesh cages (34.3 × 43.9 × 5.1 cm) for hatching and growth at 26 and 32°C. All subsequent acclimation, feeding, and daily care followed protocols described in Salinas and Munch (2012) which did not generate detectable selection on larvae and juveniles.

One week post-hatch, we randomly selected four (F_4) larvae from each family-temperature combination and placed them into individual growth chambers (8.5 cm diameter × 20.0 cm height) with mesh walls and a solid clear base to allow for tracking of individual growth trajectories and elimination of social interactions. Immediately upon hatching, larvae were fed *Rotifera* until around 5 mm. Larvae between 5 and 10 mm were fed *Artemia nauplii* and then switched to crushed TetraMin (Tetra Holding, Blacksburg, VA, United States) flakes. All feeding for larvae was *ad libitum* four times a day. Seawater was maintained at 20 ppt and photoperiod set at 14:10. Water changes were conducted daily at 10% of the total volume of water in the aquarium table to maintain high water quality. We photographed the fish weekly over 9 weeks with a Canon 40D digital camera (3888 × 2592 pixels; Canon, Japan). At this time all fish within a temperature group were randomly redistributed across aquarium tables to homogenize any table effects. After 9 weeks, we euthanized specimens with concentrated MS-222 solution and dissected them to measure wet body mass (g) and wet gonad mass (g).

Data Analysis

We measured standard length with Image J (Schneider et al., 2012) from weekly photographs. Growth rate (mm/d) was calculated from the change in body length between weeks, starting with weeks 2 and 3. GSI was calculated as the ratio of gonad wet weight to gutted wet weight. Three-way ANOVA tests and *post hoc* Tukey tests were then used to assess the significance of parent and offspring temperature on growth rate and GSI with offspring, sire and dam temperatures as fixed effects and maternal and paternal identity as random effects. Note that aquarium table was not modeled as a random effect, since offspring within a temperature rearing group were redistributed randomly at weekly intervals across tanks throughout the rearing period. To evaluate whether differences in GSI were driven by growth, we repeated the GSI analysis with growth as a covariate as maturation can be growth or size dependent in fish (Ernande et al., 2004). All of the analyses were performed with R Studio (version 1.3.1056) and the package "lmer4" (Bates et al., 2015).

RESULTS

Offspring growth rates assessed at mean parental temperature were consistent with previous trends found in Salinas and Munch (2012) in which the fastest growth occurs when parent and offspring temperatures match (**Figure 1**, **Supplementary Figure 1**, **Table 1**). Sire and dam identity were not significant for offspring growth rate (estimated variance contributed by parent ID was <0.001). For GSI, random effects were not significant for dam (variance = 0.0572) or sire (variance = 0.042). We therefore dropped parent IDs as random effects from subsequent models.

Not surprisingly, offspring growth rate was significantly correlated with offspring rearing temperature ($P < 0.001$) at all days of growth (**Table 2** and **Supplementary Tables 1**, **2**). More interestingly, we found significant interactions between Dam °C × Offspring °C ($P < 0.001$, interaction coefficient = 0.095) and Sire °C × Offspring °C ($P < 0.001$, interaction coefficient = 0.057), but we did not find a significant three-way interaction at any time period (Dam °C × Sire °C × Offspring °C, $P = 0.155$) (**Table 2**). Consequently, TGP results from the additive sum of Dam °C × Offspring °C and Sire °C × Offspring °C interactions (**Figure 1** and **Supplementary Figure 1**), whereas a significant three-way interaction would have resulted in a multiplicative or exponential influence on varied growth trajectories. Additionally, we found that average growth rates were not significantly different between sire temperatures 26 and 32°C within the 26°C offspring group, or between dam/sire temperatures 26/32 and 32/26 in either offspring temperature group (**Supplementary Figure 2**).

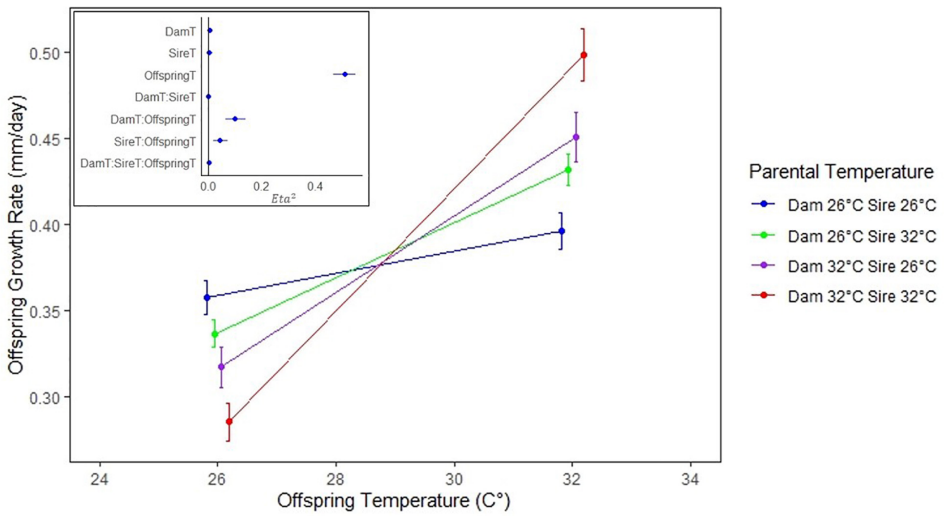

FIGURE 1 | Average growth rate (mm/d) over the first 63 days versus offspring temperature (°C). The red line indicates growth of offspring whose sire and dam were both at 32 (°C). Similarly, the purple, green, and blue lines correspond to dam/sire temperatures of 32/26, 26/32, and 26/26, respectively. Note that the fastest growing offspring at each temperature were those whose parents were both at the same temperature. Average growth rates were not significantly different between sire temperatures 26 and 32 within the 26 offspring group, or between dam/sire temperatures 26/32 and 32/26 in either offspring temperature group. Error bars denote 95% confidence intervals. Inset: Eta^2 for ANOVA results over 63 days of growth, where offspring, dam-offspring, and sire-offspring interactions were found to be significant.

After separation of offspring by sex, we found that both female and male offspring exhibited the same trends, with significant two-way interactions between both Dam °C × Offspring °C ($P < 0.001$) and Sire °C × Offspring °C ($P < 0.05$) on growth rate after 21 days of growth (**Supplementary Tables 1**, **2**). However, among female offspring, we found a significant three-way interaction by 63 days of growth (Dam °C × Sire °C × Offspring °C, $P = 0.006$) (**Supplementary Table 1**).

For both female and male offspring, GSI was most significantly affected by offspring temperature ($P < 0.001$) (**Table 3** and **Figure 2**). Additionally, the trends in GSI across parent temperature treatments paralleled that for growth rate, such that the highest GSI for both offspring sexes was observed when sires, dams, and offspring were at 32°C (**Figures 2A,B**). However, we found that the effects of parental temperature were generally not significant when compared to the effects of offspring temperature, owing to a larger variance in GSI. Only the interaction between Dam °C × Offspring °C was significant for male offspring ($P < 0.001$) (**Table 3**). Among female offspring, only the Offspring °C effect was significant ($P < 0.001$); with no significant interaction between Dam °C × Offspring °C ($P = 0.099$) or Sire °C × Offspring °C ($P = 0.309$) (**Table 3** and **Figure 2B**). In addition, growth rate did not affect GSI for either sex of offspring, as inclusion in the model did not significantly improve model fit and ANOVA with growth rate as a covariate for GSI did not alter results. Overall, we found trends of high parental contribution during the earliest weeks of growth that decreased over the first 5 weeks of age (**Figure 3**).

TABLE 1 | Offspring growth rates at 63 days by mean parent temperature.

Average parental temperature (°C)	Offspring temperature (°C)	*N*	Growth rate	sd
26	26	76	0.36	0.04
26	32	67	0.40	0.04
29	26	147	0.33	0.04
29	32	146	0.44	0.05
32	26	70	0.28	0.05
32	32	75	0.50	0.07

DISCUSSION

Our results are consistent with prior research examining thermal TGP effects on growth rate in fish including, but not limited to: sheepshead minnows, sticklebacks, and tropical reef fish (Donelson et al., 2012; Salinas and Munch, 2012; Shama and Wegner, 2014; Donelson et al., 2018). Our study extends results from previous studies in two ways. First, we found that that TGP effects on growth rate clearly comes from both sires and dams. Importantly, no three-way interaction between dam, sire, and offspring temperature was found affecting offspring growth rate, indicating that the contribution from the parents is additive rather than multiplicative. Moreover, as sire and dam both contribute to TGP effects, the mean parent environment may be sufficient to predict TGP. To evaluate this idea, we repeated the ANOVA using the average parent temperature instead of independent sire and dam temperatures. This reduced model fits the data nearly as well ($R^2 = 0.65$, compared with $R^2 = 0.66$ for the model with distinct parent temperatures). Hence, at least for sheepshead minnows, the mean parent temperature is sufficient for predicting offspring thermal performance.

Secondly, we found that TGP depends on the sex of the offspring; although offspring growth was affected by both

TABLE 2 | 3-way ANOVA with regression results for growth rate (mm day^{-1}) after 30 days of parental temperature exposure at 21, 35, and 63 days of offspring growth (Significance codes: "***" 0.001; "**" 0.05; "." 0.1).

		Growth rate 21 days				Growth rate 35 days				Growth rate 63 days			
Source	**d.f.**	**SS**	**Mean square**	***F***	***P***	**SS**	**Mean square**	***F***	***P***	**SS**	**Mean square**	***F***	***P***
Dam °C	1	0.094	0.094	21.302	<0.001***	0.063	0.063	21.681	<0.001***	0.015	0.015	6.160	0.013*
Sire °C	1	0.014	0.014	3.054	0.081 .	0.016	0.016	5.511	0.019*	0.013	0.013	5.500	0.019*
Offspring °C	1	0.415	0.415	93.947	<0.001***	0.609	0.609	210.636	<0.001***	2.100	2.100	866.770	<0.001***
Dam °C × Sire °C	1	0.003	0.003	0.742	0.389	0.019	0.019	6.432	0.012*	0.001	0.001	0.360	0.550
Dam °C × Offspring °C	1	0.261	0.261	59.097	<0.001***	0.376	0.376	130.152	<0.001***	0.408	0.408	168.370	<0.001***
Sire °C × Offspring °C	1	0.052	0.052	11.674	<0.001***	0.091	0.091	31.313	<0.001***	0.170	0.170	70.150	<0.001***
Dam °C × Sire °C × Offspring °C	1	0.000	0.000	0.036	0.850	0.003	0.003	0.856	0.355	0.005	0.005	2.030	0.155
Residuals	573	2.530	0.004			1.655	0.003			0.840	0.002		

parents regardless of sex, male offspring had no significant three-way interaction at any time point, whereas for female offspring growth, the three-way interaction between sire, dam, and offspring temperature effects were significant at 63 days of growth ($P < 0.05$) and may indicate that TGP can differentially impact growth rate (**Figure 2** and **Supplementary Tables 1**, **2**). This suggests a sex-linked epigenetic mark for certain traits. Existing research on differentiated epigenetic inheritance by sex of the parent is largely focused on maternal impacts (Dunn et al., 2011) thus far, though both paternal and maternal methylation imprints have been observed in mice (Heard and Martienssen, 2014). Recent research on paternal influences in zebrafish have revealed that patterns in paternal DNA methylation are found to be maintained throughout early development of the embryo, allowing for paternal epigenetic signatures to be passed on to offspring (Jiang et al., 2013; Skvortsova et al., 2019).

Previous studies have found a significant interaction between parental treatment temperature and offspring rearing temperature on growth rate (Salinas and Munch, 2012; Shama et al., 2014; Lee et al., 2020; Munch et al., 2021). Here, we found that transgenerational effects on growth rate extend out to 63 days post-hatch, indicating that thermal TGP persists throughout the entire juvenile stage. Consistent with previous studies on maternal effects (e.g., Gao and Munch, 2013), parental contributions were greatest early in life and decreased over the first 5 weeks of age (**Figure 3**). TGP then increased with offspring age to a maximum around 42 days. This may be due to a shift in maturation stages between seven to 8 weeks of growth (Lee et al., 2017). In contrast, other TGP studies in marine sticklebacks have found significant 3-way interactions after 90 days (Shama and Wegner, 2014).

In many fishes, mortality in larval and juvenile stages is extremely size selective (Perez and Munch, 2010) suggesting that TGP should increase offspring survival to maturity. However, we recognize that rapid juvenile growth may have trade-offs with other aspects of performance in fishes, such as swimming speed, behavioral aggression, and somatic energy storage (Schultz and Conover, 1997; dos Santos Schmidt et al., 2021; Mengistu et al., 2021; Monnet et al., 2021). In light of possible growth-fecundity trade-offs, we also examined the impacts of TGP on GSI. We found that GSI significantly increased with offspring temperature and varied with parent temperature in a manner strongly consistent with TGP, although this effect was not significant. This is consistent with the results of Munch et al. (2021), which did find significant TGP in GSI in sheepshead minnows. Hence, although recent meta-analyses have questioned the adaptive value of transgenerational effects (Sánchez-Tójar et al., 2020), the evidence presented here suggests that thermal TGP is adaptive whenever the average parental environment is positively correlated with temperatures their offspring encounter.

Kielland et al. (2017) did not find evidence for TGP in the zooplankton *Daphnia pulex* and suggested that much prior evidence for TGP resulted from experimental artifacts. In light of this, it is worth evaluating potential confounds in our results. The most obvious potential problems are: (a) genetic differences among parents assigned to each temperature treatment; (b)

TABLE 3 | ANOVA results for GSI after 30 days of parental temperature exposure and 63 days of offspring growth (Significance codes: "***" 0.001).

	Gonadosomatic index									
	Male offspring					Female offspring				
Source	**d.f.**	**SS**	**MS**	***F***	***P***	**d.f.**	**SS**	**MS**	***F***	***P***
Dam °C	1	0.780	0.780	0.75	0.388	1	1.200	1.230	0.57	0.453
Sire °C	1	0.010	0.010	0.01	0.918	1	0.100	0.100	0.05	0.832
Offspring °C	1	55.050	55.050	52.91	<0.001***	1	44.200	44.250	20.38	<0.001***
Dam °C × Sire °C	1	0.000	0.000	0.00	0.962	1	0.100	0.110	0.05	0.820
Dam °C × Offspring °C	1	16.680	16.680	16.03	<0.001***	1	6.000	5.960	2.75	0.099
Sire °C × Offspring °C	1	2.450	2.450	2.36	0.126	1	2.300	2.260	1.04	0.309
Dam °C × Sire °C × Offspring °C	1	0.470	0.470	0.46	0.500	1	0.100	0.060	0.03	0.864

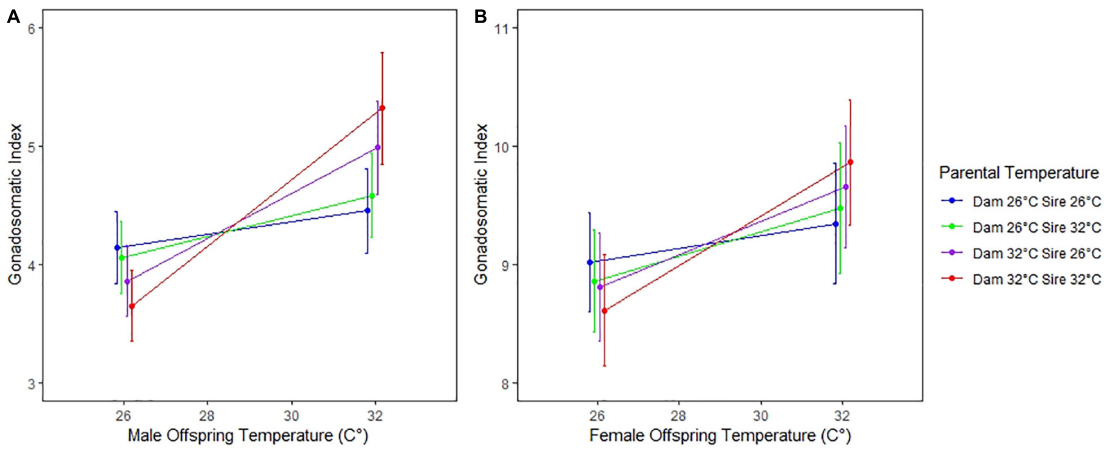

FIGURE 2 | (A) Gonosomatic index for male offspring versus offspring temperature (°C). **(B)** Gonosomatic index for female offspring versus offspring temperature (°C). The red line indicates GSI for offspring whose sire and dam were both at 32 (°C). Similarly, the purple, green, and blue lines correspond to dam/sire temperatures of 32/26, 26/32, and 26/26, respectively. Note that the GSI is largest (hence maturation fastest) for offspring whose parents were both at the same temperature. Error bars denote 95% confidence intervals.

selection on parents during temperature treatment; and (c) selection on offspring during spawning and subsequent rearing. Since the random effects of sire and dam are minimal and non-significant, there is little evidence for substantial genetic differences among parents. Moreover, since no parents died during the temperature treatment and fecundity was equalized by artificial breeding, there is no opportunity for selection on parents to affect the results. Finally, previous work on sheepshead minnows demonstrated that rearing protocols are not responsible for the differences in offspring growth associated with different parent temperature treatments (i.e., the same protocols do not produce TGP when the parent exposure time is short) (Salinas and Munch, 2012; Munch et al., 2021). Therefore, we are reasonably confident that TGP in sheepshead minnows is not an experimental artifact. Moreover, the fact that sire-driven TGP is nearly equal to that contributed by dams after 3 weeks of growth and persists to grand-offspring (Lee et al., 2020), strongly suggest that thermal TGP in offspring growth is epigenetic, though further work is needed to elucidate a specific mechanism, e.g., methylation (Jiang et al., 2013; Skvortsova et al., 2019).

Environmental conditions are changing rapidly in both marine and freshwater environments (Scavia et al., 2002) and TGP may dampen selection resulting from a change in environment (Donelson et al., 2018). As such, TGP may mitigate population decline by alleviating a "phenotype-environment mismatch," ultimately buying time for evolutionary rescue (DeWitt et al., 1998; Marshall et al., 2010; Harmon and Pfennig, 2021). However, although plasticity represents an organismal capacity for extremely rapid phenotypic changes over a single generation, it is unclear how thermal TGP will affect species responses over the long term. For instance, multiple traits may be affected in addition to growth, such as the skewing of offspring gender ratios (Donelson and Munday, 2015), thermosensory behavioral adjustments (Abram et al., 2017), migration pattern (Merlin and Liedvogel, 2019), disease resistance (Moghadam et al., 2015), transgenerational immune priming (Freitak et al., 2009), and hatching success (Stillwell and Fox, 2005).

In addition, although theoretical studies abound (Gomulkiewicz and Holt, 1995; Lande, 2009; McCaw et al., 2020) we know next to nothing about how TGP evolves in natural populations. Walsh et al. (2016) compared the degree of TGP

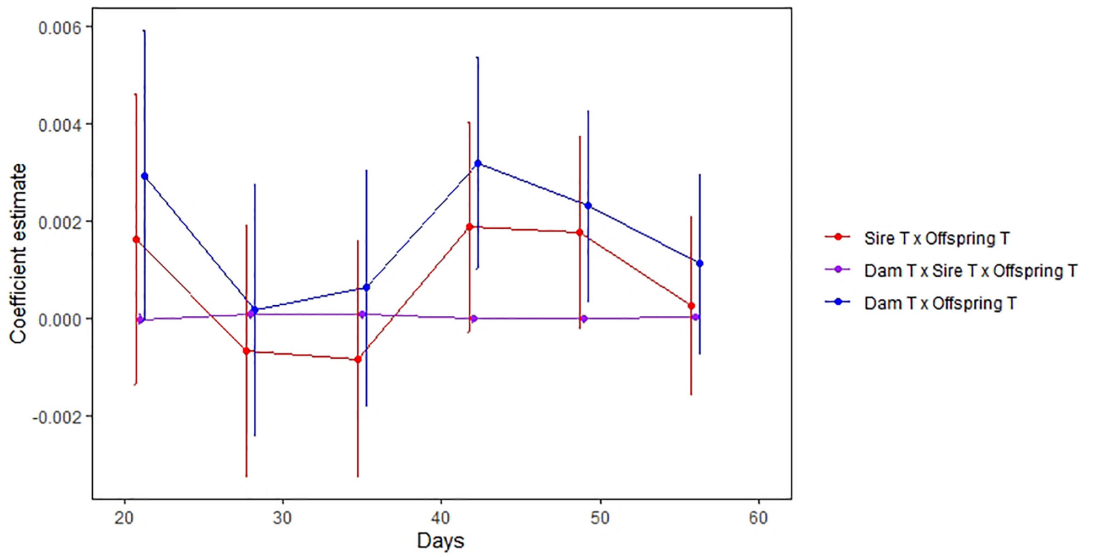

FIGURE 3 | Degree of TGP versus offspring age. The horizontal axis is the age (days) of offspring and the vertical axis is the parent temperature x offspring temperature interaction effect on offspring growth over the previous week. The interaction measures the change in the slope of the growth v. temperature reaction norm attributed to dam (blue) and sire (red) temperature treatments. Effects for dams and sires are largely parallel, with peaks at 20 and 42 days. Error bars denote residual standard error.

in response to predator cues among locally adapted populations and found that the degree of TGP depended on the predictability of predator presence in the native habitat. Moreover, Munch et al. (2021) found that the degree of TGP in sheepshead minnows from different latitudes changes in proportion to the predictability of the thermal environment. Although these geographic patterns are consistent with TGP evolving in response to environmental gradients, they do not tell us how fast TGP will evolve - a critical issue for the impact of a changing climate. In addition, climate change involves multiple drivers and future research should investigate the extent at which TGP could buffer populations with multiple environmental stressors such as hypoxia and ocean acidification (Gobler et al., 2018; Roman et al., 2019). In light of increasingly severe climatic shifts and decreasing environmental predictability, studies elucidating the extent of TGP effects on key physiological and behavioral traits critical to population persistence are an important next step.

DATA AVAILABILITY STATEMENT

The raw data supporting the conclusions of this article are available on the Open Science Forum repository (Identifier: doi: 10.17605/OSF.IO/X2U6H).

ETHICS STATEMENT

The animal study was reviewed and approved by IACUC, Office of Research Compliance, UCSC.

AUTHOR CONTRIBUTIONS

SM conceived and designed the study. SC and W-SL performed the research and conducted analyses. All authors contributed to the manuscript.

FUNDING

This research was generously supported by a Pew Marine Conservation Fellowship to SM and NSF OCE grant #1130483. W-SL was partly supported by the research, "Development of an integrated disease-ecology assessment system" (GP2021-15), funded by the Korea Environment Institute (KEI).

ACKNOWLEDGMENTS

We thank Jamie Bongard for experimental assistance.

SUPPLEMENTARY MATERIAL

The Supplementary Material for this article can be found online at: https://www.frontiersin.org/articles/10.3389/fmars.2021.734318/full#supplementary-material

Supplementary Figure 1 | Interaction plot of average offspring growth rate (mm/d) over the first 63 days versus offspring temperature (°C). The red line indicates growth of offspring at 32, and blue line growth of offspring at 26. Note that the fastest growing offspring at each temperature were those whose parents were both at the same temperature. Error bars denote 95% confidence intervals.

Supplementary Figure 2 | Tukey test for analysis of significance in growth rate between temperature treatment groups. Statistically significant groups did not have the 95% confidence bar overlap with zero difference in mean levels.

REFERENCES

Abram, P. K., Boivin, G., Moiroux, J., and Brodeur, J. (2017). Behavioural effects of temperature on ectothermic animals: unifying thermal physiology and behavioural plasticity. *Biol. Rev.* 92, 1859–1876. doi: 10.1111/brv.12312

Atkinson, D. (1995). Effects of temperature on the size of aquatic ectotherms: exceptions to the general rule. *J. Therm. Biol.* 20, 61–74. doi: 10.1016/0306-4565(94)00028-H

Bates, D., Mächler, M., Bolker, B., and Walker, S. (2015). Fitting linear mixed-effects models using lme4. *J. Stat. Softw.* 67, 1–48. doi: 10.18637/jss.v067.i01

Baxter, F. A., and Drake, A. J. (2019). Non-genetic inheritance via the male germline in mammals. *Philos. Trans. R. Soc. B Biol. Sci.* 374:20180118. doi: 10.1098/rstb.2018.0118

Bennett, W. A., and Beitinger, T. L. (1997). Temperature tolerance of the sheepshead minnow, cyprinodon variegatus. *Copeia* 1997:77. doi: 10.2307/1447842

Berkeley, S. A., Chapman, C., and Sogard, S. M. (2004). Maternal age as a determinant of larval growth and survival in a marine fish, sebastes melanops. *Ecology* 85, 1258–1264. doi: 10.1890/03-0706

Clark, R. A., Fox, C. J., Viner, D., and Livermore, M. (2003). North Sea cod and climate change – modelling the effects of temperature on population dynamics. *Glob. Change Biol.* 9, 1669–1680. doi: 10.1046/j.1365-2486.2003.00685.x

Cooney, C. A., Dave, A. A., and Wolff, G. L. (2002). Maternal methyl supplements in mice affect epigenetic variation and DNA methylation of offspring. *J. Nutr.* 132(8 Suppl), 2393S–2400S. doi: 10.1093/jn/132.8.2393S

Crean, A. J., Dwyer, J. M., and Marshall, D. J. (2013). Adaptive paternal effects? Experimental evidence that the paternal environment affects offspring performance. *Ecology* 94, 2575–2582. doi: 10.1890/13-0184.1

Curley, J. P., Mashoodh, R., and Champagne, F. A. (2011). Epigenetics and the origins of paternal effects. *Horm. Behav.* 59, 306–314. doi: 10.1016/j.yhbeh.2010.06.018

DeWitt, T. J., Sih, A., and Wilson, D. S. (1998). Costs and limits of phenotypic plasticity. *Trends Ecol. Evol.* 13, 77–81. doi: 10.1016/S0169-5347(97)01274-3

Dias, B. G., and Ressler, K. J. (2014). Parental olfactory experience influences behavior and neural structure in subsequent generations. *Nat. Neurosci.* 17, 89–96. doi: 10.1038/nn.3594

Donelson, J. M., and Munday, P. L. (2015). Transgenerational plasticity mitigates the impact of global warming to offspring sex ratios. *Glob. Change Biol.* 21, 2954–2962. doi: 10.1111/gcb.12912

Donelson, J. M., Munday, P. L., McCormick, M. I., and Pitcher, C. R. (2012). Rapid transgenerational acclimation of a tropical reef fish to climate change. *Nat. Clim. Change* 2, 30–32. doi: 10.1038/nclimate1323

Donelson, J. M., Salinas, S., Munday, P. L., and Shama, L. N. S. (2018). Transgenerational plasticity and climate change experiments: Where do we go from here? *Glob. Change Biol.* 24, 13–34. doi: 10.1111/gcb.13903

dos Santos Schmidt, T. C., Hay, D. E., Sundby, S., Devine, J. A., Óskarsson, G. J., Slotte, A., et al. (2021). Adult body growth and reproductive investment vary markedly within and across Atlantic and Pacific herring: a meta-analysis and review of 26 stocks. *Rev. Fish Biol. Fish.* 31, 685–708. doi: 10.1007/s11160-021-09665-9

Dunn, G. A., Morgan, C. P., and Bale, T. L. (2011). Sex-specificity in transgenerational epigenetic programming. *Horm. Behav.* 59, 290–295. doi: 10.1016/j.yhbeh.2010.05.004

Ernande, B., Dieckmann, U., and Heino, M. (2004). Adaptive changes in harvested populations: plasticity and evolution of age and size at maturation. *Proc. Biol. Sci.* 271, 415–423.

Freitak, D., Heckel, D. G., and Vogel, H. (2009). Dietary-dependent trans-generational immune priming in an insect herbivore. *Proc. Biol. Sci.* 276, 2617–2624. doi: 10.1098/rspb.2009.0323

Galloway, L. F., and Etterson, J. R. (2007). Transgenerational plasticity is adaptive in the wild. *Science* 318, 1134–1136. doi: 10.1126/science.1148766

Gao, J., and Munch, S. (2013). Genetic and maternal variation in early growth in the Atlantic silverside Menidia menidia. *Mar. Ecol. Prog. Ser.* 485, 211–222. doi: 10.3354/meps10333

Gillooly, J. F., Brown, J. H., West, G. B., Savage, V. M., and Charnov, E. L. (2001). Effects of size and temperature on metabolic rate. *Science* 293, 2248–2251. doi: 10.1126/science.1061967

Gobler, C. J., Merlo, L. R., Morrell, B. K., and Griffith, A. W. (2018). Temperature, acidification, and food supply interact to negatively affect the growth and survival of the forage fish, *Menidia beryllina* (*Inland Silverside*), and *Cyprinodon variegatus* (*Sheepshead Minnow*). *Front. Mar. Sci* 5:86. doi: 10.3389/fmars.2018.00086

Gomulkiewicz, R., and Holt, R. D. (1995). When does evolution by natural selection prevent extinction? *Evolution* 49, 201–207. doi: 10.2307/2410305

Grindstaff, J. L., Brodie, E. D., and Ketterson, E. D. (2003). Immune function across generations: integrating mechanism and evolutionary process in maternal antibody transmission. *Proc. Biol. Sci.* 270, 2309–2319. doi: 10.1098/rspb.2003.2485

Groothuis, T. G. G., and Schwabl, H. (2008). Hormone-mediated maternal effects in birds: mechanisms matter but what do we know of them? *Philos. Trans. R. Soc. Lond. B. Biol. Sci.* 363, 1647–1661. doi: 10.1098/rstb.2007.0007

Hani, Y. M. I., Turies, C., Palluel, O., Delahaut, L., Bado-Nilles, A., Geffard, A., et al. (2019). Effects of a chronic exposure to different water temperatures and/or to an environmental cadmium concentration on the reproduction of the threespine stickleback (*Gasterosteus aculeatus*). *Ecotoxicol. Environ. Saf.* 174, 48–57. doi: 10.1016/j.ecoenv.2019.02.032

Harmon, E. A., and Pfennig, D. W. (2021). Evolutionary rescue via transgenerational plasticity: evidence and implications for conservation. *Evol. Dev.* 23, 292–307. doi: 10.1111/ede.12373

Heard, E., and Martienssen, R. A. (2014). Transgenerational epigenetic inheritance: myths and mechanisms. *Cell* 157, 95–109. doi: 10.1016/j.cell.2014.02.045

Heckwolf, M. J., Meyer, B. S., Döring, T., Eizaguirre, C., and Reusch, T. B. H. (2018). Transgenerational plasticity and selection shape the adaptive potential of sticklebacks to salinity change. *Evol. Appl.* 11, 1873–1885. doi: 10.1111/eva.12688

Hoegh-Guldberg, O., Mumby, P. J., Hooten, A. J., Steneck, R. S., Greenfield, P., Gomez, E., et al. (2007). Coral reefs under rapid climate change and ocean acidification. *Science* 318, 1737–1742. doi: 10.1126/science.1152509

Jiang, L., Zhang, J., Wang, J.-J., Wang, L., Zhang, L., Li, G., et al. (2013). Sperm, but not oocyte, DNA methylome is inherited by zebrafish early embryos. *Cell* 153, 773–784. doi: 10.1016/j.cell.2013.04.041

Kielland, Ø. N., Bech, C., and Einum, S. (2017). No evidence for thermal transgenerational plasticity in metabolism when minimizing the potential for confounding effects. *Proc. Biol. Sci.* 284:20162494. doi: 10.1098/rspb.2016.2494

Kingsolver, J. G., and Huey, R. B. (1998). Evolutionary analyses of morphological and physiological plasticity in thermally variable environments. *Am. Zool.* 38, 545–560. doi: 10.1093/icb/38.3.545

Lande, R. (2009). Adaptation to an extraordinary environment by evolution of phenotypic plasticity and genetic assimilation. *J. Evol. Biol.* 22, 1435–1446. doi: 10.1111/j.1420-9101.2009.01754.x

Lee, W., Salinas, S., Lee, Y., Siskidis, J. A., Mangel, M., and Munch, S. B. (2020). Thermal transgenerational effects remain after two generations. *Ecol. Evol.* 10, 11296–11303. doi: 10.1002/ece3.6767

Lee, W.-S., Mangel, M., and Munch, S. B. (2017). Developmental order of a secondary sexual trait reflects gonadal development in male sheepshead minnows (*Cyprinodon variegatus*). *Evol. Ecol. Res.* 18, 531–538.

Marshall, D. J., Monro, K., Bode, M., Keough, M. J., and Swearer, S. (2010). Phenotype–environment mismatches reduce connectivity in the sea. *Ecol. Lett.* 13, 128–140. doi: 10.1111/j.1461-0248.2009.01408.x

Marteinsdottir, G., and Steinarsson, A. (1998). Maternal influence on the size and viability of Iceland cod Gadus morhua eggs and larvae. *J. Fish Biol.* 52, 1241–1258. doi: 10.1111/j.1095-8649.1998.tb00969.x

McCaw, B. A., Stevenson, T. J., and Lancaster, L. T. (2020). Epigenetic responses to temperature and climate. *Integr. Comp. Biol.* 60, 1469–1480. doi: 10.1093/icb/icaa049

McGhee, K. E., Barbosa, A. J., Bissell, K., Darby, N. A., and Foshee, S. (2021). Maternal stress during pregnancy affects activity, exploration and potential dispersal of daughters in an invasive fish. *Anim. Behav.* 171, 41–50. doi: 10.1016/j.anbehav.2020.11.003

Mengistu, S. B., Palstra, A. P., Mulder, H. A., Benzie, J. A. H., Trinh, T. Q., Roozeboom, C., et al. (2021). Heritable variation in swimming performance in Nile tilapia (*Oreochromis niloticus*) and negative genetic correlations with growth and harvest weight. *Sci. Rep.* 11:11018. doi: 10.1038/s41598-021-90418-w

Merlin, C., and Liedvogel, M. (2019). The genetics and epigenetics of animal migration and orientation: birds, butterflies and beyond. *J. Exp. Biol.* 222(Pt Suppl 1):jeb191890. doi: 10.1242/jeb.191890

Moghadam, H., Mørkøre, T., and Robinson, N. (2015). Epigenetics—potential for programming fish for aquaculture? *J. Mar. Sci. Eng.* 3, 175–192. doi: 10.3390/jmse3020175

Monnet, G., Rosenfeld, J. S., and Richards, J. G. (2021). Behavioural variation between piscivore and insectivore rainbow trout Oncorhynchus mykiss. *J. Fish Biol.* 99, 955–963. doi: 10.1111/jfb.14781

Monteleone, D. M., and Houde, E. D. (1990). Influence of maternal size on survival and growth of striped bass *Morone saxatilis* Walbaum eggs and larvae. *J. Exp. Mar. Biol. Ecol.* 140, 1–11. doi: 10.1016/0022-0981(90)90076-O

Mousseau, T. A., and Dingle, H. (1991). Maternal effects in insect life histories. *Annu. Rev. Entomol.* 36, 511–534. doi: 10.1146/annurev.en.36.010191.002455

Mousseau, T. A., and Fox, C. W. (1998). The adaptive significance of maternal effects. *Trends Ecol. Evol.* 13, 403–407. doi: 10.1016/S0169-5347(98)01472-4

Munch, S. B., Lee, W. S., Walsh, M., Hurst, T., Wasserman, B. A., Mangel, M., et al. (2021). A latitudinal gradient in thermal transgenerational plasticity and a test of theory. *Proc. Biol. Sci.* 288:20210797.

Perez, K. O., and Munch, S. B. (2010). Extreme selection on size in the early lives of fish. *Evolution* 64, 2450–2457. doi: 10.1111/j.1558-5646.2010.00994.x

Pörtner, H. O., Berdal, B., Blust, R., Brix, O., Colosimo, A., De Wachter, B., et al. (2001). Climate induced temperature effects on growth performance, fecundity and recruitment in marine fish: developing a hypothesis for cause and effect relationships in Atlantic cod (*Gadus morhua*) and common eelpout (*Zoarces viviparus*). *Cont. Shelf Res.* 21, 1975–1997. doi: 10.1016/S0278-4343(01)00038-3

Roach, D. A., and Wulff, R. D. (1987). Maternal effects in plants. *Annu. Rev. Ecol. Syst.* 18, 209–235. doi: 10.1146/annurev.es.18.110187.001233

Roman, M. R., Brandt, S. B., Houde, E. D., and Pierson, J. J. (2019). Interactive effects of hypoxia and temperature on coastal pelagic zooplankton and fish. *Front. Mar. Sci* 6:139. doi: 10.3389/fmars.2019.00139

Ruebel, M. L., and Latham, K. E. (2020). Listening to mother: long-term maternal effects in mammalian development. *Mol. Reprod. Dev.* 87, 399–408. doi: 10.1002/mrd.23336

Rutkowska, J., Lagisz, M., Bonduriansky, R., and Nakagawa, S. (2020). Mapping the past, present and future research landscape of paternal effects. *BMC Biol.* 18:183. doi: 10.1186/s12915-020-00892-3

Salinas, S., and Munch, S. B. (2012). Thermal legacies: transgenerational effects of temperature on growth in a vertebrate. *Ecol. Lett.* 15, 159–163. doi: 10.1111/j.1461-0248.2011.01721.x

Sánchez-Tójar, A., Lagisz, M., Moran, N. P., Nakagawa, S., Noble, D. W. A., and Reinhold, K. (2020). The jury is still out regarding the generality of adaptive 'transgenerational' effects. *Ecol. Lett.* 23, 1715–1718. doi: 10.1111/ele.13479

Scavia, D., Field, J. C., Boesch, D. F., Buddemeier, R. W., Burkett, V., Cayan, D. R., et al. (2002). Climate change impacts on U.S. coastal and marine ecosystems. *Estuaries* 25, 149–164. doi: 10.1007/BF02691304

Schneider, C. A., Rasband, W. S., and Eliceiri, K. W. (2012). NIH Image to ImageJ: 25 years of image analysis. *Nat. Methods* 9, 671–675. doi: 10.1038/nmeth.2089

Schultz, E. T., and Conover, D. O. (1997). Latitudinal differences in somatic energy storage: adaptive responses to seasonality in an estuarine fish (*Atherinidae*: *Menidia menidia*). *Oecologia* 109, 516–529. doi: 10.1007/s004420050112

Shama, L. N. S. (2015). Bet hedging in a warming ocean: predictability of maternal environment shapes offspring size variation in marine sticklebacks. *Glob. Change Biol.* 21, 4387–4400. doi: 10.1111/gcb.13041

Shama, L. N. S., Strobel, A., Mark, F. C., and Wegner, K. M. (2014). Transgenerational plasticity in marine sticklebacks: maternal effects mediate impacts of a warming ocean. *Funct. Ecol.* 28, 1482–1493. doi: 10.1111/1365-2435.12280

Shama, L. N. S., and Wegner, K. M. (2014). Grandparental effects in marine sticklebacks: transgenerational plasticity across multiple generations. *J. Evol. Biol.* 27, 2297–2307. doi: 10.1111/jeb.12490

Skvortsova, K., Tarbashevich, K., Stehling, M., Lister, R., Irimia, M., Raz, E., et al. (2019). Retention of paternal DNA methylome in the developing zebrafish germline. *Nat. Commun.* 10:3054. doi: 10.1038/s41467-019-10895-6

Stillwell, R. C., and Fox, C. W. (2005). Complex patterns of phenotypic plasticity: interactive effects of temperature during rearing and oviposition. *Ecology* 86, 924–934. doi: 10.1890/04-0547

Tarka, M., Guenther, A., Niemelä, P. T., Nakagawa, S., and Noble, D. W. A. (2018). Sex differences in life history, behavior, and physiology along a slow-fast continuum: a meta-analysis. *Behav. Ecol. Sociobiol.* 72:132. doi: 10.1007/s00265-018-2534-2

Uller, T. (2008). Developmental plasticity and the evolution of parental effects. *Trends Ecol. Evol.* 23, 432–438. doi: 10.1016/j.tree.2008.04.005

Upadhyaya, B., Larsen, T., Barwari, S., Louwagie, E. J., Baack, M. L., and Dey, M. (2017). Prenatal exposure to a maternal high-fat diet affects histone modification of cardiometabolic genes in newborn rats. *Nutrients* 9:407. doi: 10.3390/nu9040407

Walsh, M. R., Castoe, T., Holmes, J., Packer, M., Biles, K., Walsh, M., et al. (2016). Local adaptation in transgenerational responses to predators. *Proc. R. Soc. B Biol. Sci.* 283:20152271. doi: 10.1098/rspb.2015.2271

Wilson, A. J., and Reale, D. (2006). Ontogeny of additive and maternal genetic effects: lessons from domestic mammals. *Am. Nat.* 167, E23–E38. doi: 10.1086/498138

Conflict of Interest: The authors declare that the research was conducted in the absence of any commercial or financial relationships that could be construed as a potential conflict of interest.

Publisher's Note: All claims expressed in this article are solely those of the authors and do not necessarily represent those of their affiliated organizations, or those of the publisher, the editors and the reviewers. Any product that may be evaluated in this article, or claim that may be made by its manufacturer, is not guaranteed or endorsed by the publisher.

frontiers in Marine Science

ORIGINAL RESEARCH
published: 16 November 2021
doi: 10.3389/fmars.2021.756683

Trait Response to Nitrogen and Salinity in *Rhizophora mangle* Propagules and Variation by Maternal Family and Population of Origin

Christina L. Richards[1,2†‡], Kristen L. Langanke[1†], Jeannie Mounger[1], Gordon A. Fox[1,3‡] and David B. Lewis[1‡]*

[1] Department of Integrative Biology, University of South Florida, Tampa, FL, United States, [2] Plant Evolutionary Ecology Group, University of Tübingen, Tübingen, Germany, [3] Department of Biology, The University of New Mexico, Albuquerque, NM, United States

OPEN ACCESS

Edited by:
Lisa N. S. Shama, Alfred Wegener Institute, Helmholtz Centre for Polar and Marine Research (AWI), Germany

Reviewed by:
Ketil Koop-Jakobsen, Alfred Wegener Institute, Helmholtz Centre for Polar and Marine Research (AWI), Germany
Emily Dangremond, Roosevelt University, United States

***Correspondence:**
Christina L. Richards
clr@usf.edu

†These authors share first authorship

‡These authors have contributed equally to this work and share senior authorship

Specialty section:
This article was submitted to Global Change and the Future Ocean, a section of the journal Frontiers in Marine Science

Received: *10 August 2021*
Accepted: *24 September 2021*
Published: *16 November 2021*

Citation:
Richards CL, Langanke KL, Mounger J, Fox GA and Lewis DB (2021) Trait Response to Nitrogen and Salinity in Rhizophora mangle Propagules and Variation by Maternal Family and Population of Origin. Front. Mar. Sci. 8:756683. doi: 10.3389/fmars.2021.756683

Many coastal foundation plant species thrive across a range of environmental conditions, often displaying dramatic phenotypic variation in response to environmental variation. We characterized the response of propagules from six populations of the foundation species *Rhizophora mangle* L. to full factorial combinations of two levels of salinity (15 ppt and 45 ppt) reflecting the range of salinity measured in the field populations, and two levels of nitrogen (N; no addition and amended at approximately 3 mg N per pot each week) equivalent to comparing ambient N to a rate of addition of 75 kg per hectare per year. The response to increasing salinity included significant changes, i.e., phenotypic plasticity, in succulence and root to shoot biomass allocation. Propagules also showed plasticity in maximum photosynthetic rate and root to shoot allocation in response to N amendment, but the responses depended on the level of salinity and varied by population of origin. In addition, propagules from different populations and maternal families within populations differed in survival and all traits measured except photosynthesis. Variation in phenotypes, phenotypic plasticity and propagule survival within and among *R. mangle* populations may contribute to adaptation to a complex mosaic of environmental conditions and response to climate change.

Keywords: coastal ecosystem, conservation genetics, foundation species, mangroves, phenotypic plasticity, *Rhizophora mangle*

INTRODUCTION

Many plant species thrive across an extensive range of environmental conditions, often displaying dramatic phenotypic variation (McKee, 1995; Smith and Snedaker, 1995; Richards et al., 2005; Feller et al., 2010). This is particularly true in coastal ecosystems that are characterized by temporal cycles and spatial variation in tidal inundation, temperature, nutrient availability, and salinity (Pennings and Bertness, 2001; Krauss et al., 2008; IPCC, 2014; Proffitt and Travis, 2014; Wuebbles et al., 2014). In addition to the naturally dynamic nature of coastal habitats, anthropogenic activities can increase the input of nutrients and alter watersheds, further contributing to environmental variation (Bertness et al., 2002; Barbier et al., 2008; Gedan et al., 2009, 2011; Crotty et al., 2020). Within these dynamic conditions, foundation plant species such as mangroves provide ecosystem services. These services include providing habitat for many juvenile fish species, biotic filtering of pollutants, and buffering of storms

(Ellison et al., 2005; Zedler and Kercher, 2005; IUCN, 2007; Alongi, 2008, 2013; Costanza et al., 2008; Gedan et al., 2011; Bertness, 2020). Foundation species are defined not only as those that dominate a community assemblage numerically or in biomass, but they also determine diversity of associated taxa through a variety of interactions (Ellison, 2019). Further, foundation species modulate fluxes of nutrients and energy in their ecosystem (Ellison, 2019). Hence, these species disproportionately contribute to maintaining habitat integrity and ecosystem resilience (Bertness and Callaway, 1994; Keith et al., 2017; Ellison, 2019; Bertness, 2020; Qiao et al., 2021). Understanding how these species cope with challenges from anthropogenic impacts is key to preserving the ecosystems they create and define (Gedan et al., 2009, 2011; Guo et al., 2021).

Understanding the mechanisms of response in coastal foundation species has become increasingly important for conservation and management strategies as these species must cope with rising sea levels, increased warming, and anthropogenic disturbances (Gedan et al., 2011; Kirwan and Megonigal, 2013; Osland et al., 2013, 2017). The Food and Agriculture Organization of the United Nations (FAO) estimates that as much as 35% of global mangrove forest habitat has been destroyed since the early 1980's for the development of human settlements, agriculture and aquaculture, and industrial shipping harbors, although the rate of loss appears to have slowed in the last decade (Food and Agriculture Organization of the United Nations, 2007; Polidoro et al., 2010; Ellison et al., 2015; FAO, 2020). In some regions, mangrove trees are also harvested for wood and charcoal (Ellison et al., 2015), resulting in habitat fragmentation and isolation of existing remnant fragments (Friess et al., 2012; Haddad et al., 2015). The resultant loss of diversity could pose risks for these coastal foundation species in the future, particularly as sea levels are projected to rise between 0.2 and 2 m over the next century due to anthropogenic climate change (Melillo et al., 2014).

The vulnerability of coastal foundation plant communities to global change has been debated. Several authors have suggested that the combination of eutrophication and sea-level rise may have a synergistic effect that results in enhanced losses of coastal habitats, and requires further research (Deegan et al., 2012; Kirwan and Megonigal, 2013; Kirwan et al., 2016; Crosby et al., 2017; Schuerch et al., 2018). While coastal eutrophication may enhance growth of foundation species, nutrient enrichment studies have reported a range of impacts on coastal systems depending on the local conditions (Anisfeld and Hill, 2012; Kirwan and Megonigal, 2013). For example, nutrient cycling and marsh stability were affected by local sediment characteristics, soil nutrients, microbial processes, and shifts in allocation of the plant species (McKee et al., 2007; Turner, 2011; Deegan et al., 2012; Lewis et al., 2021).

Predicting species level responses to environmental challenges requires an understanding of the amount of phenotypic variation within and among populations, which may reflect both phenotypic plasticity and heritable differences in phenotype (Richards et al., 2006; Nicotra et al., 2010; Banta and Richards, 2018). Several studies have shown that plant species harbor heritable differences in eco-physiological traits (Arntz and Delph, 2001; Geber and Griffen, 2003; Caruso et al., 2005), and variation in plasticity of traits (Sultan, 2001; Matesanz and Sultan, 2013; Nicotra et al., 2015; Matesanz et al., 2021). However, the amount of variation in natural populations for traits that are important for response to future climates is not well known (Davis and Shaw, 2001; Parmesan, 2006; Lovelock et al., 2016). Plants that inhabit coastal and intertidal zones have putative physiological adaptations that enable them to grow and reproduce in the anoxic and saline conditions that characterize these habitats. These adaptations include adjustment of water required by the plant (Antlfinger and Dunn, 1979, 1983; Glenn and O'Leary, 1984; Donovan et al., 1996; Ball et al., 1997), adjustment of carbon uptake and nutrient absorption (Donovan et al., 1997; Lovelock et al., 2006, 2016; Flowers and Colmer, 2008), and changes in resource allocation (Cavalieri and Huang, 1979; Glenn and O'Leary, 1984; Donovan et al., 1996, 1997; Flowers and Colmer, 2008; Lovelock et al., 2016). In addition, mangrove species can moderate anoxia that results from flooding via root growth, and altered peat formation has allowed mangrove communities to keep pace with sea level rise (McKee et al., 2007). Mangroves have been shown to respond to changes in nitrogen (N) availability by altering relative growth rate, photosynthetic rate, and resource allocation (Feller, 1995; McKee, 1995; Feller et al., 2003), which could be an important response to anthropogenic activities, such as runoff from agriculture and other types of land use change (Feller et al., 2003; Alongi, 2013).

Given spatial differences in salinity, anoxia, and N in the intertidal habitat, plasticity of traits that allow for tolerating such conditions may be adaptive. We expect intertidal plants like mangroves to show plasticity in response to salinity and N conditions (Antlfinger, 1981; Pennings and Richards, 1998; Richards et al., 2010b; Vovides et al., 2014; Lovelock et al., 2016). Proffitt and Travis (2010) found plasticity in growth rate and reproductive output within and among natural *Rhizophora mangle* mangrove populations in the Tampa Bay region of Florida in the United States. However, they also found both site of origin and maternal tree of origin affected *R. mangle* growth and survival, and that these effects varied by intertidal position (significant maternal family by elevation interaction; Proffitt and Travis, 2010). On the other hand, in a study of other Tampa Bay populations, we found low genetic diversity, and little population differentiation (Mounger et al., 2021). Although genetic diversity was low, we discovered high epigenetic diversity based on DNA methylation polymorphisms (Mounger et al., 2021). This type of epigenetic diversity has been associated with phenotypic and functional diversity, and could be a mechanism underlying phenotypic plasticity (Zhang et al., 2013; Nicotra et al., 2015; Herrera et al., 2017; Jueterbock et al., 2020). Several studies have suggested that epigenetic diversity could be particularly important in genetically depauperate species, providing a non-genetic source of response to the diverse conditions experienced by natural populations (Gao et al., 2010; Verhoeven et al., 2010; Richards et al., 2012; Jueterbock et al., 2020). Further, some epigenetic differences have been shown to be heritable. In fact, we discovered that the differences in DNA methylation in *R. mangle* propagules were predicted by maternal tree indicating

a high degree of inheritance of differences in DNA methylation (Mounger et al., 2021).

In this study, we used plants from the same Tampa Bay populations to characterize within and among population level variation in putative adaptive traits in response to combinations of salinity and N in a full factorial design. Given the dynamic environment inhabited by *R. mangle* and the evidence of heritable non-genetic differences among populations, we hypothesized that propagules collected from different populations would respond differently to salinity and N amendment treatments. Our study was designed to test three predictions. First, *R. mangle* seedlings will be plastic in response to salinity and N amendment in putative adaptive traits that conserve water and adjust allocation of N. Second, response to salinity and N amendment will co-vary as plants shift resources to maintain osmotic balance. Finally, populations will vary in putative adaptive traits, and in plasticity of these traits, due to population differentiation.

MATERIALS AND METHODS

Study Species

The red mangrove, *Rhizophora mangle* L. 1753 (Malpighiales, Rhizophoraceae), is an evergreen shrub or tree found along tropical and subtropical coastlines across the Americas, East Africa, Bermuda, and on a number of outlying islands across the South Pacific (Proffitt and Travis, 2014; Tomlinson, 2016; DeYoe et al., 2020) that can grow to heights of 24 m (Bowman, 1917). Poleward expansion of the species is limited by freezing events (its current northern range limit is roughly 29°N latitude; Proffitt and Travis, 2014; Kennedy et al., 2017). *Rhizophora mangle* is considered a self-compatible species, with selfing rates in Tampa Bay estimated to be as high as 80–100% (Proffitt and Travis, 2005; Nadia and Machado, 2014). However, colder temperatures and contaminants from anthropogenic sources correspond with increased flowering and outcrossing, potentially resulting in higher genetic diversity particularly in the smaller populations at range limits from 28 to 30°N (Proffitt and Travis, 2005, 2014). *Rhizophora mangle* stands in our study area have a mean number of about 600 reproducing trees per kilometer of estuary (Proffitt and Travis, 2014). Pollinated *R. mangle* flowers mature in approximately 95 days, producing the buoyant hypocotyl also known as a propagule (Raju Aluri, 2013). The viviparous propagule germinates and matures on the maternal tree before it drops off, is dispersed pelagically, and becomes established as a seedling (McKee, 1995). *Rhizophora mangle* excludes salt in the root system through selective uptake of potassium (K^+) to sodium (Na^+) ions (Wise and Juncosa, 1989; Flowers and Colmer, 2008; Krauss et al., 2008; Medina et al., 2015), and allocates resources to manage osmotic potential (Bowman, 1917; Flowers and Colmer, 2008).

Sampling Design

We collected propagules from six populations of *R. mangle* between June 9 and June 26 of 2015, on the west coast of central Florida (USA) within the following county and state parks: Anclote Key Preserve State Park (AC), Fort De Soto Park (FD), Honeymoon Island State Park (HI), Upper Tampa Bay Conservation Park (UTB), Weedon Island Preserve (WI), and Werner-Boyce Salt Springs State Park (WB) (**Figure 1**). The sites varied in salinity, mean tidal range, and neighboring species. We measured salinity at each site with a refractometer finding that salinity ranged from 20 to 40 parts per thousand (ppt) across the sites at the time of collection. This area has a humid subtropical climate with mean monthly temperatures ranging from 15.6°C in January to 28.5°C in August (1991–2020 monthly normals, U.S. NOAA National Centers for Environmental Information, station GHCND:USC00088824, Tarpon Springs, FL, USA), and annual precipitation of 1379 mm (annual mean 1991–2020, Tarpon Springs station). Precipitation falls as rain, with 60% falling during June through September, and 40% evenly distributed among other months. Monthly mean relative humidity ranges from 67% in April and May to 76% in August and September (1948–2018, U.S. NOAA Comparative Climate Data for the USA through 2018, station GHCND:USW00012842, Tampa International Airport). Tides are semi-diurnal, with 0.57 m median amplitudes (U.S. NOAA National Ocean Service, Clearwater Beach, Florida, station 8726724). Sea-level rise is 4.0 ± 0.6 mm per year (1973–2020 trend, mean $\pm$ 95% confidence interval, NOAA NOS Clearwater Beach station).

Honeymoon Island had a near monoculture of *R. mangle* while the remaining sites contained mixtures of two other mangrove species that are common in Florida: *Laguncularia racemosa* L. and *Avicennia germinans* L. We refer to plants from different sites as members of different populations based on our previous work which found differences among sites based on molecular markers (Mounger et al., 2021). At each population, we collected 20 propagules directly from each of 10 maternal trees separated by at least 10 m from each other to maximize the range of genetic variation sampled within each population (Albrecht et al., 2013). Propagules from each maternal tree were at least half-siblings but they could be more closely related due to the high selfing rate in the study area (Proffitt and Travis, 2005).

We refrigerated the propagules at 4°C for up to 14 days until we planted them in the greenhouse at the University of South Florida Botanical Gardens. The greenhouse temperature was maintained between 18 and 29°C. In the greenhouse, propagules from four of the maternal trees at AC and nine of the maternal trees at FD failed to establish, so we returned to sample propagules from eight new maternal trees at FD on August 12 and 29, and from the same original maternal trees at AC on October 17. Hence, while most of the propagules were in the greenhouse from the end of June until mid-October before they were exposed to treatments, some propagules from these FD and AC maternal families had less acclimation time before treatments began.

Experimental Treatments

We measured the length of each propagule and planted each in a 0.5-L pot with a 50:50 mixture of sand and peat soil. We watered the plants each day with tap water until we started applying the salinity and N amendment in mid-October. We set up the experiment in five spatial blocks. Within each block we randomized the position of plants such that each block had one replicate of each family for each treatment combination [i.e.,

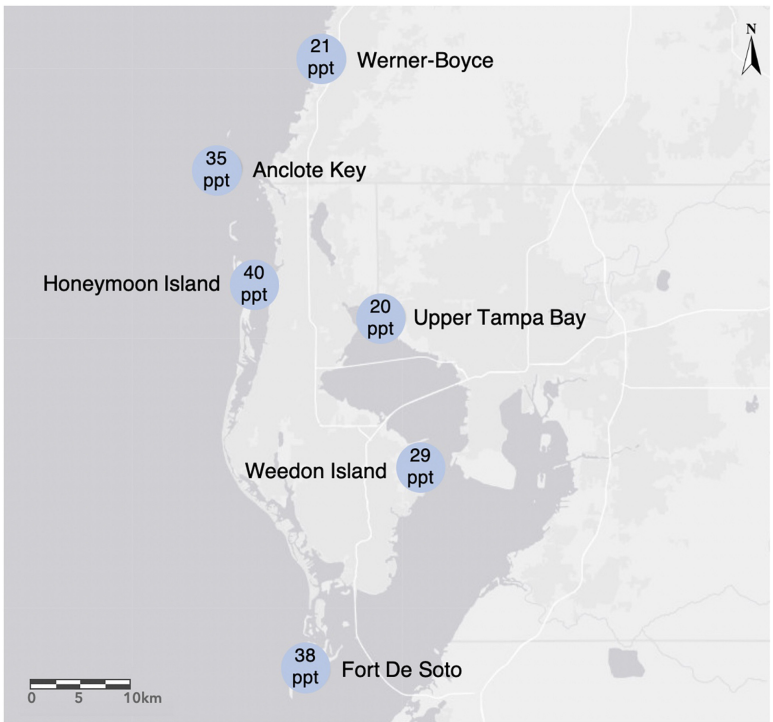

FIGURE 1 | We collected *Rhizophora mangle* propagules from the following sites in the Tampa Bay area on the west coast of Florida, USA: Werner-Boyce Salt Springs State Park, Anclote Key Preserves State Park, Honeymoon Island State Park, Upper Tampa Bay Hillsborough County Park, and Weedon Island Preserve Pinellas County Park. Salinity levels (ppt) on the date of collection for each site are indicated within the site location markers.

a full factorial randomized complete block design with $N = 6$ populations × 10 maternal families × 4 environmental treatment combinations (2 salinity × 2 N fertilization) × 5 blocks × 1 replicate/block = 1200 plants]. The treatments were a factorial combination of low and high salinity with either no addition or addition of N. The salinity treatments were made with Morton solar salt (NaCl). The low salinity treatment was 15 ppt and the high salinity was 45 ppt, reflecting a slightly wider range of salinity than we measured in the field sites considering that we only measured salinity in the field at one time point and we expect the range to be slightly greater. The N treatments were made from equal amounts (in moles N) of urea and ammonium nitrate in tap water approximating 3 mg N per pot each week. This level is similar to a rate of 75 kg N per hectare per year, based on an estimated rate of loss by soil erosion and water runoff from corn crop residue in the USA (Pimentel et al., 1989). The source water for our irrigation solution meets drinking water standards, and thus has low mineral N and phosphorous (P) concentrations, with mineral N (nitrate-N plus ammonium-N) less than 1 mg N/L and P (phosphate) less than 0.1 mg P/L (Penuela Useche, 2015). Furthermore, the aquifer that provides our water had a median sulfate concentration of 8.2 mg/L per liter (interquartile range 2.3–17.8) (Berndt et al., 2015). This sulfur (S) would not be targeted for removal via water treatment, as the Environmental Protection Agency recommended S level is <250 mg S (as SO_4)/L. This level of S would avoid plant S limitation since plants need about 1 mol S per 15–20 mol N.

At the start of treatments, we recorded seedling initial height from the soil to end of any growth. To avoid osmotic shock, the salinity treatment was applied twice a week and gradually increased by five ppt each treatment. The low salinity level (15 ppt) was reached in 2 weeks and the high salinity level (45 ppt) in 6 weeks. We started N treatments after the first week (when salinity treatments were 10 ppt), and applied N once per week from October 15, 2015 to May 1, 2016. We watered on non-treatment days with enough water to saturate the soil, but not flow through. Once per week, we watered with sufficient water to flow through the soil to prevent salt buildup. To determine if the N amendment was lost between treatments, we collected the flow-through leachate for a subset of eight plants, two of each combination of salinity and N treatment. We analyzed leachate for total dissolved N via combustion and luminescent detection (Skalar Formacs TN analyzer, Breda, Netherlands).

Traits Measured

We characterized each plant as alive, dormant, or dead at the end of the experimental treatments. We assigned plants that showed no growth and no desiccation to the dormant category. We measured five traits related to salt tolerance and overall performance for alive plants: change in height from beginning to end of treatments (cm) (hereafter, height growth), leaf mass per area or LMA (dry leaf mass in g/total leaf area cm^2), succulence (grams of water in all leaves/total leaf area cm^2), root to shoot ratio based on dry biomass, and total dry biomass (g) at harvest.

We only used healthy leaves for succulence and LMA. We defined healthy leaves as attached, a minimum of 50% green, and fully developed. For dry above ground biomass, we included leaves that were attached, but not 50% green or fully developed. We measured the biomass of above and below ground tissues of all harvested plants after the tissues were dried at 60°C until they maintained constant mass. Finally, we measured the total dry mass of leaves after drying in silica desiccant beads for a minimum of 7 days to constant mass.

In addition, we used a LI-COR 6400 to measure maximum photosynthetic rate (micromoles CO_2/m^2 s) for a subset of the plants just prior to harvest. We determined that the appropriate photosynthetically active radiation (PAR) for saturation in these plants was 1000 micromoles PAR/m^2 s based on light curves generated from six data points from each of two plants (one low salinity – no N and one high salinity – high N). We then measured maximum photosynthetic rate on one plant with at least two healthy leaves for each surviving maternal line for each treatment (n = 29 low salinity – no N; n = 31 high salinity – no N; n = 26 low salinity – high N; and n = 32 high salinity – high N, for total N = 118 total plants). We took maximum photosynthetic rate measurements at a CO_2 rate of 400 micromoles/(m^2 s) and a flow rate of 500 micromoles/s. We took the measurements on a healthy leaf from the second node of each plant after the leaf had been clamped in the LI-COR for 1 min to ensure conditions had stabilized. We measured maximum photosynthetic rate for the 118 plants in random order by block over six consecutive days from April 23 to 28, 2016, between 8:30 and 11:30 in the morning.

Statistical Analysis

We performed all statistical analyses in R, version 4.0.3 (R Core Team, 2020). All analyses reported here used either the General Linear Model (GLM) or Generalized Linear-Mixed-Model (GLMM) frameworks. GLMs are a generalization of the familiar analysis of variance framework, which allow one to use error distributions other than the restrictive Gaussian used in ANOVA. Moreover, the GLM link function allows one to fit a linear model to a dependent variable that has an essentially non-linear relationship with the predictors. For example, using a log link, one can model the log of the expected value of the data as a linear function; this is distinct from ANOVA on log-transformed data, which models the expected value of the log. GLMMs are a further generalization that allow one to model the variances, rather than expected values, of some predictors. These predictors are sometimes (incorrectly) assumed to be sampled randomly; conceptually the real distinction between these predictors and the others is whether one is interested in the mean values or variances. We fit all models as GLMMs because we were interested in the variance among the maternal families, rather than in their particular means (Bolker, 2015). However, we also fit GLMs that excluded the family terms, to determine whether maternal family contributed to improved model fits. We also treated Block as a "random" term where possible, but when such models failed to converge numerically (due to the small number of blocks) we fit the analogous model with Block as a fixed term (Bolker, 2015).

We checked the residuals to assess normality on traits as appropriate; we did not transform height growth or photosynthesis (lmer and glm), but we used the log link function (glmer) for analysis of succulence, LMA, root to shoot ratio, and total biomass. We used the function lmer or glmer implemented within the lme4 package (Bates et al., 2015) to fit a series of models and identify the best fit model for survival and for each trait (**Table 1**).

For survival and each trait, we began with a saturated model that included as fixed factors salinity, N, and their interaction as well as the random effects of block, population and maternal family nested within population. We ran subsequent models removing individual terms from the model (see details in the **Supplementary Material** file "*Rhizophora mangle* data analysis code and annotated results"). In several cases, models with random terms for block or population failed to converge (**Table 1**), most likely because there were relatively few blocks and populations. In these cases, we proceeded by treating these as fixed effects. We used AIC to evaluate the fit among all of the models that we ran for survival and for each trait. The model with the lowest AIC was considered to have the best fit. We used ANOVA (type III) in the package car (Fox and Weisberg, 2019) to evaluate the significance of fixed effects when they were included in the best model. When the random terms were found to be significant, we provided graphics of the relative differences among the maternal families, populations or blocks in the **Supplementary Material** file "Rhizophora mangle data analysis code and annotated results" to visualize the relative differences among these groups.

For survival, we assessed three states that were coded as 0 for live plants, 1 for dormant plants, and 2 for plants that died during the experiment. We modeled survival using random effects logistic regression. In one set of models, we included dormant plants as alive, and in another we excluded them. The results were qualitatively similar, so we report only the case where dormant plants were treated as alive (see results for both in **Supplementary Material** file "*Rhizophora mangle* data analysis code and annotated results"). For change in height, we included the covariate of height at the beginning of treatments in October.

To gain insight about variance explained by models, we calculated the R^2 approximations proposed by Nakagawa and Schielzeth (2013). As these authors explained, in the context of GLMMs this leads to two different sorts of R^2, a marginal R^2 that reflects variance explained by fixed factors only, and a conditional R^2 that reflects variance explained by both fixed and random factors. We reported each of these as appropriate, e.g., where the best model included only fixed factors we reported only the marginal R^2.

RESULTS

We found that some combination of salinity and N treatments were included in the best models for three of the six traits we measured: succulence, root to shoot biomass ratio, and maximum photosynthetic rate (**Table 1**). In addition, maternal families and populations were significantly different for survival and all traits

TABLE 1 | Model selection based on a series of models using the General Linear Model (GLM) or Generalized Linear-Mixed-Model (GLMM) framework.

	df	AIC	Δ_{AIC}
Survival (*N* = 1149)			
SNG ~ Salt + Pop + (1| Fam) + (1| Block)	9	561.32	0
SNG ~ Salt + Pop + (1| Fam)	8	559.32	−2
SNG ~ N + Pop + (1| Fam) + (1| Block)	9	562.19	0.86
SNG ~ N + Pop + (1| Fam)	8	560.19	−1.14
SNG ~ Pop + (1| Fam) + (1| Block)	8	560.28	−1.04
SNG ~ Pop + (1| Fam)	7	558.28	−3.04
SNG ~ (1| Fam)	2	560.56	−0.76
Height (*N* = 907)			
April ht ~ Oct ht + Salt × N + Block + (1| Pop/Fam)	9	4303.1	0
April ht ~ Oct ht + Salt + N + Block + (1| Pop/Fam)	8	4301.8	−1.4
April ht ~ Oct ht + Salt + N + (1| Pop/Fam)	8	4301.5	−1.6
April ht ~ Oct ht + Salt + (1| Pop/Fam)	6	4298.2	−4.9
April ht ~ Oct ht + (1| Pop/Fam)	5	4297.4	−5.7
Succulence (*N* = 818)			
Succulence ~ Salt × N + (1| Pop/Fam)	7	−6534	0
Succulence ~ Salt + N + (1| Pop/Fam)	6	−6533.5	0.5
Succulence ~ Salt + (1| Pop/Fam)	5	−6534.5	−0.5
LMA (*N* = 818)			
LMA ~ Salt × N + (1| Pop/Fam) + (1| Block)	8	−8041.9	0
LMA ~ Salt + N + (1| Pop/Fam) + (1| Block)	7	−8043.9	−2
LMA ~ Salt + (1| Pop/Fam)	6	−8045.9	−4
LMA ~ (1| Pop/Fam) + (1| Block)	5	−8041.8	0.1
Root to shoot biomass ratio (*N* = 899)			
RTS ~ Salt × N + (1| Pop/Fam) + (1| Block)	8	1255.1	0
Total biomass (*N* = 899)			
Total biomass ~ Salt × N + Block + (1| Pop/Fam)	8	4869.7	0
Total biomass ~ Salt × N + (1| Pop/Fam)	7	4867.8	−0.1
Total biomass ~ (1| Pop/Fam)	4	4864.5	−5.2
Maximum photosynthetic rate (*N* = 118)			
Photosynthesis ~ Salt × N + Pop + Block + (1| Fam)	14	592.9	0
Photosynthesis ~ Salt × N + Site + (1| Fam)	10	587.7	−5.1
Photosynthesis ~ Salt × N + Block + (1| Fam)	10	585.4	−7.4
Photosynthesis ~ Salt × N + (1| Fam)	6	580.4	−12.4
Photosynthesis ~ Salt × N	4	578.4	−14.5

We started with a saturated model that included salinity, N, and their interaction as fixed factors as well as the random effects of block, population and maternal family nested within population. We ran subsequent models after removing individual terms from the model (see details in ***Supplementary Material*** *file "Rhizophora mangle data analysis code and annotated results"). Fam, maternal family; ht, height; LMA, leaf mass per area (dry mass/area); Pop, population; Pop/Fam, maternal families nested within source populations; RTS, root to shoot biomass ratio; SNG, number of survivors in April. Terms in parentheses are random terms; (1\| term) indicates that a random intercept is estimated for each term. For some models, Block or Pop were fit as fixed effects if estimation as random effects failed (generally due to the small numbers of blocks and source populations). Δ_{AIC} is the difference between the saturated model (or closest model to it when saturated model was singular) and the AIC for the given model.*

measured with the exception of photosynthesis (**Table 1**). Below we report the results of model selection and assess significance of effects retained in the best model.

Treatment Validation

To ensure that our N amendment treatments were not flushed out during the once weekly flow through watering we measured the total dissolved N in leachate from a subsample of the seedlings. We found that N was not significantly different between the low salinity – no N and the high salinity – high N amended plants, and therefore, confirmed that we did not lose the N due to watering between treatments [Mean Square = 0.11, F ndf 3/ddf 48 = 0.23, Pr(>F) = 0.88].

Survival

Of 1,149 plants, 76 were unequivocally dead in April, 907 unequivocally alive, and 166 dormant. The number of plants that showed active growth ranged from 63% in HI to 92% in FD (**Figure 2**). The number of plants that did not grow, but also did not appear to be dead ranged from 3% in WB and WI to 10% in HI. We modeled survival by including these dormant plants alternatively as either alive or dead. In both cases, the best-supported model was one including a fixed effect for population and a random effect for maternal family (**Table 1**; **Supplementary Figure 1**). The model treating dormant plants as alive had conditional R^2 = 0.11 and marginal R^2 = 0.08. The model with dormant plants as dead had conditional R^2 = 0.28 and marginal R^2 = 0.13. Because there is no residual in the equation defining logistic regression, no variance component for a random residual is calculated, and thus it is not possible to calculate a meaningful scaled variance component for family here.

Trait Responses to Treatment

The only useful predictor among the fixed effects for the change in height was the height at the start of treatments in October (**Table 1**; marginal R^2 = 0.82; ANOVA chisq = 4432.67; $p < 0.0001$). The conditional R^2 was 0.92, and the marginal R^2 was 0.82, indicating that 82% of the variance in change in height was explained by a positive relationship with the fixed effect of height at the beginning of the experimental treatments (estimate = 0.9009). The variance components (scaled to sum to 1) for population and maternal family within population were 23 and 37% of the random variance, respectively. A plot of the random effects suggested that the populations were largely similar, with the exception of FD which was very different (**Supplementary Figure 2**). It is not obvious that any population had more among-family variability, but our design was limited to determine this.

For LMA (log link), the best model included only the random effects of block, population and maternal family within population. The conditional R^2 was 0.99. In this model, maternal family explained 51% of the variance, population explained 30% of the variance and block explained 17% (**Supplementary Figure 3**).

For succulence (log link) the best model included the fixed effect of salinity and the random effects of population and maternal family nested within population. The marginal R^2 = 0.39, while the conditional R^2 = 0.99. The scaled variance components for maternal family within population and population were, respectively, 0.91 and 0; in other words there was very large variance among maternal families within populations, but not among populations (**Supplementary Figure 3**). While increased salinity resulted in a statistically meaningful reduction in succulence, it was only when

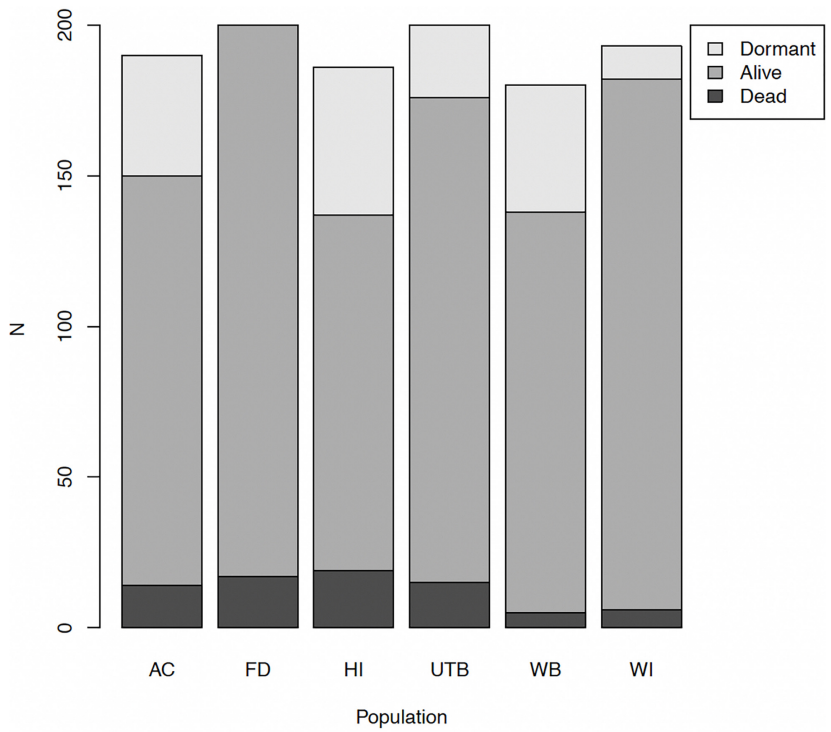

FIGURE 2 | Absolute numbers of plants in each growth state at harvest by population of origin. Dormant plants (light gray) showed no signs of desiccation or growth. Seedlings from the HI population had the lowest survival overall, while WI seedlings had the highest survival. Plants alive at harvest are medium gray, plants that had died by harvest are dark gray.

conditioned on family that it added to the explanatory power of the model.

Root to shoot biomass ratio (log link) was the only variable for which the data supported the saturated model as the best model (**Figure 3**). The conditional $R^2 = 0.206$, while the marginal $R^2 = 0.017$. An ANOVA to evaluate the fixed effects revealed that the main effect of salinity was significant (chisq = 7.38; $p = 0.007$) indicating increased root to shoot allocation in response to salinity, but not the main effect of N. In addition, the interaction of salinity × N was significant (chisq = 6.19; $p = 0.01$). At ambient N levels (no N added), root to shoot ratio was not affected by increasing salt concentration. With the addition of N fertilizer, root to shoot ratio increased in response to high salinity (**Figure 3B**). However, the small size of the marginal R^2 suggested that these effects were mainly meaningful when conditioned on the random terms. The random terms population, maternal family nested within population, and block account for 13, 24, and 6% of the random variance, respectively (**Supplementary Figure 5**).

The best model for total biomass (log link) included only the random effects of population and maternal family within population. The conditional $R^2 = 0.12$. The terms for population and family nested within population accounted for 13 and 21% of the random variance, respectively (**Supplementary Figure 6**).

The photosynthesis data were the most limited in sample size since we were only able to assess one individual with at least two healthy leaves for each surviving maternal line for each treatment ($N = 118$). The best model was one including the fixed effects salinity, N, and their interaction, but no random effects (**Table 1**). An ANOVA to evaluate these fixed effects showed the main effects of salinity and N were not significant but the interaction was (chisq = 4.46; $p = 0.035$). At ambient N levels (no N added), maximum photosynthetic rate declined with increasing salt concentration, but this negative impact of salinity was absent or reversed upon the addition of N fertilizer (**Figure 3C**).

In summary, we found plasticity to our treatments for three of the six traits we measured. Succulence decreased in response to higher salinity (**Figure 3A**), but this response varied largely by family (**Supplementary Figure 3**). For root to shoot biomass ratio and maximum photosynthetic rate the responses to experimental treatments depended on changes in both salinity and N (**Figures 3B,C**). Root to shoot ratio also varied overall in response to salinity as well as by family and population (**Supplementary Figure 4**).

DISCUSSION

We assessed the growth and survival of *R. mangle* propagules to full factorial combinations of two salt and two N levels because these are two important abiotic properties that potentially have important impacts on mangrove survival and traits, and by extension, on the biodiversity and ecosystem function of coastal wetlands. In addition to natural variation in these conditions,

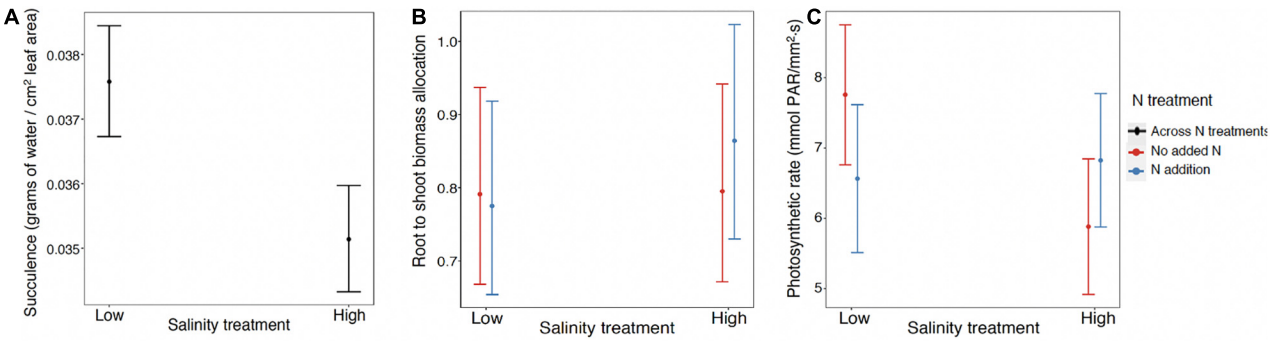

FIGURE 3 | (A) Succulence response to salt across populations with no N effect, including the random effects of maternal families within populations and populations (*N* = 818). Interaction effect for **(B)** root to shoot biomass allocation and **(C)** photosynthetic rate where response to N depends on salt treatment across all mangrove propagules. The best model for root to shoot biomass allocation (*N* = 899) also includes the fixed effect of salt and random effects of population, maternal family within population and block. The best model for photosynthetic rate (*N* = 118) does not include any of the random effects.

anthropogenic activities may result in more extreme levels of these conditions from runoff and flooding (Ellison et al., 2005; Krauss et al., 2006; Gedan et al., 2009; Kirwan and Megonigal, 2013; Lewis et al., 2014). We predicted that *R. mangle* seedlings would be plastic in response to salinity and N amendment in putative adaptive traits that conserve water and adjust allocation of N. Our study showed that only succulence and root to shoot ratio were plastic in response to salt, regardless of N treatment. Allocation to root and shoot biomass and maximum photosynthetic rate were also plastic, but response of both traits to N amendment depended on the level of salt. This supported our second prediction that response to salinity and N amendment will co-vary as plants shift resources to maintain osmotic balance. We also found support for our third prediction that populations would vary in putative adaptive traits, and in plasticity of these traits, due to population differentiation. Importantly, every trait except for photosynthesis varied among population and maternal families within populations. This was also true of survival. In fact, maternal family and population were the most consistent predictors for variation in traits and survival.

Phenotypic Plasticity in Response to Treatments

We expected that *R. mangle* propagule survival and growth would decrease in response to high salinity and increase in response to N fertilization. We also expected that N could alleviate some of the effects of salinity as indicated by an interaction of the two conditions. However, we found no response to treatments in survival, height growth, LMA or total dry biomass. This may be because the propagules were supported by resources provided by the maternal tree, which in *R. mangle* can support growth for at least a year (Ball, 2002; Proffitt and Travis, 2010). If the seedlings were supported by these maternal reserves, height growth would likely be more correlated to propagule length at collection which would be corrected for in the start-of-experiment (time zero) height measurements that we included as a covariate. Because our treatment duration was only 6 months, the lack of growth response to treatments was consistent with dependence on maternal reserves. However, we did see seedling response to treatment in succulence, allocation to root and shoot biomass and maximum photosynthetic rate.

Increased succulence is a common response to water deficiency under high salinity conditions (Rosenthal et al., 2002; Vendramini et al., 2002; Ottow et al., 2005; Karrenberg et al., 2006; Richards et al., 2008, 2010a), but in our experiment we detected reduced succulence in response to high salt. However, this could be because *R. mangle* excludes salt. Many halophytes absorb high concentrations of salt for osmotic adjustment that would normally be toxic. One strategy is to compartmentalize these ions along with increased succulence (Flowers and Colmer, 2008). On the other hand, many plants avoid this toxicity by excluding salt at the roots (Cavalieri and Huang, 1979; Donovan et al., 1996; Tester and Davenport, 2003). For example, several other halophytes that are salt excluders, including the succulent plant *Salicornia europaea* L., and another member of Rhizophoraceae, *Kandelia candel* (L.) Druce, do not increase succulence or leaf thickness in response to high salinity (Glenn and O'Leary, 1984; Kao et al., 2001). In fact, with N fertilization *K. candel* decreased leaf thickness when salinity was increased (Kao et al., 2001). Thus, one possible explanation for our results is that the N fertilized seedlings were able to reallocate resources (e.g., increased N) to salt tolerance mechanisms like compatible solutes, and still maintain positive water balance in the high salt condition without increased succulence.

Although we saw a statistically significant response to our treatments in three of the six traits, the interaction between salt and N fertilization only effected R:S and maximum photosynthetic rate. We expected maximum photosynthetic rate to increase in response to N fertilization because the enzyme RuBisCO, which catalyzes the dark reactions in photosynthesis, requires a large amount of N (Sage et al., 1987; Andersson, 2008). Further, a meta-analysis across 356 diverse species representing most biomes and growth forms showed increased maximum photosynthetic rate with increased N is a general phenomenon (Walker et al., 2014). This could lead to increased biomass

allocation to shoots relative to roots. Despite this expectation, there was no overall response to high N level independent of salt treatment. One reason might be that photosynthesis overall was limited by other nutrients, not just N, and thus increasing N alone might not have been enough to elicit a response (see e.g., Lovelock et al., 2006). In a field study, dwarf *R. mangle* did not respond to N alone, presumably because other nutrients were limiting (Feller, 1995; Lovelock et al., 2006). Dwarf mangroves did increase biomass in response to fertilization with all three nutrients: N, phosphorus (P), and potassium ions (K^+) (Feller, 1995), and in response to P addition alone (Lovelock et al., 2006). We also expected that response to N amendment would depend on salinity. We found that in plants treated with high salt, maximum photosynthetic rate was slightly enhanced by high N. Possibly, the additional N enabled the plants to synthesize N-rich compatible solutes for osmotic regulation and continued photosynthetic gain of carbon (Flowers and Colmer, 2008). Plants in high salt also responded differently in allocation of biomass with increased N; instead of increasing shoot biomass, they increased root biomass on average.

Variation Within and Among Sites

Phenotypic variation that is maintained in common garden from within and among populations would indicate *R. mangle* has heritable trait diversity which could allow for response to changing environmental conditions. Seedling survival depended on population and varied among maternal families within the six populations. We found variation in height growth, succulence, LMA, root to shoot allocation, and total dry biomass was largely determined by maternal families within populations. Proffitt and Travis (2010) also found seedling survival varied among maternal families, as well as by location in the intertidal zone. But in their study after 3 years, growth and survival did not reflect initial propagule size (Proffitt and Travis, 2010). Our results support these previous findings that propagule length is positively correlated to short term performance. This findings suggests that maternal reserves in the *R. mangle* propagule can help the seedling survive, and larger propagules contain more maternal reserves than smaller propagules (Ball, 2002; Proffitt and Travis, 2010). Because our study was a short-term, controlled greenhouse study, maximum photosynthetic rate might be the best indicator as an immediate response. Variation in maximum photosynthetic rate can ultimately manifest as variation in growth and allocation of resources, particularly once the seedling has depleted maternal reserves. The seedlings did not show significant differences in height growth or total dry biomass in response to treatments. But given the plasticity we saw in maximum photosynthetic rate, and the 1-year and 3-year growth results found in a previous study of nearby populations (Proffitt and Travis, 2010), we might have found a more dramatic response to these treatments with more time (Ball and Farquhar, 1984). However, previous work in several different systems have argued that greenhouse studies are often unable to recreate relevant field conditions, so such responses may only be registered in the field (Schittko et al., 2016; Rinella and Reinhart, 2017; Forero et al., 2019; Dostál et al., 2020).

The amount of heritable phenotypic diversity and differentiation we discovered in this study is an important indicator of the potential for this species to respond to changing conditions. The high level of diversity in response among populations and maternal families within populations may be surprising since we previously reported low genetic diversity among these plants based on molecular markers. Low genetic diversity is expected to limit the potential for different responses among individuals. On the other hand, we discovered high epigenetic diversity (Mounger et al., 2021), which could contribute to phenotypic and functional diversity, and could be a mechanism underlying the type of phenotypic differences and plasticity we found here (Zhang et al., 2013; Nicotra et al., 2015; Herrera et al., 2017; Jueterbock et al., 2020). In addition, we know very little about the interactions with the microbiome in the species, but microbes have been highlighted as important symbionts in these and other challenging environments (Bowen et al., 2017; Angermeyer et al., 2018; Jung et al., 2021). Soil microbial activity could have dramatic impacts on the future nutrient availability and stability of these coastal sediments (Deegan et al., 2012; Bowen et al., 2017; Hughes et al., 2020; Lewis et al., 2021). In fact, a recent study suggested that bacterial community composition differed among *R. mangle* maternal genotypes but not with genetic diversity (Craig et al., 2020).

CONCLUSION

Previous work suggested that *R. mangle* growth and survival depended on an interaction of intertidal elevation and maternal genotype, suggesting variation in response to flooding conditions (Proffitt and Travis, 2010). However, in addition to changes in flooding, anthropogenic activities are causing changes in salinity and N level in *R. mangle* ecosystems (McKee et al., 2007). The interacting effects of salinity, N level, and elevation are complex and potentially non-additive (McKee et al., 2007). Our experimental findings suggest that the important traits of succulence, root to shoot biomass allocation and photosynthetic rate respond to salinity, N level, or the combination of these conditions. We also discovered that seedling survival and the magnitude of almost all responses varied among populations and even maternal families within populations.

This variation in survival and important traits among families and among populations is particularly interesting considering the importance of this foundation species for the functioning of the coastal ecosystem. Our previous work showed a lack of genetic diversity, which might be alarming considering the expected limitations of low genetic variation (Allendorf et al., 2010; Estoup et al., 2016). However, accumulating studies provide important evidence that genetic variation must be interpreted with caution (Hufford and Mazer, 2003; Estoup et al., 2016) and that the emphasis on only variation in DNA sequence can be misguided (Keller, 2002, 2014; Sultan, 2015; Bonduriansky and Day, 2018). Non-genetic sources of response may contribute to the phenotypic diversity we report here that is particularly relevant under different salinity and N conditions. This may provide another source of resilience for *R. mangle* and other critical species to changing environmental conditions

and contribute to future adaptation to a complex mosaic of environmental conditions.

DATA AVAILABILITY STATEMENT

All of the data collected and analyzed for this study along with R code are included in the **Supplementary Material**, Further inquiries can be directed to the corresponding author.

AUTHOR CONTRIBUTIONS

CR, KL, GF, and DL conceived the study and designed the experiments. KL and JM collected plants and maintained the experiments. KL and GF analyzed the data. CR and KL wrote the first draft of the manuscript. All authors provided input and revisions to the manuscript.

FUNDING

This work was supported by funding from the National Science Foundation (United States) IOS-1556820 (to CR), DUE-1930451 (to DL), and the Federal Ministry of Education and Research (BMBF, Germany; MOPGA Project ID 306055 to CR).

ACKNOWLEDGMENTS

We thank Bert Anderson, Sandy Voors, Viviana Penuela Useche, M. Teresa Boquete, Mariano Alverez, and Marta Robertson for their help with analyses and review of earlier versions of this manuscript. We are grateful to Christine Brubaker, Racquel Pancho, Brianna Jerman, Vernetta Williams, Alan Franck, and Mary Mangiapia for their guidance, and Charley's Pizza for great food during greenhouse and plant processing work. We also thank Samantha Blonder, Jordan Dollbaum, Maria Nikolopoulos, Shane Palmer, Bradley Biega, Bryan Lotici, Harper Cassidy, Jelena Dosen, Nancy Sheridan, and Dawei Tang for their help in the field and the greenhouse, and our friends and family for constant support and encouragement. Finally, we acknowledge support by the Open Access Publishing Fund of University of Tübingen.

SUPPLEMENTARY MATERIAL

The Supplementary Material for this article can be found online at: https://www.frontiersin.org/articles/10.3389/fmars.2021.756683/full#supplementary-material

Supplementary Data Sheet 1 | SD1_ Code and Results.pdf = Rhizophora mangle data analysis code and annotated results (including **Supplementary Figures 1–6**).

Supplementary Data Sheet 2 | SD2_List of variable names.pdf = used in Rhizophora mangle data analysis code and annotated results.

Supplementary Data Sheet 3 | SD3_2017011 All No Calcs.csv data used to calculate survivorship.

Supplementary Data Sheet 4 | SD4_20170211 Survivors Pairs.csv data used with all plants to examine correlation.

Supplementary Data Sheet 5 | SD5_20170211 Survivors No Calcs.csv data used used for height, R:S and biomass.

Supplementary Data Sheet 6 | SD6_20160420 Final R25.csv data used for succulence and LMA data.

Supplementary Data Sheet 7 | SD7_20170728 licor FDFC.txt data used for photosynthetic rate.

REFERENCES

Albrecht, M., Kneeland, K. M., Lindroth, E., and Foster, J. E. (2013). Genetic diversity and relatedness of the mangrove *Rhizophora mangle* L. (Rhizophoraceae) using amplified fragment polymorphism (AFLP) among locations in Florida, USA and the Caribbean. *J. Coast. Conserv.* 17, 483–491. doi: 10.1007/s11852-013-0246-3

Allendorf, F. W., Hohenlohe, P. A., and Luikart, G. (2010). Genomics and the future of conservation genetics. *Nat. Rev. Genet.* 11, 697–709. doi: 10.1038/nrg2844

Alongi, D. (2013). Cycling and global fluxes of nitrogen in mangroves. *Glob. Environ. Res.* 17, 173–182.

Alongi, D. M. (2008). Mangrove forests: resilience, protection from tsunamis, and responses to global climate change. *Estuar. Coast. Shelf Sci.* 76, 1–13. doi: 10.1016/j.ecss.2007.08.024

Andersson, I. (2008). Catalysis and regulation in Rubisco. *J. Exp. Bot.* 59, 1555–1568. doi: 10.1093/jxb/ern091

Angermeyer, A., Crosby, S. C., and Huber, J. A. (2018). Salt marsh sediment bacterial communities maintain original population structure after transplantation across a latitudinal gradient. *PeerJ* 6:e4735. doi: 10.7717/peerj.4735

Anisfeld, S. C., and Hill, T. D. (2012). Fertilization effects on elevation change and belowground carbon balance in a Long Island sound tidal marsh. *Estuar. Coast.* 35, 201–211. doi: 10.1007/s12237-011-9440-4

Antlfinger, A. E. (1981). The genetic basis of microdifferentiation in natural and experimental populations of *Borrichia frutescens* in relation to salinity. *Evolution* 35, 1056–1068. doi: 10.1111/j.1558-5646.1981.tb04974.x

Antlfinger, A. E., and Dunn, E. L. (1979). Seasonal patterns of CO2 and water vapor exchange of three salt marsh succulents. *Oecologia* 43, 249–260. doi: 10.1007/BF00344952

Antlfinger, A. E., and Dunn, E. L. (1983). Water use and salt balance in three salt marsh succulents. *Am. J. Bot.* 70:561. doi: 10.2307/2443167

Arntz, M. A., and Delph, L. F. (2001). Pattern and process: evidence for the evolution of photosynthetic traits in natural populations. *Oecologia* 127, 455–467. doi: 10.1007/s004420100650

Ball, M. C. (2002). Interactive effects of salinity and irradiance on growth: implications for mangrove forest structure along salinity gradients. *Trees* 16, 126–139. doi: 10.1007/s00468-002-0169-3

Ball, M. C., Cochrane, M. J., and Rawson, H. M. (1997). Growth and water use of the mangroves *Rhizophora apiculata* and *R. stylosa* in response to salinity and humidity under ambient and elevated concentrations of atmospheric CO2. *Plant Cell Environ.* 20, 1158–1166. doi: 10.1046/j.1365-3040.1997.d01-144.x

Ball, M. C., and Farquhar, G. D. (1984). Photosynthetic and stomatal responses of the grey mangrove, avicennia marina, to transient salinity conditions. *Plant Physiol.* 74, 7–11. doi: 10.1104/pp.74.1.7

Banta, J. A., and Richards, C. L. (2018). Quantitative epigenetics and evolution. *Heredity* 121, 210–224. doi: 10.1038/s41437-018-0114-x

Barbier, E. B., Koch, E. W., Silliman, B. R., Hacker, S. D., Wolanski, E., Primavera, J., et al. (2008). Coastal ecosystem-based management with nonlinear ecological functions and values. *Science* 319, 321–323. doi: 10.1126/science.1150349

Bates, D., Mächler, M., Bolker, B., and Walker, S. (2015). Fitting linear mixed-effects models Usinglme4. *J. Stat. Softw.* 67:1. doi: 10.18637/jss.v067.i01

Berndt, M. P., Katz, B. G., Kingsbury, J. A., and Crandall, C. A. (2015). The quality of our Nation's waters: water quality in the Upper Floridan aquifer

and overlying surficial aquifers, southeastern United States, 1993-2010. *Circular* 1355:72. doi: 10.3133/cir1355

Bertness, M. (2020). *A Brief Natural History of Civilization: Why a Balance Between Cooperation and Competition Is Vital to Humanity*. Yale: Yale University Press.

Bertness, M. D., and Callaway, R. (1994). Positive interactions in communities. *Trends Ecol. Evol.* 9, 191–193. doi: 10.1016/0169-5347(94)90088-4

Bertness, M. D., Ewanchuk, P. J., and Silliman, B. R. (2002). Anthropogenic modification of New England salt marsh landscapes. *Proc. Natl. Acad. Sci. U.S.A.* 99, 1395–1398. doi: 10.1073/pnas.022447299

Bolker, B. M. (2015). "Linear and generalized linear mixed models," in *Ecological Statistics*, eds G. A. Fox, S. Negrete-Yankelevich, and V. J. Sosa (Oxford: Oxford University Press), 309–333.

Bonduriansky, R., and Day, T. (2018). *Extended Heredity*. Princeton, NJ: Princeton University Press.

Bowen, J. L., Kearns, P. J., Byrnes, J. E. K., Wigginton, S., Allen, W. J., Greenwood, M., et al. (2017). Lineage overwhelms environmental conditions in determining rhizosphere bacterial community structure in a cosmopolitan invasive plant. *Nat. Commun.* 8:433. doi: 10.1038/s41467-017-00626-0

Bowman, H. H. M. (1917). Ecology and physiology of the red mangrove. *Proc. Am. Philos. Soc.* 56, 589–672.

Caruso, C. M., Maherali, H., Mikulyuk, A., Carlson, K., and Jackson, R. B. (2005). Genetic variance and covariance for physiological traits in Lobelia: are there constraints on adaptive evolution? *Evolution* 59, 826–837. doi: 10.1111/j.0014-3820.2005.tb01756.x

Cavalieri, A. J., and Huang, A. H. C. (1979). Evaluation of proline accumulation in the adaptation of diverse species of marsh halophytes to the saline environment. *Am. J. Bot.* 66, 307–312. doi: 10.1002/j.1537-2197.1979.tb06228.x

Costanza, R., Pérez-Maqueo, O., Martinez, M. L., Sutton, P., Anderson, S. J., and Mulder, K. (2008). The value of coastal wetlands for hurricane protection. *Ambio* 37, 241–248.

Craig, H., Kennedy, J. P., Devlin, D. J., Bardgett, R. D., and Rowntree, J. K. (2020). Effects of maternal genotypic identity and genetic diversity of the red mangrove *Rhizophora mangle* on associated soil bacterial communities: a field-based experiment. *Ecol. Evol.* 10, 13957–13967. doi: 10.1002/ece3.6989

Crosby, S. C., Angermeyer, A., Adler, J. M., Bertness, M. D., Deegan, L. A., Sibinga, N., et al. (2017). Spartina alterniflora biomass allocation and temperature: implications for salt marsh persistence with sea-level rise. *Estuar. Coast.* 40, 213–223. doi: 10.1007/s12237-016-0142-9

Crotty, S. M., Ortals, C., Pettengill, T. M., Shi, L., Olabarrieta, M., Joyce, M. A., et al. (2020). Sea-level rise and the emergence of a keystone grazer alter the geomorphic evolution and ecology of southeast US salt marshes. *Proc. Natl. Acad. Sci. U.S.A.* 117, 17891–17902. doi: 10.1073/pnas.1917869117

Davis, M. B., and Shaw, R. G. (2001). Range shifts and adaptive responses to Quaternary climate change. *Science* 292, 673–679. doi: 10.1126/science.292.5517.673

Deegan, L. A., Johnson, D. S., Warren, R. S., Peterson, B. J., Fleeger, J. W., Fagherazzi, S., et al. (2012). Coastal eutrophication as a driver of salt marsh loss. *Nature* 490, 388–392. doi: 10.1038/nature11533

DeYoe, H., Lonard, R. I., Judd, F. W., Stalter, R., and Feller, I. (2020). Biological flora of the tropical and subtropical intertidal zone: literature review for *Rhizophora mangle* L. *J. Coast. Res.* 36:857. doi: 10.2112/jcoastres-d-19-00088.1

Donovan, L. A., Richards, J. H., and Muller, M. W. (1996). Water relations and leaf chemistry of *Chrysothamnus nauseosus* ssp. *Consimilis* (Asteraceae) and *Sarcobatus vermiculatus* (Chenopodiaceae). *Am. J. Bot.* 83:1637. doi: 10.2307/2445840

Donovan, L. A., Richards, J. H., and Schaber, E. J. (1997). Nutrient relations of the halophytic shrub, Sarcobatus vermiculatus, along a soil salinity gradient. *Plant Soil* 190, 105–117. doi: 10.1023/A:1004211207079

Dostál, P., Fischer, M., and Prati, D. (2020). Comparing experimental and field-measured traits and their variability in Central European grassland species. *J. Veg. Sci.* 31, 561–570. doi: 10.1111/jvs.12875

Ellison, A., Farnsworth, E., and Moore, G. (2015). *Rhizophora Mangle. IUCN Red List of Threatened Species*. Gland: IUCN.

Ellison, A. M. (2019). Foundation species, non-trophic interactions, and the value of being common. *iScience* 13, 254–268. doi: 10.1016/j.isci.2019.02.020

Ellison, A. M., Bank, M. S., Clinton, B. D., Colburn, E. A., Elliott, K., Ford, C. R., et al. (2005). Loss of foundation species: consequences for the structure and dynamics of forested ecosystems. *Front. Ecol. Environ.* 3, 479–486.

Estoup, A., Ravigné, V., Hufbauer, R., Vitalis, R., Gautier, M., and Facon, B. (2016). Is there a genetic paradox of biological invasion? *Annu. Rev. Ecol. Evol. Syst.* 47, 51–72. doi: 10.1146/annurev-ecolsys-121415-032116

FAO (2020). *Global Forest Resources Assessment 2020*. Rome: FAO.

Feller, I. C. (1995). Effects of nutrient enrichment on growth and herbivory of dwarf red mangrove (*Rhizophora mangle*). *Ecol. Monogr.* 65, 477–505. doi: 10.2307/2963499

Feller, I. C., Lovelock, C. E., Berger, U., McKee, K. L., Joye, S. B., and Ball, M. C. (2010). Biocomplexity in mangrove ecosystems. *Ann. Rev. Mar. Sci.* 2, 395–417. doi: 10.1146/annurev.marine.010908.163809

Feller, I. C., Whigham, D. F., McKee, K. L., and Lovelock, C. E. (2003). Nitrogen limitation of growth and nutrient dynamics in a disturbed mangrove forest, Indian River Lagoon, Florida. *Oecologia* 134, 405–414. doi: 10.1007/s00442-002-1117-z

Flowers, T. J., and Colmer, T. D. (2008). Salinity tolerance in halophytes. *New Phytol.* 179, 945–963. doi: 10.1111/j.1469-8137.2008.02531.x

Food and Agriculture Organization of the United Nations (2007). *The World's Mangroves 1980-2005. A Thematic Study Prepared in the Framework of the Global Forest Resources Assessment 2005 [2007]*. Rome: FAO.

Forero, L. E., Grenzer, J., Heinze, J., Schittko, C., and Kulmatiski, A. (2019). Greenhouse- and field-measured plant-soil feedbacks are not correlated. *Front. Environ. Sci.* 7:184. doi: 10.3389/fenvs.2019.00184

Fox, J., and Weisberg, S. (2019). *An R Companion to Applied Regression, Third edition*. Thousand Oaks, CA: Sage.

Friess, D. A., Krauss, K. W., Horstman, E. M., Balke, T., Bouma, T. J., Galli, D., et al. (2012). Are all intertidal wetlands naturally created equal? Bottlenecks, thresholds and knowledge gaps to mangrove and saltmarsh ecosystems. *Biol. Rev. Camb. Philos. Soc.* 87, 346–366. doi: 10.1111/j.1469-185x.2011.00198.x

Gao, L., Geng, Y., Li, B., Chen, J., and Yang, J. (2010). Genome-wide DNA methylation alterations of *Alternanthera philoxeroides* in natural and manipulated habitats: implications for epigenetic regulation of rapid responses to environmental fluctuation and phenotypic variation. *Plant Cell Environ.* 33, 1820–1827. doi: 10.1111/j.1365-3040.2010.02186.x

Geber, M. A., and Griffen, L. R. (2003). Inheritance and natural selection on functional traits. *Int. J. Plant Sci.* 164, S21–S42. doi: 10.1086/368233

Gedan, K. B., Kirwan, M. L., Wolanski, E., and Barbier, E. B. (2011). The present and future role of coastal wetland vegetation in protecting shorelines: answering recent challenges to the paradigm. *Clim. Change* 106, 7–29. doi: 10.1007/s10584-010-0003-7

Gedan, K. B., Silliman, B. R., and Bertness, M. D. (2009). Centuries of human-driven change in salt marsh ecosystems. *Ann. Rev. Mar. Sci.* 1, 117–141. doi: 10.1146/annurev.marine.010908.163930

Glenn, E. P., and O'Leary, W. (1984). Relationship between salt accumulation and water content of dicotyledonous halophytes. *Plant Cell Environ.* 7, 253–261. doi: 10.1111/1365-3040.ep11589448

Guo, J., Richards, C. L., Holsinger, K. E., Fox, G. A., Zhang, Z., and Zhou, C. (2021). Genetic structure in patchy populations of a candidate foundation plant: a case study of *Leymus chinensis* (Poaceae) using genetic and clonal diversity. *Am. J. Bot.* doi: 10.1002/ajb2.1771

Haddad, N. M., Brudvig, L. A., Clobert, J., Davies, K. F., Gonzalez, A., Holt, R. D., et al. (2015). Habitat fragmentation and its lasting impact on Earth's ecosystems. *Sci. Adv.* 1:e1500052. doi: 10.1126/sciadv.1500052

Herrera, C. M., Medrano, M., and Bazaga, P. (2017). Comparative epigenetic and genetic spatial structure of the perennial herb *Helleborus foetidus*: isolation by environment, isolation by distance, and functional trait divergence. *Am. J. Bot.* 104, 1195–1204. doi: 10.3732/ajb.1700162

Hufford, K. M., and Mazer, S. J. (2003). Plant ecotypes: genetic differentiation in the age of ecological restoration. *Trends Ecol. Evol.* 18, 147–155. doi: 10.1016/s0169-5347(03)00002-8

Hughes, A. R., Moore, A. F. P., and Gehring, C. (2020). Plant response to fungal root endophytes varies by host genotype in the foundation species *Spartina alterniflora*. *Am. J. Bot.* 107, 1645–1653. doi: 10.1002/ajb2.1573

IPCC (2014). Climate change 2014: synthesis report. *Paper Presented at the Contribution of Working Groups I, II and III to the Fifth Assessment Report of*

the Intergovernmental Panel on Climate Change, eds R. K. Pachauri and L. A. Meyer Geneva (Switzerland: IPCC).

IUCN (2007). *Environmental and Socio Economic Value of Mangroves in Tsunami Affected Areas*. Gland: IUCN.

Jueterbock, A., Boström, C., Coyer, J. A., Olsen, J. L., Kopp, M., Dhanasiri, A. K. S., et al. (2020). The seagrass methylome is associated with variation in photosynthetic performance among clonal shoots. *Front. Plant Sci.* 11:571646. doi: 10.3389/fpls.2020.571646

Jung, J. H., Reis, F., Richards, C. L., and Bossdorf, O. (2021). Understanding plant microbiomes requires a genotype × environment framework. *Am. J. Bot.* 108, 1–4. doi: 10.1002/ajb2.1742

Kao, W.-Y., Tsai, H.-C., and Tsai, T.-T. (2001). Effect of NaCl and nitrogen availability on growth and photosynthesis of seedlings of a mangrove species, *Kandelia candel* (L.) Druce. *J. Plant Physiol.* 158, 841–846. doi: 10.1078/0176-1617-00248

Karrenberg, S., Edelist, C., Lexer, C., and Rieseberg, L. (2006). Response to salinity in the homoploid hybrid species *Helianthus paradoxus* and its progenitors *H. annuus* and *H. petiolaris*. *New Phytol.* 170, 615–629. doi: 10.1111/j.1469-8137.2006.01687.x

Keith, A. R., Bailey, J. K., Lau, M. K., and Whitham, T. G. (2017). Genetics-based interactions of foundation species affect community diversity, stability and network structure. *Proc. Biol. Sci.* 284:20162703. doi: 10.1098/rspb.2016.2703

Keller, E. F. (2002). *The Century of the Gene*. Cambridge, MA: Harvard University Press.

Keller, E. F. (2014). From gene action to reactive genomes. *J. Physiol.* 592, 2423–2429. doi: 10.1113/jphysiol.2014.270991

Kennedy, J. P., Garavelli, L., Truelove, N. K., Devlin, D. J., Box, S. J., Chérubin, L. M., et al. (2017). Contrasting genetic effects of red mangrove (*Rhizophora mangle*L.) range expansion along West and East Florida. *J. Biogeogr.* 44, 335–347. doi: 10.1111/jbi.12813

Kirwan, M. L., and Megonigal, J. P. (2013). Tidal wetland stability in the face of human impacts and sea-level rise. *Nature* 504, 53–60. doi: 10.1038/nature12856

Kirwan, M. L., Temmerman, S., Skeehan, E. E., Guntenspergen, G. R., and Fagherazzi, S. (2016). Overestimation of marsh vulnerability to sea level rise. *Nat. Clim. Chang.* 6, 253–260. doi: 10.1038/nclimate2909

Krauss, K. W., Lovelock, C. E., McKee, K. L., López-Hoffman, L., Ewe, S. M. L., and Sousa, W. P. (2008). Environmental drivers in mangrove establishment and early development: a review. *Aquat. Bot.* 89, 105–127. doi: 10.1016/j.aquabot.2007.12.014

Krauss, K. W., Twilley, R. R., Doyle, T. W., and Gardiner, E. S. (2006). Leaf gas exchange characteristics of three neotropical mangrove species in response to varying hydroperiod. *Tree Physiol.* 26, 959–968. doi: 10.1093/treephys/26.7.959

Lewis, D. B., Brown, J. A., and Jimenez, K. L. (2014). Effects of flooding and warming on soil organic matter mineralization in *Avicennia germinans* mangrove forests and *Juncus roemerianus* salt marshes. *Estuar. Coast. Shelf Sci.* 139, 11–19. doi: 10.1016/j.ecss.2013.12.032

Lewis, D. B., Jimenez, K. L., Abd-Elrahman, A., Andreu, M. G., Landry, S. M., Northrop, R. J., et al. (2021). Carbon and nitrogen pools and mobile fractions in surface soils across a mangrove saltmarsh ecotone. *Sci. Total Environ.* 798:149328. doi: 10.1016/j.scitotenv.2021.149328

Lovelock, C. E., Ball, M. C., Choat, B., Engelbrecht, B. M. J., Holbrook, N. M., and Feller, I. C. (2006). Linking physiological processes with mangrove forest structure: phosphorus deficiency limits canopy development, hydraulic conductivity and photosynthetic carbon gain in dwarf *Rhizophora mangle*. *Plant Cell Environ.* 29, 793–802. doi: 10.1111/j.1365-3040.2005.01446.x

Lovelock, C. E., Krauss, K. W., Osland, M. J., Reef, R., and Ball, M. C. (2016). "The physiology of mangrove trees with changing climate," in *Tree Physiology*, eds G. Goldstein and L. S. Santiago (Cham: Springer International Publishing), 149–179.

Matesanz, S., Blanco-Sánchez, M., Ramos-Muñoz, M., de la Cruz, M., Benavides, R., and Escudero, A. (2021). Phenotypic integration does not constrain phenotypic plasticity: differential plasticity of traits is associated to their integration across environments. *New Phytol.* 231, 2359–2370. doi: 10.1111/nph.17536

Matesanz, S., and Sultan, S. E. (2013). High-performance genotypes in an introduced plant: insights to future invasiveness. *Ecology* 94, 2464–2474. doi: 10.1890/12-1359.1

McKee, K. L. (1995). Seedling recruitment patterns in a Belizean mangrove forest: effects of establishment ability and physico-chemical factors. *Oecologia* 101, 448–460. doi: 10.1007/BF00329423

McKee, K. L., Cahoon, D. R., and Feller, I. C. (2007). Caribbean mangroves adjust to rising sea level through biotic controls on change in soil elevation. *Glob. Ecol. Biogeogr.* 16, 545–556. doi: 10.1111/j.1466-8238.2007.00317.x

Medina, E., Fernandez, W., and Barboza, F. (2015). Element uptake, accumulation, and resorption in leaves of mangrove species with different mechanisms of salt regulation. *Web Ecol.* 15, 3–13. doi: 10.5194/we-15-3-2015

Melillo, J. M., Richmond, T. T. C., and Yohe, G. W. (2014). *Climate Change Impacts in the United States: The Third National Climate Assessment*. London: U.S. Global Change Research Program.

Mounger, J., Teresa Boquete, M., Schmid, M. W., Granado, R., Robertson, M. H., Voors, S. A., et al. (2021). Inheritance of DNA methylation differences in the mangrove *Rhizophora mangle*. *Evol. Dev.* 23, 351–374. doi: 10.1111/ede.12388

Nadia, T. L., and Machado, I. C. (2014). Wind pollination and propagule formation in *Rhizophora mangle* L. (Rhizophoraceae): resource or pollination limitation?. *An. Acad. Bras. Cienc.* 86, 229–238. doi: 10.1590/0001-37652014101712

Nakagawa, S., and Schielzeth, H. (2013). A general and simple method for obtainingR2from generalized linear mixed-effects models. *Methods Ecol. Evol.* 4, 133–142. doi: 10.1111/j.2041-210x.2012.00261.x

Nicotra, A. B., Atkin, O. K., Bonser, S. P., Davidson, A. M., Finnegan, E. J., Mathesius, U., et al. (2010). Plant phenotypic plasticity in a changing climate. *Trends Plant Sci.* 15, 684–692. doi: 10.1016/j.tplants.2010.09.008

Nicotra, A. B., Segal, D. L., Hoyle, G. L., Schrey, A. W., Verhoeven, K. J. F., and Richards, C. L. (2015). Adaptive plasticity and epigenetic variation in response to warming in an Alpine plant. *Ecol. Evol.* 5, 634–647. doi: 10.1002/ece3.1329

Osland, M. J., Enwright, N., Day, R. H., and Doyle, T. W. (2013). Winter climate change and coastal wetland foundation species: salt marshes vs. mangrove forests in the southeastern United States. *Glob. Chang. Biol.* 19, 1482–1494. doi: 10.1111/gcb.12126

Osland, M. J., Griffith, K. T., Larriviere, J. C., Feher, L. C., Cahoon, D. R., Enwright, N. M., et al. (2017). Assessing coastal wetland vulnerability to sea-level rise along the northern Gulf of Mexico coast: gaps and opportunities for developing a coordinated regional sampling network. *PLoS One* 12:e0183431. doi: 10.1371/journal.pone.0183431

Ottow, E. A., Brinker, M., Teichmann, T., Fritz, E., Kaiser, W., Brosché, M., et al. (2005). Populus euphratica displays apoplastic sodium accumulation, osmotic adjustment by decreases in calcium and soluble carbohydrates, and develops leaf succulence under salt stress. *Plant Physiol.* 139, 1762–1772. doi: 10.1104/pp.105.069971

Parmesan, C. (2006). Ecological and evolutionary responses to recent climate change. *Annu. Rev. Ecol. Evol. Syst.* 37, 637–669. doi: 10.1146/annurev.ecolsys.37.091305.110100

Pennings, S. C., and Bertness, M. (2001). "Salt marsh communities," in *Marine Community Ecology*, eds S. Bertness, D. Gaines, and M. Hay (Sunderland, MA: Sinauer Associates), 289–316.

Pennings, S. C., and Richards, C. L. (1998). Effects of wrack burial in salt-stressed habitats: *Batis maritima* in a southwest Atlantic salt marsh. *Ecography* 21, 630–638. doi: 10.1111/j.1600-0587.1998.tb00556.x

Penuela Useche, V. (2015). *Influences of Yard Management Intensity on Urban Soil Biogeochemistry*. Available online at: https://digitalcommons.usf.edu/cgi/viewcontent.cgi?article=6582&context=etd (accessed September 21, 2021).

Pimentel, D., Culliney, T., Butler, I., Reinemann, D., and Beckman, K. (1989). "Low-input sustainable agriculture using ecological management practices," in *Agricultural Ecology and Environment*, eds M. G. Paoletti, B. R. Stinner, and G. G. Lorenzoni (Amsterdam: Elsevier).

Polidoro, B. A., Carpenter, K. E., Collins, L., Duke, N. C., Ellison, A. M., Ellison, J. C., et al. (2010). The loss of species: mangrove extinction risk and geographic areas of global concern. *PLoS One* 5:e10095. doi: 10.1371/journal.pone.0010095

Proffitt, C. E., and Travis, S. (2014). Red mangrove life history variables along latitudinal and anthropogenic stress gradients. *Ecol. Evol.* 4, 2352–2359. doi: 10.1002/ece3.1095

Proffitt, C. E., and Travis, S. E. (2005). Albino mutation rates in red mangroves (*Rhizophora mangle* L.) as a bioassay of contamination history in Tampa Bay, Florida, USA. *Wetlands* 25, 326–334.

Proffitt, C. E., and Travis, S. E. (2010). Red mangrove seedling survival, growth, and reproduction: effects of environment and maternal genotype. *Estuar. Coast.* 33, 890–901. doi: 10.1007/s12237-010-9265-6

Qiao, X., Zhang, J., Wang, Z., Xu, Y., Zhou, T., Mi, X., et al. (2021). Foundation species across a latitudinal gradient in China. *Ecology* 102:e03234. doi: 10.1002/ecy.3234

R Core Team (2020). *R: A Language and Environment for Statistical Computing*. Vienna: R Foundation for Statistical Computing.

Raju Aluri, J. S. (2013). Reproductive ecology of mangrove flora: conservation and management. *Trans. Rev. Syst. Ecol. Res.* 15, 133–184. doi: 10.2478/trser-2013-0026

Richards, C. L., Bossdorf, O., Muth, N. Z., Gurevitch, J., and Pigliucci, M. (2006). Jack of all trades, master of some? On the role of phenotypic plasticity in plant invasions. *Ecol. Lett.* 9, 981–993. doi: 10.1111/j.1461-0248.2006.00950.x

Richards, C. L., Pennings, S. C., and Donovan, L. A. (2005). Habitat range and phenotypic variation in salt marsh plants. *Plant Ecol.* 176, 263–273. doi: 10.1007/s11258-004-0841-3

Richards, C. L., Schrey, A. W., and Pigliucci, M. (2012). Invasion of diverse habitats by few Japanese knotweed genotypes is correlated with epigenetic differentiation. *Ecol. Lett.* 15, 1016–1025. doi: 10.1111/j.1461-0248.2012.01824.x

Richards, C. L., Walls, R. L., and Bailey, J. P. (2008). Plasticity in salt tolerance traits allows for invasion of novel habitat by Japanese knotweed sl (*Fallopia japonica* and *F.*×*bohemica*, Polygonaceae). *Am. J. Bot.* 95, 931–942. doi: 10.3732/ajb.2007364

Richards, C. L., White, S. N., McGuire, M. A., and Franks, S. J. (2010b). Plasticity, not adaptation to salt level, explains variation along a salinity gradient in a salt marsh perennial. *Estuaries* 33, 840–852. doi: 10.1007/s12237-009-9186-4

Richards, C. L., Wares, J. P., and Mackie, J. A. (2010a). Evaluating adaptive processes for conservation and management of estuarine and coastal resources. *Estuar. Coasts* 33, 805–810.

Rinella, M. J., and Reinhart, K. O. (2017). Mixing soil samples across experimental units ignores uncertainty and generates incorrect estimates of soil biota effects on plants: response to Cahill et al. (2017) No silver bullet: different soil handling techniques are useful for different research questions, exhibit differential type I and II error rates, and are sensitive to sampling intensity. *New Phytol.* 216, 15–17. doi: 10.1111/nph.14432

Rosenthal, D. M., Schwarzbach, A. E., Donovan, L. A., Raymond, O., and Rieseberg, L. H. (2002). Phenotypic differentiation between three ancient hybrid taxa and their parental species. *Int. J. Plant Sci.* 163, 387–398. doi: 10.1086/339237

Sage, R. F., Pearcy, R. W., and Seemann, J. R. (1987). The nitrogen use efficiency of C(3) and C(4) plants : III. Leaf nitrogen effects on the activity of carboxylating enzymes in *Chenopodium album* (L.) and *Amaranthus retroflexus* (L.). *Plant Physiol.* 85, 355–359. doi: 10.1104/pp.85.2.355

Schittko, C., Runge, C., Strupp, M., Wolff, S., and Wurst, S. (2016). No evidence that plant-soil feedback effects of native and invasive plant species under glasshouse conditions are reflected in the field. *J. Ecol.* 104, 1243–1249. doi: 10.1111/1365-2745.12603

Schuerch, M., Spencer, T., Temmerman, S., Kirwan, M. L., Wolff, C., Lincke, D., et al. (2018). Future response of global coastal wetlands to sea-level rise. *Nature* 561, 231–234. doi: 10.1038/s41586-018-0476-5

Smith, S. M., and Snedaker, S. C. (1995). Salinity responses in two populations of viviparous *Rhizophora mangle* L. seedlings. *Biotropica* 27:435. doi: 10.2307/2388955

Sultan, S. E. (2001). Phenotypic plasticity for fitness components in polygonum species of contrasting ecological breadth. *Ecology* 82, 328–343.

Sultan, S. E. (2015). *Organism and Environment: Ecological Development, Niche Construction, and Adaptation*. Oxford: Oxford University Press.

Tester, M., and Davenport, R. (2003). Na+ tolerance and Na+ transport in higher plants. *Ann. Bot.* 91, 503–527. doi: 10.1093/aob/mcg058

Tomlinson, P. B. (2016). *The Botany of Mangroves*. Cambridge, MA: Cambridge University Press.

Turner, R. E. (2011). Beneath the salt marsh canopy: loss of soil strength with increasing nutrient loads. *Estuar. Coast.* 34, 1084–1093. doi: 10.1007/s12237-010-9341-y

Vendramini, F., Díaz, S., Gurvich, D. E., Wilson, P. J., Thompson, K., and Hodgson, J. G. (2002). Leaf traits as indicators of resource-use strategy in floras with succulent species. *New Phytol.* 154, 147–157. doi: 10.1046/j.1469-8137.2002.00357.x

Verhoeven, K. J. F., Van Dijk, P. J., and Biere, A. (2010). Changes in genomic methylation patterns during the formation of triploid asexual dandelion lineages. *Mol. Ecol.* 19, 315–324. doi: 10.1111/j.1365-294X.2009.04460.x

Vovides, A. G., Vogt, J., Kollert, A., Berger, U., Grueters, U., Peters, R., et al. (2014). Morphological plasticity in mangrove trees: salinity-related changes in the allometry of *Avicennia germinans*. *Trees* 28, 1413–1425. doi: 10.1007/s00468-014-1044-8

Walker, A. P., Beckerman, A. P., Gu, L., Kattge, J., Cernusak, L. A., Domingues, T. F., et al. (2014). The relationship of leaf photosynthetic traits - *V cmax* and *J max* - to leaf nitrogen, leaf phosphorus, and specific leaf area: a meta-analysis and modeling study. *Ecol. Evol.* 4, 3218–3235. doi: 10.1002/ece3.1173

Wise, R. R., and Juncosa, A. M. (1989). Ultrastructure of the transfer tissues during viviparous seedling development in *Rhizophora mangle* (Rhizophoraceae). *Am. J. Bot.* 76, 1286–1298. doi: 10.1002/j.1537-2197.1989.tb15110.x

Wuebbles, D., Meehl, G., Hayhoe, K., Karl, T. R., Kunkel, K., Santer, B., et al. (2014). CMIP5 climate model analyses: climate extremes in the United States. *Bull. Am. Meteorol. Soc.* 95, 571–583. doi: 10.1175/bams-d-12-00172.1

Zedler, J. B., and Kercher, S. (2005). Wetland resources: status, trends, ecosystem services, and restorability. *Annu. Rev. Environ. Resour.* 30, 39–74. doi: 10.1146/annurev.energy.30.050504.144248

Zhang, Y.-Y., Fischer, M., Colot, V., and Bossdorf, O. (2013). Epigenetic variation creates potential for evolution of plant phenotypic plasticity. *New Phytol.* 197, 314–322. doi: 10.1111/nph.12010

Conflict of Interest: The authors declare that the research was conducted in the absence of any commercial or financial relationships that could be construed as a potential conflict of interest.

Publisher's Note: All claims expressed in this article are solely those of the authors and do not necessarily represent those of their affiliated organizations, or those of the publisher, the editors and the reviewers. Any product that may be evaluated in this article, or claim that may be made by its manufacturer, is not guaranteed or endorsed by the publisher.

frontiers in Marine Science

ORIGINAL RESEARCH
published: 18 November 2021
doi: 10.3389/fmars.2021.760891

Variation in Coral Thermotolerance Across a Pollution Gradient Erodes as Coral Symbionts Shift to More Heat-Tolerant Genera

Melissa S. Naugle[1,2], Thomas A. Oliver[3], Daniel J. Barshis[4], Ruth D. Gates[5†] and Cheryl A. Logan[1]*

[1] Department of Marine Science, California State University, Monterey Bay, Seaside, CA, United States, [2] Moss Landing Marine Laboratories, Moss Landing, CA, United States, [3] National Oceanic and Atmospheric Administration, Pacific Island Fisheries Science Center, Honolulu, HI, United States, [4] Department of Biological Sciences, Old Dominion University, Norfolk, VA, United States, [5] Hawai'i Institute of Marine Biology, University of Hawai'i at Mānoa, Kāne'ohe, HI, United States

OPEN ACCESS

Edited by:
Jose M. Eirin-Lopez, Florida International University, United States

Reviewed by:
Noah Rose, Princeton University, United States
Noriyuki Satoh, Okinawa Institute of Science and Technology Graduate University, Japan

***Correspondence:**
Melissa S. Naugle
mnaugle@csumb.edu

† Deceased

Specialty section:
This article was submitted to Global Change and the Future Ocean, a section of the journal Frontiers in Marine Science

Received: *19 August 2021*
Accepted: *20 October 2021*
Published: *18 November 2021*

Citation:
Naugle MS, Oliver TA, Barshis DJ, Gates RD and Logan CA (2021) Variation in Coral Thermotolerance Across a Pollution Gradient Erodes as Coral Symbionts Shift to More Heat-Tolerant Genera. Front. Mar. Sci. 8:760891. doi: 10.3389/fmars.2021.760891

Phenotypic plasticity is one mechanism whereby species may cope with stressful environmental changes associated with climate change. Reef building corals present a good model for studying phenotypic plasticity because they have experienced rapid climate-driven declines in recent decades (within a single generation of many corals), often with differential survival among individuals during heat stress. Underlying differences in thermotolerance may be driven by differences in baseline levels of environmental stress, including pollution stress. To examine this possibility, acute heat stress experiments were conducted on *Acropora hyacinthus* from 10 sites around Tutuila, American Samoa with differing nutrient pollution impact. A threshold-based heat stress assay was conducted in 2014 and a ramp-hold based assay was conducted in 2019. Bleaching responses were measured by assessing color paling. Endosymbiont community composition was assessed at each site using quantitative PCR. RNA sequencing was used to compare differences in coral gene expression patterns prior to and during heat stress in 2019. In 2014, thermotolerance varied among sites, with polluted sites holding more thermotolerant corals. These differences in thermotolerance correlated with differences in symbiont communities, with higher proportions of heat-tolerant *Durusdinium* found in more polluted sites. By 2019, thermotolerance varied less among sites, with no clear trend by pollution level. This coincided with a shift toward *Durusdinium* across all sites, reducing symbiont community differences seen in 2014. While pollution and symbiont community no longer could explain variation in thermotolerance by 2019, gene expression patterns at baseline levels could be used to predict thermotolerance thresholds. These patterns suggest that the mechanisms underlying thermotolerance shifted between 2014 and 2019, though it is possible trends may have also been affected by methodological differences between heat stress assays. This study documents a shift in symbiont community over time and captures potential

implications of that shift, including how it affects variation in thermotolerance among neighboring reefs. This work also highlights how gene expression patterns could help identify heat-tolerant corals in a future where most corals are dominated by *Durusdinium* and symbiont-driven thermotolerance has reached an upper limit.

Keywords: coral reefs, pollution, gene expression, symbiosis, phenotypic plasticity, climate change, thermal tolerance, acclimatization

INTRODUCTION

Anthropogenic climate change presents a bleak future for many species with major declines in global biodiversity projected (Bellard et al., 2012). Rising global temperatures and other changing environmental conditions are predicted to push many species past their physiological tolerance limits (Somero, 2010). An important, yet often overlooked component of projecting the effects of climate change on species persistence is estimating both a taxa's thermal threshold for physiological stress, and its capacity for acclimatization (Seebacher et al., 2015).

Reef building corals present a good model for studying within-generation acclimatization processes (i.e., phenotypic plasticity) because they are sessile and long-lived, and have experienced rapid climate-driven declines in the past two decades, often with differential survival among individuals (Marshall and Baird, 2000; West and Salm, 2003; Hughes et al., 2017). These differences may be driven by microenvironmental differences, genetics, or phenotypic plasticity. Since corals have high species-level and individual-level differences in thermotolerance (e.g., Fuller et al., 2020; Loya et al., 2001), they are good candidates for studies investigating plastic responses to climate change.

Acclimatization processes can occur at multiple levels within a coral "holobiont." A coral holobiont is the coral animal plus all of the associated microorganisms and symbiotic algae that live on and within the coral tissue (Rohwer et al., 2002). Plasticity can occur within the coral animal itself (e.g., gene expression shifts to increase heat shock proteins or antioxidants during thermal stress; Dixon et al., 2020), or within the members of the coral holobiont community that contribute to coral thermotolerance (e.g., endosymbiont shifts toward more heat-tolerant species or "symbiont shuffling"; Berkelmans and van Oppen, 2006). Symbiont shuffling may increase thermotolerance when there is a change in the proportions of different genera within the Symbiodiniaceae family, often seen as an increase in the proportion of heat-tolerant *Durusdinium* (Berkelmans and van Oppen, 2006; Stat and Gates, 2011; Ladner et al., 2012; LaJeunesse et al., 2018). Gene expression shifts and symbiont shuffling may increase thermotolerance, but there are limits to that increase. Once symbiont shuffling has occurred and corals host entirely one species/strain of symbiont, they may have maximized their ability to improve their symbiont-driven thermotolerance (Howells et al., 2020). While other plasticity processes exist (e.g., transgenerational plasticity; Putnam and Gates, 2015), gene expression shifts and symbiont shuffling are well-studied mechanisms by which corals are known to adjust their thermotolerance within the lifetime of an individual (Berkelmans and van Oppen, 2006; Bellantuono et al., 2012) and are the focus of this study.

While gene expression shifts and symbiont shuffling have been examined in response to temperature stress, fewer studies have investigated how these processes respond when temperature stress interacts with local stressors such as pollution. Land-based pollution can carry nutrients and sediments into marine environments, affecting corals and their symbionts (Silbiger et al., 2018). There have been multiple accounts of elevated nutrients lowering thermotolerance (Wooldridge, 2009; Wiedenmann et al., 2013; Donovan et al., 2020) or conversely improving thermotolerance (Béraud et al., 2013; Zhou et al., 2017; Riegl et al., 2019; Becker et al., 2021). These discrepancies may be partially explained by differences in nutrient type or ratios among nutrient concentrations (Morris et al., 2019; Burkepile et al., 2020). While the effects of nutrient pollution have been investigated in lab-controlled studies, there are fewer instances of field-based assessments of pollution and thermotolerance (Wooldridge, 2009; Becker and Silbiger, 2020; Becker et al., 2021). Recent field-based studies of how pollution impacts thermotolerance have not explored underlying mechanisms such as symbiont shifts and coral host gene expression (Becker and Silbiger, 2020; Becker et al., 2021).

Long-term pollution stress could increase or decrease coral thermotolerance to acute heat stress. When corals are exposed to multiple stressors, many studies have shown synergistic effects, whereby the cumulative effect of two stressors is greater than each stressor independently (Kersting et al., 2015; Towle et al., 2016; Ellis et al., 2019). However, other studies have shown that multiple stressors can produce antagonistic effects in corals, whereby the cumulative effect of two stressors is less than that of each stressor alone (Zhou et al., 2017; Marangoni et al., 2019; Darling et al., 2020). Since the cellular stress response (CSR) is similar even for different types of environmental stresses (e.g., Dixon et al., 2020; Kültz, 2020), it is possible that if mild long-term pollution stress triggers macromolecular damage and increases constitutive expression of stress response genes, this could lead to higher thermotolerance during heat stress. This may be due to the "frontloading" of stress response genes in polluted waters, whereby the baseline gene expression more closely resembles CSR gene expression, better preparing the coral to tolerate acute stress (Barshis et al., 2013; Thomas et al., 2018). It is also possible that long-term pollution stress has induced symbiont community shifts in favor of more stress-tolerant symbionts, leading to higher thermotolerance (LaJeunesse et al., 2010). This concept of increased tolerance to one stressor due to exposure to a different stressor is termed "cross-tolerance"

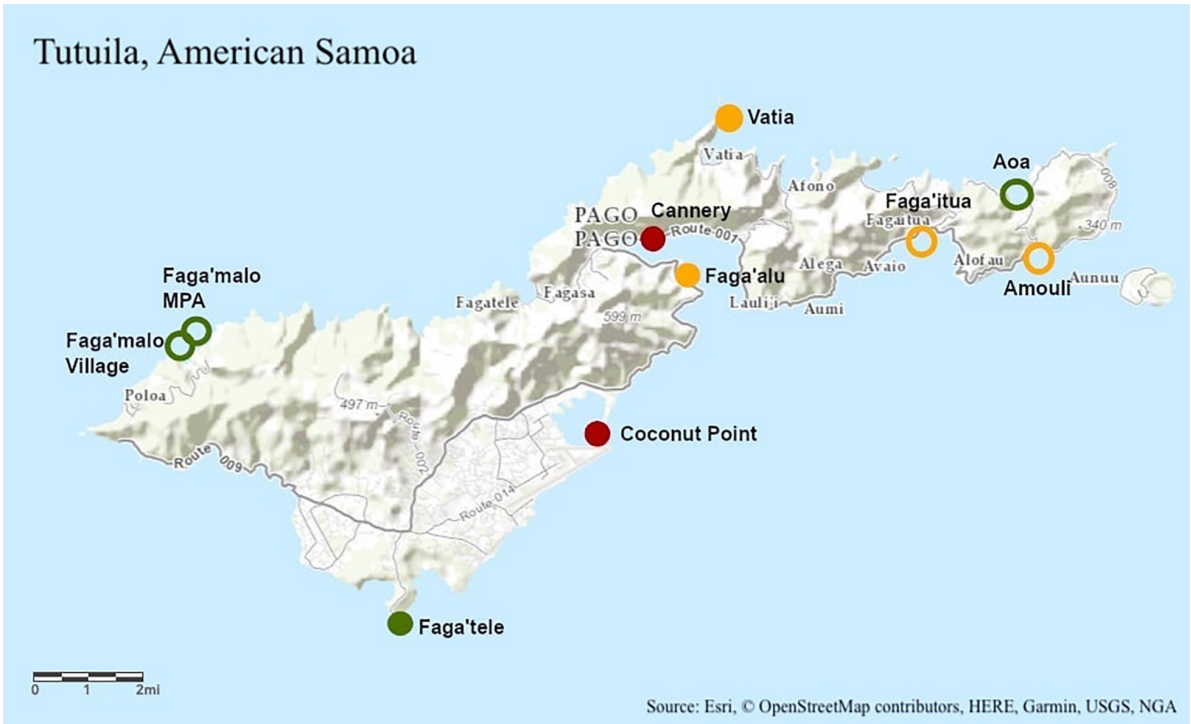

FIGURE 1 | Topographic map of Tutuila, American Samoa of Tutuila, American Samoa with study site locations labeled. Green represents low pollution, yellow represents moderate pollution, and red represents high pollution. Pollution designations were determined using human population and nutrient loading data (DiDonato, 2004; Sudek and Lawrence, 2017; Shuler et al., 2019; Shuler and Comeros-Raynal, 2020). Unfilled circles were sampled only in 2014 and filled in circles were sampled in 2014 and 2019.

and has been demonstrated in many species (Li and Hahn, 1978; Sabehat et al., 1998; Ely et al., 2014; Gunderson et al., 2016).

In this study, we investigate thermotolerance of a common reef-building coral, *Acropora hyacinthus*, on reefs of differing pollution levels around the island of Tutuila, American Samoa in 2 years, 5 years apart (2014 and 2019). During this 5 year period, mass bleaching events occurred in 4 of the 5 years on American Samoan coral reefs (**Supplementary Figure 1**, Witze, 2015; Sudek and Lawrence, 2017; Morikawa and Palumbi, 2019). We also measure two underlying mechanisms of plasticity that may affect thermotolerance: endosymbiont community composition and gene expression shifts. We investigate the role of pollution in triggering these plastic mechanisms and their effect on coral thermotolerance.

MATERIALS AND METHODS

Site Selection and Field Collections

Ten sites of differing pollution levels were chosen to represent a gradient of pollution around Tutuila, American Samoa (**Figure 1**). Sites were categorized as either "low," "moderate," or "high" pollution based on human population and nutrient loading data, following established designations (DiDonato, 2004; Sudek and Lawrence, 2017; Shuler et al., 2019; Shuler and Comeros-Raynal, 2020). In March and July 2014, ten colonies of *Acropora hyacinthus* were sampled at each of ten sites between 07:00 and 11:00 (**Figure 1**). Eight fragments of approximately 2 cm^3 were collected haphazardly from each colony, with two replicates processed for genetic sampling (stored in RNA preservation buffer). The remaining six fragments were transported back to our experimental facility (in Vaitogi in March, and Coconut Point in July), and held at 28°C overnight, with the assay to begin at sunrise the following day. Colonies were sampled at least 10 m apart to reduce the likelihood of sampling clones. All fragments were collected on snorkel and were sampled between 0 and 2 m in depth.

In August 2019, eight colonies of *A. hyacinthus* were sampled at a subset of five of the original 2014 sites between 07:00 and 11:00 (**Figure 1**). Seventeen fragments of approximately 2 cm^3 were collected haphazardly using stainless steel coral cutters from each colony: four replicates for each of four temperature treatments and one field control which was never placed in the temperature stress assay. Colonies were sampled at least 10 m apart to reduce the likelihood of sampling clones. All fragments were collected on snorkel and were sampled between 0 and 2 m in depth.

Threshold-Based Heat Stress Assay

Temperature dependent mortality in 2014 was measured using a 3-day threshold-based heat stress assay consisting of a ramp tank and a control. Replicate coral branches (n = 60 per tank,

with three replicates of each of 10 colonies from two sites) were allowed to acclimate to tank conditions at 28°C for 16 h. The temperature stress assay began at 06:00, in which the control tank was held at 28°C for the duration of the stress, and the heated tank was brought to 30°C over the course of the first 30 min, and then continuously ramped at 2°C per 12 h during "daylight hours" (06:00–18:00), held overnight at the last ramp value, and then ramped between 06:00 and 18:00 for the following two successive days (**Supplementary Figure 2**). During daylight hours (06:00–18:00), full spectrum lights were measured using a planar Apogee PAR sensor and maintained at 500 μmol m^{-2} s^{-1}. Partial water changes were performed two times per day over the course of the assay. Water temperatures were controlled using a custom-built Arduino controller linked to aquarium heaters (Finnex HMA-200S Titanium Aquarium Heater) and Nova Tec IceProbe thermoelectric chillers (Nova Tec Products, San Rafael, CA). Water temperatures were measured every minute using HOBO UA-002-64 temperature and light loggers. Temperatures were kept to within 0.5°C of the desired temperature.

Coral color paling was measured every 4 h between 06:00 and 22:00 using the CoralWatch® Coral Health Chart (Siebeck et al., 2006) and was recorded over the course of the assay until fragments experienced mortality, as measured by tissue sloughing. A fragment's thermal threshold of "degree heating days" was calculated as the number of degrees above the local bleaching threshold of 29°C, as reported by NOAA's Coral Reef Watch, multiplied by the number of elapsed days above that threshold until mortality was reached. Data from colonies with controls that experienced mortality throughout the course of the experiment were discarded.

Ramp-Hold Heat Stress Assay

Thermal resistance to temperature stress in 2019 was measured using a standardized short-term acute heat stress assay and the Coral Bleaching Autonomous Stress System (CBASS; Voolstra et al., 2020). This approach has been shown to determine differences in coral thermotolerance similarly to a classic long-term heat stress assay (Voolstra et al., 2020; Evensen et al., 2021). We chose to use this 1-day ramp-hold assay in 2019 rather than repeat the 2014-style assay due to the logistical advantage of a 1-day assay and to be more comparable to recent studies using CBASS (Voolstra et al., 2020, 2021; Cunning et al., 2021; Evensen et al., 2021; Savary et al., 2021). This assay consists of four replicate tanks to test three experimental temperature treatments and one control, for a total of eight tanks. The temperature stress assay was conducted at 13:00 for each study site and continued until the following morning at 06:00 (**Supplementary Figure 2**). Replicate coral branches (n = 16 per tank, with two replicates of each of 8 colonies) were allowed to acclimate to tank conditions at 28°C for 1 h. At 14:00, corals were exposed to ramp-hold: control (28°C), 33°C, 34°C or 35°C during a 2 h ramp, 3 h hold, 1 h ramp down to 28°C, and overnight recovery at 28°C. Light levels were measured using an Apogee underwater quantum meter twice during the assay and maintained between 210 and 250 μmol m^{-2} s^{-1}. To mimic natural field conditions, lights were turned off at 19:00 and turned on in the morning at 06:00 (Roleadro LED Aquarium Light). Partial water changes (~2 L) using water from the sampling site were performed 4–5 times over the course of the assay. Water temperatures were controlled using a custom-built Arduino controller linked to aquarium heaters (Finnex HMA-200S Titanium Aquarium Heater) and custom-built cooling loops hooked to a Hamilton Technology Aqua Euro Max Aquarium Chiller. Water temperatures were measured every minute using HOBO UA-002-64 temperature and light loggers. Temperatures were kept to within 0.5°C of the desired temperature.

Thermotolerance was measured through changes in visual color paling using the CoralWatch® Coral Health Chart (Siebeck et al., 2006) with the same observer for all trials and colorimetric analysis using an Olympus TG-5 taken by the same photographer in the same location for all measurements (*sensu* Winters et al., 2009). A subset of coral fragments (n = 4 per temperature treatment) were collected during heat stress (at 19:00) for RNAseq analysis. Samples were preserved in an RNA preservation buffer and stored at –20°C until analysis, though only the 28 and 35°C treatments were analyzed.

CoralWatch® Color Card and red pixel intensity measurements were used to generate a single metric for thermotolerance for each colony. Raw CoralWatch and red intensity values were normalized in an open interval from 0 to 1 for each temperature treatment from 28 to 35°C. Logistic curves were fit to the data across temperatures and the midpoint of the curves was used as an indication of temperature at which bleaching occurred, with a maximum of 36.5°C if curves did not reach the midpoint by 35°C (using the *nlme* function in R; Pinheiro et al., 2021). The mean of the two midpoints (CoralWatch and red intensity) was used to generate a two-variable mean threshold, in units of °C. This two-variable mean was used to determine the most and least thermotolerant corals. The highest and lowest 10, 20, and 30% of the two-variable means were used to classify the 10, 20, and 30% least and most thermotolerant corals. All data and code are available at: https://github.com/melissanaugle/SCLERA_Tutuila_Thermotolerance. All analyses were conducted in R version 4.1.0 (R Core Team, 2021).

Quantification of Symbiont Communities

For symbiont analysis, ten replicates per site were used in 2014 and eight replicates per site were used in 2019. Total genomic DNA was extracted from preserved fragments that had never entered the heat stress assay using a Qiagen DNeasy® Blood and Tissue Kit. Samples were prepared by removing excess buffer and homogenizing in a TissueLyser LT for 5 min at 50 Hz. Total DNA was measured using a NanoDrop spectrophotometer and a Qubit fluorometer. All DNA quantifications met the following criteria: > 2 ng/μl (on Qubit), 260:280 > 1.8, 260:230 > 1.59. Total DNA was prepared for qPCR using methods described in Cunning and Baker (2013) to quantify symbiont communities at each study site. Samples were run in duplicate in 2014 and triplicate in 2019, with a no-template control on a Biorad CFX96 Touch Real-Time PCR Detection System. Reaction volumes were 10 μl, with 5 μl Taqman Genotyping Master Mix and 1 μl genomic DNA template. qPCR analysis uses species-specific tags to identify *Cladocopium* and *Durusdinium*, which

comprise the majority of the Symbiodiniaceae in American Samoan *Acropora hyacinthus* (Ladner et al., 2012). Since *Durusdinium* are more thermally tolerant than *Cladocopium*, ratios between the two genera provide a metric to understand coral thermotolerance contributed by the symbiont community (Cunning and Baker, 2013).

Ratios of *Cladocopium* to *Durusdinium* cycle threshold (Ct) values were calculated using results from qPCR. Baseline thresholds were chosen for each run to remove background noise. Ct values were recorded for samples that amplified past the threshold in fewer than 40 cycles. Ct values were averaged across duplicates in 2014 and triplicates in 2019 and cell numbers of *Cladocopium* and *Durusdinium* were calculated using the following formula: $2^{(40-Ct)}$/cell copy number (where cell copy number = 9 for *Cladocopium* and 1 for *Durusdinium* (Cunning and Baker, 2013). Log base 2 *Cladocopium* to *Durusdinium* ratios were calculated using the following formula: log2(cell number *Cladocopium*/cell number *Durusdinium*). All data and code are available at: https://github.com/melissanaugle/SCLERA_Tutuila_Thermotolerance. All analyses were conducted in R version 4.1.0.

RNA Sequencing

Due to budget constraints, only the control and highest (28°C and 35°C) temperature treatments were used for mRNA sequencing and gene expression analysis. RNA extraction, cDNA library construction and sequencing were performed in two separate batches: once for Coconut Point, Faga'alu, and Faga'tele in February-March 2020 and again for Cannery and Vatia in March-April 2021. Total RNA was extracted using a Qiagen RNeasy® Plus Mini Kit, following the manufacturer's protocol. Samples were homogenized using a TissueLyser LT for 10 min at 50 Hz in 2020 and for 3 min at 50 Hz in 2021. RNA was assessed using a NanoDrop™ (Thermo Fisher Scientific), Qubit fluorometer and on a BioAnalyzer. 38 cDNA libraries were constructed from 300 ng of total RNA using the NEBNext® Ultra II RNA Library Prep Kit for Illumina® (E7530) with the NEBNext® Poly(A) mRNA Magnetic Isolation Module (E7490). Paired-end libraries were sequenced on a single HiSeq4000 150 bp lane at NovoGene in Davis, CA. Raw data obtained from sequencing was submitted to the NCBI Sequence Read Archive (SRA) database (Bioproject accession: PRJNA762371; SRA accession: SRP339664).

Differential Gene Expression Analysis

Low quality reads and adapter sequences were discarded using Trimmomatic (Bolger et al., 2014). Trimmomatic parameters were set to remove reads below 25 bp long, leading and trailing bases below quality "5," and reads that did not meet quality standards for a sliding window where in a four base sliding window, the average quality per base drops below a 5. Sequences were also trimmed of adapter sequences including standard Illumina adapters and polyT sequences. Quality of trimmed reads was assessed using FastQC.[1] Sequenced reads were aligned to the reference *A. hyacinthus* transcriptome described in Barshis et al. (2013) using bowtie2 and counted using RSEM in UNIX (Li and Dewey, 2011; Langmead and Salzberg, 2012). Out of 33,496 possible contigs, 18,387 were discarded due to low expression, following methods described in Chen et al. (2016), and 15,109 contigs were retained and used for differential gene expression analysis. Gene expression statistical analyses were conducted using edgeR with a FDR of 0.001 and a fourfold change cut-off. A weighted gene co-expression network analysis (WGCNA) was conducted to compare co-regulated gene networks and their association with pollution level, symbiont community, and thermotolerance (Langfelder and Horvath, 2008). WGCNA identifies co-expressed gene modules using hierarchical clustering of expression data and relates those modules to sample traits. WGCNA was performed on baseline gene expression from corals at control conditions, and separately on gene expression from corals under heat stress. Gene annotations were acquired from Barshis et al. (2013), and significant WGCNA modules ($p < 0.05$) were analyzed for enrichment of Biological Processes (BP) Gene Ontology (GO) terms using the GO_MWU R script (Wright et al., 2015). The GO_MWU R script uses a Mann-Whitney *U*-test and tests the kME (module membership score or eigengene-base connectivity) in among-module genes compared to other genes in the transcriptome outside the module to test if genes in the module of interest are significantly enriched (Wright et al., 2015; Huerta-Cepas et al., 2017).

Linear Mixed-Effects Models of Thermotolerance

Linear mixed-effects models were used to investigate the role of multiple variables in setting thermotolerance in 2014 and We built and present 5 mixed models, each using colony-level features (e.g., tolerance, symbionts), site-level features (e.g., pollution) or temporal data (e.g., season, year). Each model held Site as a random factor. We specifically model: the correlation of pollution level and season vs. thermal tolerance in 2014, the correlation of pollution and *Cladicopium:Durusdinium* ratio vs. thermal tolerance in 2019; the correlation of year and pollution level vs. *Cladicopium:Durusdinium* ratio; the correlation of pollution level, season, and *Cladicopium:Durusdinium* ratio vs. thermal tolerance in 2014, and the correlation of three eigengene expression modules vs. thermal tolerance in 2019.

To explore the potential for non-linearity, models were first built using a generalized additive model approach using the mgcv package in R (Wood, 2011), but due to minimal evidence of non-linearity, subsequent linear mixed-effects models were built using the lme4 package in R (Bates et al., 2015). Model assumptions were checked using the ggplot2 package in R (Wickham, 2016). Separate models were built for each year when investigating thermotolerance due to the differences in experimental design and thermotolerance metric between 2014 and 2019. To determine the importance of individual variables within each final model, we generated model sets from the final model using all-subsets regression (*dredge* in the package MuMIn), and then small sample size corrected Akaike information criterion (AICc) weight across each parameter (using *importance* in the MuMIn

[1]http://www.bioinformatics.babraham.ac.uk/projects/fastqc/

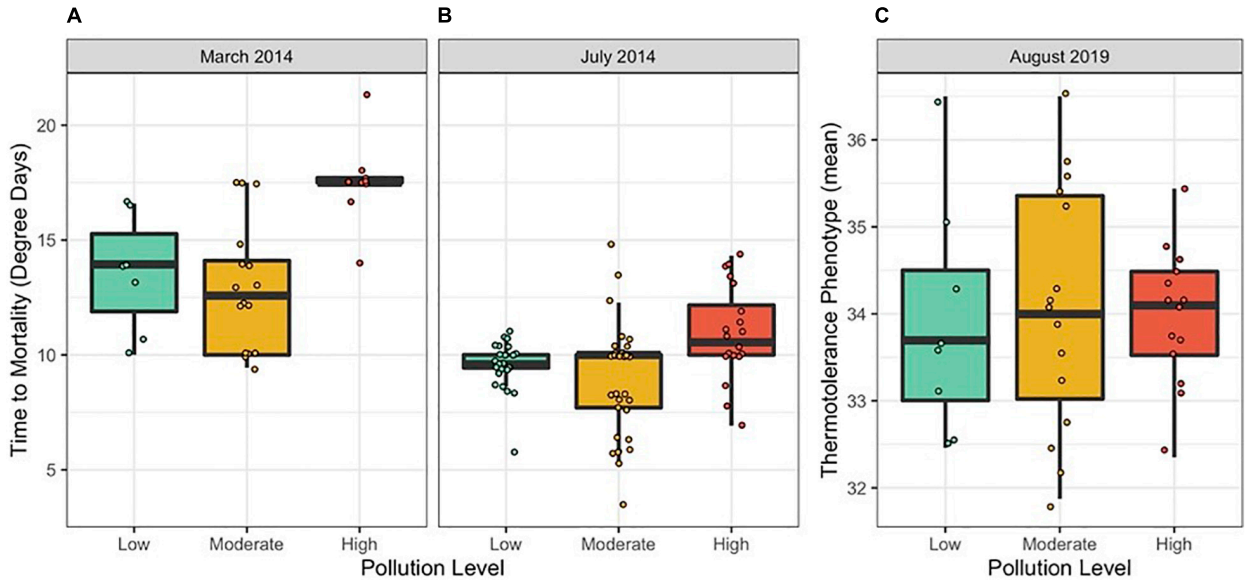

FIGURE 2 | Thermotolerance variation among colonies by pollution level in **(A)** March 2014, **(B)** July 2014, and **(C)** August 2019. Thermotolerance was measured as mortality in degree days in 2014 and as a two-variable mean in 2019. Points represent individual colonies and are jittered to prevent overlapping.

package) to generate a relative importance metric, ranging from 0 to 1 (Kamil, 2020).

In 2014, season, log2 ratio of *Cladocopium:Durusdinium*, and pollution level were included as explanatory variables of thermotolerance, measured as mortality in degree days, with site was included as a random factor. Model selection was based on AIC.

In 2019, log2 ratio of *Cladocopium:Durusdinium*, pollution level, and eigengene expression of significant WGCNA modules at baseline conditions (pre-heat stress) were included as explanatory variables of thermotolerance, measured as a two-variable mean value that represented thermotolerance. All data and code are available at: https://github.com/melissanaugle/SCLERA_Tutuila_Thermotolerance. All analyses were conducted in R version 4.1.0.

TABLE 1 | ANOVA table from a linear mixed model of thermotolerance in 2014 with site as a random effect and season and pollution category as explanatory variables.

Variable	Sum Sq	Num DF	Den DF	*F*-value	*P*-value
Season	374.50	1	94.11	84.90	8.5e-15
Pollution category	61.04	2	5.03	6.92	0.04

We show that thermotolerance was higher both in the hotter season (i.e., March) and at sites ranked as high pollution. Marginal R^2 = 0.520.

TABLE 2 | Colony-level linear mixed-effects model ANOVA table showing impact of *Cladocopium* to *Durusdinium* log2 ratio and pollution category in 2019.

Variable	Sum Sq	Mean Sq	Num DF	Den DF	*F*-value	*P*-value
Pollution category	0.40	0.20	2	2.11	0.15	0.87
C:D log2 ratio	1.91	1.91	1	31.40	1.42	0.24

Marginal R^2 = 0.038.

RESULTS

Thermotolerance Patterns in 2014 and 2019

We compared colony-level coral thermotolerance in March and July 2014 among sites, expressed as time to mortality in degree heating days (**Figures 2A,B**). Thermotolerance varied among sites, with the most thermotolerant corals found at Cannery (high pollution) in March 2014 and Cannery (high pollution), Coconut Point (high pollution), Faga'alu (moderate pollution) and Faga'itua (moderate pollution) in July 2014. The least thermotolerant corals were found at Faga'alu (moderate pollution) and Faga'itua (moderate pollution) in March 2014 and at Amouli (moderate pollution), Aoa (low pollution) and Vatia (moderate pollution) in July 2014. In 2019, thermotolerance was measured as a two-variable mean and was less variable among sites, with the most thermotolerant corals found at Vatia (moderate pollution) and the least thermotolerant corals found at Faga'tele (low pollution; **Supplementary Figure 3** and **Figure 2C**).

Sites were pooled into their pollution level categories to examine trends between pollution and thermotolerance. In linear mixed models for 2014, holding site as a random effect, we show that thermotolerance was higher both in the hotter season (i.e., March) and at sites ranked as "High" for pollution level (**Table 1** and **Figures 2A,B**; N = 115, Season $p << 0.001$, Pollution $p < 0.05$). Pollution level held no explanatory power in 2019 (**Table 2**).

TABLE 3 | Linear model of *Cladocopium* to *Durusdinium* ratio across both sampling years, with year and pollution category as explanatory variables.

Variable	Sum Sq	Num DF	Den DF	*F*-value	*P*-value
Year	310.47	1	114.00	4.82	0.03
Pollution category	1004.37	2	4.12	7.79	0.04

Marginal R^2 *= 0.402.*

Shifts in Symbiont Community Between 2014 and 2019

In both 2014 and 2019, the log2 ratio of *Cladocopium* to *Durusdinium* favored *Cladocopium* at lower pollution levels and favored *Durusdinium* at higher pollution levels (**Figure 3** and **Table 3**; N = 154, Pollution $p < 0.05$). Yet, 2014 and 2019 differed in their log2 ratio of *Cladocopium* to *Durusdinium*, with 2019 showing a stronger preference for *Durusdinium* compared to that seen in 2014 (**Figure 3** and **Table 3**; N = 154, Year $p < 0.05$). Model estimates of *Cladocopium* to *Durusdinium* ratios controlling for pollution level showed a 16.7-fold decrease in 2019 compared to 2014 (i.e., mean log2 ratio reduced by 4.07 between years), suggesting a substantial and significant shift toward *Durusdinium*. Log2 *Cladocopium* to *Durusdinium* ratios also varied by site, with most sites across time points including corals hosting a combination of *Cladocopium* and *Durusdinium*, though both high pollution sites in 2019 hosted 100% *Durusdinium* (**Supplementary Figure 4**).

Gene Expression Responses

Differential gene expression analysis was performed on coral fragments from 2019 from the five sample sites and from two treatments (heat stress at 35°C and control at 28°C). Gene expression profiles were driven strongly by temperature treatment, with 6,020 genes differentially expressed between heat and control treatments across all sites (edgeR, FDR < 0.001; **Supplementary Figure 5**).

A weighted gene co-expression network analysis (WGCNA) was conducted to investigate how gene networks (called modules) from corals at control conditions (i.e., baseline expression patterns) correlated to pollution level, presence or absence of *Cladocopium*, and thermotolerance (**Figure 4**). One module, module C9, correlated to pollution level. No modules correlated to symbiont type. However, multiple gene modules showed correlations with thermotolerance under control conditions. Two modules (C5 and C8) correlated with the top 10% most thermotolerant coral colonies and two modules (C6 and C7) correlated with the top 20–30% thermotolerant coral colonies. Two additional modules (C3 and C16) correlated with the bottom 10–20% thermotolerant coral colonies.

Gene Ontology (GO) analysis was performed on the four modules relating to the most thermotolerant corals: modules C5, C6, C7, and C8. These modules contained 496, 267, 406, 117 genes, respectively. Of these four modules, only C8 showed any significant enrichment for Biological Processes (BP) GO terms. Module C8 was enriched for genes involved primarily in immune response, cytokine production, and multi-organism processes ($p < 0.05$, **Supplementary Table 1**).

Gene Ontology (GO) analysis was performed on modules C3 and C16 to determine which gene expression patterns at control conditions correlated with poor performance under heat stress. Module C3 contained 69 genes and module C16 contained 280 genes. Module C3 contained overrepresented GO categories relating to ion transport ($p < 0.05$, **Supplementary Table 1**). Module C16 contained many overrepresented GO categories, including negative regulation of protein catabolic process,

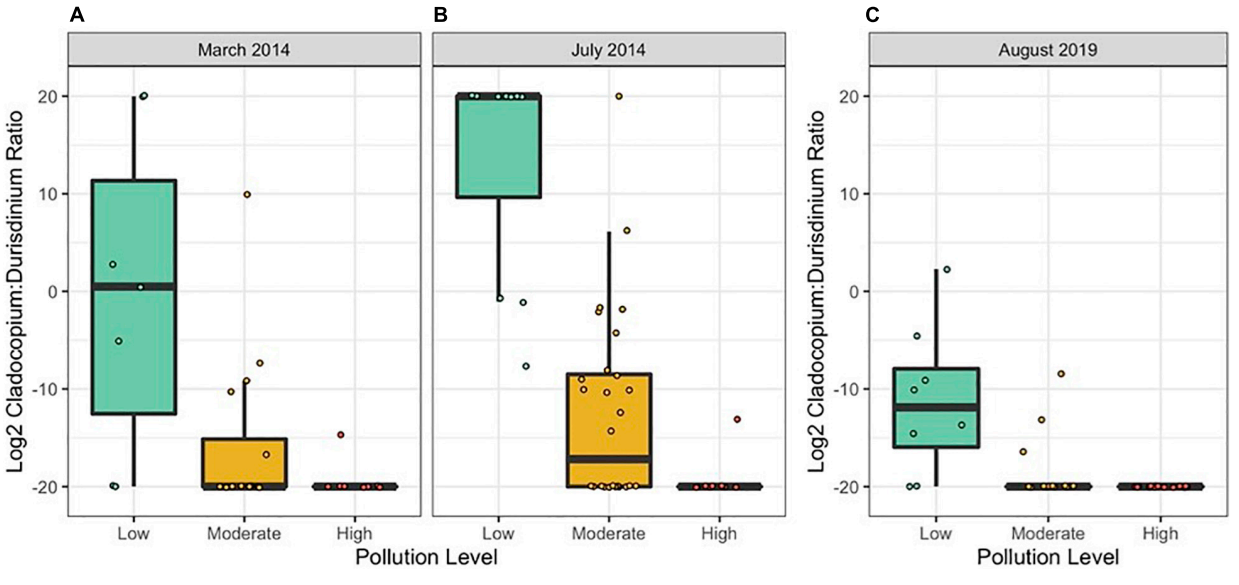

FIGURE 3 | Colony-level log2 *Cladocopium*:*Durusdinium* ratios by pollution level in **(A)** March 2014, **(B)** July 2014, and **(C)** August 2019. Each point represents one coral colony. N = 10/site in 2014 and n = 8/site in 2019. Points represent individual colonies and are jittered to prevent overlapping.

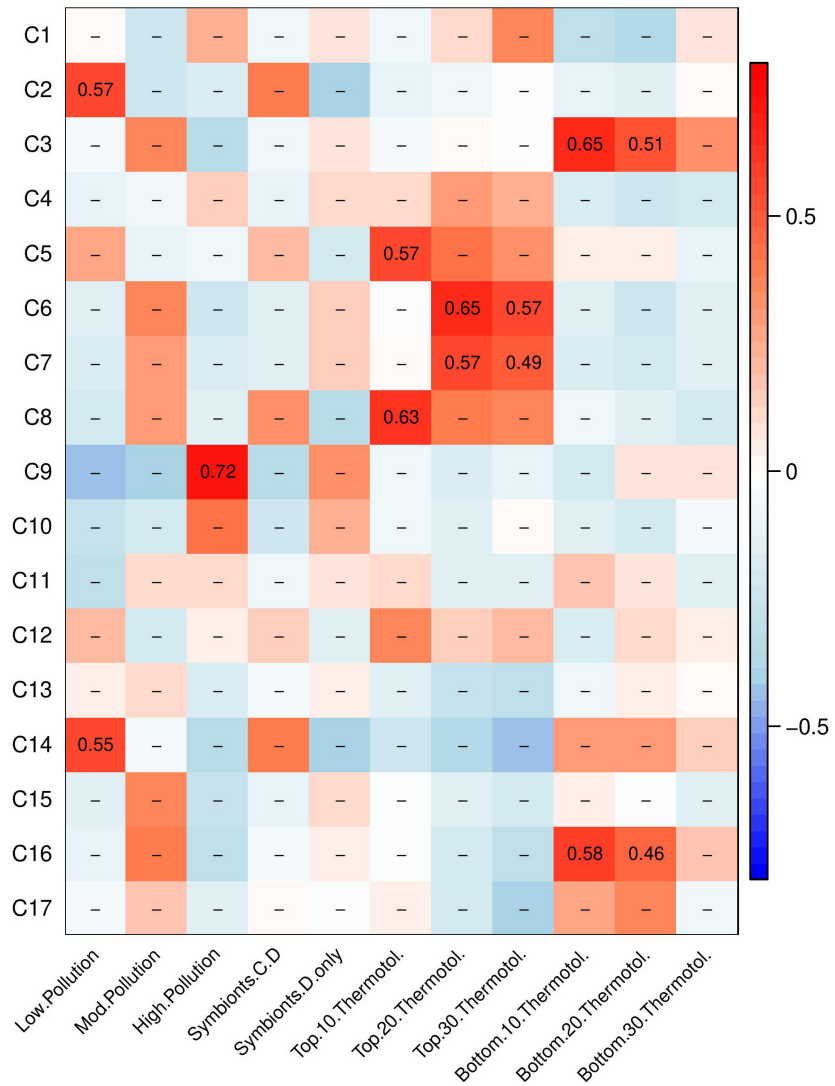

FIGURE 4 | Weighted gene co-expression network analysis (WGCNA) heatmap of module-trait correlations showing gene modules of baseline gene expression that correlate to pollution level, symbiont community, and thermotolerance. Pearson's R for significant correlations ($p < 0.05$) are reported with red indicating a positive correlation and blue indicating a negative correlation.

negative regulation of proteasomal protein catabolic process, regulation of ubiquitin-dependent protein catabolic process, regulation of protein catabolic process, intrinsic apoptotic signaling pathway by p53 class mediator, tail-anchored membrane protein insertion into endoplasmic reticulum (ER) membrane, establishment of protein localization to membrane, negative regulation of neuron differentiation, intrinsic apoptotic signaling pathway in response to ER stress, and regulation of cellular protein catabolic process ($p < 0.05$, **Supplementary Table 1**). These overrepresented categories were contained within broader, parent categories of protein catabolic process regulation, protein localization, apoptotic signaling, negative regulation of nervous system development, and mRNA processing.

A WGCNA was also performed on gene expression on corals under heat stress at 35°C to determine how gene expression under heat stress varies by pollution level, presence or absence of *Cladocopium*, and thermotolerance (**Supplementary Figure 6**). Module H5 related to high pollution; modules H3 and H4 related to low pollution. Four modules (H3, H4, H13, and H14) showed positive expression in corals hosting both *Cladocopium* and *Durusdinium* and negative expression in corals hosting only *Durusdinium*. Gene Ontology (GO) analysis for the four modules correlated to symbiont community type showed enrichment for calcium ion transport, DNA repair, RNA processing, and developmental processes, among other GO terms (**Supplementary Table 2**). Four modules (H7, H8, H13, and H14) correlated with the 10–20% most thermotolerant corals. GO analysis for the four modules correlated to high thermotolerance showed enrichment for RNA processing, gene silencing by RNA, RNA splicing, and membrane docking, among other GO

terms (**Supplementary Table 2**). Two modules (H12 and H15) correlated with the 10–20% least thermotolerant corals. GO analysis for the two modules correlated to low thermotolerance showed enrichment for MAPK activity and vesicle-mediated transport, which were upregulated in the least thermotolerant corals (**Supplementary Table 2**).

Predictors of Thermotolerance in 2014 and 2019

Linear mixed-effects models were used to identify the factors contributing to thermotolerance in 2014 and 2019. In 2014, we investigated the role of symbiont community, season, and pollution level on setting thermotolerance. Log2 *Cladocopium* to *Durusdinium* ratio, season and pollution level were all retained in a linear mixed-effects model as explanatory variables of thermotolerance, as measured in mortality in degree days (**Table 4**). Although *Cladocopium* to *Durusdinium* ratio is correlated with pollution level, pollution level adds additional explanatory power to the model, and its inclusion significantly improves the model fit and survives model simplification using likelihood ratio tests. Taken together, the model including symbiont genotype, season, and pollution level explained 46.9% of variation in thermotolerance in 2014 (marginal R^2 = 0.469; **Table 4**, N = 81). Using a model set approach to quantify the relative importance of each variable, we found that season was the strongest predictor of thermotolerance (sum of AICc weights = 1.00), followed closely by pollution level (0.92), and log2 *Cladocopium* to *Durusdinium* ratio (0.12).

Applying the same model structure to the data from 2019, however, results in a fit with almost no explanatory power. In 2019, we investigated the role of symbiont community, pollution level, and baseline gene expression on setting thermotolerance. All 2019 sampling occurred in the same season, so that parameter was invariant in 2019. Yet, neither log2 *Cladocopium* to *Durusdinium* ratio nor pollution category was significantly correlated with the thermal tolerance phenotype in 2019, with the model explaining only 3.71% of variation in thermotolerance (marginal R^2 = 0.0371%, **Table 2**; N = 37). Gene expression, however, showed substantive and significant power to predict thermotolerance phenotypes, even for a modest sample size (i.e., N = 18). After model simplification, eigengene expression values of three of the six significant WGCNA modules were retained in the model: modules C3, C5, and C8 (**Table 5**), though models retaining module C7 were competitive. While including module C7 and other modules improved model predictive power, we chose to limit the model to three predictor variables to avoid issues of overfitting. Taken together, expression of these three WGCNA modules explained 54.1% of variation in thermotolerance (N = 18). Using a model set approach to quantify the relative importance of each variable, we found that module C5 was the strongest predictor of thermotolerance (sum of AICc weights = 0.86), followed closely by module C8 (0.81), and module C3 (0.78).

TABLE 4 | Colony-level linear mixed-effects model ANOVA table showing impact of *Cladocopium* to *Durusdinium* log2 ratio and pollution category in explaining variation in thermotolerance in 2014.

Variable	Sum Sq	Mean Sq	Num DF	Den DF	*F*-value	*P*-value
Season	123.87	123.87	1	39.74	26.85	6.7e-6
Pollution category	26.00	13.00	2	3.67	2.82	0.18
C:D log2 ratio	17.83	17.83	1	75.68	3.86	0.05

Marginal R^2 = 0.469.

TABLE 5 | Colony-level linear mixed-effects model ANOVA table showing impact of baseline eigengene expression of WGCNA modules in explaining variability in thermotolerance in 2019.

Variable	Sum Sq	Mean Sq	Num DF	Den DF	*F*-value	*P*-value
Eigengene expression of module C3	4.64	4.64	1	13.82	6.88	0.02
Eigengene expression of module C5	6.39	6.39	1	13.27	9.48	0.01
Eigengene expression of module C8	5.20	5.20	1	13.53	7.72	0.02

Marginal R^2 = 0.541.

DISCUSSION

In this study we measured coral thermotolerance and symbiont communities across a gradient of pollution in 2014 and 2019. In 2014, we found variation in thermotolerance by pollution level, largely driven by symbiont community differences. By 2019, we found no variation in thermotolerance by pollution level, likely due to shifts in symbiont communities over time toward *Durusdinium*, which reduced variation in symbiont communities among sites. Instead, thermotolerance in 2019 was best predicted by gene expression of a select number of modules during our control (i.e., baseline) treatment. Our results suggest that baseline gene expression may act as an important indicator of thermotolerance variation and may be especially important after shifts to more ecologically homogeneous symbiont communities, as we saw with *Durusdinium*.

Thermotolerance Varied by Pollution Level in 2014, Driven in Part by Symbiont Community

In 2014, we found differences among sites in their degree-day mortality as an indicator of thermotolerance, with more polluted sites holding more thermotolerant corals. Variation in thermotolerance was best explained by season, followed by variation in pollution level and symbiont community. Thermotolerance was higher in March, at the end of austral summer, compared to in July, in the middle of austral winter. This finding is consistent with past work showing that thermotolerance fluctuates by season and tends to be highest during warmer months (Jurriaans and Hoogenboom, 2020). In addition to season, symbiont community was important

in driving differences in thermotolerance in 2014. Symbiont communities varied between the two time points in 2014, with a higher proportion of heat-tolerant *Durusdinium* in March compared to July (**Figure 3**). It is well established that symbiont communities within corals fluctuate by season and corals tend to host a higher proportion of thermotolerant symbionts in warmer months (Fitt et al., 2000; Chen et al., 2005; Thornhill et al., 2006).

Symbiont Communities Shifted Toward Durusdinium by 2019

At all sites over both years, the proportion of *Cladocopium* was greater at sites with lower pollution levels. This pattern of higher proportions of *Durusdinium* at high pollution sites aligns with previous work showing that corals living in more variable or stressful regions tend to favor *Durusdinium* (Fabricius et al., 2004; Oliver and Palumbi, 2009; Carballo-Bolaños et al., 2019). Some work has also linked increased proportions of *Durusdinium* to areas with higher pollution level or human impact (LaJeunesse et al., 2010). Our findings support the idea that corals exposed to chronic pollution stress, similarly to heat stress, favor *Durusdinium*. In 2014, this pattern was most apparent, with stronger differences in the *Cladocopium* to *Durusdinium* ratio between high and low pollution sites. By 2019, coral fragments at all sites shifted significantly toward *Durusdinium,* with sites considered moderately or highly polluted being at or nearly 100% *Durusdinium*. This shift over time may have occurred due to symbiont shifts after bleaching, such as after any of the four mass bleaching events that occurred between 2014 and 2019 (Witze, 2015; Sudek and Lawrence, 2017; Morikawa and Palumbi, 2019; **Figure 5**). However, it should be noted that colonies sampled in 2019 were not the same colonies as those sampled in 2014, so the significant shift toward *Durusdinium* we describe should not be interpreted as single colony "shuffling," but rather a landscape-scale phenomenon. Since *Durusdinium* outcompete other symbiont species in environmentally stressed corals, they are predicted to continue to overtake coral symbiont communities over time, especially after continual bleaching events (Stat and Gates, 2011; Logan et al., 2021). Shifts to *Durusdinium* typically increase coral thermotolerance, but are accompanied by tradeoffs, including to growth rate (Little et al., 2004). While growth rate was not included in this study, it is possible that corals with high levels of *Durusdinium* (e.g., corals in high pollution sites and/or most corals in 2019) also had lower growth rates or other physiological differences not measured here.

In 2019, we observed an interesting exception to the established idea that corals hosting more *Durusdinium* are more thermotolerant. Though the majority of 2019 colonies hosted 100% *Durusdinium*, the two most thermotolerant coral colonies both hosted a small proportion of *Cladocopium.* The qPCR method used in this study to distinguish between Symbiodiniciae genera cannot distinguish among different species of *Cladocopium*. Therefore, it is possible that we have captured multiple different *Cladocopium* species, some of which have been shown to promote higher thermotolerance (Hoadley et al., 2021). Also interestingly, even corals that hosted 100% *Durusdinium* varied in their thermotolerance, indicating that factors other than symbiont community can play a significant role in setting thermotolerance. Previous work has also shown that corals with similar symbiont communities may exhibit variation in thermotolerance due to differences in their environment (Oliver and Palumbi, 2011).

The shift in symbiont communities toward *Durusdinium* from 2014 to 2019 is likely due to severe marine heatwaves that occurred in the interim (**Supplementary Figure 1**). As symbiont communities become dominated by heat-tolerant *Durusdinium*, this facet of coral's adaptive capacity to future warming may become effectively exhausted. Global projections suggest that anthropogenic warming will favor shifts to heat-tolerant symbiont types under future climate change scenarios, and associated thermotolerance gains may reach an upper limit (Logan et al., 2021). This suggests that other types of acclimatization, such as changes in host gene and protein expression, may play an especially important role in determining thermotolerance when symbiont-driven thermotolerance is maximized for species that can undergo symbiont shifts.

Thermotolerance Did Not Vary by Pollution in 2019, and Symbiont Community Variation Was Minimal

In 2014, we found differences among sites in their degree-day mortalities as an indicator of thermotolerance; yet by

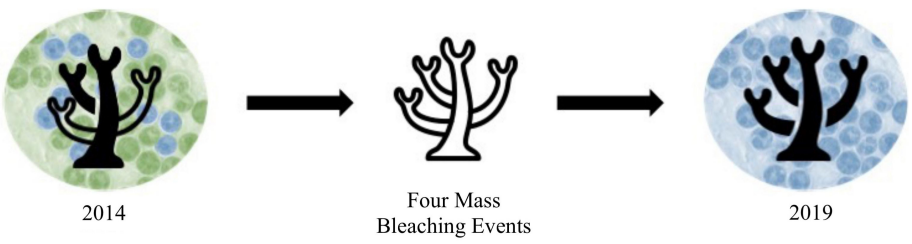

FIGURE 5 | Hypothesized mechanisms underlying thermotolerance in *A. hyacinthus* in Tutuila, American Samoa over time with green representing *Cladocopium* and blue representing *Durusdinium*. In 2014, thermotolerance varied by site, with that variation driven by symbiont community differences. Likely due to the four mass bleaching events that took place between 2014 and 2019, symbiont communities became dominated by *Durusdinium*, thereby evening out differences in thermotolerance among sites. From 2019, we expect that mechanisms other than symbiont community variation are underlying variation in thermotolerance.

2019, pollution was no longer significant in our linear mixed model (p = 0.87, **Table 2**). Thermotolerance differences in 2014 were related to variation in symbiont community among sites. By 2019, these differences were reduced and corals at all sites hosted almost entirely *Durusdinium* (with the exception of one individual). Since symbiont community was a strong predictor of thermotolerance in 2014, we attribute the minimal variation in thermotolerance in 2019 to the minimal variation in symbiont community. In a linear mixed model, we found that log2 *Cladocopium* to *Durusdinium* ratio was no longer predictive of thermotolerance in 2019 (p = 0.24, **Table 2**). The minimal predictive power of symbiont community in 2019 may be attributed to shifts toward *Durusdinium*. Previous work has shown that symbiont fidelity may promote higher thermotolerance compared to symbiont flexibility (i.e., symbiont shifts), especially as co-evolution occurs between symbionts and coral hosts (Howells et al., 2020). Our findings suggest that Tutuila corals are shifting toward *Durusdinium* dominance, and may continue to shift toward even higher proportions of *Durusdinium* after future bleaching events.

Nevertheless, it is possible that differences in thermotolerance variation between 2014 and 2019 may be attributed to the differences in the heat stress assays. In 2014, a threshold-based assay (3 days) was used to determine differences in mortality while in 2019, a ramp-hold assay (6 h) was performed to determine differences in bleaching intensity. However, prior comparisons of the acute ramp-hold assay to longer-term assays (i.e., 2–3 weeks) showed similar response differences (Voolstra et al., 2020; Evensen et al., 2021). Regardless, for this reason, we did not directly compare differences in thermotolerance over time, but focused on how differences in thermotolerance varied by other factors, including site. Yet, it is possible that variation among sites may still be affected by the difference in the assay between years. For example, the 2014 threshold-based assay tests a more sustained acute heat stress (3 days) whereby corals may exhibit greater variation in their ability to acclimate (perhaps due in part to pollution level) while the 2019 ramp-hold assay tests shorter acute heat stress (6 h) that may not allow for as much variation in acclimation by pollution level.

Gene Expression Correlates With Variation in Thermotolerance in 2019

While thermotolerance differences among sites were minimal in 2019 even after controlling for corals that host predominantly *Durusdinium*, there was variation in thermotolerance within sites. Since pollution level and symbiont community did not explain these within-site thermotolerance differences, we investigated baseline gene expression levels and gene expression responses to heat stress. Gene expression at control conditions was linked to thermotolerance during heat stress in six gene modules (**Figure 4**). Interestingly, those gene expression patterns did not appear to be dictated by sample site, meaning that regardless of site, some corals express genes that correlate with future heat stress tolerance. In a linear mixed-effects model of thermotolerance, three of those six modules explained 54.1% of the variation in thermotolerance (**Table 5**).

At control conditions, gene expression modules were correlated to thermotolerance as measured in the heat stress assay to examine the possibility of "front-loading" (*sensu* Barshis et al., 2013). We compared the genes in the four modules where baseline expression correlated to high thermotolerance (e.g., modules C5, C6, C7 and C8; **Figure 4**) with frontloaded genes identified in Barshis et al. (2013). The four modules correlating to high thermotolerance in *A. hyacinthus* matched three of the 135 genes identified in Barshis et al. (2013), on the nearby American Samoa island of Ofu. These three genes were annotated as: a large repetitive protein, a non-collagenous (NC) domain protein, and a protein kinase family protein (Barshis et al., 2013). We examined the Biological Process (BP) Gene Ontology (GO) terms for these three shared genes, though no BP annotations were available. However, one gene was annotated for oxidoreductase activity as a Molecular Function (MF) GO term. We note that the analysis of gene expression differed between the two studies, which may have led to fewer similarities in frontloading genes than expected. We also compared these four modules (e.g., modules C5, C6, C7, and C8; **Figure 4**) to three significant bleaching-associated modules from Rose et al. (2016). We found 131 genes shared with the 2459 genes in module 1, 38 genes shared with the 442 genes in module 10, and 10 genes shared with the 277 genes in module 12 (Rose et al., 2016). We examined the Biological Process GO terms in these 179 shared genes with bleaching-related genes from Rose et al. (2016) and found five occurrences of "apoptosis," "immune response" and "purine nucleotide biosynthetic process," four occurrences of "homophilic cell adhesion" and three occurrences of "defense response to virus," "DNA replication," "innate immune response," "negative regulation of viral reproduction," "proteolysis," and "regulation of transcription, DNA-dependent." The higher number of shared genes in the Rose et al. (2016) comparison vs. the Barshis et al. (2013) comparison may be due to the greater number of genes to compare against or due to the more comparable WGCNA study design. Additionally, both the Barshis et al. (2013) and the Rose et al. (2016) studies examined *A. hyacinthus* from Ofu, an island in American Samoa hosting remarkably thermotolerant corals. Regardless, these findings suggest that gene modules predictive of thermotolerance may vary regionally or over time, and that functional categories may be more important as predictors than individual genes.

In the least thermotolerant corals, baseline gene expression included upregulation of apoptosis and ion transport Gene Ontology (GO) categories, which are characteristic of the cellular stress response (CSR; Kültz, 2005). These patterns indicate that corals with baseline gene expression patterns characteristic of the CSR unexpectedly perform worse during heat stress. Expression of apoptotic or programmed cell death related genes could be indicative of severe or chronic stress. This idea has been proposed previously: constitutive expression of stress response genes may not benefit organisms if (1) overexpression of these genes is costly or (2) these genes drive tradeoffs in the stress response (Rivera et al., 2021).

Taken together, our results indicate that cytokine production and upregulation of immune response genes at baseline conditions may benefit *A. hyacinthus* during heat stress while upregulation of apoptosis-related genes may hinder

thermotolerance. The most thermotolerant corals may use other gene pathways to protect against macromolecular damage without triggering apoptosis (Rivera et al., 2021). These results align with a finding that disease-tolerant corals upregulated cytokine-related pathways under stress while disease-susceptible corals upregulated apoptotic-related pathways (Fuess et al., 2017). These differences in baseline gene expression may be due to variables that were not measured in this study, including environmental, ecological, or evolutionary variation. It is also possible that the differences in baseline gene expression are not plastic, but rather signal differences in heritable variation in thermotolerance. Since genetic differences were not explored in this study, we cannot determine whether these gene expression differences occur due to plastic processes or genetic variation, though past work on *A. hyacinthus* in American Samoa has found that both adaptation and acclimatization shape thermotolerance (Oliver and Palumbi, 2011; Palumbi et al., 2014; Barshis et al., 2018; Thomas et al., 2018).

The linear mixed model that best predicted thermotolerance in 2019 contained eigengene expression of three gene modules (**Table 5**). These modules encompassed 681 genes whose baseline expression could be used to predict 54.1% of variation in future thermotolerance. This can be compared to the 46.9% of thermotolerance variation in 2014 that could be explained by season, log2 *Cladocopium* to *Durusdinium* ratio, and pollution level. However, if we had baseline gene expression data available for 2014, it is possible that more variation in thermotolerance could have been explained by the model.

Baseline expression of these three gene modules were shown to predict a substantial amount of variation in future thermotolerance. This presents a useful tool for reef managers or restoration specialists, who may test baseline expression to identify corals with high thermotolerance. However, additional research with higher sample sizes and broader geographic areas would need to be conducted before useful baseline gene expression lists could be generated. Our gene list was useful in predicting thermotolerance of our samples, yet, when compared to published gene lists (e.g., Barshis et al., 2013; Rose et al., 2016), we find few genes overlapping. This suggests that baseline gene expression data may be context dependent and may be most useful when applied to the geographic region where they were generated. Further research into baseline gene expression and its ability to predict thermotolerance may give insight into its potential as a conservation tool.

Baseline Gene Expression Related to Pollution Level

In a WGCNA analysis of baseline gene expression patterns, module C9 showed opposing patterns in the low pollution vs. the high pollution sites (**Figure 4**). When compared to Gene Ontology (GO) categories upregulated under nutrient stress in Rosic et al. (2014), none of the categories matched Biological Processes GO terms in module C9. We also compared the GO terms of genes in module C9 to the generalized *Acropora* stress response GO terms from Dixon et al. (2020) and found five of the 190 genes shared GO terms. These five genes were primarily mini-collagen and calcium-binding proteins. While few of the GO terms in module C9 matched previous studies, many of the GO terms appear to be involved in production of methionine, which is an amino acid that has been shown to mitigate oxidative stress (Luo and Levine, 2009; Aguilar et al., 2017). Therefore, it is possible that pollution is inducing stress response genes that differ from those identified in the two previous studies. This may be due to the highly context-dependent nature of pollution, whereby differences in pollution may induce different stress response genes. This suggests that pollution may be inducing some level of cellular stress, even though pollution did not correlate with thermotolerance in 2019.

Gene Expression Under Heat Stress Related to Pollution Level, Symbiont Community, and Thermotolerance

During heat stress, gene expression correlated with pollution but showed more significant correlations with symbiont community (**Supplementary Figure 6**). Two gene modules showed opposite patterns in corals hosting entirely *Durusdinium* compared to those hosting *Cladocopium* and *Durusdinium*. This follows previous work showing that Symbiodiniaceae type can affect gene expression in the coral host (Yuyama et al., 2012; Barfield et al., 2018; Helmkampf et al., 2019). The modules that varied by Symbiodiniaceae type contained overrepresented Biological Processes (BP) Gene Ontology (GO) categories relating to RNA splicing, processing, and gene silencing. Barfield et al. (2018) also found that RNA processing and modification genes were upregulated in corals hosting *Cladocopium* compared to those hosting *Durusdinium*. This suggests that maintaining symbiosis with *Cladocopium* may require post-transcriptional modifications (Baumgarten et al., 2017; Barfield et al., 2018).

Gene expression under heat stress was also correlated to thermotolerance, with four modules related to the 10–20% most thermotolerant corals and two modules related to the 10–20% least thermotolerant corals (**Supplementary Figure 6**). Module H15, whose expression was upregulated in the least thermotolerant corals, was significantly enriched for MAPK signaling. Mitogen-activated protein kinases (MAPK) are signaling proteins involved in repairing oxidative damage that occurs during stress (Kültz, 2005). The least thermotolerant corals may express higher levels of stress response genes during heat stress because they are encountering greater macromolecular damage than more thermotolerant corals.

Interestingly, two of the modules that were upregulated in *Cladocopium*-containing corals under heat stress were also upregulated in the most thermotolerant corals. This is unexpected since previous work shows that colonies hosting entirely *Durusdinium* are typically more thermotolerant (Berkelmans and van Oppen, 2006; Stat and Gates, 2011; Howells et al., 2020). However, this pattern is driven by two individuals mentioned above hosting low levels (<1%) of *Cladocopium* which were among the top performing 10%.

CONCLUSION

This study explored the impact of pollution on coral thermotolerance, symbiont communities and gene expression

in a field-based experiment. While our field-based experiment cannot disentangle the specific impacts of pollution on these variables, it is useful to study these effects *in situ* to determine how real-world environments vary. Symbiont communities showed trends with pollution level, with more polluted sites hosting higher proportions of heat-tolerant *Durusdinium*. Yet, by 2019, all sites overwhelmingly hosted *Durusdinium,* demonstrating a noticeable shift in symbiont communities from 2014, which contained much higher levels of heat-sensitive *Cladocopium*. Thermotolerance was not determined by symbiont communities nor pollution level by 2019, but did relate to baseline gene expression patterns prior to heat stress. This suggests that differences in baseline gene expression may allow some corals to better tolerate subsequent heat stress. We found that baseline expression of three gene modules was predictive of future thermotolerance. Future work should investigate what triggers these differences in baseline gene expression to better understand how management efforts can use them in conservation efforts. This study highlights how gene expression patterns could aid in the identification of heat-tolerant corals in a future where most corals are dominated by *Durusdinium* and symbiont-driven thermotolerance has reached an upper limit. Further, the work serves as a cautionary tale that we need to routinely re-examine our assumptions about patterns of coral thermotolerance as climate change effects become increasingly manifest.

DATA AVAILABILITY STATEMENT

The datasets presented in this study can be found in online repositories. The names of the repository/repositories and accession number(s) can be found below: the raw RNA sequencing reads are available on the NCBI Sequence Read Archive (SRA) database (Bioproject accession: PRJNA762371; SRA accession: SRP339664). All data and code are available at https://github.com/melissanaugle/SCLERA_Tutuila_Thermotolerance.

AUTHOR CONTRIBUTIONS

TO, DB, and CL collected the data in 2014. MN collected the data in 2019 and wrote the first draft of the manuscript. MN and TO performed the statistical analysis. MN, TO, and CL contributed to the interpretation of the results and wrote sections of the manuscript. All authors, excepting RG who sadly could not, contributed to manuscript revision, read, and approved the submitted version. All authors contributed to the conception and design of the study.

FUNDING

The 2014 component of this project was funded by a National Oceanic and Atmospheric Administration Coral Reef Conservation Program grant to TO, RG, and CL (NA13NOS4820018). Data collection and analysis in 2019 was funded by a California State University, Monterey Bay Research, Scholarship and Creative Activity grant to CL, an Earl H. and Ethel M. Myer's Oceanographic and Marine Biology Trust grant to MN, a California State University Program for Education and Research in Biotechnology grant to MN, an Explorer's Club-Mamont Scholar grant to MN, and a California State University Council on Ocean Affairs, Science&Technology (COAST) grant to MN.

ACKNOWLEDGMENTS

We would like to thank Griffin Srednick, Hideyo Hattori, Johann Vollrath, Valentine Vaeoso, and Salvador Jorgensen for their roles in the 2014 field collections. We thank Jennifer Grossman and Casey Juliussen, who were supported by the Undergraduate Research Opportunities Center at California State University Monterey Bay (CSUMB), for their roles in 2019 field collections. We also thank J. Steve Ryan for his CBASS assistance. We additionally thank Melanie (Cuijuan) Yu, Jacoby Baker, Juliana Cornett, Arie Dash and the 2020 and 2021 Marine Experimental Physiology courses at CSUMB for their contributions to RNAseq sample preparation and preliminary data analysis. We would also like to thank two reviewers for their insightful comments and efforts toward improving our manuscript.

SUPPLEMENTARY MATERIAL

The Supplementary Material for this article can be found online at: https://www.frontiersin.org/articles/10.3389/fmars.2021.760891/full#supplementary-material

Supplementary Figure 1 | Timeline of marine heatwave occurrence from Coral Reef Watch "Samoa" virtual station, as measured by degree-heating weeks.

Supplementary Figure 2 | Visualization of heat ramp profiles for **(A)** the 2014 threshold-based heat stress assay and **(B)** the 2019 ramp-hold heat stress assay.

Supplementary Figure 3 | Thermotolerance variation among colonies by site in **(A)** March 2014, **(B)** July 2014, and **(C)** August 2019. Thermotolerance was measured as mortality in degree days in 2014 and as a two-variable bleaching metric in 2019. Sites are colored according to their pollution level with red representing high pollution, yellow representing moderate pollution and green representing low pollution. Points represent individual colonies and are jittered to prevent overlapping.

Supplementary Figure 4 | Colony-level visual representation of symbiont *Cladocopium*:*Durusdinium* ratios among sites in **(A)** March 2014, **(B)** July 2014, and **(C)** August 2019. $N = 10$ in 2014 and $n = 8$ in 2019. Sites are colored according to their pollution level with red representing high pollution, yellow representing moderate pollution, and green representing low pollution. Points represent individual colonies and are jittered to prevent overlapping.

Supplementary Figure 5 | Heatmap showing differential expression of 6,020 genes between the control and heat stress treatments (edgeR, FDR < 0.001, fold-change > 4). Green labels represent low pollution sites, orange represent moderate pollution and red represent high pollution. Expression of corals in control treatments are shown on the left and expression of heat stressed treatments are shown on the right.

Supplementary Figure 6 | Weighted gene co-expression network analysis (WGCNA) heatmap of module-trait correlations showing gene modules of gene expression during heat stress that correlate to pollution level, symbiont community, and thermotolerance. Pearson's R for significant correlations ($p < 0.05$) are reported with red indicating a positive correlation and blue indicating a negative correlation.

Supplementary Table 1 | Significantly enriched Biological Processes (BP) GO terms for the modules of baseline gene expression correlated with the most and least thermotolerant corals. GO terms were included if adjusted p-value ≤ 0.05. Modules C5, C6, C7, and C8 were upregulated in control conditions in the most thermotolerant corals. Modules C3 and C16 were upregulated in control conditions in the least thermotolerant corals.

Supplementary Table 2 | Significantly enriched Biological Processes (BP) GO terms for the modules of gene expression during heat stress that correlated with the most and least thermotolerant corals. GO terms were included if adjusted p-value ≤ 0.05. Modules H7, H8, H13, and H14 were upregulated under heat stress in the most thermotolerant corals. Modules H12 and H15 were upregulated under heat stress in the least thermotolerant corals.

REFERENCES

Aguilar, C., Raina, J.-B., Motti, C. A., Fôret, S., Hayward, D. C., Lapeyre, B., et al. (2017). Transcriptomic analysis of the response of *Acropora millepora* to hypo-osmotic stress provides insights into DMSP biosynthesis by corals. *BMC Genom.* 18:612. doi: 10.1186/s12864-017-3959-0

Barfield, S. J., Aglyamova, G. V., Bay, L. K., and Matz, M. V. (2018). Contrasting effects of *Symbiodinium* identity on coral host transcriptional profiles across latitudes. *Mol. Ecol.* 27, 3103–3115. doi: 10.1111/mec.14774

Barshis, D. J., Birkeland, C., Toonen, R. J., Gates, R. D., and Stillman, J. H. (2018). High-frequency temperature variability mirrors fixed differences in thermal limits of the massive coral *Porites lobata*. *J. Exp. Biol* 221:jeb188581. doi: 10.1242/jeb.188581

Barshis, D. J., Ladner, J. T., Oliver, T. A., Seneca, F. O., Traylor-Knowles, N., and Palumbi, S. R. (2013). Genomic basis for coral resilience to climate change. *Proc. Natl. Acad. Sci.U.S.A.* 110, 1387–1392. doi: 10.1073/pnas.1210224110

Bates, D., Mäechler, M., Bolker, B., and Walker, S. (2015). Fitting Linear mixed-effects models using lme4. *J. Stat. Softw.* 67, 1–48. doi: 10.18637/jss.v067.i01

Baumgarten, S., Cziesielski, M. J., Thomas, L., Michell, C., Esherick, L., Pringle, J., et al. (2017). Evidence for miRNA-mediated modulation of the host transcriptome in cnidarian-dinoflagellate symbiosis. *Mol. Ecol* 27, 403–418. doi: 10.1111/mec.14452

Becker, D. M., and Silbiger, N. J. (2020). Nutrient and sediment loading affect multiple facets of functionality in a tropical branching coral. *J. Exp. Biol.* 223:jeb225045. doi: 10.1242/jeb.225045

Becker, D. M., Putnam, H. M., Burkepile, D. E., Adam, T. C., Vega Thurber, R., and Silbiger, N. J. (2021). Chronic low-level nutrient enrichment benefits coral thermal performance in a fore reef habitat. *Coral Reefs* 40, 1637–165. doi: 10.1007/s00338-021-02138-2

Bellantuono, A. J., Granados-Cifuentes, C., Miller, D. J., Hoegh-Guldberg, O., and Rodriguez-Lanetty, M. (2012). Coral thermal tolerance: tuning gene expression to resist thermal stress. *PLoS One* 7:e50685. doi: 10.1371/journal.pone.0050685

Bellard, C., Bertelsmeier, C., Leadley, P., Thuiller, W., and Courchamp, F. (2012). Impacts of climate change on the future of biodiversity. *Ecol. Lett.* 15, 365–377. doi: 10.1111/j.1461-0248.2011.01736.x

Béraud, E., Gevaert, F., Rottier, C., and Ferrier-Pagès, C. (2013). The response of the scleractinian coral *Turbinaria reniformis* to thermal stress depends on the nitrogen status of the coral holobiont. *J. Exp. Biol.* 216, 2665–2674. doi: 10.1242/jeb.085183

Berkelmans, R., and van Oppen, M. J. H. (2006). The role of zooxanthellae in the thermal tolerance of corals: a 'nugget of hope' for coral reefs in an era of climate change. *Proc. Royal Soc. B. Biol. Sci.* 273, 2305–2312. doi: 10.1098/rspb.2006.3567

Bolger, A. M., Lohse, M., and Usadel, B. (2014). Trimmomatic: a flexible trimmer for Illumina sequence data. *Bioinformatics* 30, 2114–2120. doi: 10.1093/bioinformatics/btu170

Burkepile, D. E., Shantz, A. A., Adam, T. C., Munsterman, K. S., Speare, K. E., Ladd, M. C., et al. (2020). Nitrogen identity drives differential impacts of nutrients on coral bleaching and mortality. *Ecosystems* 23, 798–811. doi: 10.1007/s10021-019-00433-2

Carballo-Bolaños, R., Denis, V., Huang, Y.-Y., Keshavmurthy, S., and Chen, C. A. (2019). Temporal variation and photochemical efficiency of species in Symbiodinaceae associated with coral *Leptoria phrygia* (Scleractinia. Merulinidae) exposed to contrasting temperature regimes. *PLoS One* 14:e0218801. doi: 10.1371/journal.pone.0218801

Chen, C. A., Wang, J.-T., Fang, L.-S., and Yang, Y.-W. (2005). Fluctuating algal symbiont communities in *Acropora palifera* (Scleractinia: *Acroporidae*) from Taiwan. *Mar. Ecol. Prog. Ser.* 295, 113–121. doi: 10.3354/meps295113

Chen, Y., Lun, A. T. L., and Smyth, G. K. (2016). From reads to genes to pathways: differential expression analysis of RNA-Seq experiments using Rsubread and the edgeR quasi-likelihood pipeline. *F1000Res.* 5:1438. doi: 10.12688/f1000research.8987.2

Cunning, R., and Baker, A. C. (2013). Excess algal symbionts increase the susceptibility of reef corals to bleaching. *Nat. Clim. Change* 3:259. doi: 10.1038/nclimate1711

Cunning, R., Parker, K. E., Johnson-Sapp, K., Karp, R. F., Wen, A. D., Williamson, O. M., et al. (2021). Census of heat tolerance among Florida's threatened staghorn corals finds resilient individuals throughout existing nursery populations. *Proc. Royal Soc. B. Biol. Sci.* 288, 20211613. doi: 10.1098/rspb.2021.1613

Darling, E. S., McClanahan, T. R., and Côté, I. M. (2020). Combined effects of two stressors on Kenyan coral reefs are additive or antagonistic, not synergistic. *Conserv. Lett.* 3, 122–130.

DiDonato, G. (2004). *Developing an Initial Watershed Classification For American Samoa. Report From The American Samoa Environmental Protection Agency*. Pago Pago, AS: The American Samoa Environmental Protection Agency.

Dixon, G., Abbott, E., and Matz, M. (2020). Meta-analysis of the coral environmental stress response: *Acropora* corals show opposing responses depending on stress intensity. *Mol. Ecol.* 29, 2855–2870. doi: 10.1111/mec.15535

Donovan, M. K., Adam, T. C., Shantz, A. A., Speare, K. E., Munsterman, K. S., Rice, M. M., et al. (2020). Nitrogen pollution interacts with heat stress to increase coral bleaching across the seascape. *Proc. Natl. Acad. Sci. U.S.A.* 117, 5351–5357. doi: 10.1073/pnas.1915395117

Ellis, J. I., Jamil, T., Anlauf, H., Coker, D. J., Curdia, J., Hewitt, J., et al. (2019). Multiple stressor effects on coral reef ecosystems. *Glob. Chang. Biol.* 25, 4131–4146. doi: 10.1111/gcb.14819

Ely, B. R., Lovering, A. T., Horowitz, M., and Minson, C. T. (2014). Heat acclimation and cross tolerance to hypoxia. *Temperature* 1, 107–114. doi: 10.4161/temp.29800

Evensen, N. R., Fine, M., Perna, G., Voolstra, C. R., and Barshis, D. J. (2021). Remarkably high and consistent tolerance of a Red Sea coral to acute and chronic thermal stress exposures. *Limnol. Oceanogr.* 66, 1718–1729. doi: 10.1002/lno.11715

Fabricius, K., Mieog, J., Colin, P., Idip, D., and van Oppen, M. (2004). Identity and diversity of coral endosymbionts (zooxanthellae) from three Palauan reefs with contrasting bleaching, temperature and shading histories. *Mol. Ecol.* 13, 2445–2458. doi: 10.1111/j.1365-294X.2004.02230.x

Fitt, W., McFarland, F., Warner, M., and Chilcoat, G. (2000). Seasonal patterns of tissue biomass and densities of symbiotic dinoflagellates in reef corals and relation to coral bleaching. *Limnol. Oceanogr.* 45, 677–685. doi: 10.4319/lo.2000.45.3.0677

Fuess, L. E., Pinzón, C. J. H., Weil, E., Grinshpon, R. D., and Mydlarz, L. D. (2017). Life or death: disease-tolerant coral species activate autophagy following immune challenge. *Proc. Royal Soc. B Biol. Sci.* 284:20170771. doi: 10.1098/rspb.2017.0771

Fuller, Z. L., Mocellin, V. J. L., Morris, L. A., Cantin, N., Shepherd, J., Sarre, L., et al. (2020). Population genetics of the coral *Acropora millepora*: toward genomic prediction of bleaching. *Science* 369:eaba4674. doi: 10.1126/science.aba4674

Gunderson, A. R., Armstrong, E. J., and Stillman, J. H. (2016). Multiple stressors in a changing world: the need for an improved perspective on physiological responses to the dynamic marine environment. *Ann. Rev. Mar. Sci.* 8, 357–378. doi: 10.1146/annurev-marine-122414-033953

Helmkampf, M., Bellinger, M. R., Frazier, M., and Takabayashi, M. (2019). Symbiont type and environmental factors affect transcriptome-wide gene expression in the coral *Montipora capitata*. *Eco. Evol.* 9, 378–392. doi: 10.1002/ece3.4756

Hoadley, K. D., Pettay, D. T., Lewis, A., Wham, D., Grasso, C., Smith, R., et al. (2021). Different functional traits among closely related algal symbionts dictate stress endurance for vital Indo-Pacific reef-building corals. *Glob. Chang. Biol.* 27, 5295–5309. doi: 10.1111/gcb.15799

Howells, E. J., Bauman, A. G., Vaughan, G. O., Hume, B. C. C., Voolstra, C. R., and Burt, J. A. (2020). Corals in the hottest reefs in the world exhibit symbiont fidelity not flexibility. *Mol. Ecol.* 29, 899–911. doi: 10.1111/mec.15372

Huerta-Cepas, J., Forslund, K., Coelho, L. P., Szklarczyk, D., Jensen, L. J., von Mering, C., et al. (2017). Fast genome-wide functional annotation through orthology assignment by eggNOG-Mapper. *Mol. Biol. Evol.* 34, 2115–2122. doi: 10.1093/molbev/msx148

Hughes, T. P., Kerry, J. T., Álvarez-Noriega, M., Álvarez-Romero, J. G., Anderson, K. D., Baird, A. H., et al. (2017). Global warming and recurrent mass bleaching of corals. *Nature* 543, 373–377. doi: 10.1038/nature21707

Jurriaans, S., and Hoogenboom, M. O. (2020). Seasonal acclimation of thermal performance in two species of reef-building corals. *Mar. Ecol. Prog. Ser.* 635, 55–70. doi: 10.3354/meps13203

Kamil, B. (2020). *MuMIn: Multi-Model Inference.* R package version 1.43.17.

Kersting, D. K., Cebrian, E., Casado, C., Teixidó, N., Garrabou, J., and Linares, C. (2015). Experimental evidence of the synergistic effects of warming and invasive algae on a temperate reef-builder coral. *Sci. Rep.* 5:18635. doi: 10.1038/srep18635

Kültz, D. (2005). Molecular and evolutionary basis of the cellular stress response. *Annu. Rev. Physiol.* 67, 225–257. doi: 10.1146/annurev.physiol.67.040403.103635

Kültz, D. (2020). Evolution of cellular stress response mechanisms. *J. Exp. Zool. A Ecol. Integr. Physiol.* 333, 359–378.

Ladner, J. T., Barshis, D. J., and Palumbi, S. R. (2012). Protein evolution in two co-occurring types of *Symbiodinium*: an exploration into the genetic basis of thermal tolerance in *Symbiodinium* clade D. *BMC Evol. Biol.* 12:217. doi: 10.1186/1471-2148-12-217

LaJeunesse, T. C., Pettay, D. T., Sampayo, E. M., Phongsuwan, N., Brown, B., Obura, D. O., et al. (2010). Long-standing environmental conditions, geographic isolation and host–symbiont specificity influence the relative ecological dominance and genetic diversification of coral endosymbionts in the genus *Symbiodinium*. *J. Biogeogr.* 37, 785–800. doi: 10.1111/j.1365-2699.2010.02273.x

LaJeunesse, T. C., Parkinson, J. E., Gabrielson, P. W., Jeong, H. J., Reimer, J. D., Voolstra, C. R., et al. (2018). Systematic revision of symbiodiniaceae highlights the antiquity and diversity of coral endosymbionts. *Curr. Biol.* 28, 2570–2580.e6. doi: 10.1016/j.cub.2018.07.008

Langfelder, P., and Horvath, S. (2008). WGCNA: an R package for weighted correlation network analysis. *BMC Bioinform.* 9:559. doi: 10.1186/1471-2105-9-559

Langmead, B., and Salzberg, S. L. (2012). Fast gapped-read alignment with Bowtie 2. *Nat. Methods* 9, 357–359. doi: 10.1038/nmeth.1923

Li, B., and Dewey, C. N. (2011). RSEM: accurate transcript quantification from RNA-Seq data with or without a reference genome. *BMC Bioinform.* 12:323. doi: 10.1186/1471-2105-12-323

Li, G. C., and Hahn, G. M. (1978). Ethanol-induced tolerance to heat and to adriamycin. *Nature* 274, 699–701. doi: 10.1038/274699a0

Little, A. F., van Oppen, M. J. H., and Willis, B. L. (2004). Flexibility in algal endosymbioses shapes growth in reef corals. *Science* 304, 1492–1494. doi: 10.1126/science.1095733

Logan, C. A., Dunne, J. P., Ryan, J. S., Baskett, M. L., and Donner, S. D. (2021). Quantifying global potential for coral evolutionary response to climate change. *Nat. Clim. Change* 11, 537–542. doi: 10.1038/s41558-021-01037-2

Loya, Y., Sakai, K., Yamazato, K., Nakano, Y., Sambali, H., and van Woesik, R. (2001). Coral bleaching: the winners and the losers. *Ecol. Lett.* 4, 122–131. doi: 10.1046/j.1461-0248.2001.00203.x

Luo, S., and Levine, R. L. (2009). Methionine in proteins defends against oxidative stress. *FASEB J.* 23, 464–472. doi: 10.1096/fj.08-118414

Marangoni, L. F. B., Pinto, M. M., de, A. N., Marques, J. A., and Bianchini, A. (2019). Copper exposure and seawater acidification interaction: antagonistic effects on biomarkers in the zooxanthellate scleractinian coral *Mussismilia harttii*. *Aquat. Toxicol.* 206, 123–133. doi: 10.1016/j.aquatox.2018.11.005

Marshall, P. A., and Baird, A. H. (2000). Bleaching of corals on the Great Barrier Reef: differential susceptibilities among taxa. *Coral Reefs* 19, 155–163. doi: 10.1007/s003380000086

Morikawa, M. K., and Palumbi, S. R. (2019). Using naturally occurring climate resilient corals to construct bleaching-resistant nurseries. *Proc. Natl. Acad. Sci. U.S.A.* 116, 10586–10591. doi: 10.1073/pnas.1721415116

Morris, L. A., Voolstra, C. R., Quigley, K. M., Bourne, D. G., and Bay, L. K. (2019). Nutrient availability and metabolism affect the stability of coral-Symbiodiniaceae symbioses. *Trends Microbiol.* 27, 678–689. doi: 10.1016/j.tim.2019.03.004

Oliver, T. A., and Palumbi, S. R. (2009). Distributions of stress-resistant coral symbionts match environmental patterns at local but not regional scales. *Mar. Ecol. Prog. Ser.* 378, 93–103. doi: 10.3354/meps07871

Oliver, T. A., and Palumbi, S. R. (2011). Do fluctuating temperature environments elevate coral thermal tolerance? *Coral Reefs* 30, 429–440. doi: 10.1007/s00338-011-0721-y

Palumbi, S. R., Barshis, D. J., Traylor-Knowles, N., and Bay, R. A. (2014). Mechanisms of reef coral resistance to future climate change. *Science* 344, 895–898. doi: 10.1126/science.1251336

Pinheiro, J., Bates, D., DebRoy, S., Sarkar, D., and R Core Team (2021). *Nlme: Linear And Nonlinear Mixed Effects Models.* R package version 3.1-152.

Putnam, H. M., and Gates, R. D. (2015). Preconditioning in the reef-building coral *Pocillopora damicornis* and the potential for trans-generational acclimatization in coral larvae under future climate change conditions. *J. Exp. Biol.* 218, 2365–2372. doi: 10.1242/jeb.123018

R Core Team (2021). *R: A language and environment for statistical computing.* R Foundation for Statistical Computing. Vienna, Austria.

Riegl, B., Glynn, P. W., Banks, S., Keith, I., Rivera, F., Vera-Zambrano, M., et al. (2019). Heat attenuation and nutrient delivery by localized upwelling avoided coral bleaching mortality in northern Galapagos during 2015/2016 ENSO. *Coral Reefs* 38, 773–785. doi: 10.1007/s00338-019-01787-8

Rivera, H. E., Aichelman, H. E., Fifer, J. E., Kriefall, N. G., Wuitchik, D. M., Wuitchik, S. J. S., et al. (2021). A framework for understanding gene expression plasticity and its influence on stress tolerance. *Mol. Ecol.* 30, 1381–1397. doi: 10.1111/mec.15820

Rohwer, F., Seguritan, V., Azam, F., and Knowlton, N. (2002). Diversity and distribution of coral-associated bacteria. *Mar. Ecol. Prog. Ser.* 243, 1–10. doi: 10.3354/meps243001

Rose, N. H., Seneca, F. O., and Palumbi, S. R. (2016). Gene networks in the wild: identifying transcriptional modules that mediate coral resistance to experimental heat stress. *Genome Biol. Evol.* 8, 243–252. doi: 10.1093/gbe/evv258

Rosic, N., Kaniewska, P., Chan, C.-K. K., Ling, E. Y. S., Edwards, D., Dove, S., et al. (2014). Early transcriptional changes in the reef-building coral *Acropora aspera* in response to thermal and nutrient stress. *BMC Genom.* 15:1–17. doi: 10.1186/1471-2164-15-1052

Sabehat, A., Weiss, D., and Lurie, S. (1998). Heat-shock proteins and cross-tolerance in plants. *Physiol. Plant* 103,437–441. doi: 10.1034/j.1399-3054.1998.1030317.x

Savary, R., Barshis, D. J., Voolstra, C. R., Cárdenas, A., Evensen, N. R., Banc-Prandi, G., et al. (2021). Fast and pervasive transcriptomic resilience and acclimation of extremely heat-tolerant coral holobionts from the northern Red Sea. *Proc. Natl. Acad. Sci. U.S.A.* 118:e2023298118. doi: 10.1073/pnas.2023298118

Seebacher, F., White, C. R., and Franklin, C. E. (2015). Physiological plasticity increases resilience of ectothermic animals to climate change. *Nat. Clim. Change* 5, 61–66. doi: 10.1038/nclimate2457

Shuler, C. K., Amato, D. W., Gibson, V., Baker, L., Olguin, A. N., Dulai, H., et al. (2019). Assessment of terrigenous nutrient loading to coastal ecosystems along a human land-use gradient, Tutuila, American Samoa. *Hydrology* 6:18. doi: 10.3390/hydrology6010018

Shuler, C. K., and Comeros-Raynal, M. (2020). Ridge to reef management implications for the development of an open-source dissolved inorganic nitrogen-loading model in American Samoa. *Environ. Manage.* 66, 498–515. doi: 10.1007/s00267-020-01314-4

Siebeck, U. E., Marshall, N. J., Klüter, A., and Hoegh-Guldberg, O. (2006). Monitoring coral bleaching using a colour reference card. *Coral Reefs* 25, 453–460. doi: 10.1007/s00338-006-0123-8

Silbiger, N. J., Nelson, C. E., Remple, K., Sevilla, J. K., Quinlan, Z. A., Putnam, H. M., et al. (2018). Nutrient pollution disrupts key ecosystem functions on coral reefs. *Proc. Royal Soc. B. Biol. Sci.* 285:20172718. doi: 10.1098/rspb.2017.2718

Somero, G. N. (2010). The physiology of climate change: how potentials for acclimatization and genetic adaptation will determine 'winners' and 'losers.'. *J. Exp. Biol.* 213, 912–920. doi: 10.1242/jeb.037473

Stat, M., and Gates, R. (2011). Clade D *Symbiodinium* in scleractinian corals: a "nugget" of hope, a selfish opportunist, an ominous sign, or all of the above? *J. Mar. Biol.* 2011:730715. doi: 10.1155/2011/730715

Sudek, M., and Lawrence, A. (2017). *American Samoa Coral Reef Monitoring Program.* Progress report FY13/14. Report to the Department of Marine and Wildlife Resources, Coral Reef Advisory Group and NOAA. Pago Pago, AS: Department of Marine and Wildlife Resources.

Thomas, L., Rose, N. H., Bay, R. A., López, E. H., Morikawa, M. K., Ruiz-Jones, L., et al. (2018). Mechanisms of thermal tolerance in reef-building corals across a fine-grained environmental mosaic: lessons from Ofu, American Samoa. *Front. Mar. Sci.* 4:434. doi: 10.3389/fmars.2017.00434

Thornhill, D. J., LaJeunesse, T. C., Kemp, D. W., Fitt, W. K., and Schmidt, G. W. (2006). Multi-year, seasonal genotypic surveys of coral-algal symbioses reveal prevalent stability or post-bleaching reversion. *Mar. Biol.* 148, 711–722. doi: 10.1007/s00227-005-0114-2

Towle, E. K., Baker, A. C., and Langdon, C. (2016). Preconditioning to high CO2 exacerbates the response of the Caribbean branching coral *Porites porites* to high temperature stress. *Mar. Ecol. Prog. Ser.* 546, 75–84. doi: 10.3354/meps11655

Voolstra, C. R., Buitrago-López, C., Perna, G., Cárdenas, A., Hume, B. C. C., Rädecker, N., et al. (2020). Standardized short-term acute heat stress assays resolve historical differences in coral thermotolerance across microhabitat reef sites. *Glob. Change Biol* 26, 4328–4343. doi: 10.1111/gcb.15148

Voolstra, C. R., Valenzuela, J. J., Turkarslan, S., Cárdenas, A., Hume, B. C. C., Perna, G., et al. (2021). Contrasting heat stress response patterns of coral holobionts across the Red Sea suggest distinct mechanisms of thermal tolerance. *Mol. Ecol.* 30, 4466–4480. doi: 10.1111/mec.16064

West, J. M., and Salm, R. V. (2003). Resistance and resilience to coral bleaching: implications for coral reef conservation and management. *Conserv. Biol.* 17, 956–967. doi: 10.1046/j.1523-1739.2003.02055.x

Wickham, H. (2016). *ggplot2: Elegant Graphics For Data Analysis*. New York, NY: Springer-Verlag.

Wiedenmann, J., D'Angelo, C., Smith, E. G., Hunt, A. N., Legiret, F.-E., Postle, A. D., et al. (2013). Nutrient enrichment can increase the susceptibility of reef corals to bleaching. *Nat. Clim. Change* 3, 160–164. doi: 10.1038/nclimate1661

Winters, G., Holzman, R., Blekhman, A., Beer, S., and Loya, Y. (2009). Photographic assessment of coral chlorophyll contents: implications for ecophysiological studies and coral monitoring. *J. Exp. Mar. Biol. Ecol.* 380, 25–35. doi: 10.1016/j.jembe.2009.09.004

Witze, A. (2015). Corals worldwide hit by bleaching. *Nature* 543, 373–377. doi: 10.1038/nature.2015.18527

Wood, S. N. (2011). Fast stable restricted maximum likelihood and marginal likelihood estimation of semiparametric generalized linear models. *J. R. Stat. Soc. Ser. B Stat. Methodol.* 73, 3–36. doi: 10.1111/j.1467-9868.2010.00749.x

Wooldridge, S. A. (2009). Water quality and coral bleaching thresholds: formalising the linkage for the inshore reefs of the Great Barrier Reef, Australia. *Mar. Pollut. Bull.* 58, 745–751. doi: 10.1016/j.marpolbul.2008.12.013

Wright, R. M., Aglyamova, G. V., Meyer, E., and Matz, M. V. (2015). Gene expression associated with white syndromes in a reef building coral, *Acropora hyacinthus*. *BMC Genomics* 16:371. doi: 10.1186/s12864-015-1540-2

Yuyama, I., Harii, S., and Hidaka, M. (2012). Algal symbiont type affects gene expression in juveniles of the coral *Acropora tenuis* exposed to thermal stress. *Mar. Environ. Res.* 76, 41–47. doi: 10.1016/j.marenvres.2011.09.004

Zhou, Z., Zhang, G., Chen, G., Ni, X., Guo, L., Yu, X., et al. (2017). Elevated ammonium reduces the negative effect of heat stress on the stony coral *Pocillopora damicornis*. *Mar. Pollut. Bull.* 118, 319–327. doi: 10.1016/j.marpolbul.2017.03.018

Conflict of Interest: The authors declare that the research was conducted in the absence of any commercial or financial relationships that could be construed as a potential conflict of interest.

Publisher's Note: All claims expressed in this article are solely those of the authors and do not necessarily represent those of their affiliated organizations, or those of the publisher, the editors and the reviewers. Any product that may be evaluated in this article, or claim that may be made by its manufacturer, is not guaranteed or endorsed by the publisher.

frontiers in Marine Science

CORRECTION
published: 05 January 2022
doi: 10.3389/fmars.2021.833194

Corrigendum: Variation in Coral Thermotolerance Across a Pollution Gradient Erodes as Coral Symbionts Shift to More Heat-Tolerant Genera

Melissa S. Naugle[1,2], Thomas A. Oliver[3], Daniel J. Barshis[4], Ruth D. Gates[5†] and Cheryl A. Logan[1]*

[1] Department of Marine Science, California State University, Monterey Bay, Seaside, CA, United States, [2] Moss Landing Marine Laboratories, Moss Landing, CA, United States, [3] National Oceanic and Atmospheric Administration, Pacific Island Fisheries Science Center, Honolulu, HI, United States, [4] Department of Biological Sciences, Old Dominion University, Norfolk, VA, United States, [5] Hawai'i Institute of Marine Biology, University of Hawai'i at Mānoa, Kāne'ohe, HI, United States

Keywords: coral reefs, pollution, gene expression, symbiosis, phenotypic plasticity, climate change, thermal tolerance, acclimatization

A Corrigendum on

Variation in Coral Thermotolerance Across a Pollution Gradient Erodes as Coral Symbionts Shift to More Heat-Tolerant Genera

by Naugle, M. S., Oliver, T. A., Barshis, D. J., Gates, R. D., and Logan, C. A. (2021). Front. Mar. Sci. 8:760891. doi: 10.3389/fmars.2021.760891

In the original article, the authors neglected to include an additional funder: a California State University Council on Ocean Affairs, Science & Technology (COAST) grant to MN. The updated Funding statement appears below:

"The 2014 component of this project was funded by a National Oceanic and Atmospheric Administration Coral Reef Conservation Program grant to TO, RG, and CL (NA13NOS4820018). Data collection and analysis in 2019 was funded by a California State University, Monterey Bay Research, Scholarship and Creative Activity grant to CL, an Earl H. and Ethel M. Myer's Oceanographic and Marine Biology Trust grant to MN, a California State University Program for Education and Research in Biotechnology grant to MN, an Explorer's Club-Mamont Scholar grant to MN, and a California State University Council on Ocean Affairs, Science & Technology (COAST) grant to MN."

The authors apologize for this error and state that this does not change the scientific conclusions of the article in any way. The original article has been updated.

OPEN ACCESS

Approved by:
Frontiers Editorial Office, Frontiers Media SA, Switzerland

****Correspondence:***
Melissa S. Naugle
mnaugle@csumb.edu

†Deceased

Specialty section:
This article was submitted to Global Change and the Future Ocean, a section of the journal Frontiers in Marine Science

Received: *10 December 2021*
Accepted: *13 December 2021*
Published: *05 January 2022*

Citation:
Naugle MS, Oliver TA, Barshis DJ, Gates RD and Logan CA (2022) Corrigendum: Variation in Coral Thermotolerance Across a Pollution Gradient Erodes as Coral Symbionts Shift to More Heat-Tolerant Genera. Front. Mar. Sci. 8:833194. doi: 10.3389/fmars.2021.833194

frontiers in Marine Science

ORIGINAL RESEARCH
published: 01 February 2022
doi: 10.3389/fmars.2022.759450

Temperature-Dependent Reproductive Success of Stickleback Lateral Plate Morphs: Implications for Population Polymorphism and Range Shifts Under Ocean Warming

*Sylvia Wanzenböck[1,2], Lukas Fuxjäger[1,2], Eva Ringler[3,4], Harald Ahnelt[2,5] and Lisa N. S. Shama[1]**

[1] Coastal Ecology Section, Alfred-Wegener-Institut Helmholtz-Zentrum für Polar- und Meeresforschung, Wadden Sea Station Sylt, List, Germany, [2] Department of Evolutionary Biology, University of Vienna, Vienna, Austria, [3] Messerli Research Institute, University of Veterinary Medicine Vienna, Medical University of Vienna, Vienna, Austria, [4] Division of Behavioural Ecology, Institute of Ecology and Evolution, University of Bern, Bern, Switzerland, [5] Natural History Museum in Vienna, First Zoological Department, Vienna, Austria

OPEN ACCESS

Edited by:
Chih-hao Hsieh, National Taiwan University, Taiwan

Reviewed by:
Dian-Han Kuo, National Taiwan University, Taiwan
Lengxob Yong, University of Exeter, United Kingdom

***Correspondence:**
Lisa N. S. Shama
lisa.shama@awi.de
orcid.org/0000-0002-9017-9950

Specialty section:
This article was submitted to Global Change and the Future Ocean, a section of the journal Frontiers in Marine Science

Received: *16 August 2021*
Accepted: *11 January 2022*
Published: *01 February 2022*

Citation:
Wanzenböck S, Fuxjäger L, Ringler E, Ahnelt H and Shama LNS (2022) Temperature-Dependent Reproductive Success of Stickleback Lateral Plate Morphs: Implications for Population Polymorphism and Range Shifts Under Ocean Warming. Front. Mar. Sci. 9:759450. doi: 10.3389/fmars.2022.759450

Changing environments associated with rapid climate change can shape direct measures of fitness such as reproductive success by altering mating behavior, fecundity and offspring development. Using a polymorphic oceanic population of threespine stickleback (*Gasterosteus aculeatus*), we investigated whether a 4°C increase in sea surface temperature influenced clutch siring success, reproductive output, and offspring growth among lateral plate morphs. Since low plated morphs are thought to have a selective advantage in warmer environments, we predicted that low plated males should have higher clutch siring success in +4°C environments, and that thermal plasticity of traits (e.g., egg size, offspring growth) should reflect different trait optima in different environments among plate morphs. Parentage analysis of egg clutches revealed temperature-specific clutch siring success, in that low plated males sired more clutches in +4°C environments and completely plated males sired more clutches at ambient (seasonal) temperature. Both completely and low plated females laid larger eggs when acclimated to +4°C, but only completely plated females had smaller clutches at +4°C. Offspring of low and partially plated females grew much less at +4°C compared to those of completely plated females. Taken together, our results demonstrate that ocean warming could impact reproductive success at various levels, with differential effects depending on phenotype, in this case, lateral plate morph. Some traits (clutch siring success, egg size) showed better performance for low plated fish at +4°C, whereas others (e.g., growth) did not. Higher clutch siring success of low plated males at elevated temperature might indicate a future shift in plate morph composition for polymorphic stickleback populations, with potential implications for colonization ability during range shifts under climate change.

Keywords: climate change, environment-dependent reproductive success, phenotypic plasticity, egg size, offspring growth, parentage analysis, lateral plate morph, *Gasterosteus aculeatus*

INTRODUCTION

Rapid warming of the world's oceans is a major threat to population persistence and biodiversity of marine ecosystems (Intergovernmental Panel on Climate Change [IPCC], 2014). Organisms can respond to fast changing environmental conditions either by moving to where conditions better match their thermal optima, or by remaining in place and coping via genetic adaptation and/or phenotypic plasticity (Gienapp et al., 2007). Thermal plasticity of fitness-related traits has been documented in numerous marine species, showing that different phenotypes will be adaptive in different environments (Munday et al., 2013). Importantly, changing environmental conditions may also influence reproductive success – a direct measure of fitness – and can affect different phenotypes at several levels: (1) changing environments can alter mating preferences (Candolin, 2019), which may lead to premating isolation, and thus, reduce the frequency of certain phenotypes in the population, (2) change the fecundity of particular phenotypes (Barneche et al., 2018), with some having higher reproductive output in changed conditions than others, and (3) have developmental effects on offspring (Monaghan, 2008), such that some phenotypes produce offspring that outperform others. Some of the general effects of climate warming on reproductive success include changes to mating behavior (Pilakouta and Alund, 2021), smaller egg sizes (Barneche et al., 2018), and smaller body sizes (Daufresne et al., 2009). Also, spawning adults and early developmental stages (e.g., embryos) were recently identified as the most vulnerable life stages of teleost fishes under climate change (Dahlke et al., 2020). Hence, ocean warming can influence how both natural selection and sexual selection shape phenotypes (Safran et al., 2013), with changes to reproductive success likely influenced by a combination of all of these factors.

The threespine stickleback (*Gasterosteus aculeatus*; hereafter referred to as stickleback), is a small teleost fish that is well known for its complex biology, with morphologically divergent populations distributed throughout the Northern hemisphere (Bell and Foster, 1994; Paepke, 2002). Nevertheless, most of this complexity is known only from freshwater populations (e.g., Wootton, 2009), which are derived from ancestral oceanic (anadromous and strictly marine) populations (Walker and Bell, 2000; Reusch et al., 2001; Raeymaekers et al., 2005; McGuigan et al., 2010; Spoljaric and Reimchen, 2011; Wund et al., 2012). Stickleback are polymorphic for the pattern of their lateral plates (bony armor plates lining the body) which aid against predation (Reimchen, 1983, 2000; Bergstrom, 2002; Barrett, 2010), but also influence swimming performance (Tudorache et al., 2007; Bjærke et al., 2010; Dalziel et al., 2011). Lateral plate morph is genetically determined (primarily by the Eda gene; Colosimo et al., 2005; Jones et al., 2006; Barrett, 2010), heritable (e.g., Hagen, 1973; Hermida et al., 2002; Loehr et al., 2012; Hansson et al., 2016; Østbye et al., 2018), and under strong selection from biotic and abiotic factors (Hagen and Moodie, 1982; Baumgartner and Bell, 1984; Bergstrom, 2002; Marchinko and Schluter, 2007; Barrett, 2010; Smith et al., 2014). Oceanic stickleback populations are predominantly comprised of the completely plated morph (plates extend from the head to the caudal fin) that is capable of migrating long distances (Wootton, 1984; Bell and Foster, 1994), whereas freshwater populations consist mostly of low plated fish (plates only on the anterior part of the trunk) with superior maneuverability. A partially plated morph expresses an intermediate but variable number of plates (plates absent in the middle of the body), and often occurs in brackish water (Wootton, 1976). Contrary to most oceanic populations, those of the North Sea (e.g., German Bight) are characterized by lateral plate polymorphism, comprised of mostly completely plated morphs (as well as some partially plated), but with a small proportion of low plated morphs present (Münzing, 1963; Wootton, 2009). Plate morph polymorphism in these coastal populations is thought to be maintained by a balance between divergent selection and gene flow (Raeymaekers et al., 2014).

The geographic distribution of plate morphs is also correlated with a number of habitat characteristics, one of which is temperature (Münzing, 1963; Wootton, 1976; Hagen and Moodie, 1982; Baumgartner and Bell, 1984; Reimchen, 2000; Des Roches et al., 2020; Smith et al., 2020). In freshwater populations, those with completely plated morphs predominantly occur in regions with cold winters and high annual temperature fluctuations, whereas the low plated morph is more common in regions with relatively warm winters and low annual temperature fluctuations (Hagen and Moodie, 1982; Paepke, 2002; Smith et al., 2020, 2021). Less is known for oceanic populations, but a temperature-dependent plate morph gradient also occurs in some marine and estuarine environments (Münzing, 1963; Baumgartner and Bell, 1984; Paepke, 2002; Des Roches et al., 2020). For instance, the frequency of low plated fish is generally higher at lower latitudes along Californian (Baumgartner and Bell, 1984; Des Roches et al., 2020) and European coasts (Münzing, 1963; Smith et al., 2020), but is shifting northward with climate change due to an increase in lentic estuarine habitats associated with climate warming and decreased precipitation (Des Roches et al., 2020), and/or correlated effects of smaller body size (Smith et al., 2020).

Studies investigating stickleback mating patterns suggest that mate choice is often strongly based on body size (Dieckmann and Doebeli, 1999; McKinnon and Rundle, 2002; Conte and Schluter, 2013; Berner et al., 2016), but also trophic traits, antipredator traits and male reproductive characters can contribute to non-random mating (Blouw and Hagen, 1990; Ziuganov, 1995; Nagel and Schluter, 1998; McKinnon and Rundle, 2002; Scott, 2004; Snowberg and Bolnick, 2008; Jenck et al., 2020). However, little is known about how changing environmental conditions may affect mating preferences for certain phenotypic traits. For instance, both increased water turbidity (Candolin et al., 2007; Wong et al., 2007) and temperature (Fuxjäger et al., 2019) have been shown to alter strong visual mate choice cues like body size. In turbid water, olfactory cues played a more important role when vision was impaired (Heuschele et al., 2009), whereas at higher water temperature, smaller males had increased reproductive success (regardless of the female's body size) under the hypothesis that smaller males spent less energy on metabolism at higher temperature, and therefore, had more energy available for courtship and mating (Fuxjäger et al., 2019). Such environment-induced changes in mating success suggest

that female preference may be influenced by environment-dependent male condition (see also Heuschele et al., 2009; Robinson et al., 2012), which will differ for specific trait-environment combinations. However, almost nothing is known about mating patterns among stickleback lateral plate morphs in general (but see Ziuganov, 1995), and whether mating success among plate morph phenotypes differs with environmental conditions has not yet been investigated.

Earlier studies that investigated fecundity and offspring growth differences among stickleback lateral plate morphs suggest morph-specific trait performance. Differences in reproductive output traits among plate morphs were investigated at the population level, and compared, for example, oceanic populations (completely plated) with freshwater populations (low plated fish; Baker, 1994; Baker et al., 1998). In a survey of 43 freshwater and oceanic stickleback populations from Haida Gwaii (Canada), Oravec and Reimchen (2013) found that these populations had larger eggs and smaller clutches than those in other geographical areas, which they attributed to low environmental temperature. They also found a negative association between egg size and (population mean) number of lateral plates, however, no data on egg sizes or clutch sizes for each lateral plate morph were reported (Oravec and Reimchen, 2013). For offspring growth, a handful of studies have compared growth among stickleback plate morphs. In one study, low plated fish had higher growth rates as juveniles than completely plated fish, but completely plated fish reached a similar size by the time of sexual maturity (Bell et al., 2010). In another study, partially and low plated offspring grew better than completely plated fish in freshwater, whereas all morphs grew similarly in salt water (Marchinko and Schluter, 2007). Nevertheless, little is known about reproductive output and offspring growth differences among lateral plate morphs within polymorphic oceanic populations, and even less with regard to thermal plasticity of these traits.

Due to fast changing climate conditions, oceanic stickleback populations are facing strong environmental pressure (Ramler et al., 2014; Shama and Wegner, 2014; Shama, 2015; Fuxjäger et al., 2019). Since plate morph distributions may be influenced by environmental temperature (Hagen and Moodie, 1982; Baumgartner and Bell, 1984; Reimchen, 2000), climate warming may affect the geographic distribution of polymorphic populations in the future. Importantly, if low plated stickleback cope seemingly better with warmer temperatures than completely plated fish (Münzing, 1963; Smith et al., 2021), adaptive benefits of mating with low plated morphs could arise, and might help to mediate some of the negative consequences of climate warming. In this study, we used large, outdoor mesocosms simulating ambient and ocean warming conditions to investigate the role of changing environments on reproductive success (clutch siring success, reproductive output and offspring growth) among stickleback lateral plate morphs. Specifically, we used a polymorphic oceanic population to test (1) if clutch siring success differs among lateral plate morphs, and also varies with environmental temperature, (2) if thermal plasticity for fecundity traits differs among plate morphs, and (3) if parental plate morph influences offspring growth trajectories under ocean warming.

MATERIALS AND METHODS

Clutch Siring Success Experiment

Wild adult stickleback were caught by trawling from an oceanic population in the Sylt-Rømø Bight, Germany (55°05′ N, 8°39′ E) in February 2016. Adult fish (n = 215) were randomly divided between two large outdoor mesocosms (each 1800 l) set to two temperatures (ambient and +4°C), and were acclimated for 60 days during their reproductive conditioning phase. Mesocosms had permanent flow-through of seawater, and were heated using large heating elements connected to temperature sensors. Temperature was adjusted daily to match seasonal conditions in the Sylt-Rømø Bight, and was recorded hourly using HOBO Pendant ® Temperature/Light Data Loggers (Onset Computer Co., Bourne, MA, United States). Fish were fed daily with chironomid larvae *ad libitum*. After 2 months of temperature acclimation, all fish were caught and lateral plate morph determined by visual inspection. For low plated fish (L), lateral plates appear only on the anterior part of the trunk. The completely plated morph (C) is defined by a row of lateral plates from the head to the base of the caudal fin, and the partially plated morph (P) has a gap of at least two plates between the anterior plates and those on the caudal peduncle (Wootton, 2009). Fish were sorted by sex and plate morph, and transferred to 25 l aquaria (n = 20 fish per aquaria) in the laboratory set to the acclimation temperature.

At the start of the clutch siring success experiment, standard length (±1 mm), weight, sex and plate morph were determined for 96 fish. The first dorsal spine of these fish was clipped and stored at −20°C for later genotyping (see below). Fish were then assigned to one of eight large outdoor mesocosms (see Pansch et al., 2016 for mesocosm technical details) set to either ambient or +4°C in a full-factorial design. Specifically, each mesocosm consisted of six males (three from ambient acclimation temperature and three from +4°C, and with one male of each lateral plate morph per acclimation temperature), and six females following the same treatment combinations as males (**Figure 1**). Fish were size-matched within each mesocosm. On average, females were size-matched to ±5.63 mm and males to ±3.63 mm. The average size difference between males and females in each mesocosm was ±5.49 mm. Each mesocosm contained a mating arena comprised of a 97 × 97 cm frame enclosed with 5 mm mesh which was fixed to a platform positioned at 50 cm water depth. To allow each male to establish a possible territory and display courtship behaviors, six plastic trays were set within each mating arena to serve as nesting sites. Plastic trays (25 × 14 × 6 cm) contained a 3 cm layer of sand (1.25 kg) and 1.5 g nesting material (Wenco Nm 30/3 black sewing thread cut into 5-7 cm lengths conditioned for 2 days in seawater). Fish in the mesocosms were fed daily with chironomid larvae *ad libitum* for the duration of the experiment.

The experiment began on 28 April 2016 using water temperatures of 10°C (ambient) and 14°C (+4°C) and ended on 17 May 2016 with water temperatures of 16 and 20°C. Water temperature in the mesocosms was logged every 30 min using installed multi-sensor probes (Hydrolab DS5X Probe, OTT

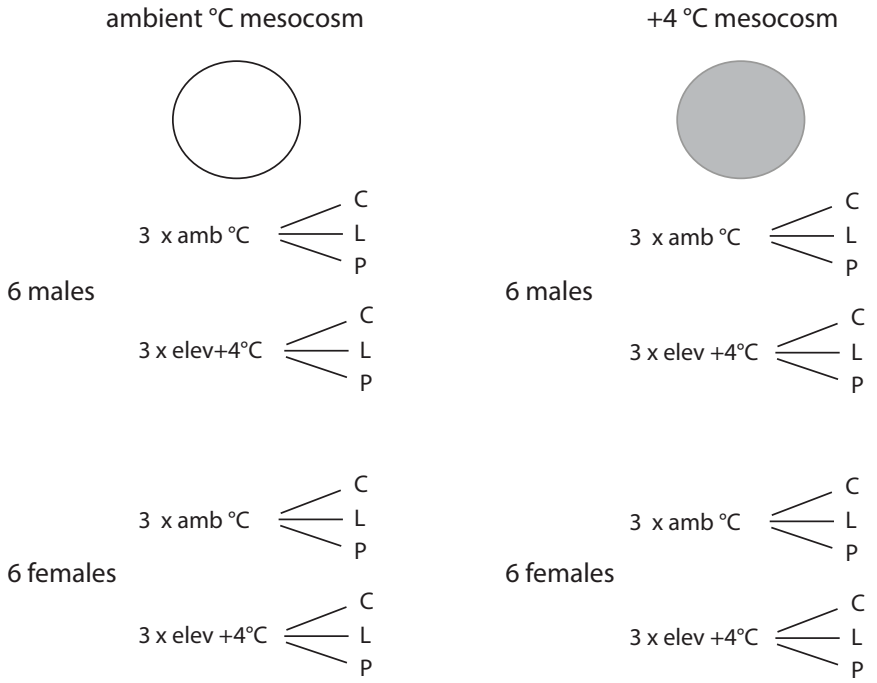

FIGURE 1 | Experimental design schematic showing the combination of six males and six females from different temperature acclimation treatments (ambient, +4°C climate change scenario) and different plate morphs (c, complete; l, low plated; p, partial) in mesocosms set to either ambient or elevated (+4°C) temperature.

Messtechnik GmbH, Kempten, Germany). A nest report was taken every day to document the status and location of each nest in the experiment. Trays with active nests were removed every fourth day to carefully detach egg clutches (performed under a dissecting microscope to minimize disturbance of the nest). Removed trays were returned to the same position in the mating arena, and were supplemented with 0.2 g replacement nesting material. The experiment was stopped after at least seven clutches from each mesocosm had been collected (on average 9.75 clutches were collected from each mesocosm). At the end of the experiment, adult fish were recaptured, and weight (±1 mg), standard length (±1 mm), sex and plate morph was determined for each individual. Fish were then euthanized in an overdose of MS222 and stored at −20°C for later genetic analyses.

Fecundity Traits

All egg clutches were photographed under a dissecting microscope for later determination of egg size and clutch size using imaging software (LEICA QWIN, Leica Microsystems Imaging Solutions Ltd., Cambridge, United Kingdom). The diameter of 10 randomly chosen eggs per clutch was used to calculate the mean egg size of each clutch. Clutch size was determined by counting the number of eggs in each clutch. Egg clutches were transferred into 1 l glass beakers containing an air supply and filtered sea water set to the corresponding mesocosm temperature (ambient or +4°C). Water was changed in the beakers every third day until larvae began to hatch. Hatching success was estimated as the proportion of live larvae in relation to total larvae (live and dead) plus dead eggs/embryos after 2 days of hatching (i.e., unfertilized eggs were not included). Three days after hatching, 24 larvae from each clutch were randomly selected, euthanized in MS222 and frozen at −20°C for later determination of larval genotype.

Growth Experiment

For the growth experiment, ten randomly chosen larvae per clutch (n = 78 clutches) were photographed under a dissecting microscope at 2 days post-hatch for determination of larval size, and were further reared in 1 l beakers until 30 days post-hatch. At this point, the 10 larvae per clutch were transferred to a 2 l aquarium connected to a flow-through seawater system set at either ambient temperature or +4°C. All juvenile fish were photographed at 30, 60, and 90 days post-hatch under a dissecting microscope for analyses of offspring size (standard length ± 0.1 mm) using imaging software (LEICA QWIN V3.5.0; Leica Microsystems Imaging Solutions Ltd., Cambridge, United Kingdom). Throughout the growth experiment, juvenile fish were fed daily with live *Artemia* sp. nauplii *ad libitum.*

Genotyping and Parentage Analysis

All 96 adult fish and 16 larvae from each of 72 randomly chosen clutches (n = 1152 larvae in total) were genotyped at five microsatellite loci (see Kalbe et al., 2009 for loci details). DNA was extracted from spine clips for adults and whole 3 days old larvae using DNeasy Blood and Tissue Kits (Qiagen, Hilden, Germany) following the manufacturer's protocol. The 20 µl multiplex PCR reactions consisted of 10 µl Multiplex Mastermix (Qiagen, Hilden, Germany), 8 µl primer mix (forward and

reverse primer of 5196 HEX, 4170 6_FAM, 1125 6_FAM, 1097 NED and 7033 NED) and 2 μl DNA. Thermal cycling for PCR consisted of: 95°C for 5 min, 30 cycles of 94°C for 1 min, 58°C for 1 min and 72°C for 1 min, and 72°C for 10 min (as in Schade et al., 2014). Amplified fragments were diluted with water (1:20), and 1 μl of diluted PCR product was denatured in 15 μl Hi-Di Formamide containing an internal size standard (ROX500; Applied Biosystems, Foster City, CA, United States). Fragments were analyzed on an ABI 3130xl sequencer. Electropherograms were manually inspected using PeakScanner 1.0 (Applied Biosystems), and Tandem 1.01 (Matschiner and Salzburger, 2009) was used to bin final allele sizes.

Parentage analysis was performed using the program COLONY 2.0 (Wang and Santure, 2009), a likelihood-based method that uses a group-wise approach to infer genealogies from multilocus genotype data (cf. Ursprung et al., 2011; Rausch et al., 2014). The full likelihood model was used with medium precision allowing for polygamous mating in both sexes. Each mesocosm was analyzed separately with males and females (six potential fathers and mothers each) representing the potential fathers and mothers for the respective clutches collected in that mesocosm (see also Fuxjäger et al., 2019). Only 'Best (ML) Configuration' assignments with the maximum likelihood obtained at the end of the computation in which COLONY found both parents (i.e., no simulated genotypes) were used for subsequent analyses. The COLONY analysis implements a full-pedigree likelihood approach which considers the likelihood of the entire pedigree structure and allows the simultaneous inference of parentage and sibship. However, it does not provide explicit p values for each of the pair assignments. To obtain high confidence in the parentage assignments, we investigated the discriminative power of the microsatellite data by conducting allele frequency analyses in Cervus (Kalinowski et al., 2007). We calculated the number of alleles per locus, polymorphic information content (PIC), as well as combined non-exclusion probabilities for parent pairs and combined non-exclusion probabilities for individual identity for each mesocosm separately using only parental genotypes.

Statistical Analysis

Clutch siring success, fecundity traits (mean egg size, clutch size) and offspring growth were analyzed as general linear mixed effect models using the *MCMCglmm* package in R (Hadfield, 2010). For all models, we ran Markov chains of 10^6 iterations, removed a burn-in of 10^5 iterations, and then kept every 1000th estimate after thinning. We fitted proper but uninformative priors covering half the variance of the trait for each random and fixed effect (i.e., $V = 0.5$, nu = 0.002) when fitting Gaussian or Poisson response variables, but fixed the variance to 1 when fitting Binomial response variables. We checked the resulting Markov chains for autocorrelation and stationarity, and only kept chains with an effective sampling size of > 500 for each estimated parameter. Mesocosm was included as a random effect in all models, and family (clutch) was included as a random effect for the offspring growth models.

Clutch siring success was investigated by determining whether potential combinations of male and female plate morphs had any offspring (siring success) in the two reproductive environment (mesocosm) temperatures. The clutch siring success analysis included all males (nest owners, non-reproducing males and sneakers) and all possible male-female combinations within the mesocosms. The proportion of clutches sired was estimated as the number of realized siring events divided by the number of all potential siring events a given male could have achieved (see also Fuxjäger et al., 2019). We analyzed this as a binomial response variable using male and female size as covariates, male and female acclimation temperature, male and female plate morph and mesocosm temperature plus all of their interactions as fixed effects. Mean egg size was analyzed as a Gaussian response variable, and we fit female size, clutch size, female acclimation temperature, female plate morph and mesocosm temperature, plus the interactions between clutch size and female acclimation temperature and plate morph, and all two-way interactions between female acclimation temperature, plate morph and mesocosm temperature. Clutch size was modeled in the same way, but as a Poisson distributed response variable and using mean egg size as a covariate. Note: we did not fit the three-way interaction between female °C, female plate morph and mesocosm temperature for egg traits as there was only one clutch in one of the three-way combinations. Offspring growth over time (at 2, 30, 60, and 90 days post-hatch) was modeled as a Gaussian response variable as a function of male and female acclimation temperature, male and female plate morph, mesocosm temperature and all two-way interactions. The three-way interactions were not modeled due to three missing three-way combinations.

RESULTS

Clutch Siring Success

We used parentage analysis to investigate whether clutch siring success differed among stickleback lateral plate morphs depending on environmental conditions, here, increased water temperature. For offspring assignments, all 96 parental fish were recovered at the end of the experiment, and their genotype could be reliably determined. During the course of the experiment (19 days), 78 clutches in total were collected from the eight mesocosms (39 clutches from ambient temperature and 39 clutches from +4°C mesocosms), and we randomly selected 72 clutches for genotyping. Of the 1152 larvae genotyped (16 larvae per clutch), 73 individuals (6.34%) could not be determined due to PCR failure. The microsatellite markers were highly informative, with a mean number of alleles per locus across mesocosms of 11.28 (SD = 0.48), an average PIC of 0.86 (SD = 0.01), an average combined non-exclusion probability per parent pair of $7.9^{*}e^{-06}$, and a combined non-exclusion probability of identity of $9.0^{*}e^{-07}$. Consequently, the power of our markers to reliably infer parentage within each mesocosm was very high.

Of the 72 clutches genotyped, 45 were single-male sirings by a nest-owner male (e.g., no extra-male fertilizations). The remaining 27 clutches were either sired by multiple males, contained eggs fertilized by sneaker males, and/or contained stolen eggs, resulting in 37.5% (27/72) of genotyped clutches

reflecting some form of alternate reproductive strategy. The number of sneaking events (any siring success by a sneaker male) was similar in both mesocosm temperatures (16 events in ambient °C and 15 events in +4°C). The plate morph distribution of sneaking males was also similar between mesocosm temperatures, with the exception of fewer completely plated sneakers in +4°C mesocosms (4 complete/3 low/3 partially plated sneaker males in ambient mesocosms vs. 1 complete/3 low/4 partially plated sneaker males in +4°C mesocosms). Of the 48 males in the experiment (i.e., both mesocosm temperatures), 39 had some form of siring success, and the plate morph distribution of these males was 11 complete/13 low/15 partially plated. In total, 43 of the 48 females in the experiment managed to reproduce, with a plate morph distribution of 14 complete/15 low/14 partial.

Our GLMM analyses revealed that clutch siring success was significantly influenced by male size, female size, male acclimation temperature and the interaction between male plate morph and mesocosm (reproductive environment) temperature (**Table 1**). Overall, there was a positive relationship between body size (male and female) and clutch siring success. However, low plated nest-owner males were significantly smaller than both complete and partially plated nest-owner males (**Figure 2**), and had higher clutch siring success in +4°C mesocosms (interaction: low plate morph x + 4°C mesocosm; estimate = –0.137, $p = 0.031$, **Supplementary Table 1**). Sneaker males, on the other hand, were smaller than non-reproducing males (except partially plated males at +4°C), and low-plated sneaker males were smaller than the other plate morphs in both mesocosm temperatures (**Figure 2**). Overall, we found that low plated males had significantly higher clutch siring success in +4°C mesocosms when paired with females of all plate morphs, whereas completely plated males showed the opposite pattern and had higher siring success in ambient temperature mesocosms when mated with all female plate morph combinations (**Figure 3**). Partially plated males showed a mixed clutch siring success pattern, with

TABLE 1 | Clutch siring success of stickleback (*Gasterosteus aculeatus*) depending on environmental (mesocosm) temperature, lateral plate morph (C, complete; L, low; P, partial), and acclimation temperature (°C) of males and females.

Clutch siring success (binomial) DIC = 1173.272

Fixed effects	***Estimate***	***95% CI***	***Effective sample***	***P***
Male size	–1.712	–3.362 to 0.065	900	**0.042**
Female size	1.008	0.098 to 1.800	900	**0.020**
Mesocosm temperature (Meso)	–1.097	–13.469 to 9.846	900	0.871
Male plate morph L	–0.203	–1.293 to 0.898	512	0.740
Male plate morph P	–0.187	–1.433 to 0.775	1018	0.747
Female plate morph L	–0.315	–1.553 to 0.868	900	0.618
Female plate morph P	0.273	–0.842 to 1.310	900	0.644
Male temperature (M°C)	–1.001	–1.865 to –0.268	816	**0.002**
Female temperature (F°C)	0.219	–0.346 to 0.882	900	0.487
Male size * Meso	0.045	–1.912 to 2.109	900	0.984
Male plate L * female plate L	–0.380	–2.168 to 1.309	900	0.700
Male plate P * female plate L	1.079	–0.421 to 2.601	900	0.160
Male plate L * female plate P	–0.294	–1.7793 – 1.163	900	0.736
Male plate P * female plate P	0.649	–0.792 to 1.980	900	0.384
Meso * male plate L	0.873	–0.589 to 2.531	634	0.280
Meso * male plate P	1.743	0.290 to 3.290	900	**0.024**
Meso * female plate L	–0.005	–1.912 to 2.116	834	0.989
Meso * female plate P	–0.173	–1.691 to 1.777	791	0.853
M°C * F°C	0.101	–1.103 to 1.238	900	0.842
M°C * Meso	0.639	–0.462 to 1.612	753	0.224
F°C * Meso	–0.361	–1.396 to 0.512	1022	0.427
Meso * male plate L * female plate L	0.828	–1.638 to 3.533	801	0.522
Meso * male plate P * female plate L	–0.942	–3.105 to 1.506	900	0.396
Meso * male plate L * female plate P	0.428	–1.910 to 2.642	900	0.676
Meso * male plate P * female plate P	–1.348	–3.473 to 0.755	599	0.222
M°C * F°C * Meso	–0.032	–1.474 to 1.500	900	0.960
Random effects	***Variance component***	***95% CI***	***Effective sample***	
Mesocosm	0.167	0.001 to 0.548	900	

Male and female size (standard length: mm) were included as covariates, and mesocosm was modeled as a random effect. Clutch siring success was estimated as the proportion of clutches sired and modeled as a binomial response. Fixed term estimates with 95% confidence intervals are given, with significant terms in bold.

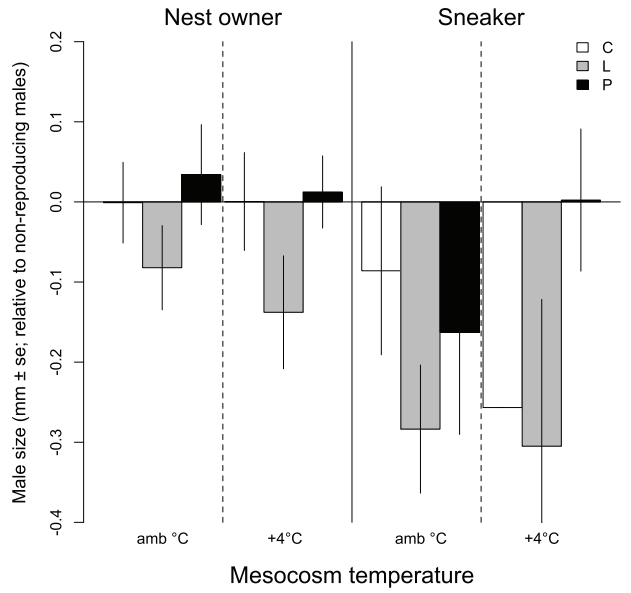

FIGURE 2 | Size of male nest owners and sneakers (mm ± SE) relative to non-reproducing males for each plate morph (C, complete; L, low; P, partial) in ambient and +4°C mesocosms.

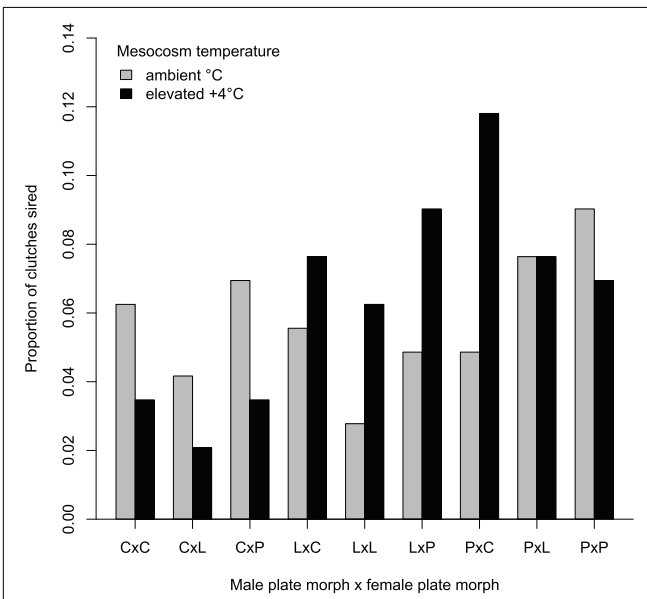

FIGURE 3 | Clutch siring success (measured as the proportion of clutches sired) for each male plate morph in combination with female plate morphs (c, complete; l, low; p, partially plated) in ambient and elevated (+4°C) temperature mesocosms.

higher success at +4°C when paired with completely plated females, lower success at +4°C when paired with partially plated females, and no difference in siring success between mesocosm temperatures when paired with low plated females (interaction: Meso x male plate P, **Table 1** and **Figure 3**).

Egg Size, Clutch Size, and Hatching Success

To investigate if thermal plasticity of fecundity traits differed among lateral plate morphs, we estimated mean egg size, clutch size and hatching success of egg clutches collected from nests within the mesocosms, with both female acclimation temperature (during reproductive conditioning) and mesocosm temperature (during egg laying) set to either ambient or +4°C. Of the 72 clutches genotyped, 39 contained eggs with single-female parentage. Only these clutches were used in the analyses of mean egg size and clutch size, since multiple-female parentage clutches may have included females from different acclimation temperatures and of different plate morph. Mean egg size was significantly influenced by female size, female acclimation temperature (female °C), the interaction between clutch size and female °C, and the interaction between female °C and plate morph (**Table 2**). Overall, there was a positive relationship between female size and egg size, but there was no difference in female size among plate morphs (ANOVA $F_{2,90} = 0.447$; $p = 0.641$) or acclimation temperatures (ANOVA $F_{1,92} = 0.838$; $p = 0.363$) at the start of the experiment. Partially and low plated females laid slightly larger eggs (1.71 ± 0.06 mm and 1.70 ± 0.06 mm, respectively) than completely plated females (1.69 ± 0.07 mm). However, completely and low plated females produced larger eggs when acclimated at +4°C, whereas partially plated females produced larger eggs when acclimated at ambient temperature (**Figure 4A**).

Clutch size was significantly influenced by female acclimation °C, the interaction between egg size and female °C, and the interaction between female °C and plate morph (**Table 2**). The number of eggs per clutch ranged from 39 to 397, and on average, completely plated females laid the largest clutches (251.67 ± 93.5), low plated females laid the smallest clutches (159.33 ± 62.0), and partially plated females were intermediate (209.33 ± 105.2). However, completely plated females laid smaller clutches when acclimated to +4°C, whereas low and partially plated females had similar sized clutches in both acclimation temperatures (**Figure 4B**). There was a tradeoff between egg size and clutch size (bigger eggs but smaller clutches), driven by females acclimated to +4°C (**Supplementary Figure 1a**), and the tradeoff was most apparent for low plated females, resulting from larger eggs laid at +4°C (**Supplementary Figure 1b**). Hatching success of the 78 clutches collected from all mesocosms was high (74.98% in ambient and 82.30% in +4°C mesocosms), and did not differ significantly between mesocosm temperatures (ANOVA $F_{1,76} = 1.814$; $p = 0.227$). For the 39 single-female parentage clutches, overall hatching success was also high (81.30%), and there were no significant effects of female °C (ANOVA $F_{1,23} = 0.572$; $p = 0.457$), female plate morph ($F_{2,23} = 2.083$; $p = 0.147$), or mesocosm temperature ($F_{1,6} = 0.402$; $p = 0.550$) on hatching success.

Offspring Growth

Since climate warming has been shown to influence fish body size (Daufresne et al., 2009), we investigated whether parental thermal history as well as lateral plate morph might

TABLE 2 | Mean egg size **(A)** and clutch size **(B)** of stickleback (*Gasterosteus aculeatus*) females of differing lateral plate morph (C, complete; L, low; P, partial) depending on acclimation temperature (F°C) and environmental (mesocosm) temperature.

(A) Mean egg size (Gaussian) DIC = −116.162

Fixed effects	***Estimate***	***95% CI***	***Effective sample***	***P***
Female size	0.025	0.011 to 0.040	900	**<0.001**
Clutch size	0.001	−0.001 to 0.002	900	0.936
Female temperature (F°C)	0.203	0.073 to 0.334	900	**<0.001**
Plate morph L	0.058	−0.010 to 0.199	900	0.442
Plate morph P	0.066	−0.080 to 0.185	680	0.340
Mesocosm temperature (Meso)	0.037	−0.072 to 0.147	900	0.496
Clutch size * F°C	−0.001	−0.002 to 0.001	900	**0.013**
Clutch size * plate morph L	0.001	−0.001 to 0.002	917	0.898
Clutch size * plate morph P	0.001	−0.001 to 0.002	900	0.336
F°C × plate morph L	0.042	−0.074 to 0.173	900	0.507
F°C × plate morph P	−0.136	−0.248 to −0.023	900	**0.022**
Plate morph L * Meso	−0.039	−0.172 to 0.111	900	0.564
Plate morph P * Meso	−0.104	−0.258 to 0.027	900	0.122
F°C * Meso	−0.063	−0.193 to 0.072	900	0.351
Random effects	***Variance component***	***95% CI***	***Effective sample***	
Mesocosm	0.000	0.000 to 0.001	900	
Units	0.002	0.001 to 0.003	949	

(B) Clutch size (Poisson) DIC = 352.927

Fixed effects	***Estimate***	***95% CI***	***Effective sample***	***P***
Female size	0.101	−0.090 to 0.277	965	0.251
Mean egg size (egg size)	0.366	−5.690 to 6.487	900	0.887
Female temperature (F°C)	10.709	0.772 to 21.302	900	**0.049**
Plate morph L	11.195	−2.636 to 23.574	762	0.091
Plate morph P	−6.636	−17.342 to 6.171	905	0.258
Mesocosm temperature (Meso)	0.477	−0.377 to 1.212	900	0.218
Egg size * F°C	−6.217	−11.891 to −0.033	900	**0.040**
Egg size * plate morph L	−6.776	−14.099 to 1.319	766	0.093
Egg size * plate morph P	3.477	−4.207 to 9.808	895	0.298
F°C * plate morph L	1.495	0.450 to 2.633	811	**0.013**
F°C * plate morph P	0.425	−0.462 to 1.288	794	0.356
Plate morph L * Meso	−0.737	−1.804 to 0.335	900	0.149
Plate morph P * Meso	0.612	−0.059 to 1.463	900	0.113
F°C * Meso	−0.710	−1.575 to 0.066	900	0.102
Random effects	***Variance component***	***95% CI***	***Effective sample***	
Mesocosm	0.008	0.000 to 0.024	670	
Units	0.201	0.086 to 0.342	900	

Female size (standard length: mm), clutch size (total number of eggs) and mean egg size were included as covariates in the models, and mesocosm was modeled as a random effect. Fixed term estimates including 95% confidence intervals are shown, and significant terms are highlighted in bold.

modulate temperature-induced changes to offspring body size. For offspring growth (body size over time) analyses, only clutches with single-couple parentage (i.e., no extra-pair fertilizations) were used (n = 27) so that potential effects of paternal or maternal acclimation temperature and plate morph could be tested. Offspring growth was significantly influenced by parental acclimation temperature, parental plate morph combination, and interactions between parental plate morph and mesocosm temperature (**Table 3**). Mesocosm temperature (offspring growth environment) interacted with parental plate morph to influence offspring size at various time points (**Figures 5A–D**). At 30 days post-hatch, offspring of completely and low plated females were significantly smaller in +4°C mesocosms, whereas offspring of partially plated females were similarly sized in both mesocosm temperatures (**Figure 5B**). However, at 60 and 90 days, offspring of low and partially plated females were markedly smaller in +4°C mesocosms, whereas offspring of completely plated females were similarly sized in both mesocosm temperatures (**Table 3**

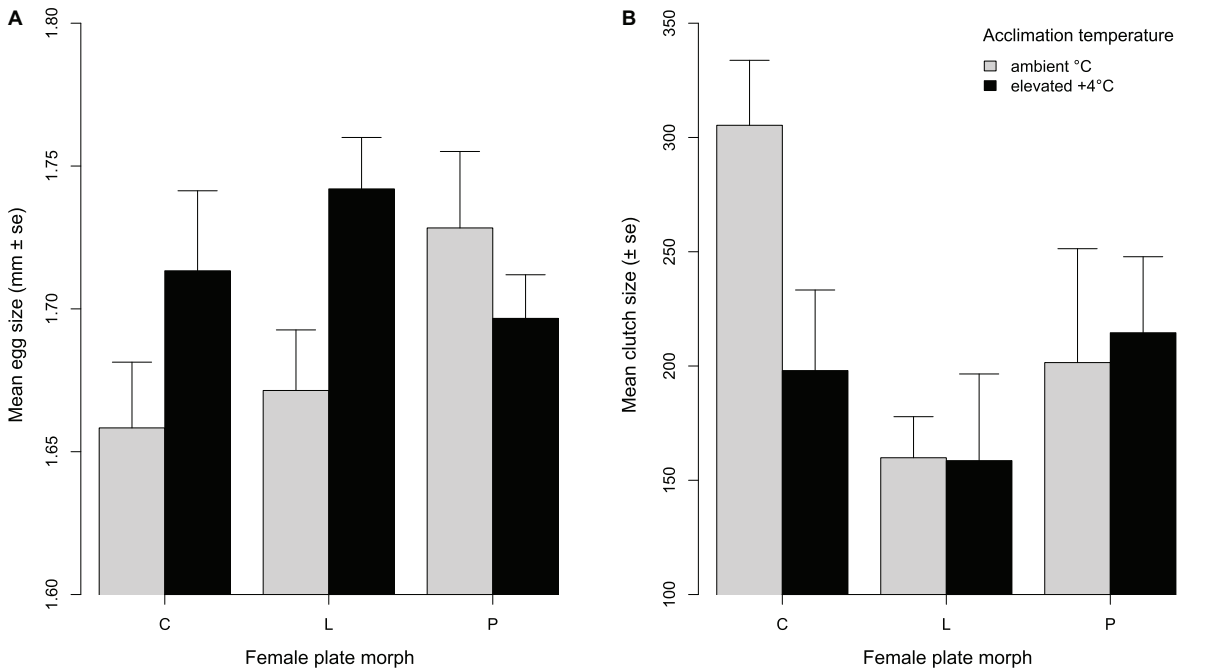

FIGURE 4 | (A) Mean egg size (mm ± SE) of complete (C), low (L), and partially (P) plated females acclimated to ambient or elevated (+4°C) temperature. **(B)** Mean clutch size (±SE) depending on female plate morph and acclimation temperature (ambient and +4°C).

and **Figures 5C,D**). Parental plate morph combination also influenced offspring size (averaged over mesocosm temperatures due to three missing three-way interaction combinations). At 2 days post-hatch, effects of LxP (male × female plate morph) parents on offspring size were only marginally significant (p = 0.058; **Table 3** and **Supplementary Figure 2a**), whereas at 30 and 90 days post-hatch, a number of parental plate morph combinations had significant effects on offspring size (**Table 3**). At 30 days, offspring with a parental plate morph combination of LxP and PxP were significantly larger than those from CxC (**Supplementary Figure 2b**), and at 90 days, offspring of PxP were still significantly larger than those from CxC (**Supplementary Figure 2d**).

DISCUSSION

Our study revealed that stickleback lateral plate morphs showed different plastic responses to simulated ocean warming for several traits related to reproductive success, a direct measure of fitness. Most interesting, we detected environment-specific clutch siring success, in that low plated males sired more clutches in elevated temperature (+4°C) environments and completely plated males sired more clutches at ambient temperature, possibly reflecting energy tradeoffs between male morphology, metabolism, courtship behavior, and thermal environment. Fecundity traits (egg size and clutch size) differed depending on female plate morph and acclimation temperature experienced during the last phases of oogenesis, and offspring growth varied depending on the interaction between parental plate morph and offspring thermal environment. Taken together, our results demonstrate that reproductive success measured at multiple levels (clutch siring success, fecundity, offspring growth) differed among lateral plate morphs depending on environmental temperature, which could, thus, lead to shifts in plate morph polymorphism and colonization ability during range shifts of oceanic stickleback populations under climate change.

Male Plate Morph and Reproductive Environment Temperature Shape Clutch Siring Success

In our siring success experiment, alternate reproductive strategies (e.g., sneaking or egg theft) were found in 37.5% of genotyped clutches. This relatively high proportion is in line with other studies (e.g., Largiadèr et al., 2001; Fuxjäger et al., 2019), demonstrating that alternate strategies may be common in stickleback, with potentially large influences on male reproductive success. Stickleback males not only steal foreign eggs, but occasionally, the sneaker returns and steals the eggs he fertilized to place them in his own nest (Largiadèr et al., 2001; Le Comber et al., 2003). For males with empty nests, egg thievery can be the first step to a successful breeding season since females prefer to spawn in nests already containing eggs (Bell and Foster, 1994; Largiadèr et al., 2001; Le Comber et al., 2003). In our experiment, sneaking events were equally distributed between mesocosm temperatures and there were no large differences among plate morphs. That is, we did not detect environment-dependent sneaking success that differed by lateral plate morph. We did find a clear pattern that (almost) all sneaking

TABLE 3 | Offspring size (standard length: mm) over time (at 2 days to 90 days post-hatch) of stickleback (*Gasterosteus aculeatus*) depending on parental acclimation temperature (M°C, F°C), offspring environment (mesocosm) temperature, and parental plate morph (C, complete; L, low; P, partial).

Offspring size (Gaussian)

Fixed effects	***Size_2d DIC = 291.472***			***Size_30d DIC = 619.356***			***Size_60d DIC = 818.962***			***Size_90d DIC = 291.472***		
	Est.	***95% CI***	***P***	***Est.***	***95% CI***	***P***	***Est.***	***95% CI***	***P***	***Est.***	***95% CI***	***P***
Male temp. (M°C)	–0.020	–0.826 to 0.653	0.949	0.123	–0.588 to 0.800	0.698	0.447	–0.558 to 1.332	0.344	0.813	–0.314 to 1.895	0.160
Female temp. (F°C)	0.054	–0.613 to 0.735	0.884	–0.220	–0.801 to 0.444	0.387	0.230	–0.723 to 1.289	0.684	0.321	–0.795 to 1.440	0.580
Mesocosm°C (Meso)	–0.229	–1.522 to 0.969	0.700	–0.137	–1.425 to 1.027	0.796	–0.452	–2.155 to 1.291	0.551	–0.172	–2.098 to 1.565	0.856
Male plate L	–0.101	–1.524 to 1.220	0.860	0.256	–1.072 to 1.281	0.638	–0.360	–2.043 to 1.116	0.629	–0.871	–2.751 to 1.176	0.382
Male plate P	0.182	–1.097 to 1.463	0.782	0.108	–1.129 to 1.316	0.829	–1.444	–2.926 to 0.188	0.082	–1.349	–3.105 to 0.902	0.196
Female plate L	–0.444	–1.705 to 0.776	0.427	–0.122	–1.214 to 0.908	0.776	0.509	–1.027 to 2.049	0.509	3.009	1.063 to 4.893	**0.004**
Female plate P	–1.095	–2.367 to 0.254	0.087	–1.497	–2.666 to –0.329	**0.018**	–0.543	–2.169 to 1.027	0.500	–0.331	–2.307 to 1.412	0.744
M°C * F°C	–0.592	–1.391 to 0.156	0.111	–0.608	–1.321 to 0.053	0.069	–1.120	–2.040 to –0.212	**0.018**	–0.853	–2.049 to 0.410	0.162
M°C * Meso	0.204	–0.792 to 1.360	0.696	0.286	–0.778 to 1.278	0.558	0.456	–0.741 to 1.937	0.493	–0.861	–2.543 to 0.792	0.329
F°C * Meso	0.172	–0.436 to 0.737	0.580	0.149	–0.383 to 0.773	0.560	0.432	–0.557 to 1.420	0.316	–0.540	–1.552 to 0.503	0.258
Male L * female L	0.402	–0.592 to 1.423	0.407	0.497	–0.381 to 1.316	0.238	0.798	–0.392 to 2.066	0.187	0.688	–0.932 to 2.206	0.393
Male P * female L	–0.109	–1.501 to 1.659	0.869	–0.412	–1.913 to 1.065	0.547	1.299	–0.613 to 3.127	0.202	–0.253	–2.702 to 2.144	0.836
Male L * female P	1.078	–0.009 to 2.197	0.058	1.226	0.275 to 2.191	**0.013**	0.907	–0.543 to 2.339	0.213	1.447	–0.230 to 3.067	0.096
Male P * female P	1.100	–0.491 to 2.758	0.198	1.670	0.118 to 3.089	**0.036**	1.994	0.049 to 4.028	0.060	2.702	0.370 to 5.352	**0.038**
Meso * male L	–0.304	–1.781 to 1.154	0.613	–0.660	–1.902 to 0.867	0.331	–0.562	–2.872 to 1.372	0.547	0.764	–1.535 to 2.974	0.502
Meso * male P	0.056	–1.499 to 1.264	0.916	0.577	–0.772 to 1.930	0.378	1.087	–0.703 to 3.126	0.220	2.627	0.609 to 4.912	**0.022**
Meso * female L	–0.074	–0.734 to 0.971	0.824	–0.128	–0.934 to 0.624	0.724	–2.142	–3.335 to –0.977	**0.004**	–4.097	–5.362 to –2.754	**<0.001**
Meso * female P	0.312	–0.577 to 1.243	0.527	1.133	0.268 to 1.987	**0.020**	–0.812	–1.885 to 0.613	0.178	–1.148	–2.479 to 0.351	0.113
Random effects	***Var.C.***	**95% CI**		***Var.C.***	**95% CI**		***Var.C.***	**95% CI**		***Var.C.***	**95% CI**	
Mesocosm	0.003	0.001 to 0.012		0.010	0.001 to 0.044		0.102	0.001 to 0.580		0.053	0.001 to 0.121	
Family (clutch)	0.079	0.007 to 0.198		0.025	0.001 to 0.152		0.025	0.001 to 0.165		0.042	0.001 to 0.277	
Units	0.156	0.131 to 0.184		0.572	0.473 to 0.680		1.244	0.104 to 1.482		1.962	1.594 to 2.336	

Mesocosm and family (clutch) were modeled as random effects (Var.C., variance component). Fixed estimates (Est.) and variance components (Var.C.) are shown with ± 95% C.I., and significant terms are in bold.

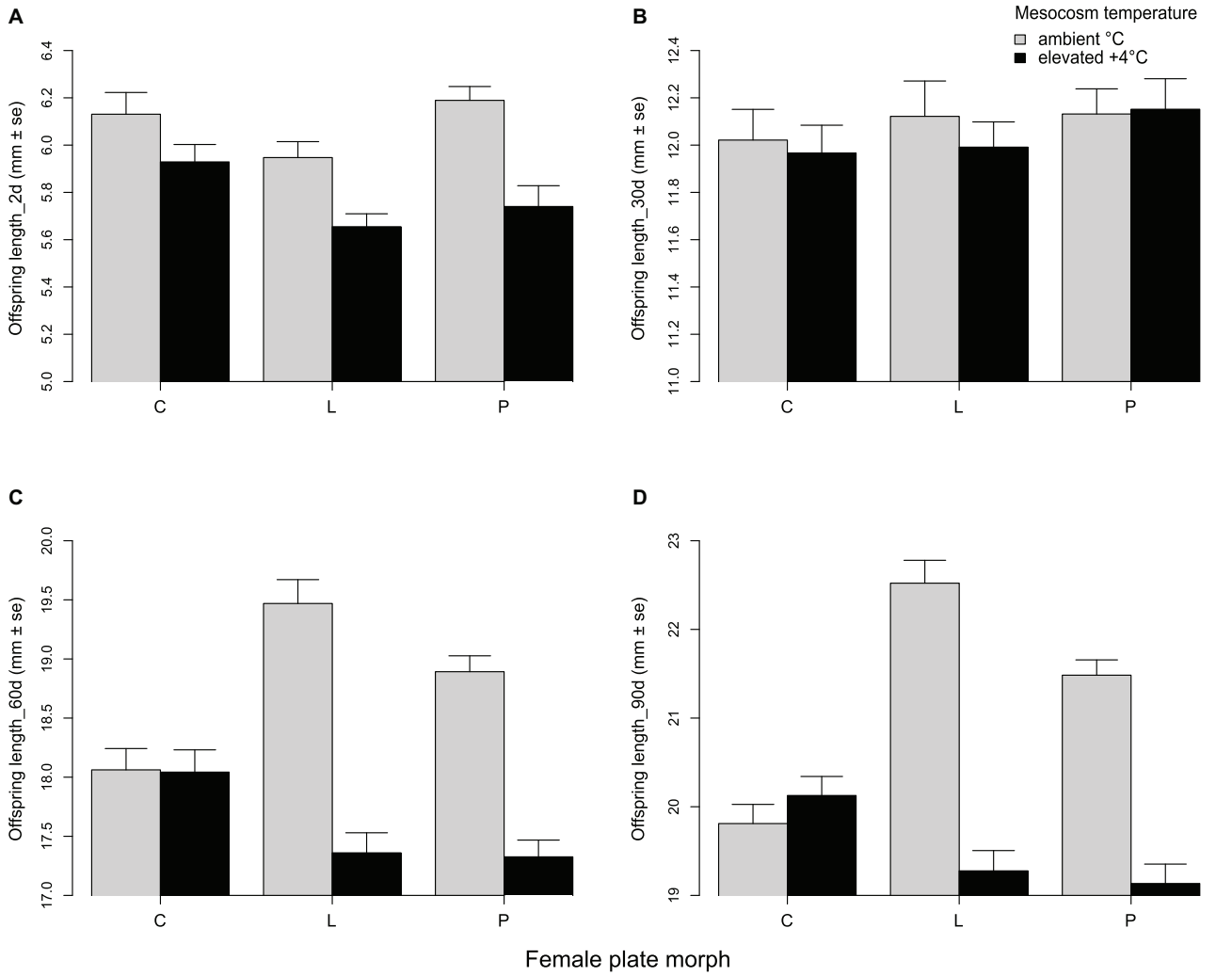

FIGURE 5 | Mean length (mm ± SE) of stickleback offspring depending on maternal plate morph (C, complete; L, low; P, partial) and environmental (mesocosm) temperature (ambient or +4°C): **(A)** 2 days post-hatch, **(B)** 30 days post-hatch, **(C)** 60 days post-hatch, and **(D)** 90 days post-hatch.

males were smaller than non-reproducing males, consistent with other studies showing that small size is often advantageous, and may even be a prerequisite for successful alternate reproductive strategies (Taborsky, 2008).

Clutch siring success of nest owners, on the other hand, differed depending on male plate morph, size and reproductive environment (mesocosm) temperature. Most interestingly, low plated nest owners were smaller than non-reproducing males, and had higher siring success in +4°C mesocosms compared to ambient temperature. Completely plated males showed the opposite pattern (higher siring success in ambient mesocosms; no size difference compared to non-reproducing males), and partially plated males showed a mixed siring success pattern in terms of body size and mesocosm temperature. Rather than assortative mating where particular morphs preferentially choose the same morph phenotype, we predicted that increasing water temperature should lead to higher reproductive success for low plated males irrespective of the plate morph of the female. Indeed, this is what we found, in that low plated males sired the most clutches in +4°C mesocosms and completely plated males sired the most at ambient °C (in both cases with all female plate morphs), suggestive of context-dependent or environment-dependent mate choice (Heuschele et al., 2009; Robinson et al., 2012; McGhee et al., 2015). However, further studies including behavioral assays and controlled choice experiments are needed to determine if female preference is the mechanism underlying the differences in mating success among lateral plate morphs found in our study.

The sexual cue underlying higher clutch siring success of low plated males at elevated temperature is unclear. One candidate trait is metabolic performance: small, low plated males may have a metabolic advantage at elevated temperature allowing them to spend more energy on courtship, mating and/or brood care (Kraak et al., 1999; Fuxjäger et al., 2019). Nevertheless, studies of metabolic rates of stickleback plate morphs have revealed contradicting results. Comparing completely plated anadromous

with low plated freshwater populations, Tudorache et al. (2007) found higher metabolic rates in completely plated fish, whereas Morozov et al. (2018) did not find any differences in metabolic rate between both eco- and morphotypes. Also, Schaarschmidt and Jürss (2003) did not detect differences in metabolic performance related to migratory behavior between non-migrating freshwater and migrating anadromous stickleback. However, to the best of our knowledge, there is currently no data on metabolic performance of low plated oceanic stickleback, especially with regard to reproductive environment temperature.

Thermal Plasticity of Fecundity Traits Differs With Female Plate Morph

Temperature-mediated variation in egg size has been shown in numerous fish species, with a common pattern of larger eggs produced at lower temperature (Barneche et al., 2018). In line with this, previous studies of the stickleback population investigated here found that mothers produced larger eggs when acclimated to ambient temperature, and smaller eggs when acclimated to a +4°C ocean warming scenario (Shama and Wegner, 2014; Shama, 2015, 2017). In the current study, we found a contrasting overall pattern of larger eggs produced at +4°C (driven by completely and low plated females, see below). However, previous studies compared 17°C (ambient) with 21°C (+4°C), and 21°C was shown to have negative effects on several traits, e.g., development (Ramler et al., 2014), growth (Shama et al., 2014; Shama and Wegner, 2014; Shama, 2015, 2017), and survival (Schade et al., 2014). In the current study, mothers were acclimated during their reproductive conditioning phase at temperatures starting at either 10 or 14°C, and laid eggs in mesocosms reaching either 16 or 20°C. It is likely that the optimum temperature range for late oogenesis and egg ripening for this population lies above 13°C but below 21°C (see Ramler et al., 2014), suggesting that 10°C may be too cold to promote high energy states necessary to induce reproduction and/or large egg size (Baker et al., 2015).

Interestingly, females allocated resources to eggs differently depending on plate morph and the temperature experienced during acclimation. Completely and low plated females produced larger eggs when acclimated at +4°C, whereas partially plated females produced larger eggs when acclimated at ambient temperature. Moreover, tradeoffs between egg size and clutch size differed not only between acclimation temperatures (as shown in many studies e.g., Bownds et al., 2010; Liefting et al., 2010), but also among plate morphs. Completely plated females laid larger eggs but smaller clutches at +4°C (and smaller eggs but larger clutches at ambient °C), whereas low and partially plated females laid similar sized clutches under both acclimation temperatures. Overall, the slope of the egg size-clutch size tradeoff was only negative when females were acclimated to +4°C, and low plated females showed the steepest slope. Several studies have found that freshwater, low plated females tend to produce large but few eggs (Baker, 1994), but thermal plasticity of egg allocation was not investigated. Our results indicate that the strong negative correlation between egg size and clutch size for low plated females is not likely due to large eggs being more energetically costly to produce (since their clutch sizes did not differ between acclimation temperatures), but may reflect different morphology – physiology – fitness relationships among plate morphs (Morozov et al., 2018). Differing tradeoffs between fecundity and egg size were also found among morphs within a polymorphic population of Arctic charr, driven by different adaptations to feeding and habitat utilization (Smalås et al., 2017), but this remains to be investigated in oceanic stickleback.

Offspring Size Varies With Parental Plate Morph and Growth Environment Temperature

Our growth experiment showed that both the lateral plate morph of parents and offspring environmental temperature influenced body size. Although we could not test all parental plate morph combinations in both temperature environments (due to three missing combinations), we found that offspring size varied depending on the interaction between maternal plate morph and mesocosm temperature at a number of time points. Here, we found that temperature-mediated differences among plate morphs became most apparent after 60 days, when offspring of low and partially plated mothers were much smaller in +4°C mesocosms, whereas offspring of completely plated mothers were less influenced by environmental temperature. We also found that offspring of low and partially plated parents grew better than those from completely plated parents (averaged over mesocosm temperature), at least up to 90 days post-hatch. Low plated morphs have been shown to differ from completely plated morphs for a number of traits important for colonization of freshwater (growth rate, foraging behavior, immune response; Østbye et al., 2018). Our results concur with these, and suggest that morph-specific growth rates of oceanic stickleback could play a role in colonization during range shifts under ocean warming.

Intriguingly, although low plated females acclimated to +4°C produced the largest eggs, these offspring did not grow best at elevated temperature. Previous studies of this population investigating the relationship between egg size and offspring size found contrasting results. In some cases, large eggs become small offspring (as in the current study), whereas in others, small eggs went on to become large offspring (e.g., Shama, 2015), suggesting that other maternal inputs to eggs (e.g., hormones, epigenetic modifications) that are unrelated to egg size play a role in shaping offspring size (Shama et al., 2016). Specifically, we previously found maternally mediated transgenerational plasticity effects on early offspring growth (0–30 days), with offspring growing best at the same temperature their mother was acclimated to Shama et al. (2014). However, growth in later stages (60–90 days) was primarily influenced by offspring environmental temperature, and offspring grew better at ambient (17°C) than at elevated temperature (21°C; see also Shama and Wegner, 2014; Shama, 2015, 2017). In the current study, we did not detect any transgenerational plasticity effects on offspring size [e.g., no parent environment (acclimation °C) by offspring environment (mesocosm °C) interaction], and perhaps, none should be expected since parents and offspring experienced

different temperatures. As stated above, mothers exposed to the +4°C scenario experienced 14°C at the start of the experiment (potentially leading to larger egg size), whereas offspring growth would have occurred at 20°C (which is above their growth thermal optimum). The ambient temperature scenario, on the other hand, was likely too cold at the start of the experiment for large egg production (10°C), but the optimum temperature for offspring growth (16°C), essentially decoupling parent and offspring environments.

Our results also showed that higher clutch siring success of low plated males in +4°C mesocosms did not translate to larger size of low plated offspring at +4°C (up to 90 days). Nevertheless, there may be other positive effects of this siring success in the next generation. Smaller offspring at elevated temperature is a common finding in climate change experiments, and is one of the universal ecological responses to global warming in aquatic systems (Daufresne et al., 2009; Shama, 2017; Fuxjäger et al., 2019). Despite some potentially negative effects of reduced body size for various aspects of their life history (e.g., male–male competition), advantages of a smaller body size should not be ignored. For instance, if smaller individuals are able to allocate resources from growth into gonad development earlier, they might be able to reach sexual maturity faster than their conspecifics with prolonged growth (Daufresne et al., 2009). Moreover, as shown here, small size may be beneficial in warmer environments due to lower metabolic demand, leaving more energy available for courtship behavior, potentially leading to higher mating success (see also Fuxjäger et al., 2019).

CONCLUSION

Our study found that a temperature increase of 4°C as predicted by several climate models (Intergovernmental Panel on Climate Change [IPCC], 2014) will influence a number of reproductive success-related traits of oceanic stickleback, and that thermal plasticity of these traits differed with lateral plate morph. Some traits (clutch siring success, egg size) showed better performance for low plated fish at elevated temperature, whereas others (e.g., growth) did not. Higher clutch siring success of low plated males at elevated temperature might indicate a future shift in plate morph composition for polymorphic populations. One key trait coupled to such a shift is sustained swimming ability, since low plated fish lack a keel on the caudal peduncle, putting them at a hydrodynamic disadvantage (Wootton, 1984). Energetic tradeoffs between sustained swimming, growth and reproduction (McKinnon et al., 2004), together with environment-dependent mate choice for low plated males could shift the morph distribution in polymorphic populations, with potential consequences for long migrations and range shifts under ocean warming.

DATA AVAILABILITY STATEMENT

The datasets presented in this study can be found in online repositories. The names of the repository/repositories and accession number(s) can be found below: https://doi.org/10.1594/PANGAEA.937325, PANGAEA.

ETHICS STATEMENT

The animal study was reviewed and approved by Ministerium für Energiewende, Landwirtschaft, Umwelt, Natur und Digitalisierung.

AUTHOR CONTRIBUTIONS

LS and HA conceived the study. SW and LF conducted the experiment, collected the genotype, and phenotypic data. SW and ER conducted the parentage analyses. LS carried out the statistical analyses. SW wrote the first draft of the manuscript. All authors contributed to the final version.

FUNDING

This study was funded by the Coastal Ecology Section of the Alfred-Wegener-Institute Wadden Sea Station Sylt. The authors acknowledge support by the Open Access Publication Funds of Alfred-Wegener-Institut Helmholtz- Zentrum für Polar- und Meeresforschung.

ACKNOWLEDGMENTS

Many thanks to Petra Kadel for setting up and maintaining the mesocosms, Kaibil Escobar Wolf for taking care of the fish, Nancy Kuehne for help with the genotyping, and Mathias Wegner for help with MCMC GLMM.

SUPPLEMENTARY MATERIAL

The Supplementary Material for this article can be found online at: https://www.frontiersin.org/articles/10.3389/fmars.2022.759450/full#supplementary-material

REFERENCES

Baker, J. A. (1994). "Life history variation in female threespine stickleback," in *The Evolutionary Biology of the Threespine Stickleback*, eds M. A. Bell and S. A. Foster (New York, NY: Oxford University Press), 144–187.

Baker, J. A., Foster, S. A., Heins, D. C., Bell, M. A., and King, R. W. (1998). Variation in female life-history traits among Alaskan populations of the threespine stickleback, *Gasterosteus aculeatus* L. (Pisces: gasterosteidae). *Biol. J. Linnean Soc.* 63, 141–159. doi: 10.1006/bijl.1997.0187

Baker, J. A., Wund, M., Heins, D., King, R. W., Reyes, M. L., and Foster, S. A. (2015). Life-history plasticity in female threespine stickleback. *Heredity* 115, 322–334. doi: 10.1038/hdy.2015.65

Barneche, D. R., Burgess, S. C., and Marshell, D. J. (2018). Global environmental drivers of marine fish egg size. *Glob. Ecol. Biogeogr.* 27, 890–898. doi: 10.1016/j.envpol.2020.114711

Barrett, R. D. H. (2010). Review paper: adaptive evolution of lateral plates in three-spined stickleback Gasterosteus aculeatus: a case study in functional analysis of natural variation. *J. Fish Biol.* 77, 311–328. doi: 10.1111/j.1095-8649.2010.02640.x

Baumgartner, J. V., and Bell, M. A. (1984). Lateral plate morph variation in California populations of the threespine stickleback, Gasterosteus aculeatus. *Evolution* 38, 665–674. doi: 10.1111/j.1558-5646.1984.tb00333.x

Bell, M. A., and Foster, S. A. (1994). "Introduction to the evolutionary biology of the threespine stickleback," in *The Evolutionary Biology of the Threespine Stickleback*, eds M. A. Bell and S. A. Foster (New York, NY: Oxford University Press), 1–27.

Bell, M. A., Gangavalli, A. K., Bewick, A., and Aguirre, W. E. (2010). Frequency of *Ectodysplasin* alleles and limited introgression between sympatric threespine stickleback populations. *Environ. Biol. Fishes* 89, 189–198. doi: 10.1007/s10641-010-9712-z

Bergstrom, C. A. (2002). Fast-start swimming performance and reduction in lateral plate number in threespine stickleback. *Canadian J. Zool.* 80, 207–213. doi: 10.1139/z01-226

Berner, D., Ammann, M., Spencer, E., Rüegg, A., Lüscher, D., and Moser, D. (2016). Sexual isolation promotes divergence between parapatric lake and stream stickleback. *J. Evol. Biol.* 30, 401–411. doi: 10.1111/jeb.13016

Bjærke, O., Østbye, K., Lampe, H. M., and Vøllestad, L. A. (2010). Covariation in shape and foraging behaviour in lateral plate morphs in the three-spined stickleback. *Ecol. Freshw. Fish* 19, 249–256. doi: 10.1111/j.1600-0633.2010.00409.x

Blouw, D. M., and Hagen, D. W. (1990). Breeding ecology and evidence of reproductive isolation of a widespread stickleback fish (Gasterosteidae) in Nova Scotia, Canada. *Biol. J. Linnean Soc.* 39, 195–217. doi: 10.1111/j.1095-8312.1990.tb00512.x

Bownds, C., Wilson, R., and Marshall, D. J. (2010). Why do colder mothers produce larger eggs? An optimality approach. *J. Exp. Biol.* 213, 3796–3801. doi: 10.1242/jeb.043356

Candolin, U. (2019). Mate choice in a changing world. *Biol. Rev.* 94, 1246–1260. doi: 10.1111/brv.12501

Candolin, U., Salesto, T., and Evers, M. (2007). Changed environmental conditions weaken sexual selection in sticklebacks. *Eur. Soc. Evol. Biol.* 20, 233–239. doi: 10.1111/j.1420-9101.2006.01207.x

Colosimo, P. F., Hosemann, K. E., Balabhadra, S., Villarreal, G. Jr., Dickson, M., Grimwood, J., et al. (2005). Widespread parallel evolution in sticklebacks by repeated fixation of Ectodysplasin alleles. *Science* 307, 1928–1933. doi: 10.1126/science.1107239

Conte, G. L., and Schluter, D. (2013). Experimental confirmation that body size determines mate preference via phenotype matching in a stickleback species pair. *Evolution* 67, 1477–1484. doi: 10.1111/evo.12041

Dahlke, F. T., Wohlrab, S., Butzin, M., and Pörtner, H.-O. (2020). Thermal bottlenecks in the life cycle define climate vulnerability of fish. *Science* 369, 65–70.

Dalziel, A. C., Vines, T. H., and Schulte, P. M. (2011). Reductions in prolonged swimming capacity following freshwater colonization in multiple threespine stickleback populations. *Evolution* 66, 1226–1239. doi: 10.1111/j.1558-5646.2011.01498.x

Daufresne, M., Lengfellner, K., and Sommer, U. (2009). Global warming benefits the small in aquatic ecosystems. *Proc. Natl. Acad. Sci. U.S.A.* 106, 12788–12793. doi: 10.1073/pnas.0902080106

Des Roches, S., Bell, M. A., and Palkovacs, E. (2020). Climate-driven habitat change causes evolution in Threespine Stickleback. *Glob. Change Biol.* 26, 597–606. doi: 10.1111/gcb.14892

Dieckmann, U., and Doebeli, M. (1999). On the origin of species by sympatric speciation. *Nature* 400, 354–357. doi: 10.1038/22521

Fuxjäger, L., Wanzenböck, S., Ringler, E., Wegner, M. K., Ahnelt, H., and Shama, L. N. S. (2019). Within-generation and transgenerational plasticity of mate choice in oceanic stickleback under climate change. *Philos. Trans. R. Soc. B* 374, 1–12. doi: 10.1098/rstb.2018.0183

Gienapp, P., Teplitsky, C., Alho, J. S., Mills, J. A., and Merliä, J. (2007). Climate change and evolution: disentangling environmental and genetic responses. *Mol. Ecol.* 17, 1–12. doi: 10.1111/j.1365-294X.2007.03413.x

Hadfield, J. D. (2010). MCMC methods for multi-response generalized linear mixed models: the MCMCglmm R package. *J. Stat. Softw.* 33, 1–22.

Hagen, D. (1973). Inheritance of numbers of lateral plates and gill rakers in *Gasterosteus aculeatus*. *Heredity* 30, 303–312. doi: 10.1038/hdy.1973.40

Hagen, D. W., and Moodie, G. E. E. (1982). Polymorphism for plate morphs in *Gasterosteus aculeatus* on the east coast of Canada and an hypothesis for their global distribution. *Canadian J. Zool.* 60, 1032–1042.

Hansson, T. H., Fischer, B., Mazzarella, A. B., Voje, K. L., and Vøllestad, L. A. (2016). Lateral plate number in low-plated threespine stickleback: a study of plasticity and heritability. *Ecol. Evol.* 6, 3154–3160. doi: 10.1002/ece3.2020

Hermida, M., Fernández, C., Amaro, R., and San Miguel, E. (2002). Heritability and "evolvability" of meristic characters in a natural population of Gasterosteus aculeatus. *Canadian J. Zool.* 80, 532–541.

Heuschele, J., Mannerla, M., Gienapp, P., and Candolin, U. (2009). Environment-dependent use of mate choice cues in sticklebacks. *Behav. Ecol.* 20, 1223–1227. doi: 10.1093/beheco/arp123

Intergovernmental Panel on Climate Change [IPCC] (2014). "Topic 1: observed changes and their causes," in *Climate Change 2014: Synthesis Report. Contribution of Working Groups I, II and III to the Fifth Assessment Report of the Intergovernmental Panel on Climate Change*, eds Core Writing Team, R. K. Pachauri, and L. A. Meyer (Geneva: IPCC), 151.

Jenck, C. S., Lehto, W. R., Ketterman, B. T., Sloan, L. F., Sexton, A. N., and Tinghitella, R. M. (2020). Phenotypic divergence among threespine stickleback that differ in nuptial coloration. *Ecol. Evol.* 10, 2900–2916. doi: 10.1002/ece3.6105

Jones, F. C., Brown, C., Pemberton, J. M., and Braithwaite, V. A. (2006). Reproductive isolation in a threespine stickleback hybrid zone. *J. Evol. Biol.* 19, 1531–1544. doi: 10.1111/j.1420-9101.2006.01122.x

Kalbe, M., Eizaguirre, C., Dankert, I., Reusch, T. B. H., Wegner, M. K., and Milinski, M. (2009). Lifetime reproductive success is maximized with optimal histocompatibility complex diversity. *Proc. R. Soc. B* 276, 925–934. doi: 10.1098/rspb.2008.1466

Kalinowski, S. T., Taper, M. L., and Marshall, T. C. (2007). Revising how the computer program CERVUS accommodates genotyping error increases success in paternity assignment. *Mol. Ecol.* 16, 1099–1106. doi: 10.1111/j.1365-294X.2007.03089.x

Kraak, S. B. M., Bakker, T. C. M., and Mundwiler, B. (1999). Sexual selection in sticklebacks in the field: correlates of reproductive, mating, and paternal success. *Behav. Ecol.* 10, 696–706.

Largiadèr, C. R., Fries, V., and Bakker, T. C. M. (2001). Genetic analysis of sneaking and egg-thievery in a natural population of the three-spined stickleback (*Gasterosteus aculeatus* L.). *Heredity* 86, 459–468. doi: 10.1046/j.1365-2540.2001.00850.x

Le Comber, S., Faulkes, C., Formosinho, J., and Smith, C. (2003). Response of territorial males to the threat of sneaking in the three-spined stickleback (*Gasterosteus aculeatus*): a field study. *J. Zool.* 261, 15–20. doi: 10.1017/s0952836903003911

Liefting, M., Weerenbeck, M., van Dooremalen, C., and Ellers, J. (2010). Temperature-induced plasticity in egg size and resistance of eggs to temperature stress in a soil arthropod. *Funct. Ecol.* 24, 1291–1298.

Loehr, J., Leinonen, T., Herczeg, G., O'Hara, R. B., and Merilä, J. (2012). Heritability of asymmetry and lateral plate number in the threespine stickleback. *PLoS One* 7:e39843. doi: 10.1371/journal.pone.0039843

Marchinko, K. B., and Schluter, D. (2007). Parallel evolution by correlated response: lateral plate reduction in threespine stickleback. *Evolution* 61, 1084–1090. doi: 10.1111/j.1558-5646.2007.00103.x

Matschiner, M., and Salzburger, W. (2009). TANDEM: integrating automated allele binning into genetics and genomics workflows. *Bioinformatics* 25, 1982–1983. doi: 10.1093/bioinformatics/btp303

McGhee, K. E., Feng, S., Leasure, S., and Bell, A. M. (2015). A female's past experience with predators affects male courtship and the care her offspring will receive from their father. *Proc. R. Soc. B* 282:20151840.

McGuigan, K., Nishimura, N., Currey, M., Hurwit, D., and Cresko, W. A. (2010). Cryptic genetic variation and body size evolution in threespine stickleback. *Evolution* 65, 1203–1211. doi: 10.1111/j.1558-5646.2010.01195.x

McKinnon, J. S., Mori, S., Blackman, B. K., David, L., Kingsley, D. M., Jamieson, L., et al. (2004). Evidence for ecology;s role in speciation. *Nature* 429, 294–298.

McKinnon, J. S., and Rundle, H. D. (2002). Speciation in nature: the threespine stickleback model systems. *Trends Ecol. Evol.* 17, 480–488. doi: 10.1016/s0169-5347(02)02579-x

Monaghan, P. (2008). Early growth conditions, phenotypic development and environmental change. *Philos. Trans. R. Soc.* 363, 1635–1645. doi: 10.1098/rstb.2007.0011

Morozov, S., Leinonen, T., Merilä, J., and McCairns, S. R. J. (2018). Selection on the morphology–physiology-performance nexus: lessons from freshwater stickleback morphs. *Ecol. Evol.* 8, 1286–1299. doi: 10.1002/ece3.3644

Munday, P. L., Warner, R. R., Monro, K., Pandolfi, J. M., and Marshall, D. J. (2013). Predicting evolutionary responses to climate change in the sea. *Ecol. Lett.* 16, 1488–1500. doi: 10.1111/ele.12185

Münzing, J. (1963). The evolution of variation and distributional patterns in European populations of the three-spined stickleback, *Gasterosteus aculeatus*. *Evolution* 17, 320–332. doi: 10.2307/2406161

Nagel, L., and Schluter, D. (1998). Body size, natural selection, and speciation in sticklebacks. *Evolution* 52, 209–218. doi: 10.1111/j.1558-5646.1998.tb05154.x

Oravec, T. J., and Reimchen, T. E. (2013). Divergent reproductive life histories in Haida Gwaii stickleback (*Gasterosteus* spp.). *Canadian J. Zool.* 91, 17–24. doi: 10.1139/cjz-2012-0175

Østbye, K., Taugbøl, A., Ravinet, M., Harrod, C., Pettersen, R. A., Bernatchez, L., et al. (2018). Ongoing niche differentiation under high gene flow in a polymorphic brackish water threespine stickleback (*Gasterosteus aculeatus*) population. *BMC Evol. Biol.* 18:14. doi: 10.1186/s12862-018-1128-y

Paepke, H. J. (2002). "Gasterosteus aculeatus Linneaus, 1758," in *The Freshwater Fishes of Europe*, Vol. 5, eds P. M. Banarescu and H. J. Paepke (Wiebelsheim: Aula-Verlag), 209–256.

Pansch, A., Winde, V., Asmus, R., and Asmus, H. (2016). Tidal benthic mesocosms simulating future climate change scenarios in the field of marine ecology. *Limnol. Oceanogr.: Methods* 14, 257–267. doi: 10.1002/lom3.10086

Pilakouta, N., and Alund, M. (2021). Sexual selection and environmental change: what do we know and what comes next? *Curr. Zool.* 67, 293–298. doi: 10.1093/cz/zoab021

Raeymaekers, J. A. M., Konijnendijk, N., Larmuseau, M. H. D., Hellemans, B., De Meester, L., and Volkaert, F. A. M. (2014). A gene with major phenotypic effects as a target for selection vs. homogenizing gene flow. *Mol. Ecol.* 23, 162–181. doi: 10.1111/mec.12582

Raeymaekers, J. A. M., Maes, G. E., Audenaert, E., and Volckaert, F. A. M. (2005). Detecting Holocene divergence in the anadromous–freshwater three-spined stickleback (*Gasterosteus aculeatus*) system. *Mol. Ecol.* 14, 1001–1014. doi: 10.1111/j.1365-294X.2005.02456.x

Ramler, D., Mitteroecker, P., Shama, L. N. S., Wegner, M. K., and Ahnelt, H. (2014). Nonlinear effects of temperature on body form and developmental canalization in the threespine stickleback. *J. Evol. Biol.* 27, 497–507. doi: 10.1111/jeb.12311

Rausch, A. M., Hödl, W., Ringler, E., Jehle, R., and Sztatecsny, M. (2014). Male body size and parental relatedness but not nuptial colouration influence paternity success during scramble competition in Rana arvalis. *Behaviour* 151, 1869–1884.

Reimchen, T. E. (1983). Structural relationships between spines and lateral plates in threespine stickleback (*Gasterosteus aculeatus*). *Evolution* 37, 931–946. doi: 10.1111/j.1558-5646.1983.tb05622.x

Reimchen, T. E. (2000). Predator handling failures of lateral plate morphs in *Gasterosteus aculeatus*: functional implications for the ancestral plate condition. *Behaviour* 137, 1081–1096.

Reusch, T. B. H., Wegner, K. M., and Kalbe, M. (2001). Rapid genetic divergence in postglacial populations of threespine stickleback (*Gasterosteus aculeatus*): the role of habitat type, drainage and geographical proximity. *Mol. Ecol.* 10, 2435–2445. doi: 10.1046/j.0962-1083.2001.01366.x

Robinson, M. R., van Doorn, S. G., Gustafsson, L., and Qvarnström, A. (2012). Environment-dependent selection on mate choice in a natural population of birds. *Ecol. Lett.* 15, 611–618. doi: 10.1111/j.1461-0248.2012.01780.x

Safran, R. J., Scordato, E. S. C., Symes, L. B., Rodriguez, R. L., and Mendelson, T. C. (2013). Contributions of natural and sexual selection to the evolution of premating reproductive isolation: a research agenda. *Trends Ecol. Evol.* 28, 643–650. doi: 10.1016/j.tree.2013.08.004

Schaarschmidt, T., and Jürss, K. (2003). Locomotory capacity of Baltic Sea and freshwater populations of the threespine stickleback (*Gasterosteus aculeatus*). *Comparat. Biochem. Physiol. Part A: Mol. Integrat. Physiol.* 135, 411–424. doi: 10.1016/s1095-6433(03)00109-0

Schade, F. M., Shama, L. N. S., and Wegner, M. K. (2014). Impact of thermal stress on evolutionary trajectories of pathogen resistance in three-spined stickleback (*Gasterosteus aculeatus*). *BMC Evol. Biol.* 14:164. doi: 10.1186/s12862-014-0164-5

Scott, R. J. (2004). Assortative mating between adjacent populations of threespine stickleback (Gasterosteus aculeatus). *Ecol. Freshw. Fish* 13, 1–7.

Shama, L. N. S. (2015). Bet hedging in a warming ocean: predictability of maternal environment shapes offspring size variation in marine sticklebacks. *Global Change Biol.* 21, 4387–4400. doi: 10.1111/gcb.13041

Shama, L. N. S. (2017). The mean and variance of climate change in the oceans: hidden evolutionary potential under stochastic environmental variability in marine sticklebacks. *Nat. Sci. Rep.* 7, 1–14. doi: 10.1038/s41598-017-07140-9

Shama, L. N. S., Mark, F. C., Strobel, A., Lokmer, A., John, U., and Wegner, M. K. (2016). Transgenerational effects persist down the maternal line in marine sticklebacks: gene expression matches physiology in a warming ocean. *Evol. Appl.* 9, 1096–1111. doi: 10.1111/eva.12370

Shama, L. N. S., Strobel, A., Mark, F. C., and Wegner, M. K. (2014). Transgenerational plasticity in marine sticklebacks: maternal effects mediate impacts of a warming ocean. *Funct. Ecol.* 28, 1–11. doi: 10.1111/jeb.12490

Shama, L. N. S., and Wegner, M. K. (2014). Grandparental effects in marine sticklebacks: transgenerational plasticity across multiple generations. *J. Evol. Biol.* 27, 2297–2307.

Smalås, A., Amundsen, P., and Knudsen, R. (2017). The trade-off between fecundity and egg size in a polymorphic population of Arctic charr (*Salvelinus alpinus* (L.)) in Skogsfjordvatn, subarctic Norway. *Ecol. Evol.* 7, 2018–2024. doi: 10.1002/ece3.2669

Smith, C., Spence, R., Barber, I., Przybylski, M., and Wootton, R. J. (2014). The role of calcium and predation on plate morph evolution in the three-spined stickleback (*Gasterosteus aculeatus*). *Ecol. Evol.* 4, 3550–3554. doi: 10.1002/ece3.1180

Smith, C., Zieba, G., and Prybylski, M. (2021). Elevated temperatures drive the evolution of armour loss in the threespine stickleback Gasterosteus aculeatus. *Funct. Ecol.* 35, 1735–1744. doi: 10.1111/1365-2435.13846

Smith, C., Zieba, G., Spence, R., Klepaker, T., and Przybylski, M. (2020). Three-spined stickleback armour predicted by body size, minimum winter temperature and pH. *J. Zool.* 311, 13–22.

Snowberg, L. K., and Bolnick, D. I. (2008). Assortative Mating by diet in a phenotypically unimodal but ecologically variable population of stickleback. *Am. Naturalist* 172, 733–739. doi: 10.1086/591692

Spoljaric, M. A., and Reimchen, T. E. (2011). Habitat-specific trends in ontogeny of body shape in stickleback from coastal archipelago: potential for rapid shifts in colonizing populations. *J. Morphol.* 272, 590–597. doi: 10.1002/jmor.10939

Taborsky, M. (2008). "Alternative reproductive tactics in fish," in *Alternative Reproductive Tactics: an Integrative Approach*, eds R. Oliveira, M. Taborsky, and H. J. Brookman (New York, NY: Cambridge University Press), 251–299.

Tudorache, C., Blust, R., and De Boeck, G. (2007). Swimming capacity and energetics of migrating and non-migrating morphs of three-spined stickleback *Gasterosteus aculeatus* L. and their ecological implications. *J. Fish Biol.* 71, 1448–1456. doi: 10.1111/j.1095-8649.2007.01612.x

Ursprung, E., Ringler, M., Jehle, R., and Hödl, W. (2011). Strong male/male competition allows for nonchoosy females: high levels of polygynandry in a

territorial frog with paternal care. *Mol. Ecol.* 20, 1759–1771. doi: 10.1111/j.1365-294X.2011.05056.x

Walker, J. A., and Bell, M. A. (2000). Net evolutionary trajectories of body shape evolution within a microgeographic radiation of threespine sticklebacks (*Gasterosteus aculeatus*). *J. Zool.* 252, 293–302. doi: 10.1111/j.1469-7998.2000.tb00624.x

Wang, J., and Santure, A. W. (2009). Parentage and sibship inference from multilocus genotype data under polygamy. *Genetics* 181, 1579–1594. doi: 10.1534/genetics.108.100214

Wong, B. B. M., Candolin, U., and Lindström, K. (2007). Environmental deterioration compromises socially enforced signals of male quality in three-spined sticklebacks. *Am. Nat.* 170, 184–189.

Wootton, R. J. (1976). *The Biology of the Sticklebacks*. London: Academic Press.

Wootton, R. J. (1984). *A Functional Biology of Sticklebacks*. Kent: Croom Helm, 265.

Wootton, R. J. (2009). The Darwinian stickleback Gasterosteus aculeatus: a history of evolutionary studies. *J. Fish Biol.* 75, 1919–1942. doi: 10.1111/j.1095-8649.2009.02412.x

Wund, M. A., Valena, S., Wood, S., and Baker, J. A. (2012). Ancestral plasticity and allometry in threespine stickleback reveal phenotypes associated with derived, freshwater ecotypes. *Biol. J. Linnean Soc.* 105, 573–583. doi: 10.5061/dryad.hb824gd4

Ziuganov, V. V. (1995). Reproductive isolation among lateral plate phenotypes (low, partial, complete) of the threespine stickleback, Gasterosteus aculeatus, from the White Sea basin and the Kamchatka peninsula, Russia. *Behaviour* 132, 1173–1181.

Conflict of Interest: The authors declare that the research was conducted in the absence of any commercial or financial relationships that could be construed as a potential conflict of interest.

Publisher's Note: All claims expressed in this article are solely those of the authors and do not necessarily represent those of their affiliated organizations, or those of the publisher, the editors and the reviewers. Any product that may be evaluated in this article, or claim that may be made by its manufacturer, is not guaranteed or endorsed by the publisher.

frontiers in Marine Science

ORIGINAL RESEARCH
published: 25 February 2022
doi: 10.3389/fmars.2022.733315

Thermal Performance of Seaweeds and Seagrasses Across a Regional Climate Gradient

Scott Bennett[1,2], Raquel Vaquer-Sunyer[3], Gabriel Jordá[4], Marina Forteza[1], Guillem Roca[1] and Núria Marbà[1]*

[1] Global Change Research Group, Institut Mediterrani d'Estudis Avançats (CSIC-UIB), Esporles, Spain, [2] Institute for Marine and Antarctic Studies, University of Tasmania, Hobart, TAS, Australia, [3] Marilles Foundation, Palma de Mallorca, Spain, [4] Centre Oceanogràfic de Balears, CN-Instituto Español de Oceanografía (CSIC), Palma de Mallorca, Spain

Comparative patterns in thermal performance between populations have fundamental implications for a species thermal sensitivity to warming and extreme events. Despite this, within-species variation in thermal performance is seldom measured. Here we compare thermal performance both within-species and between-species, for two species of seagrass (*Posidonia oceanica* and *Cymodocea nodosa*) and two species of seaweed (*Padina pavonica* and *Cystoseira compressa*) across the Mediterranean Sea. Experimental populations from four locations representing between 75 and 99% of each species thermal distribution and a 6°C gradient in summer temperatures, were exposed to 10 temperature treatments between 15 and 36°C. Experimental thermal performance displayed the greatest variability between species, with optimal temperatures differing by over 10°C within the same location. Within-species differences in thermal performance were also important for *P. oceanica* which displayed large thermal safety margins within cool and warm-edge populations and small safety margins within central populations. Our findings suggest patterns of thermal performance in Mediterranean seagrasses and seaweeds retain deep "pre-Mediterranean" evolutionary legacies, suggesting marked differences in sensitivity to warming within and between benthic marine communities.

Keywords: macroalgae, local adaptation, phenotypic plasticity, niche conservatism, climate change

OPEN ACCESS

Edited by:
Jennifer Marie Donelson, James Cook University, Australia

Reviewed by:
Juan D. Gaitan-Espitia, The University of Hong Kong, Hong Kong SAR, China
Mat Vanderklift, Commonwealth Scientific and Industrial Research Organisation (CSIRO), Australia

****Correspondence:***
Scott Bennett
scott.bennett0@utas.edu.au

Specialty section:
This article was submitted to Global Change and the Future Ocean, a section of the journal Frontiers in Marine Science

Received: *30 June 2021*
Accepted: *13 January 2022*
Published: *25 February 2022*

Citation:
Bennett S, Vaquer-Sunyer R, Jordá G, Forteza M, Roca G and Marbà N (2022) Thermal Performance of Seaweeds and Seagrasses Across a Regional Climate Gradient. Front. Mar. Sci. 9:733315. doi: 10.3389/fmars.2022.733315

INTRODUCTION

Ocean warming is altering the distribution and abundance of species across the globe (Hoegh-Guldberg and Bruno, 2010). Benthic foundation species of seaweeds and seagrasses can be particularly sensitive to warm temperatures and have undergone extensive thermal stress, mortality and range contraction in recent decades (Marba and Duarte, 2010; Wernberg et al., 2016; Strydom et al., 2020). While many of these impacts have been concentrated in warm edge populations (Wernberg et al., 2016), cooler, central populations can also be highly sensitive to extirpation (Marba and Duarte, 2010; Bennett et al., 2015), highlighting that not all species or locations are equally susceptible to warming. The difference in temperature between an organism's upper thermal limits and its upper environmental temperatures (herein, thermal safety margin), can vary considerably both within a species and between species due to differences in thermal physiology and through geographic differences in thermal regimes (Bennett et al., 2019). This variation presents a

taxonomically and geographically diverse range of responses to warming and raises fundamental questions about the ecological and evolutionary drivers of thermal performance patterns.

Comparative measurements of thermal performance (e.g., metabolism, growth, motor function, survival) across a species range are critical to test established ecological theories about thermal sensitivity and identify potential hotspots or refuges from climate warming. For example, if individuals display similar thermal limits irrespective of range position, then thermal safety margins will decrease toward the warm edge of a species range, creating a gradient of increasing thermal sensitivity from cool to warm edge populations (Bennett et al., 2019). This is a common assumption used in many species distribution models, for example, that rely on the realised distribution of species to predict the likelihood of extirpation or range shifts under climate change (Araújo and Peterson, 2012; but see Martínez et al., 2014; Valladares et al., 2014). If, on the other hand, thermal limits differ between populations – through local adaptation or phenotypic plasticity – then thermal sensitivity may not reflect geography or remain constant across a species range (Bennett et al., 2015, 2021). Furthermore, maximum growth rates and physiological performance can be higher among populations that are adapted to warmer temperatures (e.g., hotter-is-better hypothesis), as rate depressing effects of cool temperatures on biochemical reactions are not overcome by phenotypic plasticity or genetic adaptation (Bennett, 1987; Knies et al., 2009). For the vast majority of species, within-species patterns of thermal sensitivity remain unknown, forcing climate change predictions to rely on measurements of thermal performance from a single location (Pinsky et al., 2019) or the realised thermal distribution of a species (Stuart-Smith et al., 2015). Understanding the variability in thermal performance between populations and verifying the extent to which thermal performance reflects local environmental conditions, realised species distributions, or other factors, is crucial to accurately predict climate change impacts and adaptively manage ecosystems in the Anthropocene.

The Mediterranean Sea presents a fascinating region to study within-species and between-species patterns in thermal performance and sensitivity. Seaweeds and seagrasses are the dominant habitat forming species throughout the region, where they harbour high biodiversity and provide essential ecosystem services (Bianchi et al., 2012). Many of the species that characterise rocky reefs (e.g., *Padina pavonica*) and seagrass meadows (e.g., *Posidonia oceanica*) in the Mediterranean Sea today, have deep evolutionary histories in the region dating back over 65 million years (Aires et al., 2011; Silberfeld et al., 2013). What's more, these species have survived a remarkably dynamic climatic history, spanning from tropical origins during the Cretaceous, drying out of the basin during the Messinian salinity crisis (6 Mya; Hsü et al., 1977), to repeated glaciations during the Pleistocene (2.6–0.012 Mya). These upheavals have shaped the regions unique biodiversity to include species with tropical and boreal phylogeographic origins (Por, 2009; Bianchi et al., 2012). The Mediterranean Sea settled to its current climatic conditions approximately 2000 years ago (Bianchi et al., 2012), characterised by a steep 6°C climatic gradient from west to east. Despite their evolutionary resilience, seaweeds and seagrasses are susceptible to contemporary warming in the Mediterranean. Marine heatwaves, for example, have caused severe impacts to central populations of seagrass (*P. oceanica;* Diaz-Almela et al., 2009; Marba and Duarte, 2010), leading to predictions that the species will face functional extinction by 2100 (Jordà et al., 2012; Chefaoui et al., 2018). By comparing populations in a field translocation study, however, Bennett et al. (2021) found cool-edge and warm-edge populations demonstrated higher survivorship and growth than central populations in response to thermal stress, highlighting that performance does not necessarily reflect thermal geography and *P. oceanica* may have greater resilience to warming than previously recognised. The study by Bennett et al. (2021) does not, however, identify the upper thermal limits of cool- and warm-edge populations of *P. oceanica*, or whether such geographical differences in thermal sensitivity reflects a more general phenomenon among primary producers in the region.

In this study we compare the thermal performance of four pan-Mediterranean species of seagrasses and seaweed from four locations each, spanning 8° in latitude and 30° in longitude across the Mediterranean Sea. Specifically, we ask: (1) Do growth rates within a species differ between locations across a 6°C gradient in ocean temperatures? (2) Do species with similar realised thermal distributions display similar thermal optima and upper thermal limits? (3) How do experimentally derived thermal performance metrics for each population compare to (a) local environmental temperatures at each location and (b) the realised thermal distribution of species?

Our study examines how experimentally derived growth metrics of thermal performance reflect expectations of thermal sensitivity based on a species thermal geography. This work addresses underlying differences in thermal sensitivity predictions that arise from scaling issues in climate change ecology and contributes toward more nuanced, scalable links between geography and thermal physiology.

MATERIALS AND METHODS

Field Collections

Thermal tolerance experiments were conducted on two seagrass species (*P. oceanica* and *Cymodocea nodosa*) and two brown seaweed species (*Cystoseira compressa* and *P. pavonica*) from four locations spanning 8° in latitude and 30° in longitude across the Mediterranean (**Figure 1** and **Supplementary Table 1**). These four species were chosen as they are dominant foundation species and cosmopolitan across the Mediterranean Sea. Thermal performance experiments from Catalonia and Mallorca were conducted simultaneously in June 2016 for seaweeds (*P. pavonica* and *C. compressa*) and in August 2016 for seagrasses (*P. oceanica* and *C. nodosa*). Experiments for all four species were conducted in July 2017 for Crete and in September 2017 for Cyprus.

Sea Temperature Measurements and Reconstruction

Sea surface temperature data for each collection site were based on daily SST maps with a spatial resolution of 1/4°, obtained from the National Centers for Environmental Information

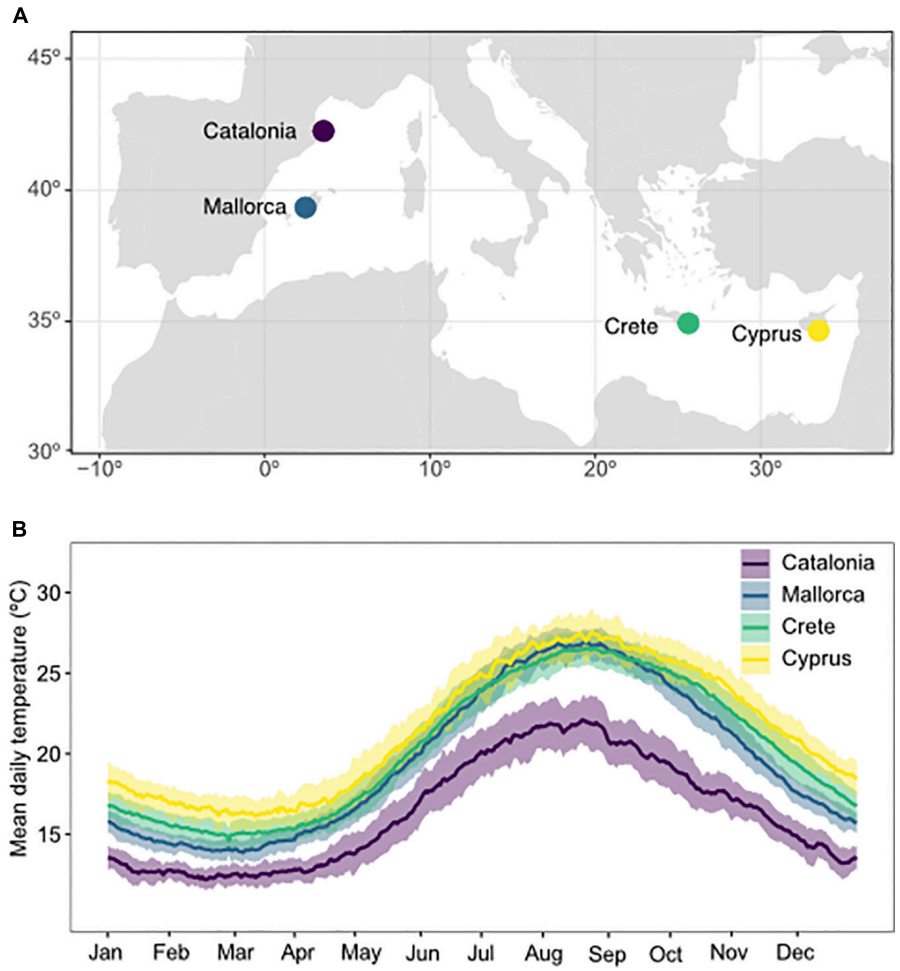

FIGURE 1 | Map of experimental collection sites **(A)** and daily temperature profiles **(B)** in Catalonia, Mallorca, Crete, and Cyprus. Temperatures represent mean daily temperatures averaged over the period 1981–2019. Shaded areas represent the standard deviation in daily temperatures between years.

(NCEI; Reynolds et al., 2007)[1]. These maps have been generated through the optimal interpolation of Advanced Very High Resolution Radiometer (AVHRR) data for the period 1981–2019. Underwater temperature loggers (ONSET Hobo pro v2 Data logger) were deployed at each site and recorded hourly temperatures throughout 1 year. In order to obtain an extended time series of temperature at each collection site, a calibration procedure was performed comparing logger data with sea surface temperature from the nearest point on SST maps. In particular, SST data were linearly fitted to logger data for the common period. Then, the calibration coefficients were applied to the whole SST time series to obtain corrected-SST data and reconstruct daily habitat temperatures from 1981 to 2019.

Species Description and Distribution

The species used in this study are all common species throughout the Mediterranean Sea, although differ in their biological traits, evolutionary histories and thermo-geographic affinities (**Supplementary Figure 1**). *P. oceanica* is endemic to the Mediterranean Sea with the all other *Posidonia* species found in temperate Australia (Aires et al., 2011). The distribution of *P. oceanica* is restricted to the Mediterranean, spanning from Gibraltar in the west to Cyprus in the east and north into the Aegean and Adriatic seas (Telesca et al., 2015; **Supplementary Figure 1A**).

Cymodocea nodosa distribution extends across the Mediterranean Sea and eastern Atlantic Ocean, where it is found from south west Portugal, down the African coast to Mauritania and west to Macaronesia (Alberto et al., 2008; **Supplementary Figure 1B**). Congeneric species of *C. nodosa* are found in tropical waters of the Red Sea and Indo-Pacific, suggesting origins in the region at least prior to the closure of the Suez Isthmus, approximately 10 Mya.

Like *C. nodosa, Cystoseira compressa* has a distribution that extends across the Mediterranean and into the eastern Atlantic, where it is found west to Macaronesia and south to northwest Africa (**Supplementary Figure 1C**). The genus *Cystoseira* has recently been reclassified to include just four

[1]www.ncdc.noaa.gov/oisst

species with all congeneric *Cystoseira* spp. having warm-temperate distributions from the Mediterranean to the eastern Atlantic (Orellana et al., 2019).

The distribution of *Padina pavonica* is conservatively considered to resemble *C. nodosa* and *C. compressa*, spanning throughout the Mediterranean and into the eastern Atlantic. We considered the poleward distribution limit of *P. pavonica* to be the British Isles 50°N (Herbert et al., 2016). *P. pavonica* was previously thought to have a global distribution, but molecular analysis of the genus has found no evidence to support this (Silberfeld et al., 2013). Instead it has been suggested that *P. pavonica* was potentially misclassified outside of the Mediterranean, due to morphological similarity with congeneric species (Silberfeld et al., 2013). *Padina* is a monophyletic genus with a worldwide distribution from tropical to cold temperate waters (Silberfeld et al., 2013). Most species have a regional distribution, with few confirmed examples of species spanning beyond a single marine realm (sensu Spalding et al., 2007).

Sample Collection

Sample collections were conducted at two sites, separated by approximately 1 km, within each location. Collections were conducted at the same depth (1–3 m) at each location and were spaced across the reef or meadow to try and minimise relatedness between shoots or fragments. Upon collection, fragments were placed into a mesh bag and transported back to holding tanks in cool, damp, dark conditions (following Bennett et al., 2021). Fragments were kept in aerated holding tanks in the collection sites at ambient seawater temperature and maintained under a 14:10 light-dark cycle until transport back to Mallorca, where experiments were performed. Prior to transport, *P. oceanica* shoots were clipped to 25 cm length (from meristem to tip), to standardise initial conditions and remove old tissue for transport. For transport back to Mallorca, fragments were packed in layers within cool-boxes. Cool-packs were wrapped in damp tea towels (rinsed in seawater) and placed between layers of samples. Samples from Catalonia, Crete, and Cyprus experienced approximately 12 h of transit time. On arrival at the destination, samples were returned to holding tanks with aerated seawater and a 14:10 light-dark cycle.

Experimental Design: Thermal Performance Experiments

All experiments were run in climate-controlled incubation facilities of the Institut Mediterrani d'Estudis Avançats (Mallorca, Spain). Following 48 h under ambient (collection site) conditions, samples were transferred to individual experimental aquaria, which consisted of a double layered transparent plastic bag filled with 2 L of filtered seawater (60 μm) (following Savva et al., 2018). Sixteen experimental bags were suspended within 80 L temperature-controlled baths. In total, ten baths were used, one for each experimental temperature treatment. Bath temperatures were initially set to the acclimatization temperature (i.e., *in situ* temperatures) and were subsequently increased or decreased by 1°C every 24 h until the desired experimental temperature was achieved. Experimental temperatures were: 15, 18, 21, 24, 26, 28, 30, 32, 34, and 36°C (**Supplementary Table 2**). For each species, four replicate aquarium bags were used for each temperature treatment with three individually marked seagrass shoots or three algal fragments placed into each bag. For *P. oceanica,* each marked plant was a single shoot including leaves, vertical rhizome and roots. For *C. nodosa*, each marked individual consisted of a 10 cm fragment of horizontal rhizome containing three vertical shoots. Individually marked seaweeds contained the holdfast, and 4–5 fronds of *P. pavonica* (0.98 ± 0.06 g FW; mean ± SE) or a standardised 5–8 cm fragment with meristematic tip for *C. compressa* (3.67 ± 0.1 g FW; mean ± SE). Experimental plants were cleaned of conspicuous epiphytes. Once the targeted temperatures were reached in all of the baths, experiments ran for 14 days for the algal species and 21 days for seagrasses to allow for measurable growth in all species at the end of the experiment. Experiments were conducted inside a temperature-controlled chamber at constant humidity and air temperature (15°C). Bags were arranged in a 4 × 4 grid within each bath, enabling four species/population treatments to be run simultaneously. Bags were mixed within each bath so that one replicate bag was in each row and column of the grid, to minimise any potential within bath effects of bag position. Replicate bags were suspended with their surface kept open to allow gas exchange and were illuminated with a 14 h light:10 h dark photoperiod through fluorescent aquarium growth lamps. The water within the bags were mixed with aquaria pumps. The light intensity within each bag was measured via a photometric bulb sensor (LI-COR) and ranged between 180 and 258 μmol m^{-2} s^{-1}. Light intensity was constant between experiments and did not significantly differ between experimental treatments ($p > 0.05$). The temperature in the baths was controlled and recorded with an IKS-AQUASTAR system, which was connected to heaters and thermometers. The seawater within the bags was renewed every 72 h and salinity was monitored daily with an YSI multi-parameter meter. Distilled water was added when necessary to ensure salinity levels remained within the range of 36–39 PSU, typical of the study region. Carbon and Nitrogen concentrations in the leaf tissue were measured at the end of the experiment for triplicates of the 24°C treatment for each species and location (**Supplementary Figure 2**) at Unidade de Técnicas Instrumentais de Análise (University of A Coruña, Spain) with an elemental analyser FlashEA 112 (Thermo Finnigan).

Growth Measurements and Statistical Analyses

Net growth rate of seagrass shoots was measured using leaf piercing-technique (Short and Duarte, 2001). At the beginning of the experiment seagrass shoots were pierced just below the ligule with a syringe needle and shoot growth rate was estimated as the elongation of leaf tissue in between the ligule and the mark position of all leaves in a shoot at the end of the experiment, divided by the experimental duration. Net growth rate of macroalgae individuals was measured as the difference in wet weight at the end of the experiment from the beginning of the experiment divided by the duration of the experiment. Moisture on macroalgae specimens was carefully

removed before weighing them. Patterns of growth in response to temperature were examined for each experimental population using a Gaussian function:

$g=ke^{[-0.5(TMA-\mu)^2/\sigma^2]}$, where k = amplitude, μ = mean, and σ = standard deviation of the curve. Best fit values for each parameter were determined using a non-linear least squares regression using the "nlstools" package (Baty et al., 2015) in R (R Core Team, 2020). 95% CI for each of the parameters were calculated using non-parametric bootstrapping of the mean centred residuals. The relationship between growth metrics and the best-fit model was determined by comparing the sum of squared deviations (SS) of the observed data from the model, to the SS of 10^4 randomly resampled datasets. Growth metrics were considered to display a significant relationship to the best-fit model if the observed SS was smaller than the 5th percentile of randomised SS. Upper thermal limits were defined as the optimal temperature + 2 standard deviations (95th percentile of curve) or where net growth = 0. Samples that had lost all pigment or structural integrity by the end of the experiment were considered dead and any positive growth was treated as zero.

Metabolic Rates

Net production (NP), gross primary production (GPP), and respiration (R) were measured for all species from the four sites for five different experimental temperatures containing the *in situ* temperature during sampling up to a 6°C warming (see **Supplementary Table 3** for details). Individuals of the different species were moved to methacrylate cylinders containing seawater treated with UV radiation to remove bacteria and phytoplankton, in incubation tanks at the five selected temperatures. Cylinders were closed using gas-tight lids that prevent gas exchange with the atmosphere, containing an optical dissolved oxygen sensor (ODOS® IKS), with a measuring range from 0 to 200% saturation and accuracy at 25°C of 1% saturation, and magnetic stirrers inserted to ensure mixing along the height of the core. Triplicates were measured for each species and location, along with controls consisting in cylinders filled with the UV-treated seawater, in order to account for any residual production or respiration derived from microorganisms (changes in oxygen in controls was subtracted from treatments). Oxygen was measured continuously and recorded every 15 min for 24 h.

Changes in the dissolved oxygen (DO) were assumed to result from the biological metabolic processes and represent NP. During the night, changes in DO are assumed to be driven by R, as in the absence of light, no photosynthetic production can occur. R was calculated from the rate of change in oxygen at night, from half an hour after lights went off to half an hour before light went on (NP in darkness equalled R). NP was calculated from the rate of change in DO, at 15 min intervals, accumulated over each 24 h period. Assuming that daytime R equals that during the night, GPP was estimated as the sum of NP and R. To derive daily metabolic rates, we accumulated individual estimates of GPP, NP, and R resolved at 15 min intervals over each 24 h period during experiments and reported them in mmol O_2 m^{-3} day^{-1}. A detailed description of calculation of metabolic rates can be found at Vaquer-Sunyer et al. (2015).

Thermal Distribution and Thermal Safety Margins

We estimated the realised thermal distribution for the four experimental species by downloading occurrence records from the Global Biodiversity Information Facility [GBIF.org (11/03/2020) GBIF Occurrence Download]. Occurrence records from GBIF were screened for outliers and distributions were verified from the primary literature (Alberto et al., 2008; Draisma et al., 2010; Win et al., 2010; Silberfeld et al., 2013; Telesca et al., 2015; Orellana et al., 2019) and Enrique Ballesteros (pers. comms.) (**Supplementary Figure 1**). Mean, 1st and 99th percentiles of daily SST's were downloaded for each occurrence site for the period between 1981 and 2019 using the SST products described above (**Supplementary Table 4**). Thermal range position of species at each experimental site were standardised by their global distribution using a Range Index (RI; Sagarin and Gaines, 2002). Median SST at the experimental collection sites were standardized relative to the thermal range observed across a species realized distribution, using the equation: $RI = 2(S_M - D_M)/D_B$ where S_M = the median temperature at the experimental collection site, D_M = the thermal midpoint of the species global thermal distribution, and D_B = range of median temperatures (°C) that a species experiences across its distribution. The RI scales from −1 to 1, whereby "−1" represents the cool, leading edge of a species distribution, "0" represents the thermal midpoint of a species distribution and "1" represents the warm, trailing edge of a species distribution (Sagarin and Gaines, 2002). Thermal safety margins for each population were calculated as the difference between empirically derived upper thermal limits for each population and the maximum long term habitat temperatures recorded at collection sites. Each population's thermal safety margin was plotted against its range position to examine patterns in thermal sensitivity across a species distribution.

RESULTS

Thermal Profiles of Experimental Sites and Global Distribution

Annual temperatures at experimental sites ranged from 10.8 ± 0.1°C to 24.4 ± 0.18°C (mean ± SE, averaged from 1981 to 2019) in Catalonia, 13.15 ± 0.12°C to 27.79 ± 0.14°C in Mallorca, 13.91 ± 0.14°C to 27.52 ± 0.16°C in Crete, and 14.0 ± 0.18°C to 29.17 ± 0.15°C in Cyprus (**Figure 1** and **Supplementary Table 1**). Combining all experimental sites, this represents the 1st – 99th percentile of the global thermal distribution of *P. oceanica*, 12th – 96th percentile for *C. nodosa*, 20th – 97th percentile for *C. compressa*, and 12th – 99th percentile of the global thermal distribution for *P. pavonica*.

Thermal Performance: Growth

Optimal and critical upper temperature limits of Mediterranean macrophytes varied both between populations and species (**Figure 2**). Overall, 11/15 experimental populations displayed significant normal growth distributions in response to temperature. Of these, 10/11 significant distributions were

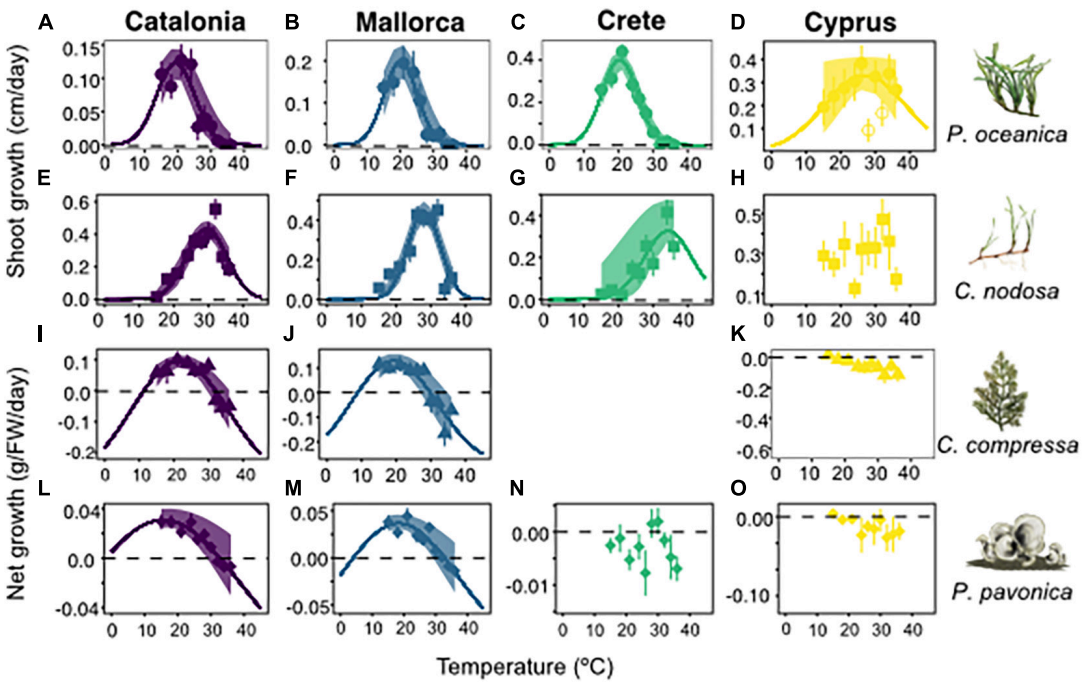

FIGURE 2 | Growth rates of experimental populations from Catalonia, Mallorca, Crete, and Cyprus, in response to temperatures from 15 to 36°C. Rows represent *Posidonia oceanica* (circles), *Cymodocea nodosa* (squares), *Cystoseira compressa* (triangles), and *Padina pavonica* (diamonds), respectively. Species illustrations and names displayed at end of each row columns represent Catalonia (purple), Mallorca (blue), Crete (green), and Cyprus (yellow). Line of best fit for *P. oceanica* from Cyprus, displays model without 28 and 32°C outliers. *C. compressa* from Crete was removed from the analysis due to poor condition of the plants at the commencement of the experiment. Shaded envelopes show 95% confidence intervals.

recorded in experiments from Catalonia, Mallorca and Crete, whereas experimental populations from Cyprus displayed variable growth responses to temperature (**Figure 2** and **Supplementary Table 5**). For *P. oceanica*, optimal growth temperatures were recorded at 19 ± 1°C for Catalonia and 20 ± 0.7°C for Mallorca and Crete, while upper limits were recorded at 30°C for Catalonia, Mallorca, and Crete. Growth patterns in Cyprus samples displayed a non-significant relationship with temperature when all data was included. By removing 28 and 32°C outliers, the growth relationship with temperature improved (p = 0.055) and was characterised by a 27 ± 13°C optimal temperature (**Figure 2** and **Supplementary Table 5**). *P. oceanica* from Cyprus also recorded the highest growth rates of any location during the experiments, averaging 0.2–0.4 cm day^{-1} including in the warmest treatments 30–36°C.

Cymodocea nodosa recorded higher optimal and lethal temperature limits than *P. oceanica* in all locations, except Cyprus. Optimal growth temperatures were 29 ± 0.5°C, 28 ± 0.4°C, and 34 ± 5°C in Catalonia, Mallorca, and Crete, respectively (**Figures 2E–G**). Critical upper limits were estimated at 41, 37.5, and 48°C for Catalonia, Mallorca, and Crete, respectively, based on best-fit growth models. *C. nodosa* in Cyprus displayed a non-significant growth relationship with temperature, despite recording relatively high growth rates across all temperature treatments. *C. compressa* and *P. pavonica* displayed wider growth curves than *P. oceanica* and *C. nodosa*. Optimal growth temperatures were 21 ± 1°C and 19 ± 1.5°C for *C. compressa* and 15.5 ± 0.5°C and 18 ± 0.4°C for *P. pavonica*, in Catalonia and Mallorca, respectively. Upper thermal limits for *C. compressa* and *P. pavonica* were recorded at 32°C in Catalonia, and 30°C for *C. compressa* and 32°C for *P. pavonica* in Mallorca. Growth curves for *C. compressa* and *P. pavonica* in Crete and Cyprus were non-significant (**Supplementary Table 5**).

Metabolic Rates

At the population level, patterns in gross primary productivity (GPP) and respiration (R) were relatively flat or variable for 8/15 and 11/15 populations, respectively, meaning that a peak in metabolic rates could not be defined. Among the populations where maximum GPP could be defined, temperatures ranged between 28 ± 4°C for Mallorca and Cyprus populations of *C. nodosa* and *C. compressa* and 32 ± 8°C for Crete and Cyprus populations of *P. pavonica* (**Supplementary Figure 3** and **Supplementary Table 6**). Metabolic rates were primarily heterotrophic (i.e., GPP < R) across temperatures in the upper portion of each populations thermal range. NP significantly decreased with increasing temperature for all species except *C. nodosa* when populations were pooled together (**Supplementary Figure 4**). *C. compressa* reduced its NP by 4.72 ± 1.65 μmol O_2/ g FW per Celsius degree (R^2 = 0.13, p < 0.007), *P. pavonica* reduced NP by 3.33 ± 0.84 μmol O_2/ g FW per Celsius degree (R^2 = 0.23, p < 0.001), and *P. oceanica* reduced NP by 0.58 ± 0.14 μmol O_2/ g FW per Celsius degree (R^2 = 0.26, p < 0.001). The temperature at which NP became

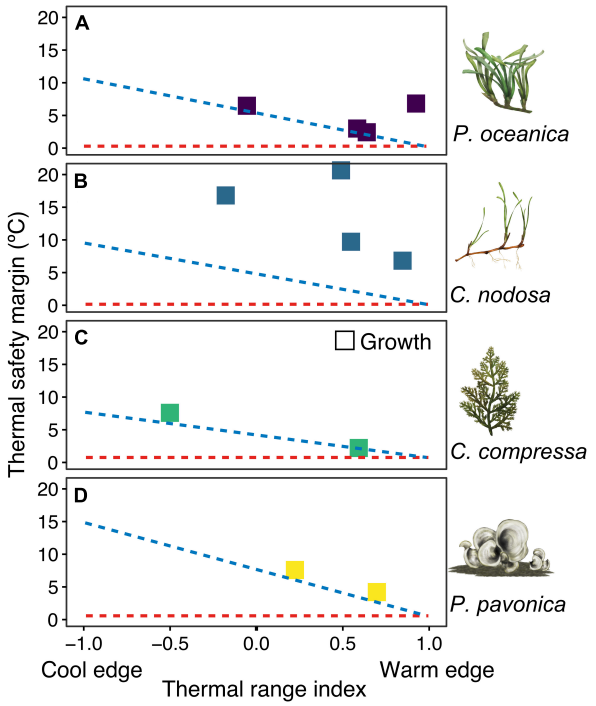

FIGURE 3 | Thermal safety margins (TSM) of experimental populations in relation to the range position. Panels **(A–D)** represent the four species. Each species name and illustration is displayed next to corresponding panel. TSMs represent the difference between experimental upper thermal limits and maximum temperatures at the collection site. Thermal range index illustrates where the maximum habitat temperatures lie in relation to the range of maximum temperatures observed across a species thermal distribution. The blue diagonal line represents expected TSM if a species fundamental (i.e., experimental) and realised thermal distribution limits were the same. The red horizontal line illustrates the TSM if fundamental thermal limits and maximum local temperatures were the same (TSM = 0). TSM estimates are based on growth rates. Upper thermal limit estimates for *P. oceanica* and *C. nodosa* in Cyprus are conservatively considered here to be 36°C, based on observed growth and survival rates in experiments.

negative, changing from net autotrophy to net heterotrophy was 22.2 ± 0.4°C for *P. oceanica*, 23.7 ± 0.5°C for *C. compressa*, and 26.2 ± 0.4°C for *P. pavonica*.

Patterns in Thermal Safety Margins Across Species Range

Thermal safety margins between experimental upper thermal limits and maximum temperatures at collection sites declined from cooler to warmer sites in accordance with expectation of thermal niche conservatism in 7 out of 12 populations (**Figure 3**). Consistent upper thermal limits for *P. oceanica* in Catalonia, Mallorca, and Crete, for example, resulted in declining thermal safety margins from 6.5 to 2.4°C from cooler to warmer locations and on average, 1 ± 0.16°C above the maximum realised habitat temperatures for the species. *P. oceanica* in Cyprus was a notable exception to this pattern, whereby thermal safety margins were >6°C as a result of higher thermal tolerance at the warm range edge. Thermal safety margins of *C. nodosa* varied between 16.8°C in the cooler Catalonia population, to 9.7 and 20.6°C in warmer Mallorca and Crete populations, respectively. All locations displayed larger thermal safety margins than predicted based on the realised thermal distribution of the species (**Figure 3**). Similar thermal limits in *C. compressa* and *P. pavonica* populations in both Catalonia and Mallorca, resulted in declining thermal safety margins from 7 to 2°C in the cooler and warmer location, respectively. Upper thermal limits were 1.9°C higher than the maximum realised habitat temperatures for *C. compressa* and 2.1°C higher than the maximum realised temperatures across *P. pavonica's* range. No experimental populations displayed upper thermal limits lower than the corresponding species distribution limit.

DISCUSSION

Quantifying spatial and taxonomic variability in thermal performance is critically important to identify potential hotspots and refuges from thermal stress in response to climate change. Here we quantified the thermal performance of four dominant habitat forming species of seaweed and seagrass, from four locations across the Mediterranean Sea. We found major differences in thermal performance between species as well as subtle, albeit important differences between populations within species. Most notably, thermal optima and upper limits in the seagrass *C. nodosa,* were over 10°C higher than the seagrass *P. oceanica,* highlighting potential differences in response to warming between species. One exception to this finding was the high thermal tolerance of *P. oceanica* in Cyprus. Cyprus represents the warm distribution edge of *P. oceanica* and experimental plants displayed high upper thermal limits resulting in larger thermal safety margin than cooler locations. Observed differences in thermal performance between species and within species provide important context about the potential vulnerability of benthic marine ecosystems to warming and contributes to a general understanding about the underlying drivers of thermal sensitivity.

Major differences in thermal performance between species was the standout finding from this study. This finding is significant, because of the close similarities these species share in their realised thermal distributions. Realised thermal limits are a commonly used metric of thermal sensitivity (Araújo and Peterson, 2012). Yet, despite all species having realised upper thermal limits between 29 and 30°C, under experimental conditions thermal limits ranged from 30°C in *P. oceanica* to over 40°C in *C. nodosa.* Interestingly, these differences in experimental thermal performance were broadly consistent with the contrasting genus-level thermal distributions of *Posidonia* and *Cymodocea*. *Posidonia* and *Cymodocea* both have Indo-Pacific distributions outside of the Mediterranean, reflecting the historical connection between the Mediterranean and Indian Ocean prior to the closure of Suez Isthmus, approximately 10 Mya. The contemporary distribution of *Posidonia* genus is bi-temperate, with all other *Posidonia* species found in temperate Australia, following their separation around 65 Mya (Aires et al., 2011). By contrast, with the exception of *C. nodosa,* all congeneric

species of *Cymodocea,* have a tropical distribution throughout the Indo-Pacific (Short et al., 2007). Previous experiments on congeneric species found that *Cymodocea serrulata* displayed severe loss of biomass at temperatures >40°C (George et al., 2018), consistent with estimated upper limits of *C. nodosa* in the current study. We are not aware of comparable thermal performance experiments on congeneric *Posidonia* spp. However, following an extreme marine heatwave in 2011, warm-edge populations of *Phragmites australis* were tolerant of temperatures up to 29°C (Strydom et al., 2020), 3.8°C above the long term average (Fraser et al., 2014). The experimental thermal performance *of P. pavonica* was also consistent with the distribution of *Padina* spp. globally. *Padina* spp. is distributed globally, from the equator to cool-temperate regions (Silberfeld et al., 2013). The broad thermal distribution of *Padina* spp (−1.8 to 31°C), parallels with the broad thermal niche breadth of *P. pavonica* observed in experiments, relative to other species. Contrasting patterns in the global thermal distribution of congeneric species parallel the differences in the thermal limits of Mediterranean species, suggesting that these differences may reflect deep evolutionary differences in thermal affinity between species.

The differences in thermal tolerance between species is also remarkable given the shared selection pressures that have acted on these species. Following the final closure of the Suez Isthmus, the Mediterranean Sea underwent repeated climatic disturbances that fundamentally affected biodiversity in the basin (Taviani, 2002; Por, 2009). At the beginning of the Pleistocene (2.6 Mya) the Mediterranean Sea underwent rapid cooling, leading to mass extinction of much of its tropical-affiliated biota (Bianchi et al., 2012). Glacial and interglacial periods then resulted in alternating waves of cool-affiliated and tropical species colonizing the Mediterranean from the Atlantic, only to become extinct or have their distribution restricted during the subsequent cool or warm cycle (e.g., *Sparisoma cretense*). Despite these profound climatic disturbances, *P. oceanica, C. nodosa, C. compressa,* and *P. pavonica* remain dominant throughout the Mediterranean, suggesting a high degree of plasticity in all four species. Moreover, differences in thermal tolerance between species persist despite strong thermal selection pressures over several million years.

While species-level differences in thermal performance were most conspicuous, more subtle differences in thermal performance were also observable between some populations. Most notably was the thermal performance of *P. oceanica* in Cyprus, which displayed the highest growth rates of any populations and did not display a decline in growth at higher temperatures as observed in other populations. This finding contrasts with the prevailing paradigm that thermal sensitivity will be highest in warm edge populations. Warm edge populations, face the highest habitat temperatures of any population across a species range by definition, which if thermal limits are conserved between populations, mean they also have the highest sensitivity to warming. Instead the high growth rates and high thermal tolerance of *P. oceanica* within warm edge populations was consistent with the "hotter-is-better" hypothesis of thermal adaptation (Knies et al., 2009). The short-term nature of these experiments limits interpretation of the specific role of phenotypic plasticity or genetic adaptation in driving these results. Nevertheless, our findings indicate a u-shaped pattern in thermal safety margins, with central populations living closest to their upper thermal limit and cool and warm range edge displaying the highest thermal safety margins.

This finding provides context for the paradigm that *P. oceanica* is highly sensitive to warming (Marba and Duarte, 2010; Jordà et al., 2012) and supports the emerging idea that edge populations of *P. oceanica* may provide a hope-spot for *P. oceanica* in response to climate change (Bennett et al., 2021). The idea of high thermal sensitivity in *P. oceanica* emerged through studies conducted in the western Mediterranean, specifically Mallorca, where temperatures above 28°C have driven severe declines in shoot density of *P. oceanica* (Diaz-Almela et al., 2009; Marba and Duarte, 2010). Our findings support this previous work insofar as thermal limits of *P. oceanica* in Mallorca were estimated to be 30°C, very close to the maximum temperatures that previously led to population declines. However, our findings also help to explain how *P. oceanica* can thrive at its warm distribution limit in Cyprus where average daily summer temperatures are already 29°C and peak daily summer temperatures frequently exceed 30°C.

For metabolic rates, increasing temperatures resulted in a reduction of net production in all species except for *C. nodosa*. A decrease of NP with temperature suggests that warming could result in a change to heterotrophic metabolism. A net reduction of NP owing to a steeper increase in respiration rates than in gross primary production has been predicted by the Metabolic Theory of Ecology (Brown et al., 2004) owing to the fact that activation energies for autotrophs are half that of heterotrophs (Harris et al., 2006; Sarmento et al., 2010). Previous studies have shown a higher increase of respiration than primary production for planktonic communities in response to warming (Müren et al., 2005; Harris et al., 2006; Sarmento et al., 2010; Vaquer-Sunyer et al., 2010; Yvon-Durocher et al., 2010; Regaudie-de-Gioux and Duarte, 2012), whereas for benthic-dominated communities this prediction has been questioned (Vaquer-Sunyer and Duarte, 2013). Our results demonstrate that macrophyte species can also increase their respiration rates faster than primary production with warming, resulting in heterotrophic metabolic rates at high temperatures.

Finally, experimental artefacts need to be considered in relation to the variable thermal performance results. Thermal performance under experimental conditions is contingent on the experimental conditions (e.g., light intensity, nutrient levels of seawater), acclimation rates and seasonality, among other factors (Bates and Morley, 2020). As such, thermal performance measured under experimental conditions needs to be considered as a relative, not absolute estimate of the ecological reality that might occur in a natural ecosystem. For example, light conditions were kept constant during daylight hours under experimental conditions, but fluctuate under natural conditions due to shading, weather conditions, water clarity and latitude – all of which can influence growth rates. While experimental conditions were simplifications of natural conditions, standardised methodologies of collection, transportation, acclimation, and experimentation minimised

methodological variation and enabled comparability in thermal performance results between experiments.

Seasonal timing was one potential source of variation that may have influenced results of experiments. While all experiments took place around summer, timing of experiments ranged between June and September. For seaweeds, poor condition of *C. compressa* from Crete at the time of collection (July) was likely due to seasonal senescence and resulted in it being removed from the analysis. For *P. oceanica,* it is unlikely that seasonality was responsible for the poor growth relationship to temperature in Cyprus. Growth rates of *P. oceanica* from Cyprus were the highest recorded in any experiments, suggesting that the poor growth relationship was not an artefact of poor performance. Performance of seagrasses may, however, have been influenced by experimental conditions as a result of their clonal growth physiology. Seagrasses are clonal plants connected by rhizomes and are dependent on the connectivity between ramets for nutrient translocation (Marbà et al., 2002). Growth rates observed in the current experiment were lower than growth rates reported for natural meadows from the same populations, but were similar to growth rates observed in a field translocation study, where fragments were transplanted into natural substrate adjacent to meadows (Bennett et al., 2021). These patterns suggest that seagrasses are less suited to growing in fragments under experimental conditions than seaweeds which source their nutrients from the water column.

Our findings reveal the thermal performance of four dominant habitat forming species across their geographical range in the Mediterranean Sea. Between species differences in optimal and upper thermal limits were pronounced despite all species sharing similar geographical distributions. Within species thermal performance was relatively conserved between populations across a 6°C climate gradient in the Mediterranean, with the clear exception of *P. oceanica* at its warm range edge. Our findings highlight nuanced inter and intra-specific patterns in thermal performance that would be overlooked through a reliance on realised distributions or measurements from a single population. Contemporary patterns in thermal performance for Mediterranean macrophytes potentially reflect deep evolutionary legacies of species and local differences in the historical and contemporary marine climates. Population-specific patterns in thermal performance have important implications for the distribution, abundance and conservation of Mediterranean benthic habitats in response to climate change.

DATA AVAILABILITY STATEMENT

The datasets presented in this study can be found in online repositories. The names of the repository/repositories and accession number(s) can be found below: https://doi.org/10.5061/dryad.d2547d81r.

ETHICS STATEMENT

Collections of plant material for this project were conducted in accordance with institutional, national, and international guidelines and legislation. Permissions for collections of plant material were obtained from local governing bodies.

AUTHOR CONTRIBUTIONS

SB, NM, and RV-S conceived and designed the study. SB, NM, GR, and RV-S conducted the field work. SB, RV-S, NM, GR, and MF conducted the experiments. GJ provided all temperature data. SB wrote the manuscript with contributions from all authors. All authors contributed to the article and approved the submitted version.

FUNDING

SB received funding from the European Union's Horizon 2020 Research and Innovation Programme under grant agreement No. 659246 and Juan de la Cierva Formación (FJCI-2016-30728). RV-S was funded by Juan de la Cierva – Incorporación (IJCI-2015-23163), NM, SB, and RV-S received funding from the Spanish Ministry of Economy, Industry and Competitiveness (MedShift, CGL2015-71809-P). NM received funding from the Spanish Ministry of Science, Innovation and Universities (SUMAECO, RTI2018-095441-B-C21).

ACKNOWLEDGMENTS

We thank Demetris Kletou, Ioannis Savva, Perikilis Kleitou, and Charalampos Antoniou in Limassol for logistical support. Eugenia Apostolaki in Crete and Teresa Alcoverro from Catalonia facilitated experimental collections. Carlos Alejandro Morell, Elvira Álvarez, Mika Noguera, Olga Sánchez, and Daniel Salom helped to conducting the experiments. Marlene Wesselmann assisted in fieldwork. Enrique Ballesteros provided advice about taxonomy and species distributions. Species illustrations were drawn by Helena Twose.

SUPPLEMENTARY MATERIAL

The Supplementary Material for this article can be found online at: https://www.frontiersin.org/articles/10.3389/fmars.2022.733315/full#supplementary-material

REFERENCES

Aires, T., Marba, N., Cunha, R. L., Kendrick, G. A., Walker, D. I., Serrao, E. A., et al. (2011). Evolutionary history of the seagrass genus *Posidonia*. *Mar. Ecol. Prog. Ser.* 421, 117–130. doi: 10.3354/meps08879

Alberto, F., Massa, S., Manent, P., Diaz-Almela, E., Arnaud-Haond, S., Duarte, C. M., et al. (2008). Genetic differentiation and secondary contact zone in the seagrass *Cymodocea nodosa* across the Mediterranean–Atlantic transition region. *J. Biogeogr.* 35, 1279–1294. doi: 10.1111/j.1365-2699.2007.01876.x

Araújo, M. B., and Peterson, A. T. (2012). Uses and misuses of bioclimatic envelope modeling. *Ecology* 93, 1527–1539. doi: 10.1890/11-1930.1

Bates, A. E., and Morley, S. A. (2020). Interpreting empirical estimates of experimentally derived physiological and biological thermal limits in ectotherms. *Can. J. Zool.* 98, 237–244. doi: 10.1139/cjz-2018-0276

Baty, F., Ritz, C., Charles, S., Brutsche, M., Flandrois, J.-P., and Delignette-Muller, M.-L. (2015). A toolbox for nonlinear regression in R: the package nlstools. *J. Stat. Softw.* 66, 1–21. doi: 10.18637/jss.v066.i05

Bennett, A. F. (1987). "Evolution of the control of body temperature: is warmer better," in *Comparative Physiology: Life in Water and on Land*, eds P. Dejour, et al. (Padova: Liviana Prass), 421–431.

Bennett, S., Alcoverro, T., Kletou, D., Antoniou, C., Boada, J., Buñuel, X., et al. (2021). Resilience of seagrass populations to thermal stress does not reflect regional differences in ocean climate. *New Phytol.* Online ahead of print doi: 10.1111/nph.17885

Bennett, S., Duarte, C. M., Marbà, N., and Wernberg, T. (2019). Integrating within-species variation in thermal physiology into climate change ecology. *Philos. Trans. R Soc. Lond. B Biol. Sci.* 374, 20180550. doi: 10.1098/rstb.2018.0550

Bennett, S., Wernberg, T., Joy, B. A., de Bettignies, T., and Campbell, A. H. (2015). Central and rear-edge populations can be equally vulnerable to warming. *Nat. Commun.* 6, 10280. doi: 10.1038/ncomms10280

Bianchi, C. N., Morri, C., Chiantore, M., Montefalcone, M., Parravicini, V., and Rovere, A. (2012). "Mediterranean Sea biodiversity between the legacy from the past and a future of change," in *Life in the Mediterranean Sea: a Look at Habitat Changes*, ed. N. Stambler (New York, NY: Nova Science Publishers Inc).

Brown, J. H., Gillooly, J. F., Allen, A. P., Savage, V. M., and West, G. B. (2004). Toward a metabolic theory of ecology. *Ecology* 85, 1771–1789. doi: 10.1890/03-9000

Chefaoui, R. M., Duarte, C. M., and Serrão, E. A. (2018). Dramatic loss of seagrass habitat under projected climate change in the Mediterranean Sea. *Glob. Change biol.* 24, 4919–4928. doi: 10.1111/gcb.14401

Diaz-Almela, E., Marba, N., Martinez, R., Santiago, R., and Duarte, C. M. (2009). Seasonal dynamics of *Posidonia oceanica* in Magalluf Bay (Mallorca, Spain): temperature effects on seagrass mortality. *Limnol. Oceanogr.* 54, 2170–2182. doi: 10.4319/lo.2009.54.6.2170

Draisma, S. G., Ballesteros, E., Rousseau, F., and Thibaut, T. (2010). DNA sequence data demonstrate the polyphyly of the genus cystoseira and other sargassaceae genera (*Phaeophyceae*) 1. *J. Phycol.* 46, 1329–1345. doi: 10.1111/j.1529-8817.2010.00891.x

Fraser, M. W., Kendrick, G. A., Statton, J., Hovey, R. K., Zavala-Perez, A., and Walker, D. I. (2014). Extreme climate events lower resilience of foundation seagrass at edge of biogeographical range. *J. Ecol.* 102, 1528–1536. doi: 10.1111/1365-2745.12300

George, R., Gullström, M., Mangora, M. M., Mtolera, M. S., and Björk, M. (2018). High midday temperature stress has stronger effects on biomass than on photosynthesis: a mesocosm experiment on four tropical seagrass species. *Ecol. Evol.* 8, 4508–4517. doi: 10.1002/ece3.3952

Harris, L. A., Duarte, C. M., and Nixon, S. W. (2006). Allometric laws and prediction in estuarine and coastal ecology. *Estuaries Coasts* 29, 340–344. doi: 10.1007/bf02782002

Herbert, R. J., Ma, L., Marston, A., Farnham, W. F., Tittley, I., and Cornes, R. C. (2016). The calcareous brown alga Padina pavonica in southern Britain: population change and tenacity over 300 years. *Mar. Biol.* 163, 46. doi: 10.1007/s00227-015-2805-7

Hoegh-Guldberg, O., and Bruno, J. F. (2010). The impact of climate change on the world's marine ecosystems. *Science* 328, 1523–1528. doi: 10.1126/science.1189930

Hsü, K. J., Montadert, L., Bernoulli, D., Cita, M. B., Erickson, A., Garrison, R. E., et al. (1977). History of the Mediterranean salinity crisis. *Nature* 267, 399. doi: 10.1038/267399a0

Jordà, G., Marbà, N., and Duarte, C. M. (2012). Mediterranean seagrass vulnerable to regional climate warming. *Nat. Clim. Change* 2, 821–824. doi: 10.1038/nclimate1533

Knies, J. L., Kingsolver, J. G., and Burch, C. L. (2009). Hotter is better and broader: thermal sensitivity of fitness in a population of bacteriophages. *Am. Nat.* 173, 419–430. doi: 10.1086/597224

Marba, N., and Duarte, C. M. (2010). Mediterranean warming triggers seagrass (*Posidonia oceanica*) shoot mortality. *Sea. Glob. Change biol.* 16, 2366–2375. doi: 10.1111/j.1365-2486.2009.02130.x

Marbà, N., Hemminga, M. A., Mateo, M. A., Duarte, C. M., Mass, Y. E., Terrados, J., et al. (2002). Carbon and nitrogen translocation between seagrass ramets. *Mar. Ecol. Prog. Ser.* 226, 287–300. doi: 10.3354/meps226287

Martínez, B., Arenas, F., Trilla, A., Viejo, R. M., and Carreño, F. (2014). Combining physiological threshold knowledge to species distribution models is key to improving forecasts of the future niche for macroalgae. *Glob. Change Biol.* 21, 1422–1433. doi: 10.1111/gcb.12655

Müren, U., Berglund, J., Samuelsson, K., and Andersson, A. (2005). Potential effects of elevated sea-water temperature on pelagic food webs. *Hydrobiologia* 545, 153–166. doi: 10.1007/s10750-005-2742-4

Orellana, S., Hernández, M., and Sansón,, M. (2019). Diversity of Cystoseira sensu lato (*Fucales*, *Phaeophyceae*) in the eastern Atlantic and Mediterranean based on morphological and DNA evidence, including Carpodesmia gen. emend. and Treptacantha gen. emend. *Eur. J. Phycol.* 54, 447–465. doi: 10.1080/09670262.2019.1590862

Pinsky, M. L., Eikeset, A. M., McCauley, D. J., Payne, J. L., and Sunday, J. M. (2019). Greater vulnerability to warming of marine versus terrestrial ectotherms. *Nature* 569, 108. doi: 10.1038/s41586-019-1132-4

Por, F. (2009). Tethys returns to the Mediterranean: success and limits of tropical re-colonization. *BioRisk* 3, 5. doi: 10.3897/biorisk.3.30

R Core Team. (2020). *R: A Language and Environment for Statistical Computing*. Vienna: R Foundation for Statistical Computing.

Regaudie-de-Gioux, A., and Duarte, C. M. (2012). Temperature dependence of planktonic metabolism in the ocean. *Glob. Biogeochem. Cycles* 26, GB1015. doi: 10.1029/2010GB003907

Reynolds, R. W., Smith, T. M., Liu, C., Chelton, D. B., Casey, K. S., and Schlax, M. G. (2007). Daily high-resolution-blended analyses for sea surface temperature. *J. Clim.* 20, 5473–5496. doi: 10.1175/2007JCLI1824.1

Sagarin, R. D., and Gaines, S. D. (2002). Geographical abundance distributions of coastal invertebrates: using one-dimensional ranges to test biogeographic hypotheses. *J. Biogeogr.* 29, 985–997. doi: 10.1046/j.1365-2699.2002.00705.x

Sarmento, H., Montoya, J. M., Vázquez-Domínguez, E., Vaqué, D., and Gasol, J. M. (2010). Warming effects on marine microbial food web processes: how far can we go when it comes to predictions? *Philos. Trans. R. Soc. B Biol. Sci.* 365, 2137–2149. doi: 10.1098/rstb.2010.0045

Savva, I., Bennett, S., Roca, G., Jordà, G., and Marbà,, N. (2018). Thermal tolerance of Mediterranean marine macrophytes: vulnerability to global warming. *Ecol. Evol.* 8, 12032–12043. doi: 10.1002/ece3.4663

Short, F. T., and Duarte, C. M. (2001). Methods for the measurement of seagrass growth and production. *Glob. Seagrass Res. Methods* 2001, 155–198. doi: 10.1016/B978-044450891-1/50009-8

Short, F., Carruthers, T., Dennison, W., and Waycott, M. (2007). Global seagrass distribution and diversity: a bioregional model. *J. Exp. Mar. Biol. Ecol.* 350, 3–20. doi: 10.1016/j.jembe.2007.06.012

Silberfeld, T., Bittner, L., Fernández-García, C., Cruaud, C., Rousseau, F., de Reviers, B., et al. (2013). Species diversity, phylogeny and large scale biogeographic patterns of the genus Padina (*Phaeophyceae*, *Dictyotales*). *J. Phycol.* 49, 130–142. doi: 10.1111/jpy.12027

Spalding, M. D., Fox, H. E., Allen, G. R., Davidson, N., Ferdaña, Z. A., Finlayson, M., et al. (2007). Marine ecoregions of the world: a bioregionalization of coastal and shelf areas. *BioScience* 57, 573–583. doi: 10.1641/B570707

Strydom, S., Murray, K., Wilson, S., Huntley, B., Rule, M., Heithaus, M., et al. (2020). Too hot to handle: unprecedented seagrass death driven by marine heatwave in a World Heritage Area. *Sea. Glob. Change Biol.* 26, 3525–3538. doi: 10.1111/gcb.15065

Stuart-Smith, R. D., Edgar, G. J., Barrett, N. S., Kininmonth, S. J., and Bates, A. E. (2015). Thermal biases and vulnerability to warming in the world's marine fauna. *Nature* 528, 88–92. doi: 10.1038/nature16144

Taviani, M. (2002). The Mediterranean benthos from late Miocene up to present: ten million years of dramatic climatic and geologic vicissitudes. *Biol. Mar. Mediterr.* 9, 445–463.

Telesca, L., Belluscio, A., Criscoli, A., Ardizzone, G., Apostolaki, E. T., Fraschetti, S., et al. (2015). Seagrass meadows (*Posidonia oceanica*) distribution and trajectories of change. *Sci. Rep.* 5, 12505. doi: 10.1038/srep12505

Valladares, F., Matesanz, S., Guilhaumon, F., Araújo, M. B., Balaguer, L., Benito-Garzón, M., et al. (2014). The effects of phenotypic plasticity and local adaptation on forecasts of species range shifts under climate change. *Ecol. Lett.* 17, 1351–1364. doi: 10.1111/ele.12348

Vaquer-Sunyer, R., and Duarte, C. M. (2013). Experimental evaluation of the response of coastal Mediterranean planktonic and benthic metabolism to warming. *Estuaries Coasts* 36, 697–707. doi: 10.1007/s12237-013-9595-2

Vaquer-Sunyer, R., Conley, D. J., Muthusamy, S., Lindh, M. V., Pinhassi, J., and Kritzberg, E. S. (2015). Dissolved organic nitrogen inputs from wastewater treatment plant effluents increase responses of planktonic metabolic rates to warming. *Environ. Sci. Technol.* 49, 11411–11420. doi: 10.1021/acs.est.5b00674

Vaquer-Sunyer, R., Duarte, C. M., Santiago, R., Wassmann, P., and Reigstad, M. (2010). Experimental evaluation of planktonic respiration response to warming in the European Arctic Sector. *Pol. Biol.* 33, 1661–1671. doi: 10.1007/s00300-010-0788-x

Wernberg, T., Bennett, S., Babcock, R. C., de Bettignies, T., Cure, K., Depczynski, M., et al. (2016). Climate-driven regime shift of a temperate marine ecosystem. *Science* 353, 169–172. doi: 10.1126/science.aad8745

Win, N. N., Hanyuda, T., Arai, S., Uchimura, M., Prathep, A., Draisma, S. G., et al. (2010). Four new species of Padina (*Dictyotales*, *Phaeophyceae*) from the western Pacific Ocean, and reinstatement of Padina japonica. *Phycologia* 49, 136–153. doi: 10.2216/09-54.1

Yvon-Durocher, G., Jones, J. I., Trimmer, M., Woodward, G., and Montoya, J. M. (2010). Warming alters the metabolic balance of ecosystems. *Philos. Trans. R. Soc. B Biol. Sci.* 365, 2117–2126. doi: 10.1098/rstb.2010.0038

Conflict of Interest: The authors declare that the research was conducted in the absence of any commercial or financial relationships that could be construed as a potential conflict of interest.

Publisher's Note: All claims expressed in this article are solely those of the authors and do not necessarily represent those of their affiliated organizations, or those of the publisher, the editors and the reviewers. Any product that may be evaluated in this article, or claim that may be made by its manufacturer, is not guaranteed or endorsed by the publisher.

Advantages of publishing in Frontiers

OPEN ACCESS
Articles are free to read for greatest visibility and readership

FAST PUBLICATION
Around 90 days from submission to decision

HIGH QUALITY PEER-REVIEW
Rigorous, collaborative, and constructive peer-review

TRANSPARENT PEER-REVIEW
Editors and reviewers acknowledged by name on published articles

Frontiers
Avenue du Tribunal-Fédéral 34
1005 Lausanne | Switzerland

Visit us: www.frontiersin.org
Contact us: frontiersin.org/about/contact

REPRODUCIBILITY OF RESEARCH
Support open data and methods to enhance research reproducibility

DIGITAL PUBLISHING
Articles designed for optimal readership across devices

FOLLOW US
@frontiersin

IMPACT METRICS
Advanced article metrics track visibility across digital media

EXTENSIVE PROMOTION
Marketing and promotion of impactful research

LOOP RESEARCH NETWORK
Our network increases your article's readership